Geometry and emplacement controls of dolerite sill complexes in the Karoo basin

by

André Coetzee

Dissertation presented for the degree of Doctor of Earth Sciences in the Faculty of Science at Stellenbosch University

Promoter:
Professor Alexander F.M. Kisters
Department of Earth Sciences
Stellenbosch University

March 2020

Declaration

By submitting this dissertation electronically, I declare that the entirety of the work contained herein is my own, original work, that I am the sole author thereof (except where explicitly otherwise stated), that reproduction and publication thereof by Stellenbosch University will not infringe any third party rights and that I have not previously in its entirety or in part submitted it for obtaining any qualification.

André Coetzee

March 2020

Abstract

This dissertation is a compilation of three case studies that integrates drilling, field and geophysical data on dolerite sill complexes across the Karoo basin to constrain the emplacement processes, feeder systems and regional controls during the formation of the Karoo Large Igneous Province (KLIP) at ca. 183 Ma.

Chapter 4 describes the relationships between several saucer-shaped sills in the sedimentary strata of the northern Karoo basin and underlying Archaean to Neoproterozoic basement strata of the Kalahari craton. The three-dimensional geometry of numerous individual sills across an area of 7400 km² were reconstructed using extensive drill hole and mining data up to a depth of 2.5 km. Saucer-shaped sills, largely confined to the Karoo Supergroup and representing various geometries, dip towards distinct narrow, funnel-like dolerite structures seated exclusively within the basement layers that likely represent a connection to deep-seated feeders. Importantly, many of these funnel-shape structures are localised near or rooted in older, dykes and normal faults in the basement strata. This highlights the significance of pre-existing basement structures in facilitating magma transport through the upper crust and into the Karoo basin. Furthermore, the wide spatial distribution of magma feeders across the Kalahari craton is more aligned with thermal incubation of the sub-lithospheric mantle than the development of mantle plumes beneath Gondwana.

Chapter 5 constrains the emplacement controls of sills in the central Karoo basin through field and drill hole data from the Victoria West sill complex. The sill complex consists of five successively emplaced saucers-shaped sills across an area of 2000 km^2 that formed though magmatic underaccretion beneath earlier sills. Rigid and fully crystallised earlier sills served as stress barriers to the upwards propagation of later sill feeders which resulted in a nested sill structure marked by a sill-in-sill configuration. The close spatial overlap between the individual

saucer-shaped sills and NW-SE trend of the sill complex suggest the reutilization of the same feeder system, most likely the rim of a large underlying sill.

Emplacement controls of the Victoria West sill complex indicates sill formation occurred under a mild compressional stress regime at the onset of Karoo magmatism. The changeover from sill complexes at 184-180 Ma to later dyke swarms at 182-174 Ma suggest a switch in the prevailing stress field prior to Gondwana break-up. Thermal loading followed by lithospheric subsidence due to the rapid emplacement of >350 000 km^3 of sills and outpouring of >10^6 km^3 of lavas across southern Africa and Antarctica may have triggered extension and the subsequent intrusion of dyke swarms along cratonic margins. Therefore, inherited basin and lithospheric architecture was crucial in the later development of Karoo magmatism.

Chapter 6 represents a study of the distinct variations of sill geometries and associated intrusive structures across the Karoo basin in relation to the basal elevation of the Drakensberg Group lavas. These spatial variations in the mode of emplacement of sills are attributed to emplacement depth in addition to changes in sedimentary facies and driving magma pressures. The northern Karoo basin is characterised by shallow (<500m) emplacement depths with sills typically showing small (<10 km) diameters and thicknesses up to 40 m. The central Karoo basin represent intermediate emplacement depths of up to 700 m with sill diameters over 30 km and thicknesses below 100 m. Advanced emplacement depths of <2 km is found in the southern Karoo basin where sills reach sizes of 50-80 km and thicknesses of 35 m. Local dyke networks show similar depth dependent relationships across the Karoo basin. Dense systematic and non-systematic dyke networks are associated with respective shallow (<500 m) and intermediate (<700 m) emplacement depths whereas greater depths (<2 km) are largely devoid of dykes. Additionally, the asymmetric distribution of different sedimentary rock types and southward thickening of layers in addition to differential magma pressures across the Karoo basin further influenced sill emplacement processes and associated structural features.

Generally, the wide spatial and stratigraphic occurrence of sills throughout the Karoo basin is more consistent with many distributed feeders emplaced in the underlying basement rocks than a single plume-related source along the rift margins of southern Africa.

Acknowledgements

And so we conclude another three years of study. The time and effort spent on my PhD has been the most exciting and rewarding part of my early career, especially when findings add substantial value to both the mining industry and the wider research community. Although the workload was demanding at times, I managed to persevere due the overwhelming support received from the people below.

First and foremost, I am thankful to my supervisor, Prof. Alex Kisters, for his patience and dedication in supervising my research over the last five years of part-time post-graduate studies. I appreciate the sharing of knowledge and particularly enjoyed our long talks during fieldwork about dolerite emplacement, life and work experiences. Thanks for unlocking my potential and laying the foundation for my future academic endeavours.

Special thanks to the people involved in the project, including the geologists (Walter Seymore and Paul Mambane) at Evander Gold Mine, farmers that provided access to key outcrop sites in the Karoo and, above all, Luc Chevallier for the sharing of information and ideas without which this study would not be possible. I am also indebted to Sasol Mining for their willingness to provide access to a wealth of data across the coalfields of the Karoo basin in addition to modelling software that proved crucial for the visualization of complex sill geometries. Furthermore, I recognize other experts in my field for their constructive and meticulous reviews which greatly improved the content of the publications.

Finally, I am grateful to my family and especially my wife for their constant backing and motivation to reach my goal throughout this period.

Contents

List of figures

Chapter 4: Craton-hosted sill feeders

Chapter 5: Sill emplacement controls

Chapter 6: Spatial variations of sills

Chapter 1: Introduction

1.1 Preface

Over the course of several decades our understanding of mafic sills and their emplacement processes have evolved significantly and we have come to acknowledge their geometric complexity and distinct emplacement processes. Initially studies have largely focussed on the factors that influence the dyke to sill transition. Anderson (1951) proposed that sill formation is driven by repeated dyke injection into the crust that induces stress rotation into the horizontal plane (Anderson, 1951). However, Pollard (1973) have shown the influence of stress field orientation alone is an oversimplification especially in anisotropic rocks. Instead, it is the interplay of the stress field with host rock discontinuities and rigidity contrasts (Young's modulus ratios) that control the propagation direction of a sheet-like intrusion. Later analogue experiments expanded on this model by suggesting that dyke arrest occurs between layers with a high rigidity ratio and that sill formation only initiates when the interface between two layers was weak creating a favourable parting surface (Kavanagh et al., 2006). On this basis solidified sills within sedimentary wall rocks represents a very suitable emplacement horizon for later sill emplacement (Menand, 2008; Gudmundsson, 2011).

In addition to the above-mentioned dyke to sill transition models are others more specific to explaining the formation of saucer-shaped sills and their distinct geometry defined by a central inner sill surrounded by an inclined sheet and structurally higher flat outer sill (Fig. 1.1). Bradley (1965) proposed that sills intrude along a surface of equipotential pressure where magma pressure equals the lithostatic pressure. This implies that stratigraphically high parts of the sill correspond to topographic lows while stratigraphically low areas coincide with topographic highs. Conversely, Francis (1982) suggested saucers-shaped sills are influenced by neutral buoyancy and gravitational flow. A sill is induced from a feeder dyke due to

reorientation of stresses from vertical to horizontal followed by magma flow in the down-dip direction towards the centre of the saucer-shaped geometry due to increased magma density relative to the surrounding wall rocks. In order for the magma to maintain a hydrostatic equilibrium it may start propagating upwards again forming a saucer-shaped structure.

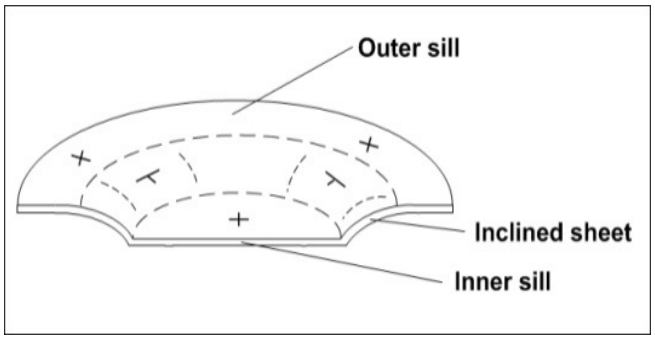

Figure 1.1: *The structural geometry of a saucer-shaped sill and constituent segments.*

However, these models were subsequently disproved by analogue and numerical experiments which instead proposed the upwards growth of saucer-shaped sills through multiple stages from a central underlying feeder (e.g. Mathieu et al., 2008; Galland et al., 2009; Galerne et al., 2011). The full visualization of entire sill networks by the more recent introduction of seismic reflectance data supported these experiments (Thomson and Hutton, 2004; Cartwright and Hansen, 2006; Magee et al., 2016; Schofield et al., 2017). The imaging of connections seemingly between individual stacked saucer-shaped sills at different stratigraphic levels made a strong case for sill-feeding-sill networks (Cartwright and Hansen, 2006) as a likely alternative to the commonly proposed dyke-based plumbing systems (Chevallier and Woodford, 1999; Galerne at al., 2011). Nonetheless, the interpretation of seismic imagery of dense sill networks often presented several challenges due to (1) interference of thick overburden rocks or closely-spaced sills, (2) sill thicknesses that are below the detectability of the seismic data and (3) the decrease in vertical resolution with depth obscuring thicker sills that would ordinarily be visible at shallower depths (Cartwright and Hansen, 2006; Schofield et al., 2017; Eide et al., 2017). Considering the limitations of seismic resolution, thinly stacked or closely overlapping sill geometries may instead be imaged as a single, more simplified intrusive body if it can be

resolved at all (Eide et al., 2017). This is confirmed by well logs that have shown large amounts of unidentified sills in seismic data (Schofield et al., 2017).

It is apparent from the remaining uncertainties linked to seismic reflection data that we require more detailed data sets to constrain the magma emplacement mechanics and feeder relationships of sill complexes. This dissertation focusses on the structural controls of mafic magma transport and emplacement processes based on examples from the Karoo basin.

1.2 Research rationale

In the Karoo Large Igneous Province sill complexes are of particular interest as it represents the primary feeder system to the overlying Drakensberg Group flood basalts that covered much of southern Africa at ca. 183-178 Ma (Marsh, 1987; Cox, 1992; Encarnacion et al., 1996; Duncan et al., 1997; Jourdan et al., 2005, 2007; Svensen et al., 2012). Although sills commonly occur throughout the Karoo and other subsidiary basins, such as the Kalahari, Ellisras, Spingbok Flats, etc. basins (e.g. Chevallier and Woodford, 1999; Galerne et al., 2011; Coetzee and Kisters, 2016; Barbolini et al., 2019), it is still unclear how these sill networks and their deeper crustal feeders facilitated such vast volumes of magma over a period of less than 500 ka (Svensen et al., 2012). This problem is aggravated by a lack of well-preserved basal sill exposures in the field and the total absence of Karoo-aged feeders in the outcropping Archaean to Neoproterozoic rocks of the Kalahari craton. Feeder relationships provide insight into the architecture of sill networks and the factors that control magma injection and dispersal throughout the Karoo basin which, in turn, contributes towards our understanding of the broader geodynamic evolution of the Karoo Large Igneous Province.

The extensive coal and gold mining complexes situated along the northern reaches of the Karoo basin, provide an exclusive view into the structure of mafic sills. Although largely eroded and obscured by vegetation on the surface, mining and drill hole data present a wealth of

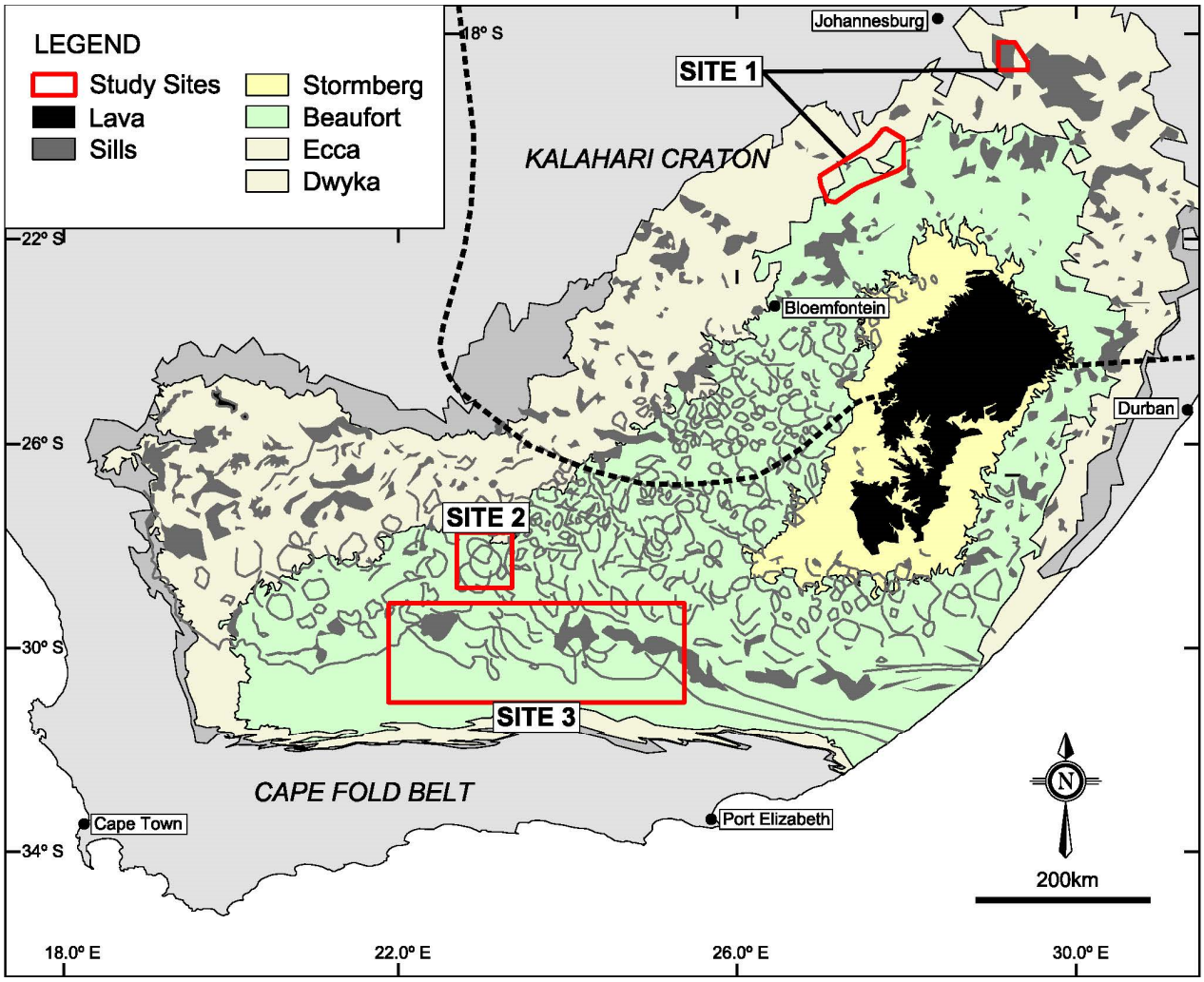

Figure 1.2: *Geological map of the Karoo basin showing the positions of the three study sites. Site 1 consist of two separate areas near the respective towns of Secunda and Sasolburg. Site 2 is located next to Victoria West whereas site 3 include a wider area between Beaufort West and Graaff-Reinet.*

information on the sub-surface occurrence of sills. Here, coal mines in particular, commit vast resources to locate and understand sills and their associated wall-rock deformation and thermal aureoles. Stratigraphic and structural data obtained from historic drill hole and mining developments represent information gathered for well over 60 years by different mining houses that extend across an area of 7400 km^2 and up to a depth of 2.5 km (Fig. 1.2 Site 1). Conversely, the semi-arid climate of the central and southern Karoo basin (Fig. 1.2 Site 2 and 3) preserves in situ sill geometries and local features that are otherwise not apparent from the detailed sub-surface data in the north. Road cuttings and short drill holes in addition to aeromagnetic and

seismic images define sill outlines, local flow directions and regional controls on magma emplacement as well as the overall structure of the underlying feeder network. Thus, the unique data sets from various sites across the Karoo basin represent an excellent opportunity to test and evaluate both analogue and theoretical models of mafic magma emplacement in the upper crust.

1.3 Structure of the dissertation

This dissertation incorporates field work and mining data of sill complexes in the Karoo basin by presenting the cumulative results of three separate projects that deal with (1) craton-hosted feeders to saucers-shaped sills and their structural controls, (2) emplacement controls of sills and their feeders and (3) the regional variations of sills across the Karoo basin.

This dissertation is laid out as follows:

- Chapter 2 describes the broader Karoo basin and Karoo Large Igneous Province
- Chapter 3 elaborates on the different data sets and methodology applied during three-dimensional modelling
- Chapter 4 relates to several scattered saucer-shaped sills with feeders rooted in older faults and dykes within the underlying basement rocks of the Kalahari craton.
- Chapter 5 describes the emplacement controls of sills in the central Karoo basin and their regional implications.
- Chapter 6 describes the spatial variations and controls of sills and associated structures across a north-south traverse of the Karoo basin.
- Chapter 7 summarizes the overarching conclusions and implications of the three case studies.

REFERENCES

Anderson, E.M. (1951). The dynamics of faulting and dyke formation with applications to Britain. Edinburgh, Oliver and Boyd, 206 pp.

Barbolini, N., Nxumalo, V., Wagner, N., Kramers, J., Vorster, C., Cairncross, B., Barnford, M.K. (2019). Palynostratigraphic correlation of the Springbok Flats coalfield to other coal-bearing successions in the Karoo basins of southern Africa, South African Journal of Geology 122, 1-16.

Bradley, J. (1965). Intrusion of major dolerite sills. Transactions of the Royal Society of New Zealand, Geology 3, 27-55.

Cartwright, J., Hansen, D.M. (2006). Magma transport through the crust via interconnected sill complexes. Geology 34, 929–932. Basin Research 10, 417–439.

Chevallier, L., Woodford, A. (1999). Morpho-tectonics and mechanism of emplacement of the dolerite rings and sills of the western Karoo, South Africa. South African Journal of Geology 102, 43–54.

Coetzee, A., Kisters, A.F.M. (2016). The 3D geometry of regional-scale dolerite saucer complexes and their feeders in the Secunda Complex, Karoo basin. J. Volcanology Geothermal Research 317, 66–79.

Cox, K. G. (1992). Karoo igneous activity and the early stages of the break-up of Gondwanaland, in Magmatism and the Causes of Continental Break-up. Geological Society, London, Special Publications 68, 137-148.

Duncan, R.A., Hooper, P.R., Rehacek, J., Marsh, J.S., Duncan, A.R. (1997). The timing and duration of the Karoo igneous event, southern Gondwana. Journal of Geophysical Research 102, 127-138.

Eide, C.H., Schfield, N., Lecomte, I., Buckley, S.J., Howell, J.A. (2017). Seismic interpretation of sill complexes in sedimentary basins: implications for the sub-sill imaging problem. Journal of the Geological Society 175, 193-209.

Encarnacion, J., Fleming, T.H., Elliot, D.H., Eales, H.V. (1996). Synchronous emplacement of Ferrar and Karoo dolerites and the early break-up of Gondwana. Geology 24, 535–538.

Francis, T.J.G. (1982). Thermal-Expansion Effects in Deep-Sea Sediments: Nature 299, 334-336.

Galland, O., Planke, S., Neumann, E.R., Malthe-Sørenssen, A. (2009). Experimental modelling of shallow magma emplacement: application to saucer-shaped intrusions. Earth and Planetary Science Letters 277, 373–383.

Galerne, C.Y., Galland, O., Neumann, E., Planke, S. (2011). 3D relationships between sills and their feeders: evidence from the Golden Valley Sill Complex (Karoo Basin) and experimental modelling. Journal of Volcanology and Geothermal Research 202, 189–199.

Gudmundsson, A. (2011). Deflection of dykes into sills at discontinuities and magma chamber formation. Tectonophysics 500, 50–64.

Jourdan, F., Féraud, G., Bertrand, H., Kampunzu, A.B., Tshoso, G., Watkeys, M.K., Le Gall, B. (2005). The Karoo large igneous province: brevity, origin, and relation with mass extinction questioned by new 40Ar/39Ar age data. Geology 33, 745–748.

Jourdan, F., Féraud, G., Bertrand, H., Watkeys, M.K. (2007). From flood basalts to the inception of oceanization: example from the 40Ar/39Ar high-resolution picture of the Karoo large igneous province. Geochemistry. Geophysics. Geosystems. 8, 989–1006.

Kavanagh, J.L., Menand, T., Sparks, R.S.J. (2006). An experimental investigation of sill formation and ropagation in layered elastic media. Earth Planet. Sci. Lett. 245, 799–813.

Magee, C.J., Muirhead, J.D., Karvelas, A., Holford, S.P., Jackson, C.A.L., Bastow, I.D., Schofield, N., Stevenson, C.S.T., McLean, C., McCarthy, W., Shtukert, O. (2016). Lateral magma flow in mafic sill complexes. Geosphere 12 (3), 809-841.

Marsh, J.S. (1987). Basalt geochemistry and tectonic discrimination within continental flood basalt provinces. Journal of Volcanology and Geothermal Research. 32, 35–49.

Mathieu, L., Van Wyk de Vries, B., Holohan, E.P., Troll, V.R. (2008). Dykes, cups, saucers and sills: Analogue experiments on magma intrusion into brittle rocks. Earth and Planetary Science Letters 271, 1–13.

Menand, T. (2008). The mechanics and dynamics of sills in layered elastic rocks and their implications for the growth of laccoliths and other igneous complexes. Earth and Planetary Letters 267, 93–99.

Pollard, D.D. (1973). Derivation and evaluation of a mechanical model for sheet intrusions. Tectonophysics 19, 233–269.

Schofield, N., Holford, S., Millett, J., Brown, D., Jolley, D., Passey, S.R., Muirhead, D., Grove, C., Magee, C., Murray, J., Hole, M., Jackson, C.A.L., Stevenson, C. (2017). Regional magma plumbing and emplacement mechanisms of the Faroe-Shetland Sill Complex: implications for magma transport and petroleum systems within sedimentary basins. Basin Research 29, 41–63.

Svensen, H., Corfu, F., Polteau, S., Hammer, Hammer, O., Planke, S. (2012). Rapid magma emplacement in the Karoo Large Igneous Province. Earth and Planetary Science Letters 325–326, 1–9.

Thomson, K., Hutton, D. (2004). Geometry and growth of sill complexes: insights using 3D seismic from the North Rockall Trough. Bulletin of Volcanology 66, 364–375.

Chapter 2: Background

The Karoo retro-arc foreland basin forms part of a larger series of basins across southern Africa that developed in response to lithospheric flexure and orogenic loading along the southern margin of Gondwana. The main Karoo basin in particular represents the deposition of sedimentary rocks from the late Carboniferous to early Jurassic in a southward-deepening syncline which includes the Dwyka, Ecca, Beaufort and Stormberg Groups (Fig. 2.1). Besides a strong tectonic control on basin development and sedimentary provenance, the stratigraphic sequence record a change in the prevailing climatic conditions from cold and semi-arid to warm and humid and later arid.

Basement rocks to the Karoo Supergroup are heterogeneous and show a large variation in age, internal structure and composition across the basin. In the north, the basin is underlain by Archaean TTG-greenstone rocks and Archaean to Proterozoic cover sequences of the Kalahari Craton (Fig. 2.1). In the south, the deeper parts of the basin are made up of Mesoproterozoic gneisses and metasediments of the Namaqua-Natal metamorphic belt (Fig. 2.1). The high-grade rocks are, in turn, overlain by the Ordovician to Carboniferous (500-330 Ma) Cape Supergroup forming a gently south-dipping wedge beneath the Karoo Supergroup that gradually tapers northwards from a maximum thickness of 8-10 km in the south to the north, where it is not developed. In the far west of the basin, the Karoo Supergroup unconformably overlies Neoproterozoic to early Phanerozoic metasedimentary sequences of the Nama and Vanrhynsdorp Groups (Fig. 2.1). The latter represent variably deformed molasse-type deposits formed during the later stages in the foreland of the Pan-African Gariep and Saldania belts at ca. 545-520 Ma (Gresse and Germs, 1993).

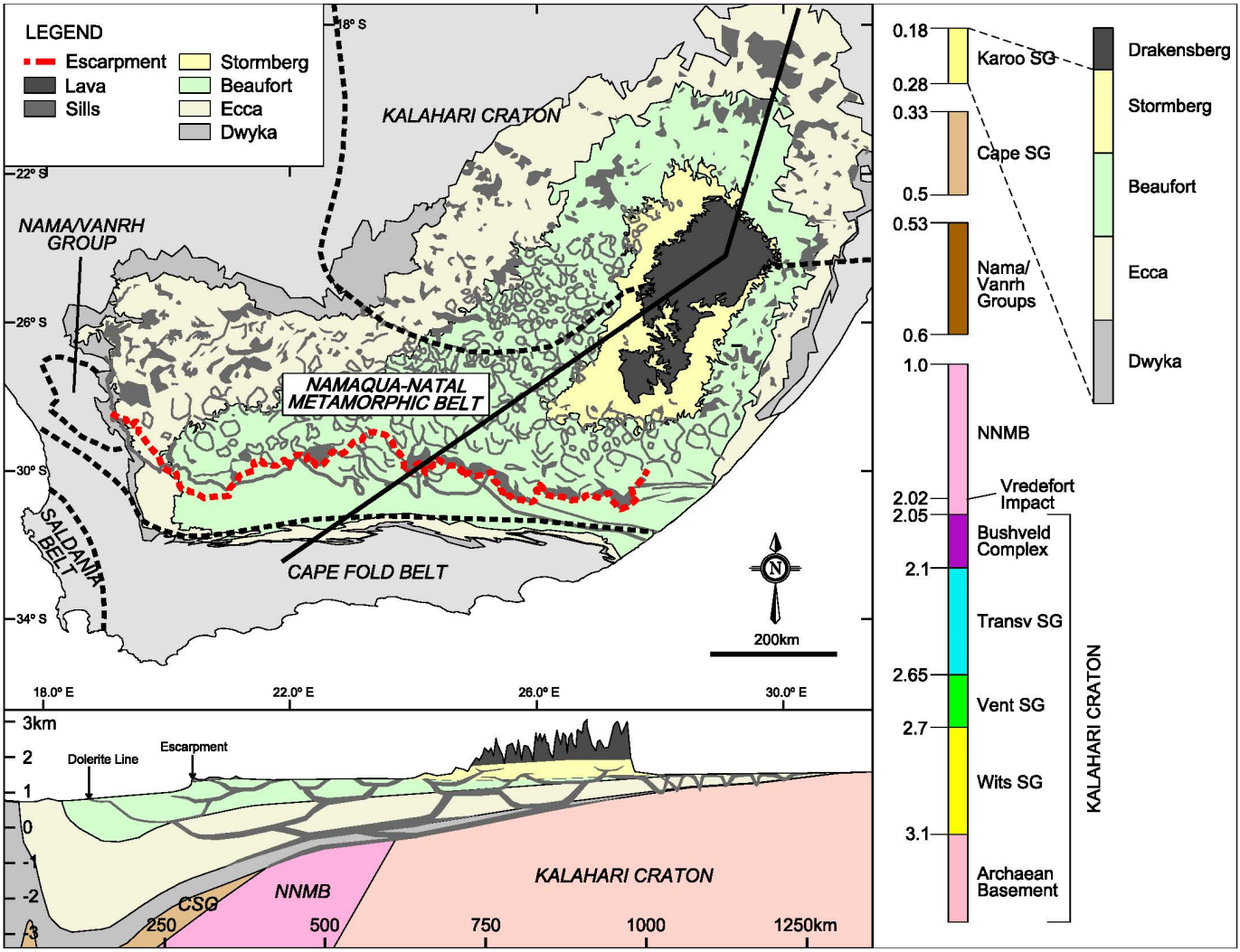

Figure 2.1: *A geological map of the Karoo basin with a regional cross-section showing the spatial distribution of the Karoo Supergroup in relation to the underlying basement terranes and their constituent litho-stratigraphic units and ages in Ga. CSG – Cape Supergroup, NNMB – Namaqua-Natal Metamorphic Belt*

The Cape Fold Belt (CFB) is the major structural feature bounding the southern margin of the Karoo basin (Fig. 2.1). The CFB forms part of the c. 6000 km long Pan-Gondwanide Mobile Belt generated during northward-directed subduction and convergence and associated accretion of terranes along the southern margin of Gondwana (Fig. 2.2) (Catuneanu, 2004). Deformation has affected Pan-African basement as well as rocks of the Cape and Karoo Supergroups (Fig. 2.1). Available age data point to progressive shortening between 281 Ma and 246 Ma (Hälbich et al., 1983; Gresse et al., 1992; Hansma et al, 2015; Blewett and Phillips, 2016). The southern

Cape Fold Belt is thick-skinned with thrusts commonly re-activating pre-existing crustal weaknesses in basement rocks (de Beer, 1995; Paton et al., 2006). Thick-skinned thrusting in the south and at deeper levels gives way to thin-skinned deformation in the north and in the shallow crust (de Beer, 1995; Paton et al., 2006; Tankard et al., 2009). This is associated with progressively more open folds and lower fold amplitudes. The general decrease in strain towards the north is also reflected by the lack of a prominent Karoo-age foredeep that would indicate orogenic loading due to the advancing thrust front, and the more or less unaffected Cape Supergroup and Namaqua-Natal metamorphic belt beneath the southern Karoo basin (Fig. 2.1) (Lindeque et al., 2011). Thin-skinned deformation of the Karoo Supergroup occurred, at least locally, detached from the Cape Supergroup through the development of low amplitude folds in the upper Karoo Supergroup and shallow listric thrusts rooted in décollement surfaces confined to the Cape Supergroup and lower Ecca and Dwyka Groups (Lindeque et al., 2011; Lanci et al., 2013).

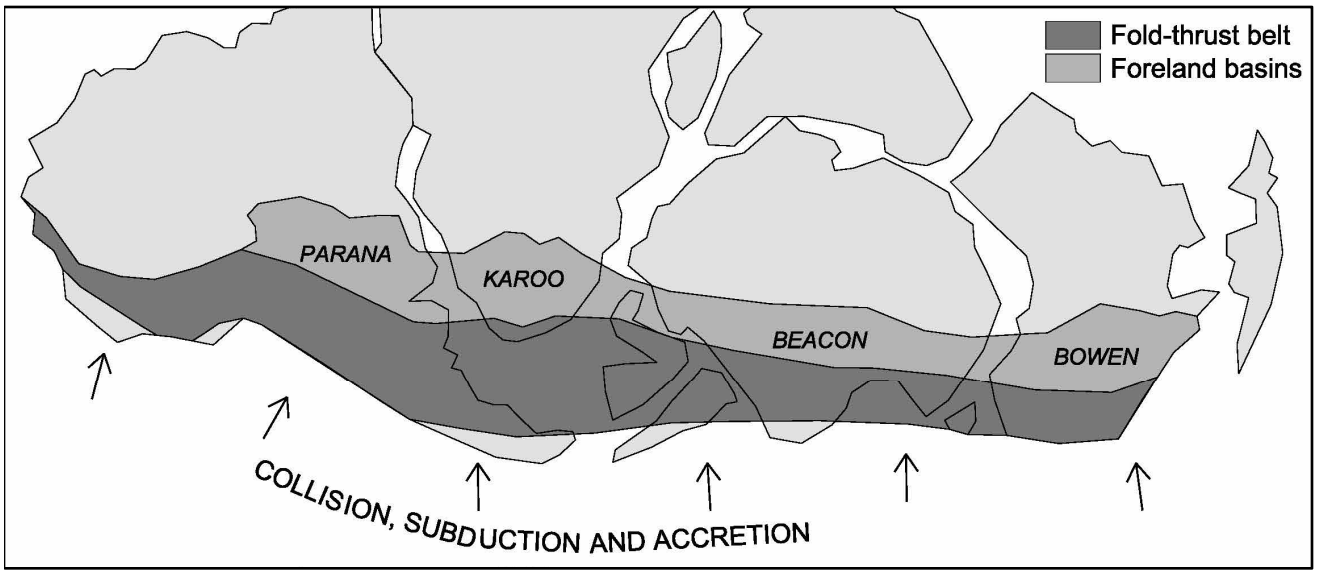

Figure 2.2: *Reconstruction of the Pan-Gondwanide Mobile Belt showing the northerly subduction of the palaeo-Pacific plate beneath southern Gondwana and the resulting foreland basins (after Catuneanu, 2004).*

The Karoo Large Igneous Province represents a period of protracted magmatic activity (184-174 Ma) across southern Africa that is associated with the injection of over 10^6 km^3 of mafic magma through the crust prior to the break-up of Gondwana. Karoo magmatism is commonly believed to have initiated from the impact of a mantle plume at the intersection between the Okavango, Save-Limpopo and Northern Lebombo dyke swarms (Fig. 2.3) (e.g. Cox, 1989; White and McKenzie, 1989; Storey and Kyle, 1997; White, 1997). Regional-scale sill complexes and dyke swarms served as an intricate plumbing system to the outpouring of over 1.4 km of continental flood basalts (Fig. 2.3) (e.g. Marsh, 1987; Cox, 1992; Encarnacion et al, 1996; Duncan et al, 1997; Chevallier and Woodford, 1999; Le Gall et al., 2002; Riley et al, 2006; Jourdan et al, 2004, 2005, 2007a, 2008; Galerne et al., 2008, 2011; Svensen et al., 2012). The vast majority of this feeder system is made up of sills emplaced within the subhorizontal sedimentary rocks of the Karoo Supergroup. Individual sills may be up to 100 m thick, but field relationships and geochemical results show they commonly occur as nested sill complexes that record the emplacement of multiple successive magma pulses (Schofield et al., 2010; Galerne et al., 2008, 2011; Neumann et al., 2011; Coetzee and Kisters, 2016). Sill complexes along the southern margin of the KLIP form a prominent escarpment (Fig. 2.1), accentuated by the uplift induced by a regional thermal anomaly that persisted well after the rifting of Gondwana at ca. 170 Ma (Marsh 1987; Cox 1992; Duncan et al., 1997; Hawkesworth et al., 1999; Jourdan et al., 2007b). Notably, the formation of the continental escarpment is associated with renewed uplift across southern Africa related to the African Superswell mantle anomaly at 30 - 15 Ma (Burke and Gunnell, 2008 and references therein). The escarpment represents a significant drop in elevation across the Karoo basin from an inland plateau preserving sill complexes at elevations between 1200-1600 m to a low lying (600-800 m) shale-rich plain largely devoid of dolerite intrusions (Fig. 2.1).

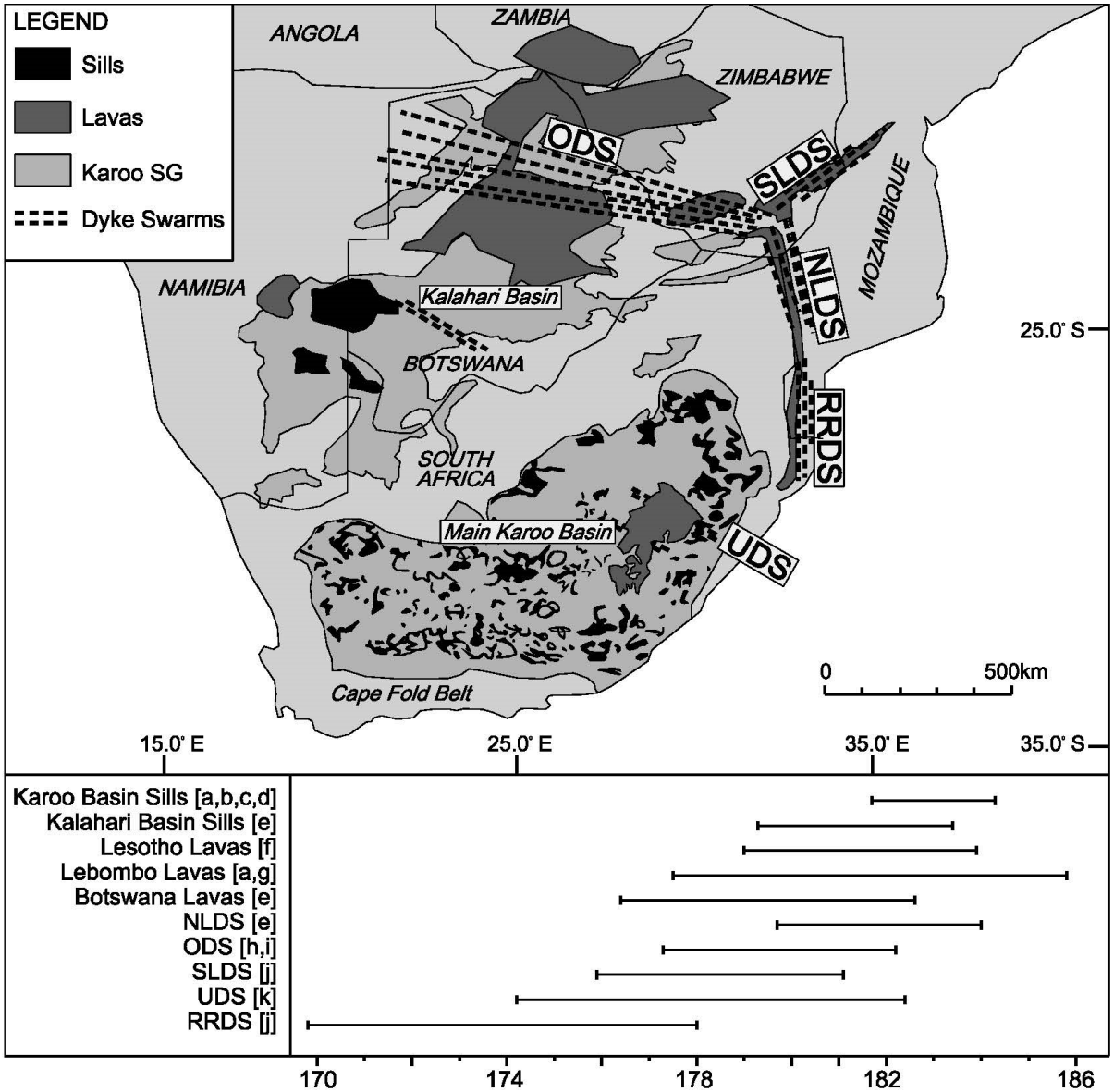

Figure 2.3: *Geological map showing the remnants of lavas, sills and dyke swarms related to the Karoo Large Igneous Province. ODS, Okavango dyke swarm; SLDS, Save-Limpopo dyke swarm; NLDS, Northern Lebombo dyke swarm; RRDS, Rooi Rand dyke swarm; UDS, Underberg dyke swarm. Age ranges are after Duncan et al. (1997) [a]; Encarnacion et al., 1996 [b]; Svensen et al. (2007) [c]; Svensen et al. (2012) [d]; Jourdan et al. (2005) [e]; Jourdan et al. (2007a) [f]; Riley et al., 2004 [g]; Le Gall et al. (2002) [h]; Jourdan et al. (2004) [i]; Jourdan et al. (2007b) [j]; Riley et al. (2006) [k]*

REFERENCES

Blewett, S., Phillips, D. (2016). An Overview of Cape Fold Belt Geochronology: Implications for Sediment Provenance and the Timing of Orogenesis. In B. Linol, M.J. de Wit (Editors). Origin and Evolution of the Cape Mountains and Karoo Basin. Nelson Mandela Metropolitan University, Port Elizabeth, South Africa, 45-55.

Burke, K., Gunnell, Y. (2008). The African Erosion Surface: A Continental-Scale Synthesis of Geomorphology, Tectonics, and Environmental Change over the Past 180 Million Years. Geological Society of America Memoir 201, 66.

Catuneanu, O. (2004). Basement control on flexural profiles and the distribution of foreland facies: The Dwyka Group of the Karoo Basin, South Africa. Geology 32, 517–520.

Chevallier, L., Woodford, A. (1999). Morpho-tectonics and mechanism of emplacement of the dolerite rings and sills of the western Karoo, South Africa. South African Journal of Geology 102, 43–54.

Coetzee, A., Kisters, A.F.M. (2016). The 3D geometry of regional-scale dolerite saucer complexes and their feeders in the Secunda Complex, Karoo Basin. J. Volcanol. Geotherm. Res. 317, 66-79.

Cox, K.G. (1992). Karoo igneous activity, and the early stages of the break-up of Gondwanaland. In: Storey, B.C., Alabaster, T., Pankhurst, R.J. (Eds.), Magmatism and the Causes of Continental Break-up, vol. 68. Geological Society of London Special Publication, pp. 37-148.

Cox, K.G. (1989). The role of mantle plumes in the development of continental drainage patterns. Nature 342, 873–877.

De Beer, C.H. (1995). Fold interference from simultaneous shortening in different directions: the Cape fold belt syntaxis. Journal of African Earth Sciences 21, 157–169.

Duncan, R.A., Hooper, P.R., Rehacek, J., Marsh, J.S., Duncan, A.R. (1997). The timing and duration of the Karoo igneous event, southern Gondwanaland. J. Geophys. Res. 102, 18127-18138.

Encarnacion, J., Fleming, T.H., Elliot, D.H., Eales, H.V. (1996). Synchronous emplacement of Ferrar and Karoo dolerites and the early break-up of Gondwana. Geology 24, 535-538.

Galerne, C.Y., Neumann, E., Planke, S. (2008). Emplacement mechanisms of sill complexes: information from the geochemical architecture of the golden valley sill complex, South Africa. J. Volcanol. Geotherm. Res. 177, 425-440.

Galerne, C.Y., Galland, O., Neumann, E., Planke, S. (2011). 3D relationships between sills and their feeders: evidence from the Golden Valley Sill Complex (Karoo Basin) and experimental modelling. Journal of Volcanology and Geothermal Research 202, 189–199.

Gresse, P.G., Theron, J.N., Fitch, F.J. and Miller, J.A. (1992). Tectonic inversion and radiometric resetting of the basement in the Cape Fold Belt. In: M.J. de Wit and I.G.D. Ransome (Editors). Inversion tectonics of the Cape Fold Belt, Karoo and Cretaceous Basins of Southern Africa. Balkema, Rotterdam, Netherlands, 217–228.

Gresse, P.G., Germs, G.J.B. (1993). The Nama foreland basin: sedimentation, major unconformity bounded sequences and multisided active margin advance. Precambrian Research, 63, 247-272.

Hälbich, I.W., Fitch, F.J. and Miller, J.A. (1983). Dating the Cape Orogeny. In: A.P.G. Söhnge and I.W. Hälbich (Editors), Geodynamics of the Cape Fold Belt. Special Publications of the Geological Society of South Africa, Johannesburg, 12, 75–100.

Hansma, J., Tohver, E., Schrank, C., Jourdaan, F. and Adams, D. (2015). The timing of the Cape Orogeny: New 40Ar/39Ar age constraints on deformation and cooling of the Cape Fold Belt, South Africa. Gondwana Research 32, 122-137.

Hawkesworth, C., Kelley, S., Turner, S., Le Roex, A., Storey, B. (1999). Mantle processes during Gondwana break-up and dispersal. J. Afr. Earth Sci. 28, 239–261.

Jourdan, F., G. Féraud, H. Bertrand, A. B. Kampunzu, G. Tshoso, B. Le Gall, J. J. Tiercelin, and P. Capiez (2004), The Karoo triple junction questioned: Evidence from 40Ar/39Ar Jurassic and Proterozoic ages and geochemistry of the Okavango dike swarm (Botswana), Earth Planet. Sci. Lett., 222, 989–1006.

Jourdan, F., G. Féraud, H. Bertrand, A. B. Kampunzu, G. Tshoso, M. K. Watkeys, and B. Le Gall. (2005), The Karoo large igneous province: Brevity, origin, and relation with mass extinction questioned by new 40Ar/39Ar age data, Geology, 33, 745–748.

Jourdan, F., G. Fe´raud, H. Bertrand, M. K. Watkeys, and P. R. Renne (2007a), Distinct brief major events in the Karoo large igneous province clarified by new 40Ar/39Ar ages on the Lesotho basalts, Lithos, 98, 195–209.

Jourdan, F., Féraud, G., Bertrand, H., Watkeys, M.K. (2007b). From flood basalts to the inception of oceanization: example from the 40Ar/39Ar high-resolution picture of the Karoo large igneous province. Geochemistry, Geophysics, Geosystems 8, 989–1006.

Lanci, L., Tohver, E., Wilson, A., Flint, S. (2013). Upper Permian magnetic stratigraphy of the lower Beaufort Group, Karoo Basin. Earth and Planetary Science Letters 375, 123–134.

Le Gall, B., G. Tshoso, F. Jourdan, G. Fe´raud, H. Bertrand, J. J. Tiercelin, A. B. Kampunzu, M. P. Modisi, M. Dyment, and J. Maia (2002), 40Ar/39Ar geochronology and structural data from the giant Okavango and related mafic dike swarms, Karoo igneous province, Botswana, Earth Planet. Sci. Lett., 202, 595–606.

Lindeque, A., De Wit, M.J., Ryberg, T., Weber, M., Chevallier, L. (2011). Deep crustal profile across the southern Karoo basin and Beattie magnetic anomaly, South Africa: an integrated interpretation with tectonic implications. South African Journal of Geology 114, 265-292.

Paton, D.A., Macdonald, D.I.M., Underhill, J.R. (2006). Applicability of thin or thick skinned structural models in a region of multiple inversion episodes; southern Africa. Journal of Structural Geology 28, 1933–1947.

Riley, T.R., Millar, I.L., Watkeys, M.K., Curtis, M.L., Leat, P.T., Klausen, M.B., Fanning, C.M. (2004). U–Pb zircon (SHRIMP) ages for the Lebombo rhyolites, South Africa: refining the duration of Karoo volcanism. J. Geol. Soc. (Lond.) 161, 547–550.

Riley, T. R. Curtis, M.L., Leat, P.T. Watkeys, M.K., Duncan, R.A., Millar, I.L., Owens, W.H. (2006). Overlap of Karoo and Ferrar Magma Types in KwaZulu-Natal, South Africa. J. of Petrography 47(3), 541–566.

Schofield, N., Stevenson, C., Reston, T. (2010). Magma fingers and host rock fluidization in the emplacement of sills. Geology 38, 63-66.

Storey, B.C., Kyle, P.R. (1997). An active mantle mechanism for Gondwana breakup. S. Afr. J. Geol. 100, 283–290.

Svensen, H., Sverre, P., Chevallier, L., Malthe-Sørenssen, A., Corfu, F., Jamtveit, B. (2007). Hydrothermal venting of greenhouse gases triggering Early Jurassic global warming. Earth Planet. Sci. Lett. 256, 554–566.

Svensen, H., Corfu, F., Polteau, S., Hammer, O., Planke, S. (2012). Rapid magma emplacement in the Karoo large igneous province. Earth Planet. Sci. Lett. 325-326, 1-9.

Tankard, A., Welsink, H., Aukes, P., Newton, R., Stettler, E. (2009). Tectonic evolution of the Cape and Karoo basins of South Africa. Marine and Petroleum Geology 26, 1379-1412.

White, R.S. (1997). Mantle plume origin for the Karoo and Ventersdorp flood basalts, South Africa. S. Afr. J. Geol. 100, 271–282.

White, R.S., McKenzie, D. (1989). Magmatism at rift zones: the generation of volcanic continental margins and flood basalts. J. Geophys. Res. 94, 7685–7729.

Chapter 3: Data and Methods

3.1 Vertical drill holes

Since the late 1950's gold exploration companies have targeted the larger extent of the Witwatersrand basin (Fig. 3.1.) in search of potential minable reserves outside of the more established gold fields. Holes were usually drilled up to the first appearance of the Kimberley reef at depths between 1 km and 2.5 km and spaced several kilometres apart (Fig. 3.2). More closely-spaced and detailed drill work were limited to areas with higher grade, such as in the Welkom gold field and Evander basin. All drilling data was captured on log sheets and handed to the Council for Geoscience (CGS) for safe keeping to be shared with future prospecting companies. This data, containing detailed descriptions of intersected lithologies and structures, was incorporated into this study and converted into electronic copies to assess the general occurrence of mafic intrusions in the basement rocks.

Similarly, Sasol Mining performed extensive diamond drilling programs across the Free State, Sasolburg-Vereeniging and Highveld coal fields (Fig. 3.1) over several decades in order to expand its mineable reserves and maintain a constant feedstock to its coal-to-liquid operations. Drill holes typically extend through the entire Karoo Supergroup sequence and stop once the underlying basement strata is intersected (Fig. 3.2). Drill

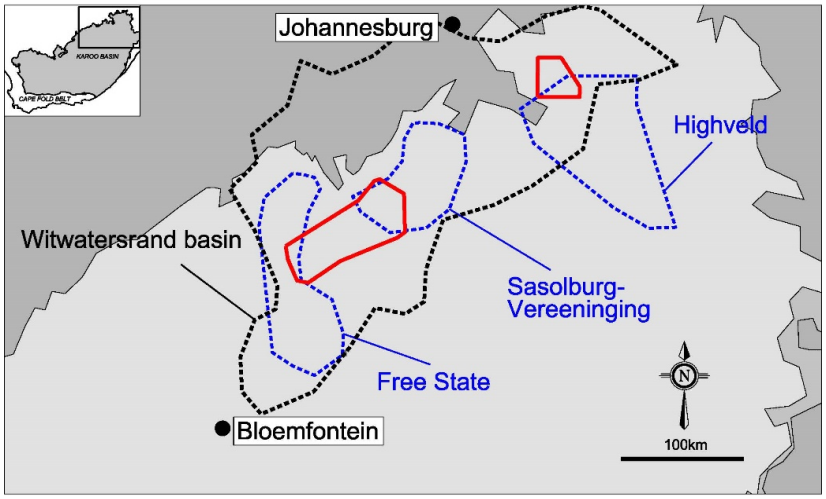

Figure 3.1: *Map of the northern Karoo basin showing the outlines of the coal fields in blue and the underling extent of the Witwatersrand basin in black in relation to the studied areas in red.*

hole densities of at least 1:25 ha or a spacing of 200-300 m are maintained in prospecting blocks which is later increased to 1:15 ha or a spacing of 100-200 m during mining operations. However, since the studied areas looks somewhat beyond the limits of prospecting and mining blocks the overall drilling density drops to 1:34 ha and 1:83 ha in the Highveld (Fig. 3.1, 3.3a) and the wider Free State and Sasolburg-Vereeniging (Fig. 3.1, 3.3b) areas respectively. Drill core data such as lithologies, thicknesses and properties were recorded by different geologists and stored in a company database for later use. This data proved crucial in identifying distinct sill complexes and modelling their three-dimensional extents in relation to the basement contact and surface topography.

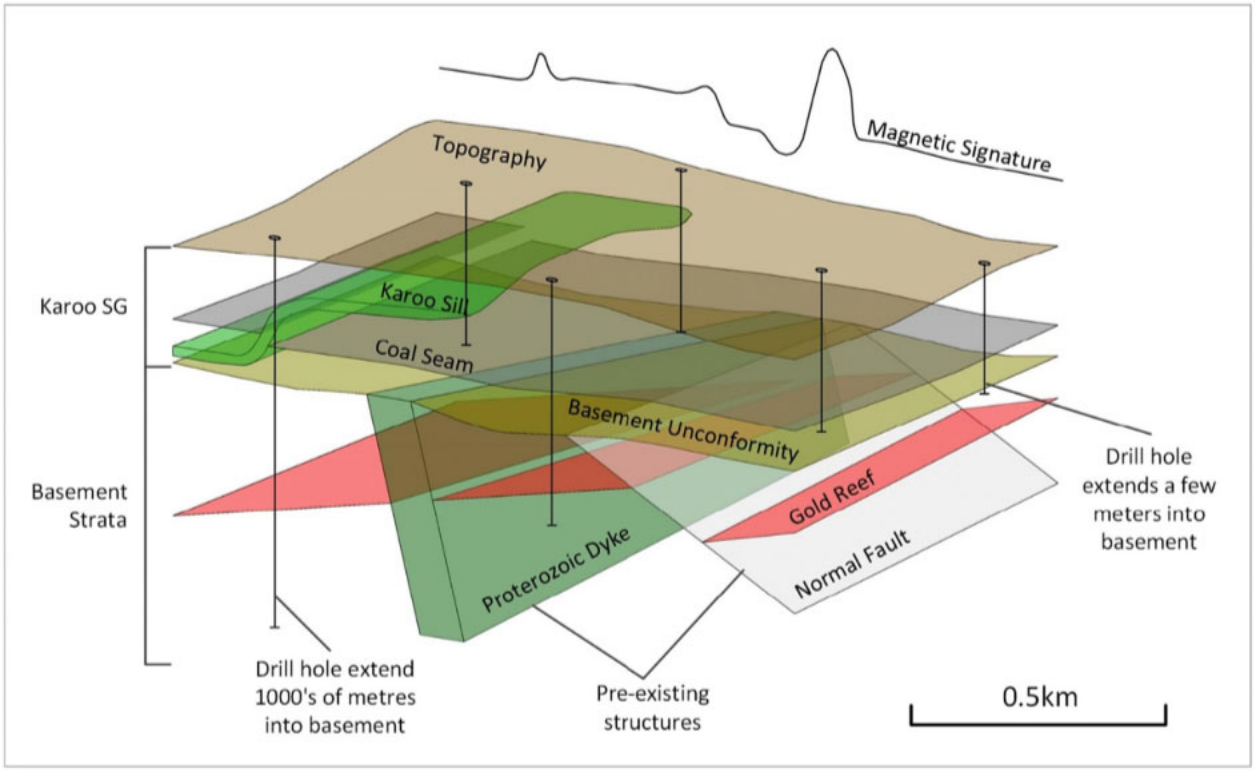

Figure 3.2: *Schematic diagram that illustrates the combination of geological data that is typically available in the northern Karoo basin from exploration drilling. Most of the drill holes intersect the Karoo Supergroup and stop a few metres into the basement strata whereas some extend 1000's of metres beyond that.*

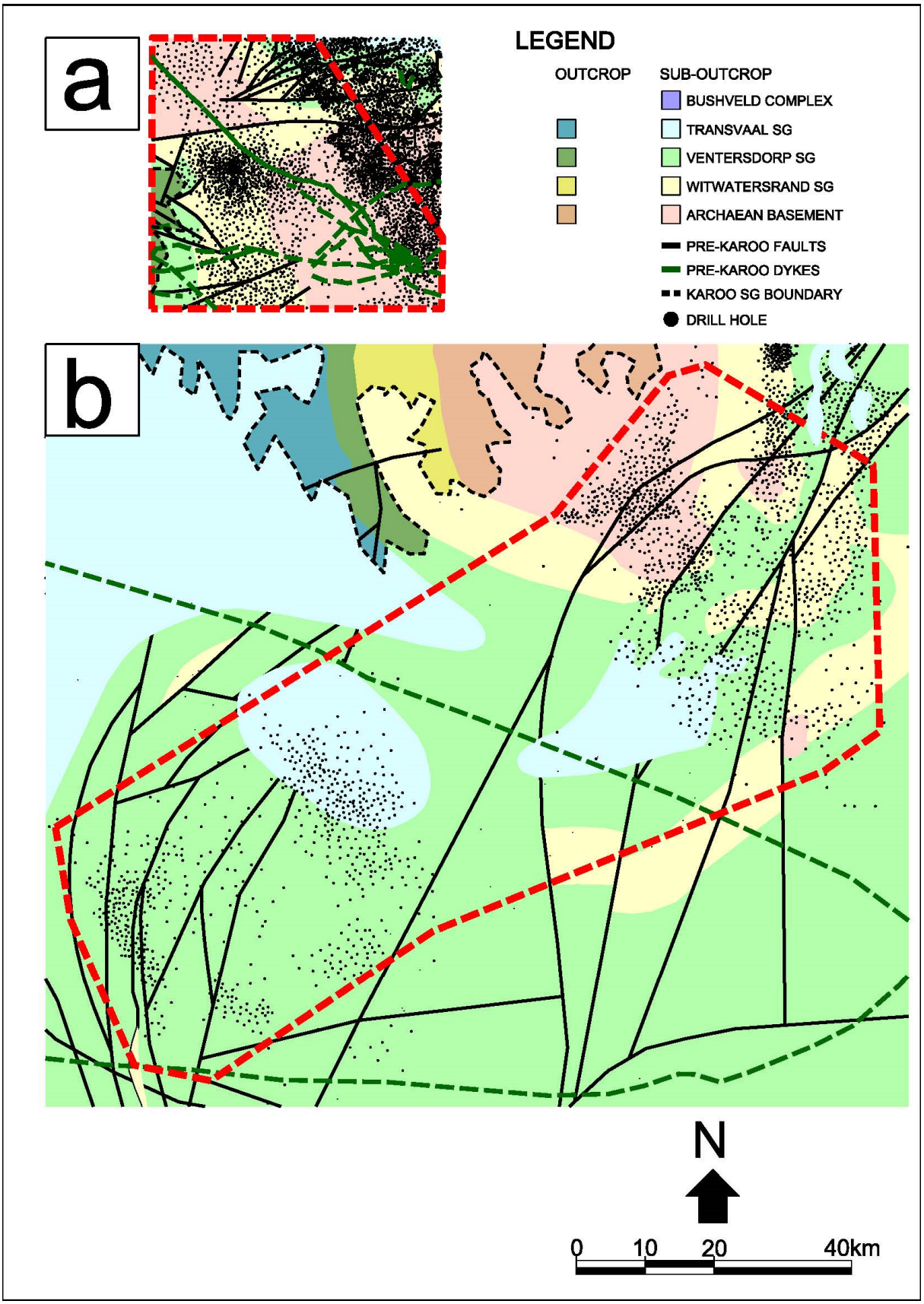

Figure 3.2: *A geological map presenting the spatial distribution of over 7000 drill holes from both gold and coal exploration in the (a) Highveld and (b) Free State areas. Although the overall drill hole density in the Free State region is low (1:83 ha), local densities can be as high as 1:25 ha.*

Other historic data includes several closely-spaced and 200-250 m deep percussion drill holes used to assess the controls of sills on groundwater aquifers in the Victoria West area (e.g. Chevallier et al., 2001). Also, oil exploration by Soekor (Sou th African Oil Exploration Corporation) in the 1960's to late 1970's across the entire Karoo basin provide a detailed account of lithologies and structures encountered in the Karoo Supergroup and the underlying basement rocks. Although spaced hundreds of kilometres apart, they remain the only source of information about deep-level lithologies and sills. The log sheets and coordinates of aforementioned drill holes were obtained from the CGS and converted into digital format for use in the study. The drilling coordinates and logs are made available in Appendix B.

3.2 Geophysical data

Mafic intrusions in the Karoo Supergroup and underlying basement in particular, were further constrained with regional (1 km line spacing) and local high resolution (~200m line spacing) aeromagnetic images obtained from the CGS and Sasol Mining. The lower resolution regional magnetic images were used in conjunction with deeper drill hole intersections to identify prominent signatures and to delineate different basement lithology types and structures (Fig. 3.1). Conversely, high resolution magnetic data assisted with the delineation of shallow-level sill outlines obscured beneath weathered material.

Additionally, published Soekor seismic data from the literature (see Appendix B) was also used in conjunction with drill hole data to visualize the deeper-level occurrence of sills beneath the dolerite line in the southern Karoo basin.

3.3 Underground mining data

Maps in the literature (e.g. Anhaeusser and Maske, 1986) and published underground reports of drilled and exposed geological structures by mining companies, such as Sibanye Gold (Beatrix – Fig 3.3 and Burnstone mines) and Pan African Resources (Evander Gold mine) provided additional constraints on the timing and occurrence of basement structures. Underground visits to regional normal faults in the Evander basin also allowed for closer evaluation of the wider fault zone and associated features in the hanging- and footwall rocks.

3.4 Three-dimensional modelling

All spatial data, particularly drill holes and outcrop positions, are imported into 3D modelling software in order to better visualize the different sill geometries across the Karoo basin. Drill hole sections are firstly generated in Datamine Strat3D, a software tool designed for stratified ore deposits, to verify the integrity of the data and to define the geological limits of the Karoo Supergroup and individual sills. Thereafter, modelling is done using a nearest neighbour interpolation method at a typical block size of 150 × 150 m to allow for higher resolution images and wireframes. Modelling occasionally requires manual intervention to limit wireframes within areas of higher certainty or increased drill density and to eliminate the occurrence of isolated and eroded sill segments that does not form part of the main sill body.

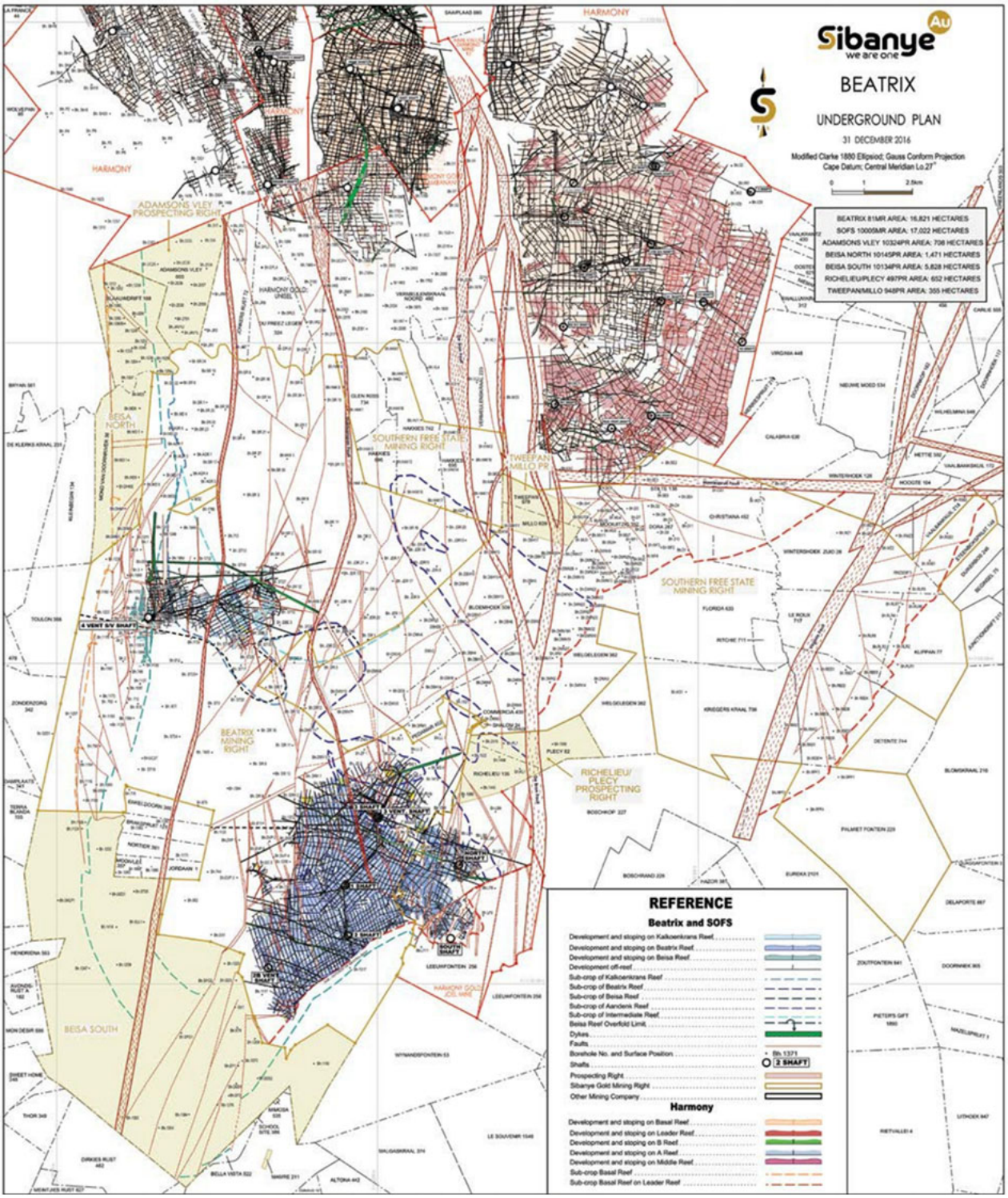

Figure 3.3: *Published underground map of Beatrix mine from Sibanye's annual report showing predominantly north-south trending normal faults.*

REFERENCES

Anhaeusser, C.R.; Maske, S. (eds.). (1986). Mineral deposits of Southern Africa, vol. 1. Geological Society of South Africa, Johannesburg.

Chevallier, L., Goedhart, M., Woodford, A.C. (2001). The Influences of Dolerite Sill and Ring Complexes on the Occurrence of Groundwater in Karoo Fractured Aquifers: A Morpho-Tectonic Approach. Water Resource Commission Reports. WRC Report No. 937/1/01: 165.

Scheiber-Enslin, S.E., Webb, S.J., Ebbing, J. (2014). Geophysically plumbing the main Karoo basin, South Africa. South African Journal of Geology 117, 2.

Chapter 4: Craton-hosted sill feeders

This chapter constitutes a presentation of the published research paper: ***The elusive feeders of the Karoo Large Igneous Province and their structural controls***[1] by Coetzee and Kisters.

This paper was first authored by André Coetzee with standard supervision entailing academic guidance and editorial support from Alex Kisters. The following aspects were carried out independently by André Coetzee: (1) drilling and underground data collection, (2) data consolidation, processing and interpretation, (3) three-dimensional modelling, (4) preparation and submission of the manuscript and (5) manuscript revision and successful resubmission.

[1]Coetzee, A., Kisters, A.F.M. (2018). The elusive feeders of the Karoo Large Igneous Province and their structural controls. *Tectonophysics, 747-748, 146-162.*

Tectonophysics 747–748 (2018) 146–162

Contents lists available at ScienceDirect

Tectonophysics

journal homepage: www.elsevier.com/locate/tecto

The elusive feeders of the Karoo Large Igneous Province and their structural controls

André Coetzee*[,1], Alexander F.M. Kisters

Department of Earth Sciences, University of Stellenbosch, Matieland, 7602 Stellenbosch, South Africa

ARTICLE INFO

Keywords:
Saucer-shaped sills
Karoo Basin
Dolerite intrusions
Pipe-like feeders
Pre-existing structures
Thermal incubation

ABSTRACT

Dolerite sills in the central parts of the Karoo large igneous province on the Kalahari Craton in South Africa record the emplacement of mafic magmas over 350,000 km^3, but the feeders to the voluminous magmatism have yet to be identified. Extensive exploration and mining data across a 7400 km^2 area and to a depth of 2.5 km in the northern Karoo Basin provide unprecedented access to the subsurface geometry of dolerite sills and their relationship to underlying basement strata. The data show saucer-shaped sills in the Karoo Supergroup with distinctly funnel-shaped geometries along their base that are seated within basement rocks. The funnel-shaped dolerite structures are interpreted to represent the feeders to the overlying regional-scale sill-saucer complexes. Four distinct saucer geometries can be identified (1) cone-shaped saucers that extend outwards from a single funnel-shaped point (Type A), (2) elongated saucers that dip towards multiple aligned funnel-shaped points (Type B), (3) the more commonly described elongated saucers with flat inner sills (Type C) and (4) elongated saucers with a combination of Type B and C geometries (Type D). Type A and C saucer geometries and point-like contacts are consistent with analogue models of saucers for respective pipe-like and linear feeders. However, the multiple pipe-like feeders associated with Type B and combination thereof with sheet-like feeders (Type D) represent saucer-feeder relationships thus far not modelled. Notably, the lower dolerite funnels are commonly rooted in older faults and/or dykes within the basement rocks. This spatial correlation emphasizes the sig-nificance of pre-existing basement structures in the Kalahari craton for the long-range transfer of the magmas through the crust. The distributed occurrence of numerous magma feeders across much of the craton is more consistent with thermal incubation of the sub-lithospheric mantle beneath Gondwana than the impact of a mantle plume.

1. Introduction

Large igneous provinces (LIP's) record the intrusion and extrusion of voluminous (> 10^6 km^3) mafic, mantle derived magmas over very large (> 10^6 km^2) areas and typically short (< 5 Ma) periods of time (e.g. Marsh, 1987; Duncan et al., 1997; Storey and Kyle, 1997; Jourdan et al., 2007; Saunders et al., 2007; Ernst, 2014; Ernst and Youbi, 2017). The sheer scale of LIP's not only raises questions about the broader geodynamic environments and processes of melt generation (Cox, 1989; White, 1997; Encarnacion et al., 1996; Duncan et al., 1997; Elliot and Fleming, 2000, 2004, 2008; Marsh, 2002; Ernst and Buchan, 2003; Jourdan et al., 2006; White et al., 2009; Svensen et al., 2012; Hastie et al., 2014), but also the nature and geometry of the plumbing systems that accommodated the transfer of the voluminous magmas from their mantle sources to the shallow-crustal emplacement sites (Magee et al., 2016; Cruden and Weinberg, 2018). Mafic dykes and sills of the Karoo LIP in southern Africa (Fig. 1) illustrate the internal architecture of at least the upper parts of this magma plumbing system (Chevallier and Woodford, 1999; Galerne et al., 2008, 2011; Schofield et al., 2010; Coetzee and Kisters, 2016, 2017). The dolerites form part of a much more extensive LIP including the Ferrar LIP in Antarctica (Elliot and Fleming, 2000, 2004, 2008) and document the emplacement of vast volumes of mafic magmas at ca. 183 Ma, shortly before the break-up of Gondwana (Cox, 1992; Encarnacion et al., 1996; Duncan et al., 1997; Svensen et al., 2012). Karoo dolerites describe two main geometries, including (1) dykes and up to 100 km wide and > 1500 km long dyke swarms, mainly along the northern and eastern margins of the Karoo Basin (Fig. 1) and (2) regional-scale sill complexes largely confined to the central parts of the Karoo Basin (Fig. 1). This paper deals with the emplacement and the nature of the feeders to sills in the central Karoo

* Corresponding author.
E-mail address: acoetzee90@gmail.com (A. Coetzee).
[1] Present address: Sasol Mining (Pty) Ltd, Sigma Colliery, PO Box 1, Sasolburg 1947, South Africa.

https://doi.org/10.1016/j.tecto.2018.09.007
Received 22 March 2018; Received in revised form 8 September 2018; Accepted 12 September 2018
Available online 14 September 2018

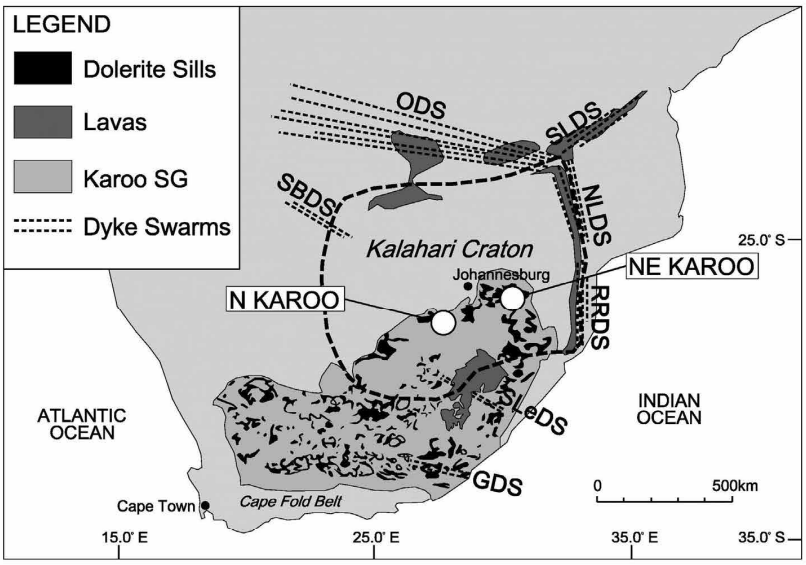

Fig. 1. Geological map of Southern-Africa showing the distribution of the main Karoo Basin in relation to the major Jurassic dyke swarms, i.e. Okavango (ODS), Save-Limpopo (SLDS), Northern Lebombo (NLDS), Rooi Rand (RRDS), Southern Botswana (SBDS), Southern Lesotho (SLeDS), and Gap (GDS) dyke swarms. The studied areas in the northern (N) and north-eastern (NE) Karoo Basin are also indicated.

and implications for the broader tectonic setting of the Karoo LIP.

Dolerite sills in the central Karoo intruded subhorizontal to gently folded strata of the Permo-Jurassic Karoo Supergroup (Fig. 1) (Chevallier and Woodford, 1999; Galerne et al., 2011; Schofield et al., 2010; Coetzee and Kisters, 2016). Sills have a combined volume of > 350,000 km^3 and are distributed over an area of > 500,000 km^2 (Svensen et al., 2012). Individual sills are up to 200 m thick and can laterally be traced for tens of kilometres. For the most part, sills form vertically stacked clusters or geometrically more complex saucer-shaped structures that step through the host-rock stratigraphy (Chevallier and Woodford, 1999). Petrographic, textural and geochemical similarities indicate (1) the emplacement of multiple magma pulses and (2) the extensive lateral transfer of magmas through interconnected sill complexes in large parts of the Karoo Basin. For dolerites of the Ferrar LIP, Leat (2008) and Airoldi et al. (2016) suggested the lateral transport of mafic magmas through interconnected sills over distances of several thousand kilometres. U-Pb zircon and baddeleyite geochronology on sills from throughout the basin indicate their intrusion between 183 ± 0.5 and 182.3 ± 0.6 Ma, possibly over a period as short as 0.47 Ma, which would translate into high time-integrated magma flux of up to 0.78 km^3/yr (Svensen et al., 2012). Despite this evidently dramatic magmatic event in the central Karoo, feeders to the sills have remained elusive. Dykes associated with the sill complexes are typically short, forming interconnected dyke networks mainly rooted in underlying sills. These dykes are unlikely to have acted as feeders to the sills and rather represent structures that accommodated the emplacement and inflation of the much larger sills, the cracked lid phenomenon described by Muirhead et al. (2014) and Coetzee and Kisters (2017).

Several regional-scale dyke swarms have been identified, mainly along the northern and eastern margins of the present-day Karoo Basin (Fig. 1). While the dyke swarms are obvious candidates for the transfer of magmas from the mantle to the shallow-crustal emplacement sites, the controls of the dyke swarms and connection to the source regions of the magmas are controversial (Uken and Watkeys, 1997; Elburg and Goldberg, 2000; Jourdan et al., 2004; Le Gall et al., 2005; Klausen, 2009; Hastie et al., 2011, 2014).

Field and geochronological studies indicate most dyke swarms intruded after the central Karoo sills, by as much as 3–5 Ma (Le Gall et al., 2002; Jourdan et al., 2004, 2005, 2007; Riley et al., 2006) rendering any direct feeding relationship between dyke swarms and sills in the broader Karoo Basin unlikely. This leaves the question as to the actual feeders of the voluminous dolerite sills in the central Karoo. In recent years, seismic reflectance data has provided unique insights into the formation and connectivity of sill networks which form the basis for sill-feeding-sill models (Thomson and Hutton, 2004; Cartwright and Hansen, 2006; Hansen and Cartwright, 2006; Magee et al., 2013; Schofield et al., 2017). However, the general inability of seismic data to image vertical structures represents a serious shortcoming that requires detailed sub-surface data on sill contacts to properly resolve. In contrast, the deeper parts of the Karoo Basin are, at least in parts, documented through coal mining and exploration of the Karoo Supergroup in addition to gold mining of the underlying Witwatersrand Supergroup. These mining activities provide a unique three-dimensional window into the architecture of basement rocks and occurrence and geometry of Karoo dolerites that potentially allow for the identification of the otherwise elusive dolerite feeders (Coetzee and Kisters, 2016, 2017). This study is based on two case histories where both mining and extensive borehole data can be utilized to reconstruct the geometries of regional-scale sills and the basement geology. Experiments and theoretical models for saucer-shaped sills relate their geometry to the shape of the underlying feeder (Malthe-Sørenssen et al., 2004; Galland et al., 2009; Kavanagh et al., 2006; Mathieu et al., 2008; Gressier et al., 2010; Galerne et al., 2011). Point- or pipe-like sources result in circular saucer geometries, whereas linear, dyke- or sheet-like magma feeders rather form elongated saucer geometries (Mathieu et al., 2008; Galland et al., 2009; Galerne et al., 2011). Magma flow patterns suggest sill propagation upwards and outwards away from the feeder (Thomson and Schofield, 2008). Dolerite dykes or sheets are most commonly invoked as the likely feeders of saucer-shaped sills (Chevallier and Woodford, 1999; Galerne et al., 2011), but actual dyke-saucer relationships have not been described from anywhere in the field. Ultimately the aim of this paper is to address the structure and controls of the elusive long-range magma transfer in the central Karoo Basin and whether sill complexes are fed by dyke swarms, hitherto unidentified, through long-range lateral magma transfer from some distant feeders, via isolated sheets or dykes, or from rather point-like sources. Furthermore, the overall distribution of sill feeders in the underlying basement rocks provides insights into the lateral extent of underplating magma and the transport of melt at lower crustal levels beneath southern Gondwana.

2. Karoo Basin

From the Late-Carboniferous to the mid-Jurassic, the main Karoo Basin represented an extensive retro-arc foreland basin north of an inferred volcanic arc and related fold-thrust belt situated in southern Gondwana. The strongly asymmetric basin structure is emphasized by significantly thicker (> 10 km) and folded Karoo strata in the south grading into much thinner (ca. 200 m) and largely undeformed Karoo rocks along the northern edge of the basin (Veevers et al., 1994; Visser, 1993; Catuneanu, 2004). The sedimentary rocks record a range of depositional environments from glaciomarine tillites and shales in the older Dwyka to shallow marine sand- and siltstones in the overlying Ecca Group. Fluvial sand- and siltstone sequences dominate the Beaufort and lower Stormberg Groups while eolian sandstones characterise the upper Stormberg Group towards the top of the Karoo Supergroup (Smith et al., 1993; Catuneanu et al., 2005). Sedimentation ceased with the onset of Karoo magmatism and the eruption of the Drakensberg flood basalts in the mid Jurassic around 183 Ma (Cox, 1992; Duncan et al., 1997).

In its central parts, the Karoo Basin is underlain by Archaean to Neoproterozoic rocks of the Kalahari Craton (Fig. 1). The oldest basement rocks are Meso-Archaean (> 3.1 Ga) Tonalite-Trondhjemite-Granodiorite (TTG) gneisses and supracrustal greenstone belts. The late-Archaean (ca. 3.08 Ga) volcanosedimentary strata of the Dominion Group is only developed west of the Vredefort dome and, for the most part, the TTG-greenstone basement is unconformably overlain by the thick metasedimentary Witwatersrand Supergroup (2.98–2.7 Ga) and the largely mafic, ca. 2.7 Ga Ventersdorp Supergroup. These Archaean successions are, in turn, unconformably overlain by the carbonate-dominated and siliciclastic 2.64–2.1 Ga Transvaal Supergroup. The supracrustal rocks above the TTG-greenstone basement document a complex structural history with at least three main phases of deformation related to (1) syn-Witwatersrand shortening: folding and thrusting of the strata, particularly along the margins of the basin, (2) post-Witwatersrand extension: normal and strike-slip faulting, and (3) post-Transvaal folding, tilting and mainly normal faulting (Myers et al., 1990). The first two stages show the development of reverse faults followed by grabens and half-grabens (Myers et al., 1990; Dankert and Hein, 2010). The post-Transvaal deformation is, in large parts, related to the Vredefort impact event (2.02 Ga) with impact-related folding and faulting recorded over > 150 km from the preserved centre of the impact crater (Wieland et al., 2005). The emplacement of the ca. 2050 Ma Bushveld Complex and associated dykes and sills in the north-eastern part of the Kalahari craton preceded the impact event by some 27 Ma (Kamo et al., 1996). Other mafic sills and dykes were emplaced during the Ventersdorp (2.7 Ga), Transvaal (Hekpoort Formation - 2.22 Ga) and Waterberg (1.88–1.9 Ga) eras.

Dolerite sills of the central Karoo Basin typically have distinct ring-like or saucer-shaped geometries defined by a central, flat inner sill with a circumferential inclined sheet that connects to a flat outer sill at a slightly higher stratigraphic level (Chevallier and Woodford, 1999; Galerne et al., 2011; Schofield et al., 2010; Coetzee and Kisters, 2016). Saucer-shaped sills show lateral extents of several tens of kilometres and typically occur in complex intrusive clusters at several levels in the sedimentary strata (Chevallier and Woodford, 1999) (Fig. 1). Sill complexes represent a significant component of lateral magma transfer within the Karoo Basin, but their deep-seated feeders have hitherto not been identified. In the following sections, we look closely at the relationship between saucer-shaped sills and the immediate underlying basement geology in the far north-eastern and northern parts of the Karoo Basin (Figs. 1, 2a, b).

3. North-eastern Karoo Basin

The towns of Secunda, Standerton and Balfour bound an area of 1400 km^2 in the north-eastern parts of the Karoo Basin (Fig. 2b). Coal mining and exploration have established the geology of the area through surface mapping and over 4000 boreholes with a borehole density of 1:34 ha. The boreholes are between 180 and 250 m deep and intersect the Karoo stratigraphy, intrusive Karoo dolerites and typically extend for short distances into underlying basement rocks. Additional subsurface information comes from several hundred boreholes drilled to depths of 1000–2500 m during gold exploration of the underlying Witwatersrand Supergroup (Fig. 3). Here we use drill hole and underground mapping data from both collieries in the Karoo Supergroup and gold mines of the Evander and South Rand Basins of the Witwatersrand Supergroup in addition to low- and high-resolution aeromagnetic data to construct and interpret the geometry of Karoo dolerites and the complex basement geology.

3.1. Regional geology

The geology of the Secunda area is dominated by the lower parts of the Karoo Supergroup, namely the Dwyka and Ecca Groups that unconformably overlie basement rocks. The basement is made up of Meso-Archaean TTG gneisses of the Devon and Cedarmont domes. In the Evander and South Rand Basins, these basement highs are overlain by rocks of the Witwatersrand and Ventersdorp Supergroups (Fig. 2b). The sub-outcropping Witwatersrand and Ventersdorp Supergroups represent planar, north-dipping strata covered to the north by the younger Transvaal Supergroup and mafic igneous rocks that form the southern limb of the Bushveld Complex. The basement strata are displaced by numerous steeply (70°) south-dipping normal faults with downthrows of 100–700 m. The northeast and southeast striking faults are subsidiary faults to the east-trending, over 200 km long, first-order Sugarbush fault (Fig. 2b). The cores of the normal faults are only 0.5 to 1.5 m wide and typically intensely quartz veined (Fig. 4a), but the damage zones around the fault cores is considerably wider at up to 100 m and commonly associated with the formation of secondary faults and fault splays, quartz veins and near-vertical joint sets. The central steep dipping (> 75°) Sugarbush fault is associated with a maximum throw of 4600 m of normal displacement in addition to significant left-lateral movement (Myers et al., 1990). The core of the Sugarbush fault is an up to 5 m wide mylonite and protomylonite, surrounded by pervasively foliated and, in places tightly folded wall rocks (Fig. 4b) containing quartz vein arrays as well as secondary faults (Myers et al., 1990). This process or damage zone may extend for several kilometres away from the fault core, probably forming part of a wide anastomosing pattern of faults that constitute the Sugarbush Fault Zone. In addition to faults, several dark-green, chloritized dolerite dykes, tens of metres wide, are intrusive into basement strata (Fig. 2b). Where intersected, the dykes are capped by a several metre deep, weathered horizon along the basement unconformity indicating a pre-Karoo emplacement for these dykes (Fig. 4c, d). The majority of dykes trend northwest-southeast and east-west cross-cutting most of the basement stratigraphy. These dyke orientations correspond to the prevailing trends associated with the emplacement of the Bushveld Complex (2.05 Ga) and post-Waterberg Group magmatism (1.88–1.9 Ga) (Uken and Watkeys, 1997). In contrast, north-easterly dyke trends are most likely related to the Olifants River dyke swarm (> 851 Ma) (Jourdan et al., 2006).

3.2. Karoo dolerites

The general absence of demonstrably Karoo-aged dolerite intrusions in the basement strata contrasts with the extensive networks of intrusions found throughout the overlying Karoo sediments. Dolerite intrusions in the Karoo Supergroup are represented as several regional-scale sills, tens of kilometres in diameter, that are closely associated with dense arrays of thin (< 5 m), localised dykes. In this locality, we focus on two sill complexes, namely sill #4 and sill #8 (Fig. 2c). These grey-green coloured sills are distinguished by their unique aphanitic textures. Sill #4 has a fine grained, ophitic texture with plagioclase and

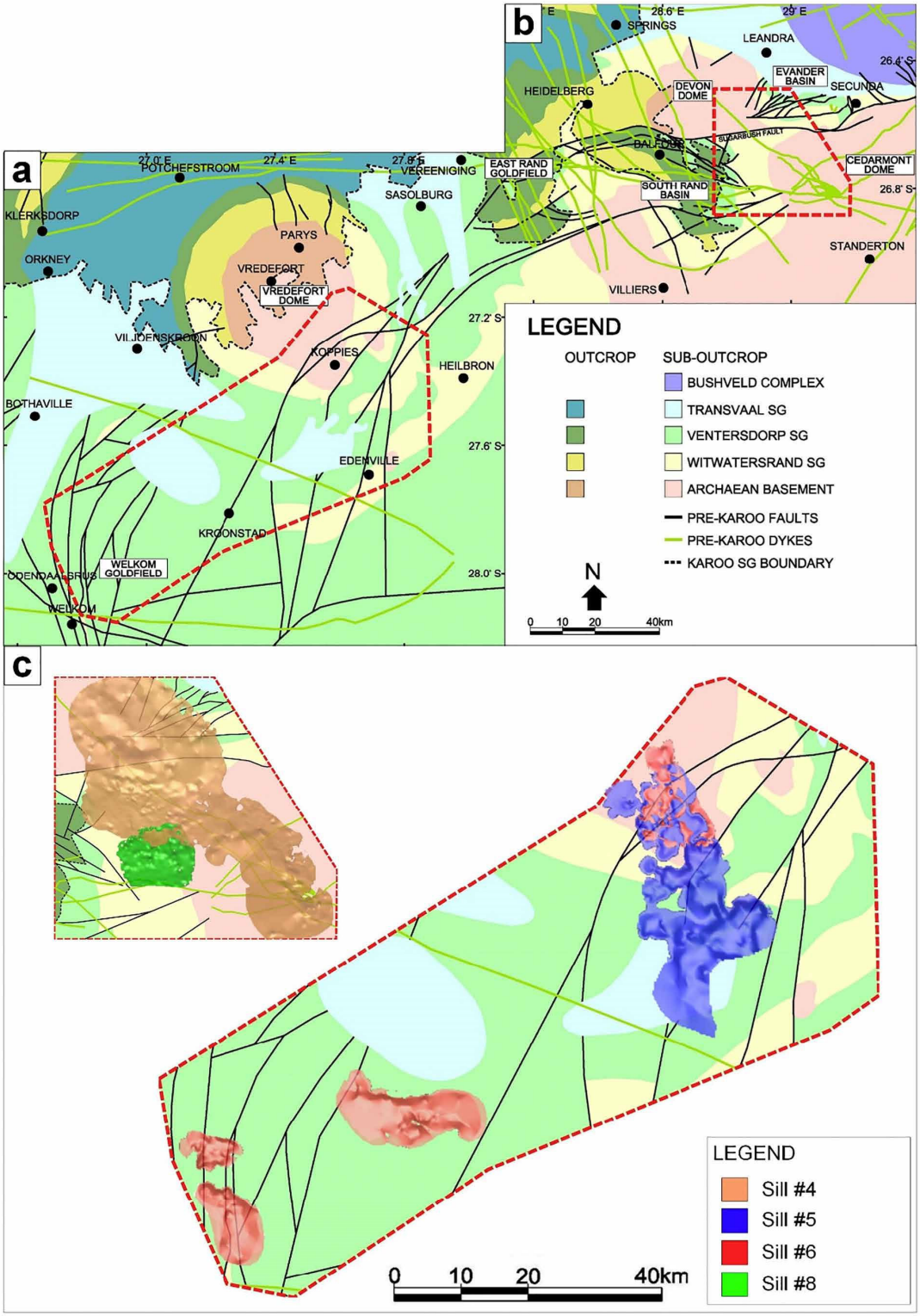

Fig. 2. a and b) Geological maps of the known regional basement geology underlying the Karoo Supergroup and the spatial layout of the different sill complexes (c) that occur within each studied area (red outlines).

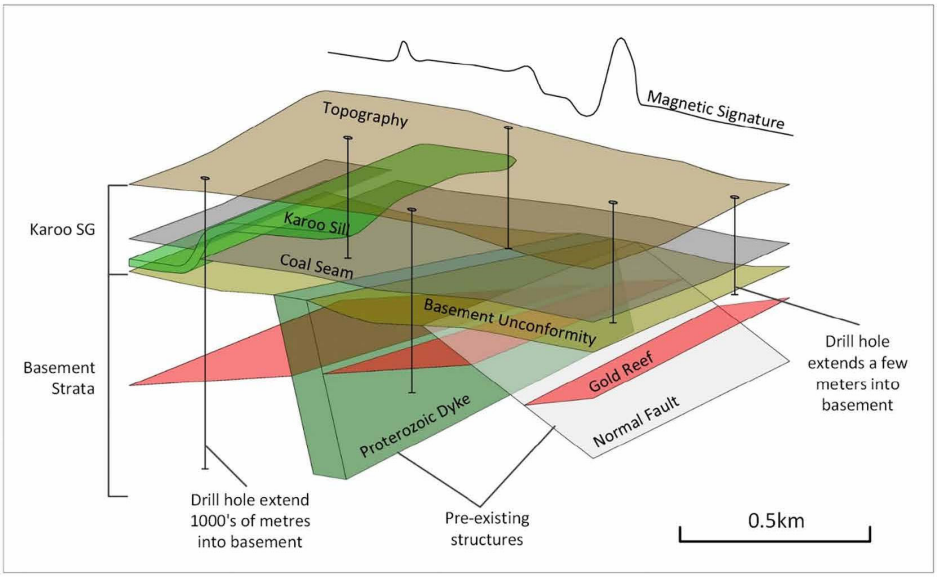

Fig. 3. A schematic diagram that illustrates the combination of geological data that is typically available at the different study sites. Most of the drill holes intersect the Karoo Supergroup and stop a few metres into the basement strata whereas some extend 1000's of metres beyond that. Furthermore, underground mine development along coal seams and gold reefs provide further structural information on the respective Karoo and Witwatersrand Supergroups. Aeromagnetic surveys identify prominent dyke occurrences in both the Karoo sediments and underlying basement rocks.

clinopyroxene as the main rock-forming minerals and minor amounts of quartz and oxide minerals (Fig. 4d). Sill #8 has a porphyritic texture defined by needle-like plagioclase crystals in a fine-grained mass of clinopyroxene, plagioclase, olivine and oxide minerals (Fig. 4e) (Bussio, 2012). Serpentine, chlorite and calcite are secondary alteration minerals found in both sills. Sills #4 and #8 have fine textured, up to 1.5 m wide chilled margins against the wall rocks, coarsening towards their central parts.

3.2.1. Sill #4 – geometry and basement contacts

Sill #4 represents a 30–45 m thick intrusive complex elongated along a north-western axis. The sill complex consist of a circular northern saucer (S4-1) 25 km wide in addition to a north-westerly elongated southern saucer (S4-2) with dimensions 25 × 10 km (see Table 1, Fig. 5a). The inner sills typically occur along the basement and Dwyka-Ecca Group contacts at elevations between 1360 and 1470 m (A.M.S.L.) (Fig. 5b, c). Transgressive inclined sheets cut through over 200 m of stratigraphy and connect to the layer parallel flat outer sill at 1540–1610 m. The inclined sheet is primarily a single, shallow-dipping sheet (20–30°), but often comprises a series of 20–40 m upward steps that involve steeper segments alternating with layer concordant segments (Fig. 5b, c). The outer sill protrudes laterally away from the inclined sheet at a higher stratigraphic level and is often eroded away at topographic lows (Fig. 5a, b).

The circular saucer (S4-1) overlies rocks of the Archaean basement of the Evander and South Rand Basins containing the gently undulating, easterly to south-easterly striking Sugarbush fault and a prominent, older northwest trending dolerite dyke (Fig. 5a, b). Notably, the inner sill has a distinct funnel-like geometry towards its lower parts, 0.8 × 0.8 km in extent and 40 m thick, where the inner sill cuts up to 25 m into the basement strata near the intersection of the Sugarbush fault and the north-west trending dolerite dyke (Fig. 5b).

The elongated saucer (S4-2) overlies multiple dolerite dykes, such as two anastomosing branches of the north-west striking dyke in addition to east-west and north-east trending dykes (Fig. 5a). The long axis of the northwest-trending saucer is parallel to the north-westerly strikes of the underlying, older dykes (Fig. 5b, c). The elongated saucer reaches 10 m into the basement strata at two distinct funnel-shaped points, 0.5 × 0.5 km in extent and 30 m thick, along the length of these older dolerite dykes (Fig. 5c).

3.2.2. Sill #8 – geometry and basement contacts

Sill #8 is a laterally continuous 20–25 m thick sheet that comprises three small depressions or saucer-shaped structures at its centre (Fig. 6a, b). The eastern (S8-1), southern (S8-2) and western (S8-3) saucers have elongated geometries with respective north-westerly, northerly and north-easterly strikes. Inner sills vary in size from 0.6 × 1 km to 1.6 × 5 km (see Table 1) and undulate within the Dwyka and Ecca Groups from 1320 to 1420 m. The inclined sheets climb at gentle angles (10–20°) through 100–180 m of strata until connecting to the outer sill at 1500 m (Fig. 6c).

Known basement structures are largely absent beneath the three saucers except for two older east-west trending dolerite dykes (Fig. 6a). Each saucer dips individually towards a single localised area 0.6 × 0.6 km, 25 m thick where the inner sill occurs 10 m inside the meta-sedimentary rocks of the Witwatersrand Supergroup (Fig. 6c).

4. Northern Karoo Basin

The study area of 6000 km^2 along the northern rim of the Karoo Basin stretches from Koppies in the north to Welkom in the south (Fig. 2a). Here, geological data include 3300 drill holes (density of 1:83 ha) through the Karoo Supergroup with several extending up to 2500 m into the basement layers. Regional maps of the Vredefort dome and adjacent basement outcrops allow for interpretations of the sub-outcropping basement rocks further south. Additional information comes from historic gold exploration data, seismic and aeromagnetic surveys. This data combined with underground maps from the nearby East Rand and Welkom goldfields provide additional constraints on regional-scale structural features.

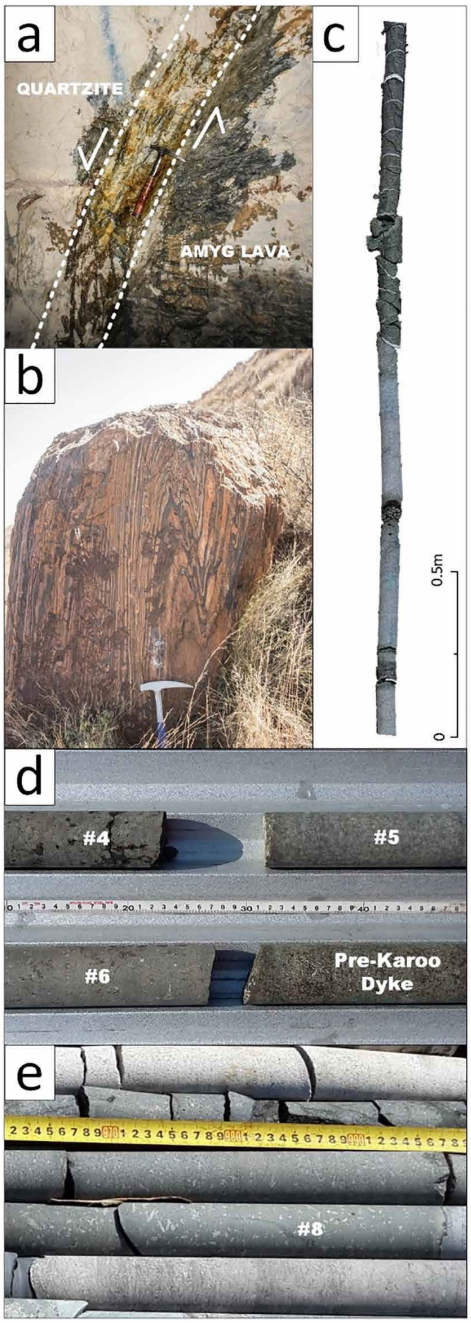

Fig. 4. (a) An underground section of a regional normal fault in the basement strata of the Evander Basin. The white surfaces represent cementation applied to protect exposed wall rocks from deterioration. (b) Ductile footwall deformation along at an outcrop exposure of the Sugarbush fault taken outside Balfour, Mpumalanga province. (c) A typical drill hole intersection of a Proterozoic dolerite dyke with weathered upper contact at the basement unconformity. (d) Drill hole intersections of sills #4, #5 and #6 in addition to a Proterozoic dolerite dyke. (e) Drill hole intersections of sill #8.

4.1. Regional geology

The Karoo Supergroup comprises the Dwyka and Ecca groups with the exception of the far south, where lower Beaufort Group sediments appear. The stratigraphy is similar to that of the north-eastern Karoo Basin, but rock types and depositional setting are significantly different in that the basement unconformity is marked by a pronounced palaeotopography that formed in pre-Karoo times during erosion of the complexly deformed strata around the Vredefort dome (Fig. 2a). The palaeotopography imparts a gentle dip to the onlapping Karoo strata. Dips vary from sub-horizontal in depressions and up to 15° along the flanks of basement highs.

The Vredefort dome partially exposes a 45 km wide core of TTG gneisses bounded by concentric, steeply dipping to overturned supracrustal rocks of the Archaean and Proterozoic Witwatersrand, Ventersdorp and Transvaal Supergroups, the so-called Vredefort collar rocks (Fig. 2a). The Vredefort impact at 2023 Ma resulted in the folding and thrusting of strata in an up to 300 km wide circular zone surrounding the impact site (Kamo et al., 1996). Basement strata have also been displaced by a series of grabens and half-grabens consisting of northerly to northeasterly trending normal faults with strike lengths > 100 km and associated displacements between 100 m and > 1000 m. Mafic intrusions in the basement rocks are limited to a few regional dolerite dykes found to the south and north of the study area showing westerly and northwesterly strikes. Based on the trends and cross-cutting relationships, these dykes are most likely related to the ca. 2050 Ma Bushveld magmatism (Uken and Watkeys, 1997).

4.2. Karoo dolerites

The three-dimensional data reveals up to three dolerite sill complexes in the Karoo Supergroup in this area. In contrast, no Karoo-aged intrusions can be distinguished in the underlying basement strata. Sills primarily consist of bedding concordant sheets that constitute more than half of the Karoo stratigraphy at any one area. We mapped the two main sill complexes, locally referred to as sills #5 and #6 where good regional coverage through borehole data and mining is available (Fig. 2a, c).

Both sills are dark grey in colour with fine grained aphanitic textures, sill #6 is distinct in that it contains star-like masses of plagioclase phenocrysts in addition to clinopyroxene and oxides (Fig. 4d). Chilled margins at the wall-rock contacts are often associated with a dark colouration and very fine-grained texture.

4.2.1. Sill #5 – geometry and basement relationships

Sill #5 represents an intrusive structure with a variable thickness from 20 m up to 80 m. The sill comprises two elongated saucers (S5-1, S5-2), a triangular saucer (S5-3) and a further three circular saucers (S5-4–S5-6) laterally connected within the Karoo Supergroup (Table 1, Fig. 7a, b). The elongated saucers are represented by S5-1, a north trending structure 6 × 16 km, and S5-2, a 30 × 6 km saucer with an arched or curved geometry orientated in the north-eastern direction (Fig. 7c). Elongated saucers extend out- and upwards from their base in the Dwyka Group (1150–1280 m) through shallow dipping (20°) inclined sheets to the outer sills at > 1360 m (Fig. 7b, c).

The triangular saucer (S5-3) has overall dimensions of 13 × 13 × 13 km. The inner sill undulates within the Dwyka Group and describes three zones about 7 × 3 km (1200–1280 m) that diverge from a central point into north-eastern, western and south-eastern directions before linking onto a gently dipping (20–30°) inclined sheet and later outer sill seated at > 1350 m (Fig. 7c).

Conversely, the circular saucers (S5-4, S5-5 and S5-6) describe much smaller 4.5 km wide cone-like structures (Fig. 7c). Inner sills generally occur within the Dwyka and lower Ecca Groups between 1200 m and 1300 m. The bounding inclined sheets are shallow dipping at 20° and link to the flat outer sill at an elevation of > 1400 m

Table 1
Detailed geometries and basement relationships of saucers interpreted from drill hole data in the north-eastern and northern Karoo basin.

Saucer no	Saucer geometry			Basement relationships			
	Geometry	Dimensions (km)	Strike	Contact geometry	Dimensions (km)	Basement rock types	Basement structures
North-eastern Karoo basin							
S4-1	Circular	25 × 25		Funnel-like (×1)	0.8 × 0.8	Archaean gneiss, Witwatersrand quartzite	Sugarbush fault, dyke
S4-2	Elongated	25 × 10	NW	Funnel-like (×2)	0.5 × 0.5	Archaean gneiss	Dykes
S8-1	Elongated	> 5 × 1.6	NW	Funnel-like (×1)	0.6 × 0.6	Witwatersrand quartzite	None
S8-2	Elongated	> 1 × 0.6	N	Funnel-like (×1)	0.6 × 0.6	Witwatersrand quartzite	None
S8-3	Elongated, curved	> 2.4 × 0.6	NE	Funnel-like (×1)	0.6 × 0.6	Witwatersrand quartzite	None
Northern Karoo basin							
S5-1	Elongated	16 × 6	N	Funnel-like (×3)	0.5 × 0.5	Archaean gneiss	Normal faults
S5-2	Elongated, curved	30 × 6	NE	Flat area (×2)	2 × 1	Transvaal dolomite	None
S5-3	Triangular	13 × 13 × 13		Flat area (×1)	7 × 1.3	Proterozoic gneiss, quartzite, lava	Normal fault
S5-4	Circular, cone-shaped	5.5 × 5.5		Funnel-like (×1)	0.7 × 0.7	Archaean gneiss	None
S5-5	Circular, cone-shaped	4.5 × 4.5		Funnel-like (×1)	0.7 × 0.7	Witwatersrand quartzite	None
S5-6	Circular, cone-shaped	5 × 5		Funnel-like (×1)	0.7 × 0.7	Ventersdorp lava	None
S6-1	Circular, cone-shaped	5 × 5		Funnel-like (×1)	0.25 × 0.25	Archaean gneiss	None
S6-2	Circular, cone-shaped	5 × 5		Funnel-like (×1)	0.25 × 0.25	Archaean gneiss	None
S6-3	Circular	4.5 × 4.5		Funnel-like (×1)	0.25 × 0.25	Ventersdorp lava	None
S6-4	Elongated	7.3 × 4.5	NW	Flat area (×1)	4.5 × 1.5	Ventersdorp lava	None
S6-5	Elongated	25 × 6	E	Narrow flat area (×2); funnel-like (×1)	5 × 1.6; 2.5 × 0.7; 0.8 × 0.8	Ventersdorp lava	None
S6-6	Elongated	9.5 × 2.7	E	Funnel-like (×2)	0.5 × 0.5	Ventersdorp lava	Normal faults
S6-7	Elongated	6 × 2.3	E	Funnel-like (×2)	0.5 × 0.5	Ventersdorp lava	Normal faults
S6-8	Elongated	6 × 3	NW	Narrow flat area	4 × 0.5	Ventersdorp lava	Normal fault
S6-9	Elongated	10 × 5.5	N	Narrow flat area	7.1 × 2.7	Ventersdorp lava	Normal faults

(Fig. 7c).

Elongated saucer S5-1 directly overlies the Archaean gneisses of the Vredefort dome as well as a prominent north-east striking graben structure (Fig. 7b, c). The inner sill reaches 20 m into the basement rocks at three funnel-shaped points, 0.5 km in diameter and 50 m thick. Two of these points occur along the strike of the east dipping (< 60°) normal fault while the other directly overlies the west dipping (< 60°) normal fault bounding the central graben structure (Fig. 7b, c). Conversely, the inner sill (60 m thick) of saucer S5-2 extends 30–60 m into the dolomite rocks of the Transvaal Supergroup along a wide, flat-lying zone roughly 2 × 1 km (Fig. 7b, c). This area is largely devoid of any known sub-outcropping basement structures (Fig. 7b, c).

The triangular saucer (S5-3) cuts 5–10 m into the Archaean gneisses, Witwatersrand Supergroup quartzites and Ventersdorp Supergroup lavas across a narrow area of 7 × 1.3 km (Fig. 7b, c) where the sill reaches a thickness of 20 m. This area overlaps with a steep (> 70°) westerly dipping regional normal fault with a displacement of > 1000 m (Fig. 7c).

Cone-shaped saucers S5-4, S5-5 and S5-6 are 50 m thick at their base and seated 5 m inside a variety of basement rocks from Archaean gneisses in the north to rocks of the Witwatersrand and Ventersdorp Supergroups further south (Fig. 7). However, these saucers are not in contact with any known or prominent basement structures that can be discerned from the mining data (Fig. 7b, c).

4.2.2. Sill #6 – geometry and basement relationships

Sill #6 is typically 15–40 m thick and consists of nine individual structures, three circular (S6-1–S6-3) and six elongated saucers (S6-4–S6-9) spread across the entire study area (Figs. 2c, 8, 9, Table 1). The circular saucers are 4.5–5.5 km in diameter and have a distinctly axi-symmetric cone-like geometry that converges towards a small (0.25–2.0 km wide) inner sill seated along the basement contact at 1180–1260 m (Figs. 8b, c, 9b). The inclined sheets show dips of 20° at the inner sill connection with gradually gentler dips towards the top as the inclined sheets merge with the outer sill at 1380–1420 m (Figs. 8b, 9b).

The elongated saucers are typically 25–6 km long and 6–2.5 km wide with north-westerly, easterly and northerly strikes (Table 1, Fig. 9a). The inner sills undulate between the basement unconformity and the lower parts of the Ecca Group at 1100–1220 m and are surrounded by a gently dipping (< 20°) inclined sheet that transgresses the stratigraphy before linking onto the outer sill at 1300–1380 m (Fig. 9b, c).

Cone-shaped saucers cut 5–10 m into the Archaean gneisses and Ventersdorp lavas at individual funnel-like points that are 0.25 km in diameter (Figs. 8b, c, 9b) and 10–20 m in thickness. These saucers are without a connection to any known basement structures at the resolution of the borehole data (Figs. 8, 9).

Elongated saucers have basal thicknesses of 30–50 m and extend up to 10 m into the Ventersdorp lavas. These saucers show a variety of basement contact geometries (Fig. 9c). Saucers S6-4, S6-8 and S6-9 are seated within the basement rocks across large parts (> 4 × 0.5 km) that often coincide with older regional normal faults (Fig. 9c, d). Conversely, saucers S6-6 and S6-7 are each characterised by two funnel-shaped points along the length of their base with dimension 0.5 × 0.5 km. These localised basement contacts usually occur near older normal faults (Fig. 9b, c). Saucer S6-5 is unique in that it shows a combination of two laterally extensive basement contacts (5 × 1.6 and 2.5 × 0.7 km) in addition to one small point-like basement contact (0.8 × 0.8 km). All three basement contacts are without any link to known underlying structures (Fig. 9b).

5. Discussion

The three-dimensional data set presented here covers an area of altogether 7400 km^2 in the northern parts of the Karoo Basin. Mapping of dolerite saucers and the wall-rock and basement geology from mining and exploration data indicate a significant number of either

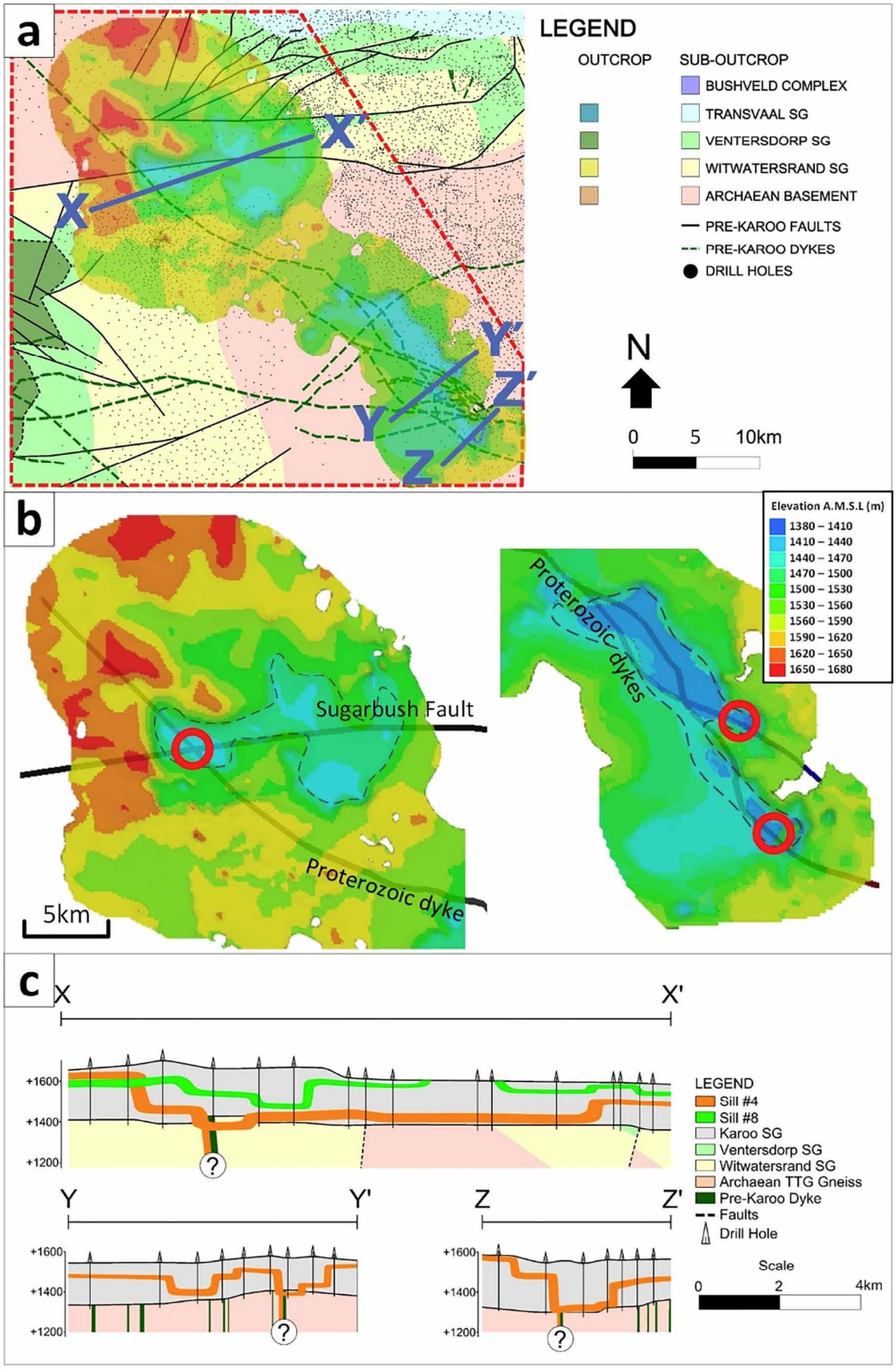

Fig. 5. (a) Map showing the spatial occurrence and relationship between saucers of sill #4 (S4-1, S4-2) and the underlying sub-outcropping basement strata and structures. (b) Elevation contour plots of the northern (S4-1) and southern saucers (S4-2) in relation to underlying Proterozoic dolerite dykes. The broken lines and red circles indicate the respective inner sill boundaries and their positions inside the basement rocks. (c) Cross-sections along lines as shown in Panel a with a vertical exaggeration factor of 5. (For interpretation of the references to colour in this figure legend, the reader is referred to the web version of this article.)

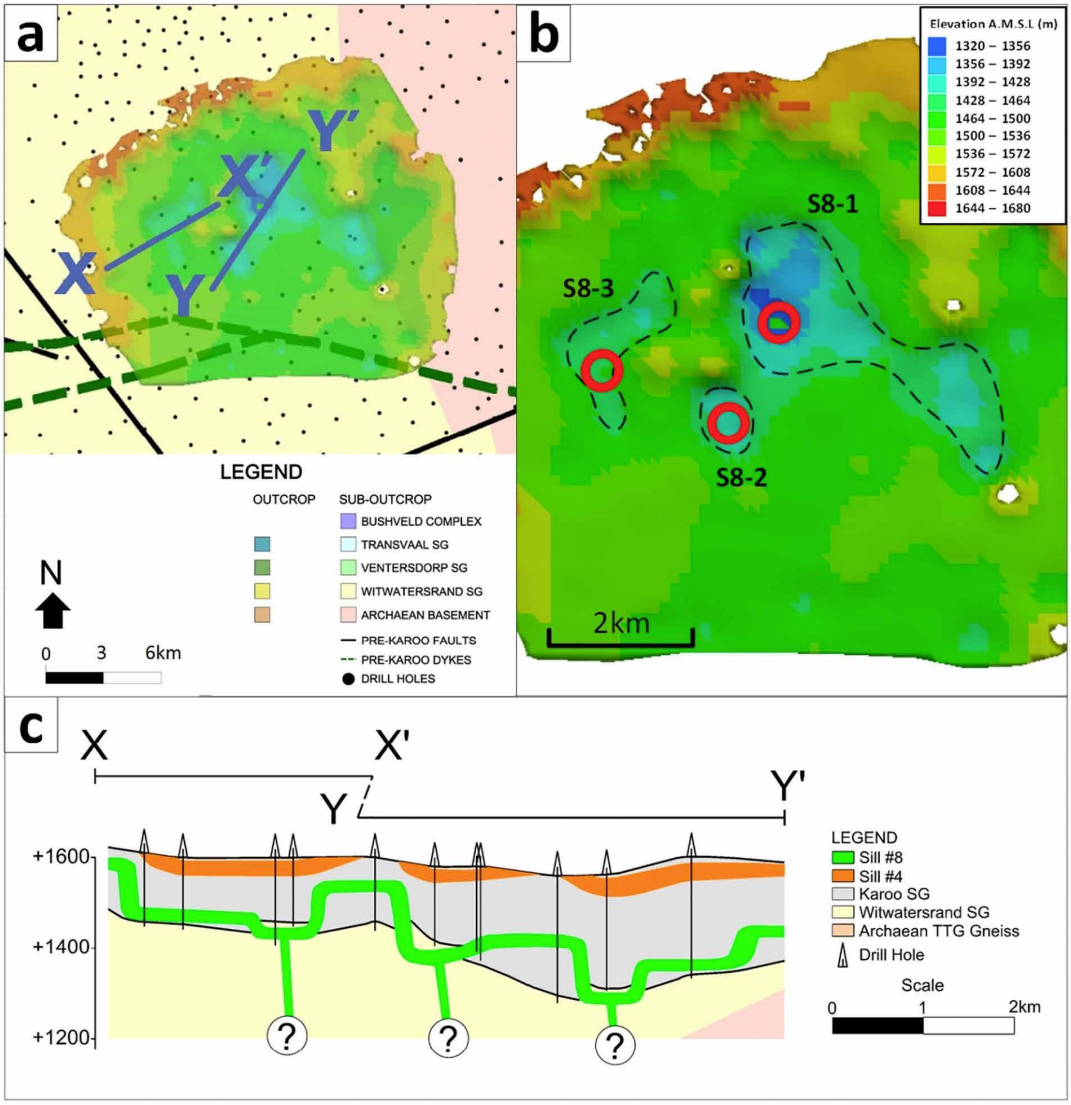

Fig. 6. (a) Map of sill #8 and its constituent saucers (S8-1, S8-2 and S8-3) in relation to the underlying basement geology. (b) Elevation contour plot of saucers S8-1–3 with their inner sill outlines and basement contacts. (c) Cross-section of sill #8 as shown in Panel a with a vertical exaggeration factor of 5.

cone-shaped or elongated saucer geometries within the Karoo Supergroup that dip towards and cut into basement rocks. Importantly, most of the contacts between Karoo dolerites and basement rocks are at or near pre-Karoo faults, particularly normal faults that form part of larger graben structures, and/or older pre-Karoo dykes.

5.1. Saucer-feeder relationships

Saucer-shaped sills are commonly interpreted to have formed though the injection of magma from an underlying feeder into the inner sill from where the magma spreads up- and outwards into the inclined sheet and outer sill. This has been shown in experimental models, but also field studies, for which the Karoo province forms one of the type localities (Chevallier and Woodford, 1999; Malthe-Sørenssen et al., 2004; Cartwright and Hansen, 2006; Kavanagh et al., 2006; Mathieu et al., 2008; Galland et al., 2009; Galerne et al., 2011; Magee et al., 2016). Analogue models, in particular, demonstrate a close spatial and geometric relationship between saucer geometry and the geometry of the underlying feeders (Mathieu et al., 2008; Galland et al., 2009; Galerne et al., 2011). Circular saucers or cones are characteristic of pipe-like feeders while elongated, more oval-shaped saucers are linked to sheet-like feeders (Mathieu et al., 2008; Galland et al., 2009; Galerne et al., 2011; Coetzee and Kisters, 2016). Magma from a linear or pipe-like basement feeder is only expected to spread laterally to form a sill along a lithological contact with a prominent rigidity contrast where further vertical fracture propagation is inhibited and magma pressures rather favour the propagation of horizontal, bedding parallel fractures. Basement-cover unconformities are common sites for this dyke-sill transition, exemplified by the location of many prominent sills along the basement-Karoo unconformity or the contact between Dwyka and Ecca groups in the Karoo Basin (Chevallier and Woodford, 1999; Coetzee and Kisters, 2016). Therefore, it is commonly recognised in the data that the occurrence of saucers several metres inside the basement rocks are most likely controlled by the position and geometry of an

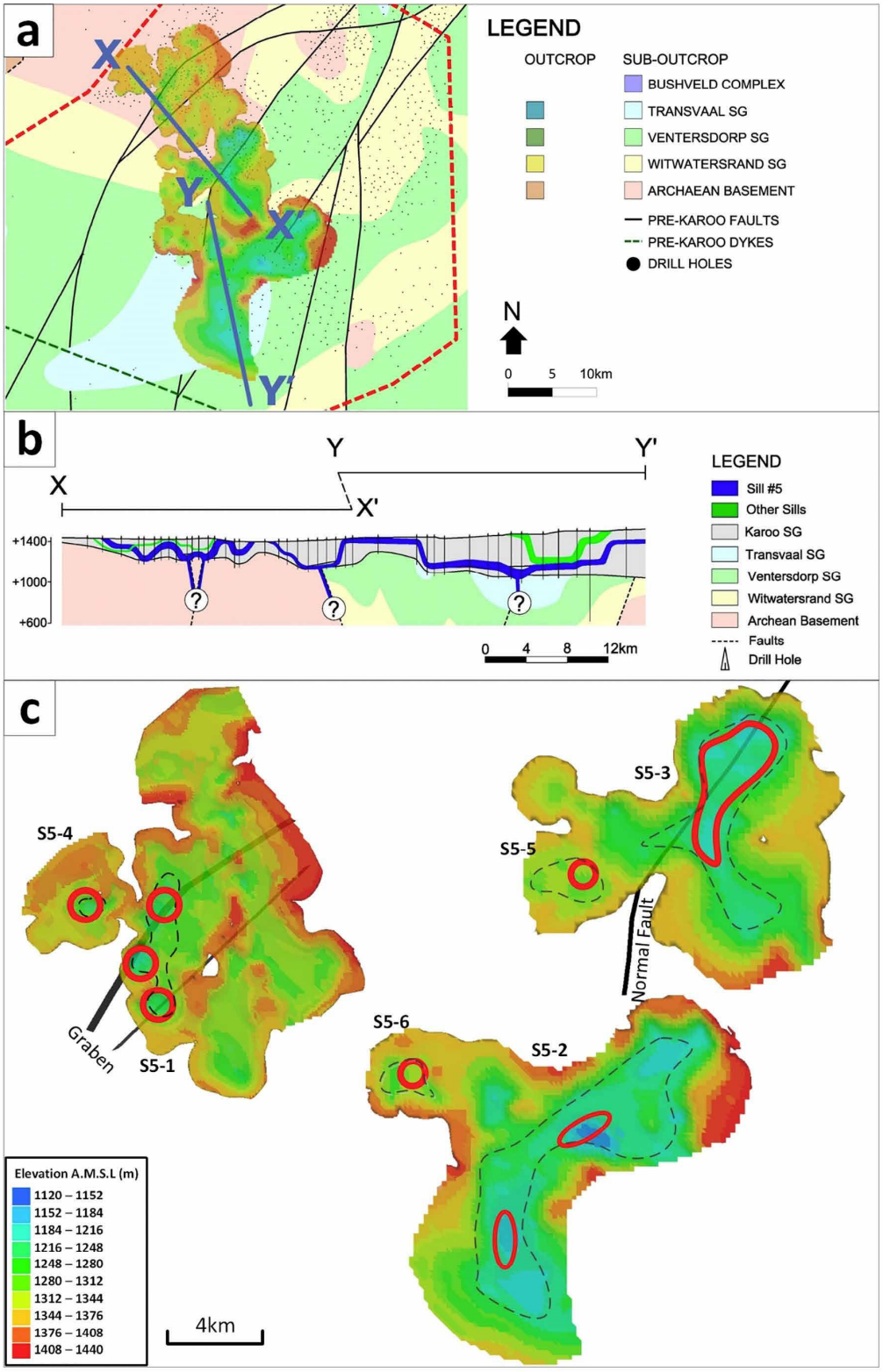

Fig. 7. (a) Plan view illustration of the spatial layout of sill #5 saucers and the underlying basement rocks. (b) Cross-section of sill #5 along lines shown in panel a with a vertical exaggeration factor of 5. (c) Elevation contour plot showing the inner sill outlines and basement contacts of the cone-shaped (S5-4 to S5-6), elongated (S5-1 and S5-2) and triangular (S5-3) saucers.

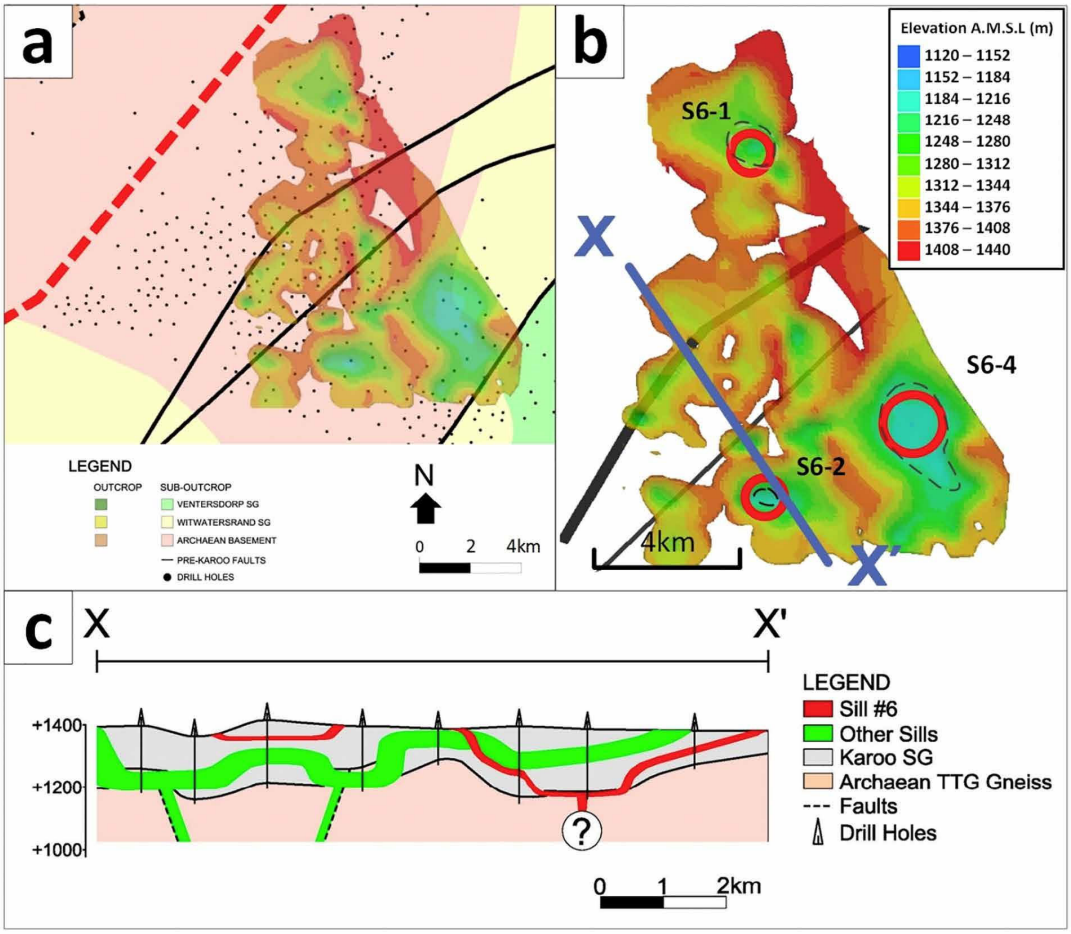

Fig. 8. (a) Plan view of the northern saucers (S6-1, S6-2, S6-4) of sill #6 in relation to the sub-outcropping basement strata and structures. (b) Elevation contour plot of saucers S-1, S6-2 and S6-4 with their inner sill outlines (broken lines) and basement contacts (red circles). (c) Cross-section of cone-shaped saucer of sill #6 with a vertical exaggeration factor of 5. (For interpretation of the references to colour in this figure legend, the reader is referred to the web version of this article.)

underlying basement feeder.

Field evidence from the north-eastern and northern parts of the Karoo Basin shows that saucer-basement relationships can be conceptualised into four main saucer geometries, henceforth referred to as Type A, B, C and D (Fig. 10a). Type A are circular or cone-shaped saucers that dip towards a single funnel-shaped point that connects to the basement rocks. Type B form elongated saucers with several aligned funnel-shaped points seated within the basement, while Type C represent elongated saucers with flat inner sills that connect to the basement over large lateral distances. Type D are elongated saucers characterised by a combination of Type A and C basement contacts.

Type A or cone-shaped saucers extend up- and outwards from single deep-seated and funnel-shaped points located either at the centre or rim of the inner sill (Fig. 10a). These funnels form isolated occurrences in rocks of the Vredefort and Cedarmont domes as well as the South Rand Basin and Welkom goldfield (Figs. 5–9, 10b). Also, while cases of Type A saucers overlying older dykes exist, their basement contacts, particularly that of S5-4 to S5-6 and S6-1 to S6-3, generally lack clear structural controls (Figs. 6–9, 10b). Type A saucer geometries display remarkable similarities to experimental results for saucers fed from pipe-like feeders. The distinct cup-shaped geometries around the central feeders (Mathieu et al., 2008; Galland et al., 2009) and circular saucer geometries demonstrated above feeders located off centre from the saucer base (Galland et al., 2009; Galerne et al., 2011) closely resemble saucer-basement contacts and geometries of Type A saucers.

On a regional scale, the long axes of the elongated Type B saucers show no preferred orientation. The saucers dip and close towards several funnel-shaped points seated within the basement rocks of the Vredefort and Cedarmont domes in addition to the Ventersdorp and Transvaal Supergroups (Fig. 10). Funnels are typically aligned parallel to the long axis of the saucers and, importantly, often coincide with either pre-existing normal faults or older dykes (Figs. 5, 7, 9). Although sheet-like feeders such as dykes are often invoked as feeders to elongated saucers (Galerne et al., 2011), the taper of Type B saucers towards a few small funnel-shaped points seated in the basement rocks is not expected for linear feeders that are in contact with the full length of the inner sill (Coetzee and Kisters, 2016). Given the numerous funnel-shaped connections of the saucers against the basement, it seems likely that Type B saucers were fed from multiple point sources or pipe-like feeders (Fig. 10a). The propagation and coalescence of magma from several coeval and aligned pipe-like feeders during saucer formation could also create the elongated geometries observed here.

Type C saucers are not associated with underlying funnel-like structures (Fig. 10a). Instead these saucers have flat inner sills with large parts extending into a variety of basement rocks, often at older normal faults (Figs. 7, 9). In contrast to the probably pipe-like feeders of

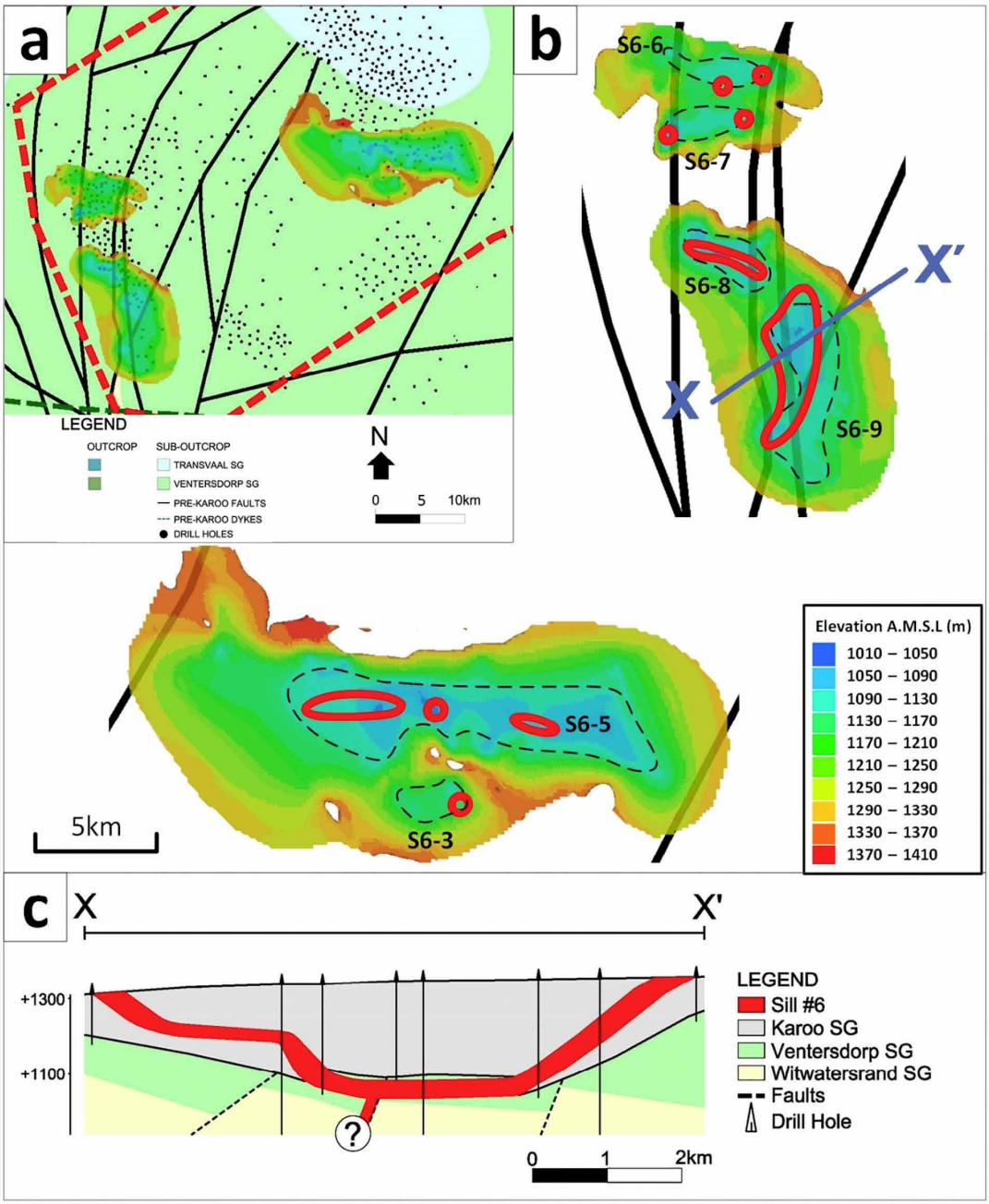

Fig. 9. (a) Plan view of the southern saucers (S6-3, S6-5–S6-9) of sill #6 with their underlying basement geology. (b) Elevation contour plots of saucers S6-3 and S6-5–S6-9 showing their inner sills and basement contacts in relation to older basement faults. (c) Cross-section of saucer S6-9 along X-X′ line in panel b with a vertical exaggeration factor of 5.

Type A and B saucers, the geometry of the elongated Type C saucers and their flat inner sills would rather point to the presence of linear, sheet-like feeders (Fig. 10a) (Galerne et al., 2011; Coetzee and Kisters, 2016). Given that the long axis of a saucer is normally limited to the length of the underlying feeder, sheet-like feeders in the northern Karoo Basin are expected to be no longer than 2.5–7 km.

Type D saucers are far less common with only one recorded case in the northern Karoo Basin. These saucers have a combination of pipe-like and linear sheet-like feeders (Fig. 10a) and lack any known connection to older pre-existing basement structures (Fig. 9). Thus, the field evidence and presence of Type A and C saucers documented here underpins the results of experiments that suggest the presence of single point-like or sheet-like feeders to saucers (Mathieu et al., 2008; Galland et al., 2009; Galerne et al., 2011). In contrast, Type B and D saucers and their multiple entry and feeder points have not been produced in experiments highlighting the need for models that replicate more intricate saucer-feeder relationships.

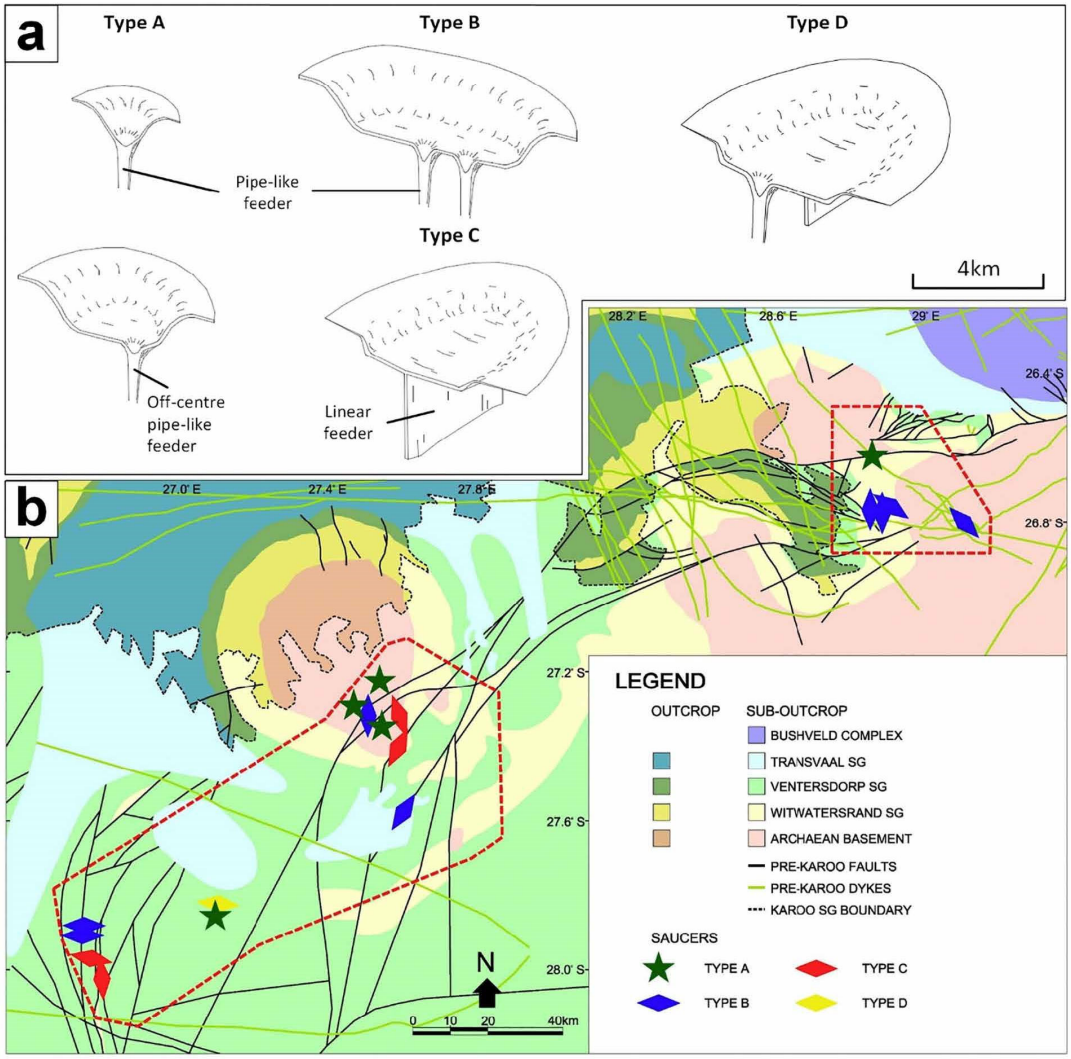

Fig. 10. (a) Schematic representation of the different saucer-basement contacts found in the northern Karoo basin and their likely underlying feeders. Type A saucers are circular or cone-shaped and dip towards a single pipe-like feeder. Type B saucers are elongated and connect to several aligned pipe-like feeders. Type C saucers have elongated geometries with a linear or dyke-like feeder. Type D saucers are elongated with a combination of pipe-like and linear underlying feeders (b) A geological map of the spatial distribution of Type A (stars), B (blue diamonds), C (red diamonds) and D (yellow diamonds) saucers. The orientation of elongated saucers (Types B, C and D) are reflected by the long axis of the diamond shapes. (For interpretation of the references to colour in this figure legend, the reader is referred to the web version of this article.)

5.2. *Basement feeders and their structural controls*

The close spatial association between Karoo saucers and basement rocks along pre-existing normal faults and/or older dolerite dykes (Figs. 5, 7–9, 10b) suggest pre-existing basement structures controlled the localisation of feeders during Karoo magmatism. Similar controls of magmatism through pre-existing structures, particularly normal faults, are recorded for other LIP's or volcanic margins (e.g. Valentine and Krogh, 2006; Hansen and Cartwright, 2006; Gaffney et al., 2007; Thomson and Schofield, 2008; Lavallée et al., 2009; Bédard et al., 2012; Muirhead et al., 2012; Magee et al., 2013; Schofield et al., 2017). In the northern Karoo Basin elongated Type B and C saucers predominantly overlie and dip towards sub-outcropping normal faults (Fig. 10b). The distinct location of several aligned funnel-shaped points along the graben structure (Fig. 7c) shows significant parallels to the occurrence of volcanic centres along graben faults in the Central Volcanic Zone of the Andes (Lavallée et al., 2009). Here, the tectonic evolution of the graben controlling later magma ascent and the subsequent formation of isolated volcanic edifices may represent an analogue for point-like feeders associated with Type B saucers.

An equivalent structural control can be demonstrated for the Type A and B saucers of the sill #4 complex that show contacts with basement rocks parallel to and along underlying Proterozoic dykes (Figs. 5, 10b). This points to the re-utilization of older c. 2.05 to 1.88 Ga Bushveld or Waterberg structures and/or dolerite dykes by the much younger Karoo-aged feeders. The overprint and apparent re-utilization of older dykes and dyke swarms by Karoo aged dykes is not unique and has similarly been recorded in the Okavango dyke swarm (Elburg and Goldberg, 2000; Jourdan et al., 2004), and Save-Limpopo dyke swarm (Fig. 1) (Jourdan et al., 2006; Hastie et al., 2014). In these cases, pre-

existing Proterozoic dyke swarms of vastly different ages (1672–851 Ma) are difficult to distinguish both in outcrop and composition from the Karoo-aged dykes along their margins. This implies that magma emplacement is strongly influenced by the difference in tensile strengths between intact wall rocks and the typically foliated, veined, or brecciated pre-existing faults or dyke margins. High fracture toughness and the absence of open fractures in the surrounding wall rocks will promote the exploitation of these crustal weaknesses by rising magma. Furthermore, regional stresses may be locally modified by the occurrence of major basement structures and residual stresses around pre-existing structures. Numerical stress models have shown that structures can influence the local stresses such that the principal compressive stress is reorientated into parallelism to nearby structures (Barnett et al., 2013). Consequently, the orientation of a later dyke may follow the orientation of the local stress field around the older structure. The modification of regional stresses by pre-existing structures may explain the occurrence of Type A and B saucers along northeast trending Proterozoic dykes (Fig. 10b). Local stress fields around basement structures such as the Sugarbush fault or other regional dykes could have modified the prevailing northerly or easterly compressive stresses parallel to the north-eastern basement dyke, thus inducing dilation and in turn magma emplacement along the margins.

In contrasts to the close spatial correlation between mainly Type B and C saucers and basement structures, it is particularly cone-shaped saucers (Type A) that do not show evidence of any recognisable underlying geological structures (Figs. 6–9, 10b). In these cases, we cannot rule out that the lack of controlling structures may merely represent an artefact of the poor resolution of subsurface data and smaller scale, subsidiary faults may go undetected in areas of more widely spaced coverage.

5.3. Feeder geometries

The formation of seemingly pipe-like feeder geometries along and within the generally planar discontinuities of faults or older dykes is still unclear. Mafic sheet intrusions are typically segmented and form through the growth and linkage of several magma segments or lobes that channelize magma along preferred pathways (Pollard et al., 1975; Hansen and Cartwright, 2006; Schofield et al., 2010). The links between these segments are often preserved as distinct steps or bridges in the otherwise continuous sheet (Nicholson and Pollard, 1985; Schofield et al., 2012). Uneven and anastomosing fault zones in addition to the different types of fault infill (vein networks, mylonites, fault gauge, breccias, etc.) may further complicate magma pathways and promote the branching and coalescence of the magma front in different parts along the fault plane (Fig. 11a). Likewise, baked and deformed host rock remains, chilled dolerite fragments along dyke margins or hydrothermal veins and fault cements may cause the segmentation of magma fronts (Fig. 11b) (Pollard et al., 1975; Rickwood, 1990). The development of segmented magma fronts in faults and dyke margins may also be driven by local surges in magma pressure. Once a preferred flow channel is established it drains magma away from the trailing magma front, thereby promoting the formation of narrow magma fingers or horns ahead of the main magma sheet. Later coalescence of several magma fingers may again form wider sheets along the length of fault planes and dyke contacts (Fig. 11a) (Pollard et al., 1975). The resulting geometry of the magma front, whether sheet- or finger-like, that arrives at the emplacement level of the Karoo strata will ultimately determine the shape of overlying saucers. Singular or multiple narrow magma fingers will form Type A or B saucers while more laterally extensive sheets representing several coalesced fingers would form Type C saucers. Alternatively, a combination of narrow magma fingers and wider sheets will result in Type D saucers.

Despite comprehensive data sets from drill holes, magnetic surveys and underground mappings, actual intersections of basement feeders with Karoo saucer-shaped sills remain elusive. Even in areas of high density drill holes and occasional deep reach of boreholes we could not find evidence of laterally continuous sheets below the saucers. Moreover, deep-level gold mining within the Witwatersrand Supergroup only rarely crosses Karoo-aged dolerite sheets that systematically exploit older faults. Similarly, anomalies of the magnitude expected of intrusions that may serve as regional feeders to the Karoo dolerites are largely absent on seismic and magnetic surveys. Rather pipe-like feeder geometries may also explain the apparent lack of feeders that can be missed in such large data sets. The lateral extent of feeder structures is simply too narrow and occurrence too isolated to be either intersected in a typical drill pattern or to produce significant geophysical signatures that are discernible from the pre-existing structures the Karoo magmas have exploited. While the funnel-shaped contacts between dolerite saucers and basement rocks are consistent with the proposed feeder geometries and lateral off-set between saucers, the actual formation processes of magma fingers and more point-like feeders must remain speculative at this stage.

5.4. Implication for Karoo magmatism

Results of this study indicate the distributed occurrence of numerous, localised feeders beneath the Karoo Supergroup. The spacing of clusters of feeders at distances of several tens of kilometres, mainly along older basement structures, across an area of > 7000 km^2 of the central Karoo Basin, does not support the proposed mantle plume positions in the rift between SE Africa and Antarctica (Burke and Dewey, 1973; Cox, 1989; White and McKenzie, 1989; Storey et al., 1992; Storey, 1995; Storey and Kyle, 1997; White, 1997; Elliot and Fleming,

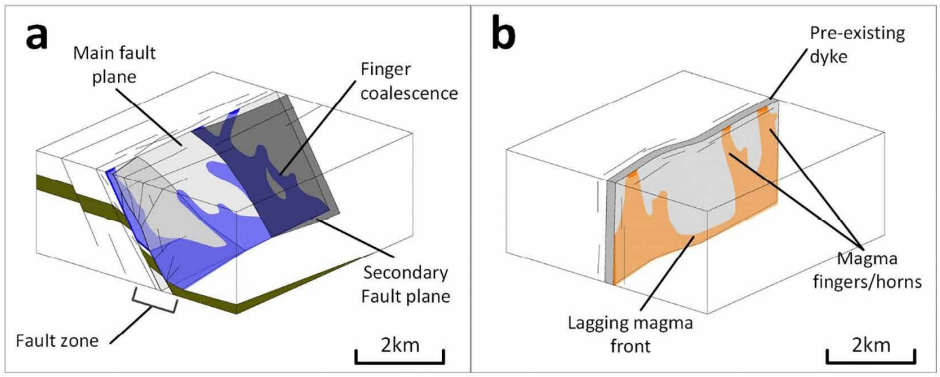

Fig. 11. Block diagrams illustrating the proposed flow patterns associated with magma exploiting pre-existing (a) dykes and (b) normal faults within the competent basement strata. Preferred magma flow channels form several narrow finger-like intrusions that feed saucers at the Karoo Supergroup emplacement level.

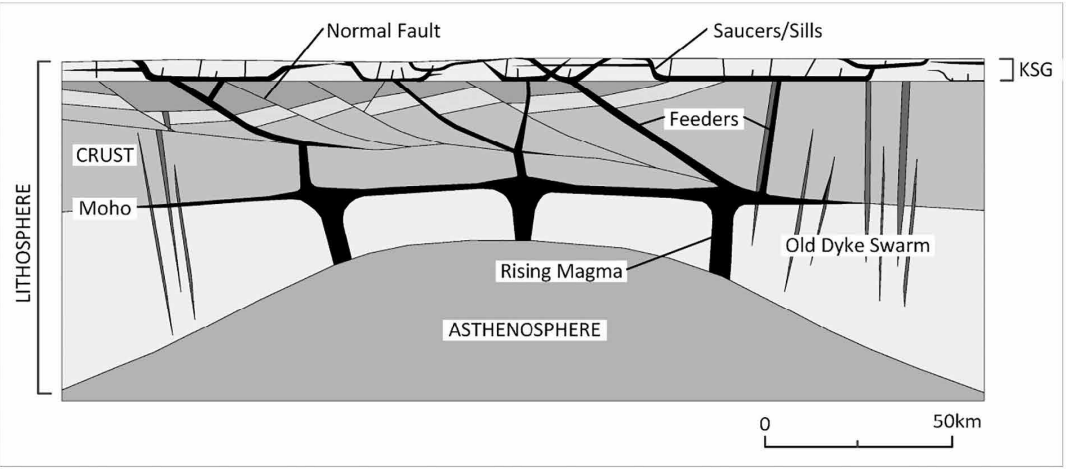

Fig. 12. A schematic diagram for the proposed magma feeder system to the Karoo sills prior to the break-up of Gondwana. Thinning lithosphere allows for the upward migration and underplating of mantle derived magmas beneath the crust that subsequently exploit pre-existing faults and dykes. Once magma feeders hit the interface of the Karoo Supergroup (KSG) magma emplacement is deflected laterally into sills and associated vertical dykes.

2000; Curtis et al., 2008). The emplacement of magma through the thicker lithosphere of the Kalahari craton suggest melting was not restricted to the localised zones of asthenospheric upwelling typically associated with mantle plumes. The insulating effect of a supercontinent such as Gondwana has a significant impact on the temperature distribution and convection within the sub-continental mantle (Coltice et al., 2007). Widely-spaced feeders to the Karoo sills may, thus, be consistent with the thermal structure associated with regional-scale thermal anomalies (Fig. 12) rather than a plume head (Anderson, 1994; Hawkesworth et al., 1999).

6. Conclusions

The three-dimensional mapping of dolerite sill complexes based on mining and exploration data sets in the north-eastern and northern Karoo Basin has yielded the following insights into the deeper feeder system of regional saucer-shaped sills below the Karoo Supergroup and the nature of melt generation during Gondwana magmatism.

1. Dolerite saucers in the Karoo Supergroup show cone- or funnel-shaped geometries at depth seated within basement rocks. The actual point-like contacts over relatively small areas would suggests the existence of narrow finger- or pipe-like feeders to sill complexes rather than laterally extensive sheets or dykes as commonly proposed.
2. Karoo-aged sheets or dykes cannot be identified in basement rocks despite the extensive mining and exploration data in the underground workings. Dykes in basement rocks are mainly pre-Karoo in age. This may corroborate the rather point- or finger-like geometry of feeders to dolerite sills in the Karoo Basin.
3. The close spatial relationship between saucers and underlying basement structures, irrespective of their orientation, emphasizes the prominent role of pre-existing basement structures, particularly older dolerite dykes and normal faults, for the transport of the Karoo dolerites and the controls of feeders to saucers of the central Karoo Basin. The regional stress field and modification thereof by local geological structures and residual stresses likely influenced the dilation of pre-existing basement structures and their subsequent exploitation by magma.
4. The multitude of feeders and their distributed spacing suggests the transfer of Karoo magmas across much of the Kalahari craton rather than being related to a few isolated feeders ("plume heads") or regional-scale dyke swarms. The emplacement of Karoo sill feeders through the Kalahari craton probably resulted from the thermal incubation of the sub-continental mantle beneath Gondwana.

Ideally, further studies on the basement relationships of saucers elsewhere in the Karoo Basin, particularly to the south along the Namaqua-Natal metamorphic belt, are needed to expand our knowledge on the more basin-wide dispersal of magma and the generation of melts during Karoo magmatism.

Acknowledgements

This study was supported by Sasol Mining (Pty) Ltd., Evander Gold Mine (Pan African Resources PLC), Taung Gold International Ltd. and the Council for Geoscience through the sharing of both new and historic geological data. We express our gratitude to Paul Mambane, Walter Seymore and Danie Thompson for organising underground visits and sharing their insights into the regional basement geology. We also thank Luc Chevallier for his long discussions on Karoo dolerites. We extend our gratitude to Craig Magee and one anonymous reviewer, whose insightful and constructive comments greatly improved the content of this paper.

References

Airoldi, G.M., Muirhead, J.D., Long, S.M., Zanella, E., White, J.D., 2016. Flow dynamics in mid-Jurassic dikes and sills of the Ferrar large igneous province and implications for long-distance magma transport. Tectonophysics 683, 182–199.

Anderson, D.L., 1994. Superplumes or supercontinents? Geology 22, 39–42.

Barnett, W., Jelsma, H., Watkeys, M., Freeman, L., Bloem, A., 2013. How structure and stress influence kimberlite emplacement. In: Pearson, D.G., et al. (Eds.), Proceedings of 10th International Kimberlite Conference. Special Issue of the Journal of the Geological Society of India, vol. 2https://doi.org/10.1007/978-81-322-1173-0_4.

Bédard, J.H., Naslund, H.R., Nabelek, P., Winpenny, A., Hryciuk, M., Macdonald, W., Hayes, B., Steigerwaldt, K., Hadlari, T., Rainbird, R., Dewing, K., Girard, É., 2012. Fault-mediated melt ascent in a Neoproterozoic continental flood basalt province, the Franklin sills, Victoria Island, Canada. Geol. Soc. Am. Bull. 124, 723–736.

Burke, K., Dewey, J.F., 1973. Plume generated triple junctions. Key indicators in applying plate tectonics to old rocks. J. Geol. 81, 403–433.

Bussio, J.P., 2012. Effect of Dolerite Intrusions on Coal Quality in the Secunda Coal Fields of South Africa (MSc Thesis). University of Pretoria, pp. 100.

Cartwright, J., Hansen, D.M., 2006. Magma transport through the crust via interconnected sill complexes. Geology 34, 929–932.

Catuneanu, O., 2004. Retroarc foreland systems—evolution through time. J. Afr. Earth Sci. 38, 225–242.

Catuneanu, O., Wopfner, H., Eriksson, P.G., Cairncross, B., Rubidge, B.S., Smith, R.M.H., Hancox, P.J., 2005. The Karoo basins of south-central Africa. J. Afr. Earth Sci. 43,

211–253.
Chevallier, L., Woodford, A., 1999. Morpho-tectonics and mechanism of emplacement of the dolerite rings and sills of the western Karoo, South Africa. S. Afr. J. Geol. 102, 43–54.
Coetzee, A., Kisters, A.F.M., 2016. The three-dimensional geometry of regional-scale dolerite saucer complexes and their feeders in the Secunda Complex, Karoo Basin. J. Volcanol. Geotherm. Res. 317, 66–79.
Coetzee, A., Kisters, A.F.M., 2017. Dyke-sill relationships in Karoo dolerites as indicators of propagation and emplacement processes of mafic magmas in the shallow crust. J. Struct. Geol. 97, 172–188.
Coltice, N., Phillips, B.R., Bertrand, H., Ricard, Y., Rey, P., 2007. Global warming of the mantle at the origin of flood basalts over supercontinents. Geology 35, 391–394.
Cox, K.G., 1989. The role of mantle plumes in the development of continental drainage patterns. Nature 342, 873–877.
Cox, K.G., 1992. Karoo igneous activity, and the early stages of the break-up of Gondwanaland. In: Storey, B.C., Alabaster, T., Pankhurst, R.J. (Eds.), Magmatism and the Causes of Continental Break-up. Geological Society of London Special Publication, vol. 68. pp. 37–148.
Cruden, A.R., Weinberg, R.F., 2018. Mechanisms of magma emplacement and storage in the lower and middle crust-magma segregation, ascent and emplacement. In: Burchardt, S. (Ed.), Volcanic and Igneous Plumbing Systems – Understanding Magma Transport, Storage and Evolution in the Earth's Crust. Elsevier, Amsterdam, pp. 13–53.
Curtis, M.L., Riley, T.R., Owens, W.H., Leat, P.T., Duncan, R.A., 2008. The form, distribution and anisotropy of magnetic susceptibility of Jurassic dykes in H.U. Sverdrupfjella, Dronning Maud Land, Antarctica. Implications for dyke swarm emplacement. J. Struct. Geol. 30, 1429–1447.
Dankert, B.T., Hein, K.A.A., 2010. Evaluating the structural character and tectonic history of the Witwatersrand Basin. Precambrian Res. 177, 1–22.
Duncan, R.A., Hooper, P.R., Rehacek, J., Marsh, J.S., Duncan, A.R., 1997. The timing and duration of the Karoo igneous event, southern Gondwanaland. J. Geophys. Res. 102, 18127–18138.
Elburg, M., Goldberg, A., 2000. Age and geochemistry of Karoo dolerite dykes from northeast Botswana. J. Afr. Earth Sci. 31, 539–554.
Elliot, D.H., Fleming, T.H., 2000. Weddell triple junction: the principal focus of Ferrar and Karoo magmatism during initial breakup of Gondwana. Geology 28, 539–542.
Elliot, D.H., Fleming, T.H., 2004. Occurrence and dispersal of magmas in Jurassic Ferrar large igneous province, Antarctica. Gondwana Res. 7, 223–237.
Elliot, D.H., Fleming, T.H., 2008. Physical volcanology and geological relationships of the Jurassic Ferrar large igneous province, Antarctica. J. Volcanol. Geotherm. Res. 172, 20–37.
Encarnacion, J., Fleming, T.H., Elliot, D.H., Eales, H.V., 1996. Synchronous emplacement of Ferrar and Karoo dolerites and the early break-up of Gondwana. Geology 24, 535–538.
Ernst, R.E., 2014. Large Igneous Provinces. Cambridge University Press, Cambridge.
Ernst, R.E., Buchan, K.L., 2003. Recognizing mantle plumes in the geological record. Annu. Rev. Earth Planet. Sci. 31, 469–523.
Ernst, R.E., Youbi, N., 2017. How large igneous provinces affect global climate, sometimes cause mass extinctions, and represent natural markers in the geological record. Palaeogeogr. Palaeoclimatol. Palaeoecol. 478, 30–52.
Gaffney, E.S., Damjanac, B., Valentine, G.A., 2007. Localization of volcanic activity: 2. Effects of pre-existing structure. Earth Planet. Sci. Lett. 263, 323–338.
Galerne, C.Y., Neumann, E., Planke, S., 2008. Emplacement mechanisms of sill complexes: information from the geochemical architecture of the golden valley sill complex, South Africa. J. Volcanol. Geotherm. Res. 177, 425–440.
Galerne, C.Y., Galland, O., Neumann, E., Planke, S., 2011. Three-dimensional relationships between sills and their feeders: evidence from the Golden Valley Sill Complex (Karoo Basin) and experimental modelling. J. Volcanol. Geotherm. Res. 202, 189–199.
Galland, O., Planke, S., Neumann, E.R., Malthe-Sørenssen, A., 2009. Experimental modelling of shallow magma emplacement: application to saucer-shaped intrusions. Earth Planet. Sci. Lett. 277, 373–383.
Gressier, J., Mougues, R., Bodet, L., Matthieu, J., Galland, O., Cobbald, P., 2010. Control of pore fluid pressure on depth of emplacement of magmatic sills: an experimental approach. Tectonophysics 489, 1–13.
Hansen, D.M., Cartwright, J., 2006. Saucer-shaped sill with lobate morphology revealed by three-dimensional seismic data: implications for resolving a shallow-level sill emplacement mechanism. J. Geol. Soc. 163, 509–523.
Hastie, W.W., Watkeys, M.K., Aubourg, C., 2011. Significance of magnetic and petrofabric in Karoo-feeder dykes, northern Lebombo. Tectonophysics 513, 96–111.
Hastie, W.W., Watkeys, M.K., Aubourg, C., 2014. Magma flow in dyke swarms of the Karoo LIP: implications for the mantle plume hypothesis. Gondwana Res. 25, 736–755.
Hawkesworth, C., Kelley, S., Turner, S., Le Roex, A., Storey, B., 1999. Mantle processes during Gondwana break-up and dispersal. J. Afr. Earth Sci. 28, 239–261.
Jourdan, F., Féraud, G., Bertrand, H., Kampunzu, A.B., Tshoso, G., Le Gall, B., Tiercelin, J.J., Capiez, P., 2004. The Karoo triple junction questioned: evidence from $^{40}Ar/^{39}Ar$ Jurassic and Proterozoic ages and geochemistry of the Okavango dike swarm (Botswana). Earth Planet. Sci. Lett. 222, 989–1006.
Jourdan, F., Féraud, G., Bertrand, H., Kampunzu, A.B., Tshoso, G., Watkeys, M.K., Le Gall, B., 2005. The Karoo large igneous province: brevity, origin, and relation with mass extinction questioned by new $^{40}Ar/^{39}Ar$ age data. Geology 33, 745–748.
Jourdan, F., Féraud, G., Bertrand, H., Watkeys, M.K., Kampunzu, A.B., Le Gall, B., 2006. Basement control on dyke distribution in large igneous provinces: case study of the Karoo triple junction. Earth Planet. Sci. Lett. 241, 307–322.
Jourdan, F., Féraud, G., Bertrand, H., Watkeys, M.K., 2007. Fromflood basalts to the inception of oceanization: example from the $^{40}Ar/^{39}Ar$ high-resolution picture of the Karoo large igneous province. Geochem. Geophys. Geosyst. 8, 989–1006.
Kamo, S.L., Reimold, W.U., Krogh, T.E., Colliston, W.P., 1996. A 2023 Ga age for the Vredefort impact crater and first report of shock metamorphosed zircons in pseudotachylitic breccias and granophyre. Earth Planet. Sci. Lett. 144, 369–387.
Kavanagh, J.L., Menand, T., Sparks, R.S.J., 2006. An experimental investigation of sill formation and ropagation in layered elastic media. Earth Planet. Sci. Lett. 245, 799–813.
Klausen, M.B., 2009. The Lebombo monocline and associated feeder dyke swarm: diagnostic of a successful and highly volcanic rifted margin? Tectonophysics 468, 42–62.
Lavallée, Y., De Silva, S.L., Salas, G., Byrnes, J.M., 2009. Structural control on volcanism at the Ubinas, Huaynaputina, and Tiscani Volcanic Group (UHTVG), southern Peru. J. Volcanol. Geotherm. Res. 186, 253–264.
Le Gall, B., Tshoso, G., Jourdan, F., Féraud, G., Bertrand, H., Tiercelin, J.J., Kampunzu, A.B., Modisi, M.P., Dyment, M., Maia, J., 2002. $^{40}Ar/^{39}Ar$ geochronology and structural data from the giant Okavango and related mafic dike swarms, Karoo igneous province, Botswana, Earth Planet. Sci. Lett. 202, 595–606.
Le Gall, B., Tshoso, G., Dyment, J., Kampunzu, A.B., Jourdan, F., Feraud, G., Bertrand, H., Aubourg, C., Vetel, W., 2005. The Okavango giant mafic dyke swarm (NE Botswana): its structural significance within the Karoo large igneous province. J. Struct. Geol. 27, 2234–2255.
Leat, P.T., 2008. On the Long-distance Transport of Ferrar Magmas, Structure and Emplacement of High-level Magmatic Systems. Special Publications, Geological Society, London, pp. 45–61.
Magee, C., Jackson, C.A.L., Schofield, N., 2013. The influence of normal fault geometry on igneous sill emplacement and morphology. Geology 41 (4), 407–410.
Magee, C.J., Muirhead, J.D., Karvelas, A., Holford, S.P., Jackson, C.A.L., Bastow, I.D., Schofield, N., Stevenson, C.S.T., McLean, C., McCarthy, W., Shtukert, O., 2016. Lateral magma flow in mafic sill complexes. Geosphere 12 (3), 809–841.
Malthe-Sørenssen, A., Planke, S., Svensen, H., Jamtveit, B., 2004. Formation of saucer-shaped sills. In: Breitkreuz, C., Petford, N. (Eds.), Physical Geology of High-level Magmatic Systems. Geological Society, London, Special Publications 234. pp. 215–227.
Marsh, J.S., 1987. Basalt Geochemistry and tectonic discrimination within continental flood basalt provinces. J. Volcanol. Geotherm. Res. 32, 35–49.
Marsh, J.S., 2002. The geophysical mapping of Mesozoic dyke swarms in southern Africa and their origin in the disruption of Gondwana. J. Afr. Earth Sci. 30, 499–513.
Mathieu, L., Van Wyk de Vries, B., Holohan, E.P., Troll, V.R., 2008. Dykes, cups, saucers and sills: analogue experiments on magma intrusion into brittle rocks. Earth Planet. Sci. Lett. 271, 1–13.
Muirhead, J.D., Airoldi, G., Rowland, J.V., Whitec, J.D.L., 2012. Interconnected sills and inclined sheet intrusions control shallow magma transport in the Ferrar large igneous province, Antarctica. Geol. Soc. Am. Bull. 124, 162–180.
Muirhead, J.D., Airoldi, G., Whitec, J.D.L., Rowland, J.V., 2014. Cracking the lid: sill-fed dikes are the likely feeders of flood basalt eruptions. Earth Planet. Sci. Lett. 406, 187–197.
Myers, R.E., McCarthy, T.S., Stanistreet, I.G., 1990. A tectono-sedimentary reconstruction of the development and evolution of the Witwatersrand basin with particular emphasis on the Central Rand Group. S. Afr. J. Geol. 93, 180–201.
Nicholson, R., Pollard, D.D., 1985. Dilation and linkage of en echelon cracks. J. Struct. Geol. (5), 583–590.
Pollard, D.D., Muller, O.H., Dockstader, D.R., 1975. The form and growth of fingered sheet intrusions. Geol. Soc. Am. Bull. 86, 351–363.
Rickwood, P., 1990. The anatomy of a dyke and the determination of propagation and magma flow directions. In: Mafic Dykes and Emplacement Mechanisms, pp. 81–100.
Riley, T.R., Curtis, M.L., Leat, P.T., Watkeys, M.K., Duncan, R.A., Millar, I.L., Owens, W.H., 2006. Overlap of Karoo and Ferrar magma types in KwaZulu-Natal, South Africa. J. Pet. 47 (3), 541–566.
Saunders, A.D., Jones, S.M., Morgan, L.A., Pierce, K.L., Widdowson, M., Xu, Y.G., 2007. Regional uplift associated with continental large igneous provinces: the roles of mantle plumes and the lithosphere. Chem. Geol. 241 (2007), 282–318.
Schofield, N., Stevenson, C., Reston, T., 2010. Magma fingers and host rock fluidization in the emplacement of sills. Geology 38, 63–66.
Schofield, N., Heaton, L., Holford, S.P., Archer, S.G., Jackson, C.A.L., Jolley, D.W., 2012. Seismic imaging of 'broken bridges': linking seismic to outcrop-scale investigations of intrusive magma lobes. J. Geol. Soc. 169, 421–426.
Schofield, N., Holford, S., Millett, J., Brown, D., Jolley, D., Passey, S.R., Muirhead, D., Grove, C., Magee, C., Murray, J., Hole, M., Jackson, C.A.L., Stevenson, C., 2017. Regional magma plumbing and emplacement mechanisms of the Faroe-Shetland Sill Complex: implications for magma transport and petroleum systems within sedimentary basins. Basin Res. 29, 41–63.
Smith, R.M.H., Eriksson, P.G., Botha, W.J., 1993. A review of the stratigraphy and sedimentary environments of the Karoo-aged basins of Southern Africa. J. Afr. Earth Sci. 16, 143–169.
Storey, B.C., 1995. The role of mantle plumes in continental breakup: case histories from Gondwanaland. Nature 377, 301–308.
Storey, B.C., Kyle, P.R., 1997. An active mantle mechanism for Gondwana breakup. S. Afr. J. Geol. 100, 283–290.
Storey, B.C., Alabaster, T., Hole, M.J., Pankhurst, R.J., Wever, H.E., 1992. Role of subduction plate boundary forces during the initial stages of Gondwana break-up: evidence from the proto-Pacific margin of Antarctica. In: Storey, B.C., Alabaster, T., Pankhurst, R.J. (Eds.), Magmatism and the Causes of Continental Break-up. Geological Society of London Special Publication 68. pp. 149–163.
Svensen, H., Corfu, F., Polteau, S., Hammer, O., Planke, S., 2012. Rapid magma emplacement in the Karoo large igneous province. Earth Planet. Sci. Lett. 325–326, 1–9.
Thomson, K., Hutton, D., 2004. Geometry and growth of sill complexes: insights using

three-dimensional seismic from the North Rockall Trough. Bull. Volcanol. 66, 364–375.
Thomson, K., Schofield, N., Thomson, K., 2008. Lithological and structural controls on the emplacement and morphology of sills in sedimentary basins. In: peTforD, N. (Ed.), Structure and Emplacement of High-level Magmatic Systems. Geological Society, London, Special Publications 302. pp. 31–44.
Uken, R., Watkeys, M.K., 1997. An interpretation of mafic dyke swarms and their relationship with major mafic magmatic events on the Kaapvaal Craton and Limpopo Belt. S. Afr. J. Geol. 100 (4), 341–348.
Valentine, G.A., Krogh, K.E.C., 2006. Emplacement of shallow dikes and sills beneath a small basaltic volcanic center—the role of pre-existing structure (Paiute Ridge, southern Nevada, USA). Earth Planet. Sci. Lett. 246, 217–230.
Veevers, J.J., Cole, D.I., Cowan, E.J., 1994. Southern Africa: Karoo basin and Cape Fold Belt. In: Veevers, J.J., Powell, C.McA. (Eds.), Permian-Triassic Pangean Basins and Foldbelts along the Panthalassan Margin of Gondwanaland. Geol. Soc. America, Boulder, Colorado, Memoir 184. pp. 223–279.
Visser, J.N.J., 1993. Sea-level changes in a back-arc—foreland transition: the Late Carboniferous-Permian Karoo Basin of South Africa. Sediment. Geol. 83, 115–131.
White, R.S., 1997. Mantle plume origin for the Karoo and Ventersdorp flood basalts, South Africa. S. Afr. J. Geol. 100, 271–282.
White, R.S., McKenzie, D., 1989. Magmatism at rift zones: the generation of volcanic continental margins and flood basalts. J. Geophys. Res. 94, 7685–7729.
White, J.D.L., Bryan, S.E., Ross, P.-S., Self, S., Thordarson, T., 2009. Physical volcanology of 30 continental large igneous provinces: update and review. In: Thordarson, T., Self, S., Larsen, G., 31 Rowland, S.K., Hoskuldsson, A. (Eds.), Studies in Volcanology: The Legacy of George Walker. 55 1 Special Publications of IAVCEI. 2. Geological Society, London, pp. 291–321.
Wieland, F., Gibson, R.L., Reimold, W.U., 2005. Structural analysis of the collar of the Vredefort Dome. South Africa—significance for impact-related deformation and central uplift formation. Meteorit. Planet. Sci. 40, 1–18.

The following represents supplementary sill thickness data not included in the original publication above

North-eastern Karoo basin

Sill #4 – Thickness

The thickness of both the circular (S4-1) and elongated (S4-2) saucer (Fig. 13a) decreases from a constant 40-50 m along the inner sills to 30-40 m within the inclined sheets. The outer sills largely taper off from a maximum of 30 m due to the effect of surface erosion except to the northeast of S4-1 where the outer sill width increases to over 80 m.

Sill #8 – Thickness

Inner sills are largely below 25 m except at the basement contacts of saucers S8-1 and S8-3 where sill widths reach 30 m (Fig. 13b). The saucer thicknesses gradually decrease to <25 m along the inclined sheets while the outer sills thin out against the topographic level.

Northern Karoo basin

Sill #5 – Thickness

The triangular saucer (S5-3) (Fig. 13c) shows a general thickness of 10-25 m along the inner sill that increases to 40 m in places along the outer sill before tapering off due to surface erosion.

Conversely, the elongated saucers show a marked increase in width along their inner sills from an average of 40 m to over 60 m (S5-1) and 80 m (S5-2) near basement contacts (Fig. 13c). Inclined sheets and outer sills maintain thicknesses upwards of 40 m except where cut off by the weathered horizon.

Circular saucers (S5-4, S5-5 and S5-6) (Fig. 13c) are typically <40 m thick with the exception of S5-4 that attains a maximum width of 60-70 m along the basement contact.

Sill #6 – Thickness

Circular saucers (S6-1, S6-2, S6-3) (Fig. 13d, e) largely maintain thicknesses of 15-20 m along their inner sills and inclined sheets before thinning abruptly at the outer sills.

Likewise saucers S6-5, S6-6, S6-7 and S6-8 (Fig. 13e) are between 30 m and 40 m thick at the inner sills and inclined sheets before tapering off.

Saucers S6-4 and S6-9 (Fig. 13d, e) show abrupt thickness increases where the inner sills cut into the basement rocks from 15 m to 20 m and 40 m to 60 m respectively. Inclined sheet and outer sill widths drop to below 15 m (S6-4) and 40 m (S6-9) depending on the local topographic level.

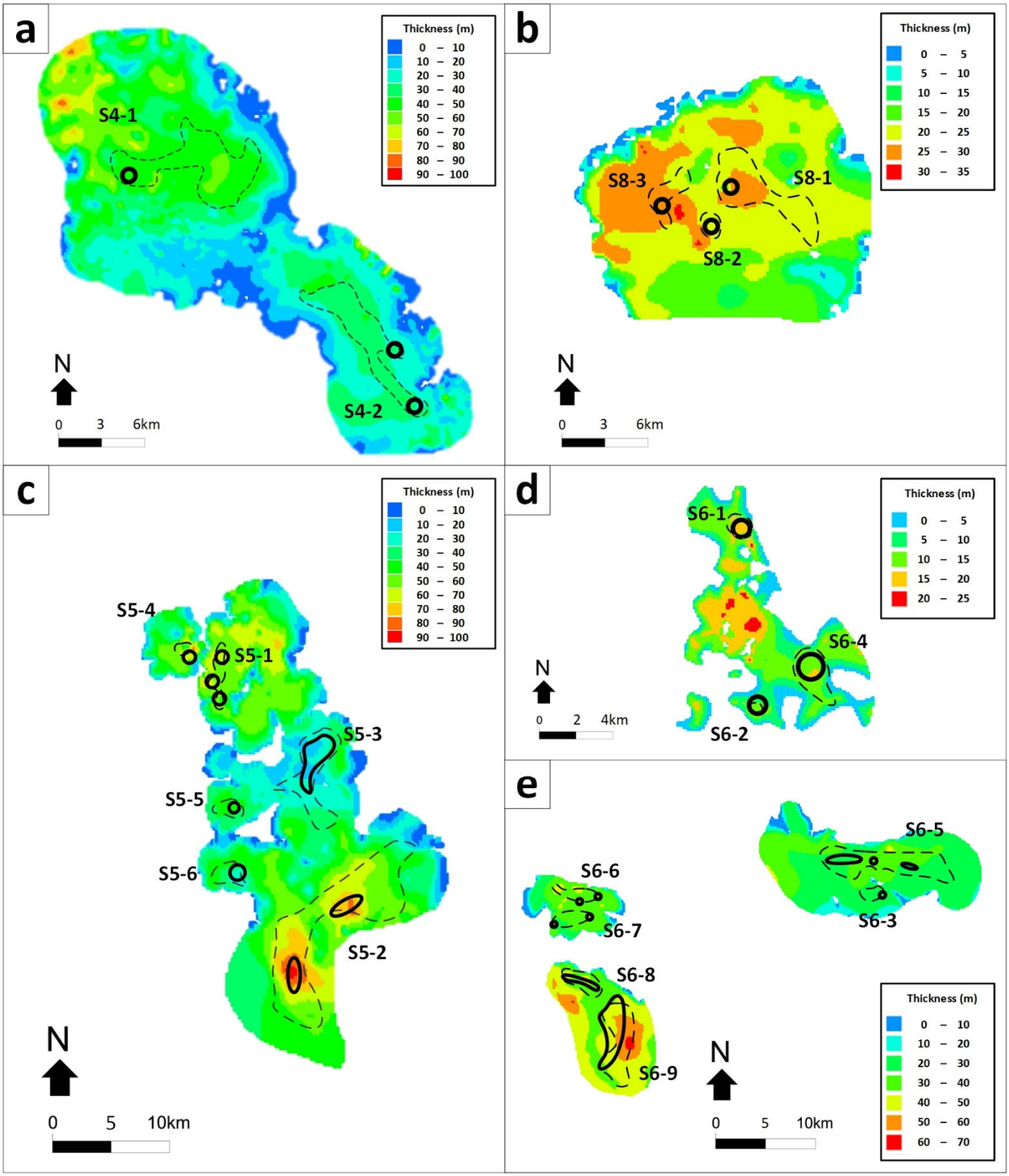

Figure 13: *Thickness contour plots of (a) sill #4, (b) sill #8, (c) sill #5 and (d and e) sill #6. The broken lines and black circles indicate the respective inner sill boundaries and their positions inside the basement rocks.*

Chapter 5: Sill emplacement controls

This chapter constitutes a presentation of the published research paper: ***Sill complexes in the Karoo LIP: emplacement controls and regional implications***[1] by Coetzee, Kisters and Chevallier.

This paper was authored by André Coetzee with standard supervision entailing academic guidance and editorial support from Alex Kisters. The following aspects were carried out independently by André Coetzee: (1) field work and data collection, (2) data consolidation, processing and interpretation, (3) three-dimensional modelling, (4) preparation and submission of the manuscript and (5) manuscript revision and successful resubmission.

[1]Coetzee, A., Kisters, A.F.M., Chevallier, L. (2019). Sill complexes in the Karoo LIP: emplacement controls and regional implications. Journal of African Earth Sciences 158, 103517.

Journal of African Earth Sciences 158 (2019) 103517

Contents lists available at ScienceDirect

Journal of African Earth Sciences

journal homepage: www.elsevier.com/locate/jafrearsci

Sill complexes in the Karoo LIP: Emplacement controls and regional implications

A. Coetzee[a,*], A.F.M. Kisters[a], L. Chevallier[b]

[a] Department of Earth Sciences, University of Stellenbosch, Matieland, 7602, Stellenbosch, South Africa
[b] Council for Geoscience, PO Box 572, Bellville, 7535, Cape Town, South Africa

ARTICLE INFO

Keywords:
Saucer-shaped sills
Dyke swarms
Karoo LIP
Gondwana break-up
Magma emplacement processes
Sedimentary basin
Rigidity contrasts

ABSTRACT

Field and sub-surface data from the Victoria West sill complex in the Karoo Large Igneous Province (ca. 180 Ma) of South Africa are used to constrain the emplacement controls of the regional-scale sill complexes in the central Karoo basin. Cross-cutting relationships point to the presence of five distinct and successively emplaced saucer-shaped sills. Growth of the sill complex was achieved through magmatic underaccretion of magma batches below earlier sills and associated uplift of the overlying strata. The magmatic underaccretion suggests that earlier sills were fully crystallized during the emplacement of later magma pulses and that the rigid (high E) dolerites, in particular, acted as stress barriers that impeded further upward propagation of steep feeder sheets. The resulting nested structure of sills-in-sills within a confined area of less than 2000 km^2 also suggests the reutilization of the same or similar feeder system even after full crystallization thereof.

The emplacement controls of sills in the central Karoo through stress barriers implies that sill emplacement occurred under very low deviatoric stresses or in a mildly compressional stress regime prior to the break-up of Gondwana. The swap from earlier (184-180 Ma), mainly sill complexes to later (182-174 Ma) dykes and dyke swarms is indicative of a switch in the stress field during the early stages of Gondwana break-up. We speculate that loading, thermal subsidence and lithospheric flexure associated with the emplacement of the earlier, stacked and voluminous sill complexes in the Karoo basins may have determined the formation of the large Karoo dyke swarms, particularly when coinciding with deeper crustal structures. The original and inherited basin geometry and lithospheric structure is pivotal in the development of later Karoo magmatism.

1. Introduction

The mafic magmatism of the Karoo Large Igneous Province (LIP) in southern Africa heralds the break-up of Gondwana in the middle Jurassic at ca. 180 Ma (Cox, 1992; Encarnacion et al., 1996; Duncan et al., 1997). The intrusive and extrusive rocks are developed as flood basalts, such as the stacked lava flows of the Drakensberg or Lebombo Groups (Jourdan et al., 2007a, 2007b; Klausen, 2009), shallow-crustal, interconnected sill complexes in the flat lying Permo-Jurassic Karoo Supergoup (Chevallier and Woodford, 1999; Schofield et al., 2010; Galerne et al., 2011; Jourdan et al., 2008; Svensen et al., 2012; Coetzee and Kisters, 2016, 2017, 2018), or as dyke swarms seemingly concentrated around intrusive centres (Uken and Watkeys, 1997; Elburg and Goldberg, 2000; Jourdan et al., 2004, 2005; Riley et al., 2004, 2006; Le Gall et al., 2002, 2005; Hastie et al., 2011, 2014). In total, Karoo magmatism may have covered an area of over 1000 000 km^2 in southern Africa (Marsh, 1987). Traditionally, the sills and dykes have been regarded as the subvolcanic vestiges of the interconnected magma plumbing system underlying and feeding the Karoo flood basalts (e.g., Duncan et al., 1997). However, there is a distinct spatial disconnect between sill complexes and dyke swarms. Sill complexes are mainly confined to the central parts of the main Karoo and Kalahari basins. Regional dyke swarms, in contrast, are chiefly developed in the northern and north-eastern parts of the Karoo LIP (Fig. 1). Moreover, existing age data indicates that sills and flood basalts were, by and large, intruded prior to the emplacement of regional dyke swarms (Fig. 1), pointing to a change in emplacement style. This may potentially signal changes in the regional stress field prior to and during the early stages of Gondwana break-up (e.g., Cox, 1992; Grantham et al., 2018).

In this paper, we investigate the controls of sill emplacement of the prominent Victoria West sill complex situated in the southern parts of the central Karoo basin. We integrate outcrop-scale observations of sill contacts with drill hole and aeromagnetic data to constrain the

* Corresponding author. Sasol Mining (Pty) Ltd, Sigma Colliery, PO Box 1, Sasolburg, 1947, South Africa.
E-mail address: andre.coetzee2@sasol.com (A. Coetzee).

https://doi.org/10.1016/j.jafrearsci.2019.103517
Received 14 March 2019; Received in revised form 31 May 2019; Accepted 3 June 2019
Available online 06 June 2019
1464-343X/

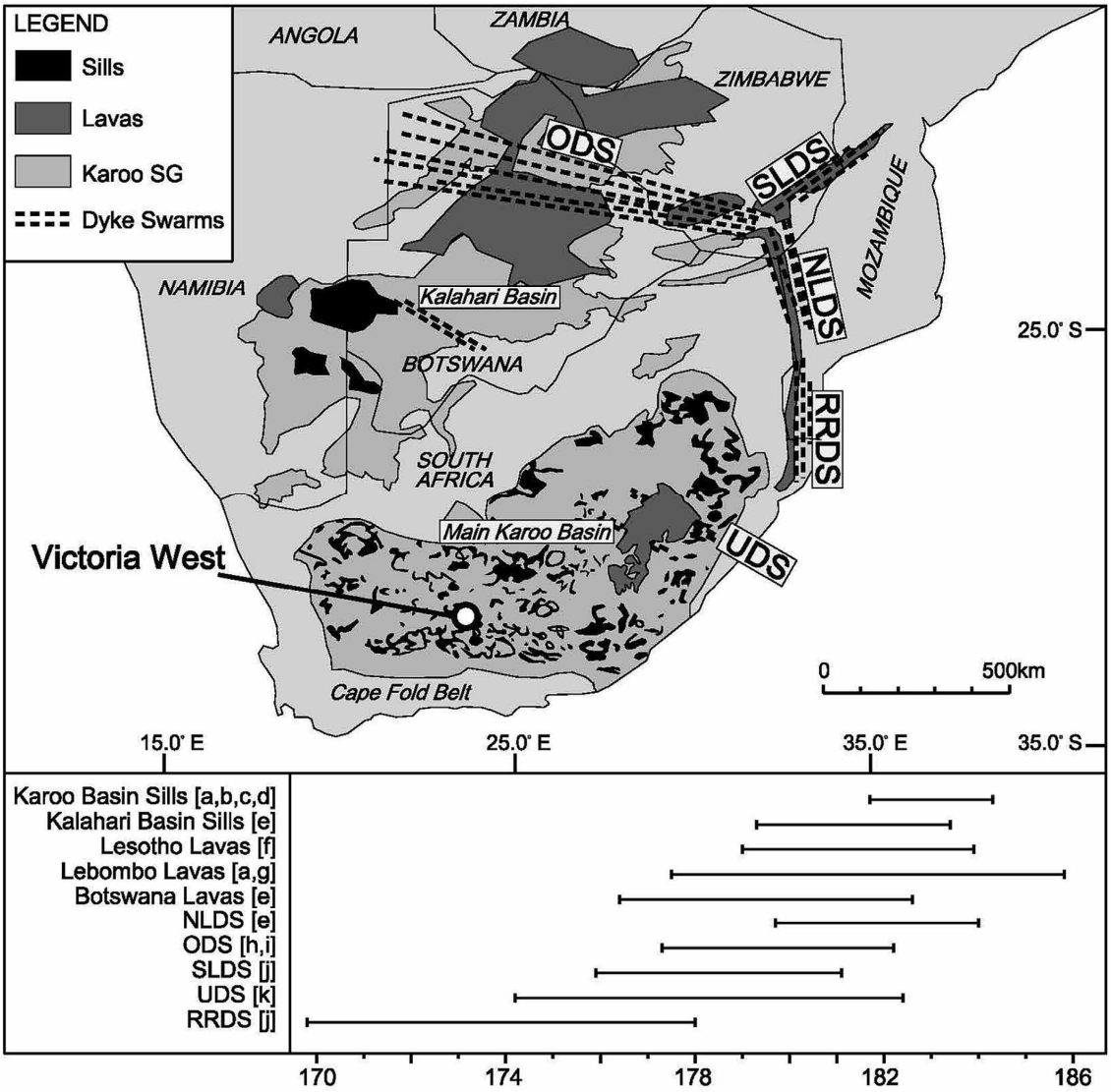

Fig. 1. Geological map showing the remnants of lavas, sills and dyke swarms related to the Karoo Large Igneous Province. ODS, Okavango dyke swarm; SLDS, Save Limpopo dyke swarm; NLDS, Northern Lebombo dyke swarm; RRDS, Rooi Rand dyke swarm; UDS, Underberg dyke swarm. Age ranges are after Duncan et al. (1997) [a]; Encarnacion et al., 1996 [b]; Svensen et al. (2007) [c]; Svensen et al. (2012) [d]; Jourdan et al. (2005) [e]; Jourdan et al. (2007a) [f]; Riley et al., 2004 [g]; Le Gall et al. (2002) [h]; Jourdan et al. (2004) [i]; Jourdan et al. (2007b) [j]; Riley et al. (2006) [k].

geometry, sequence of intrusive events, wall-rock dolerite contacts and likely feeder locations that have controlled sill emplacement and assess the implications thereof for the tectonic controls of the Karoo magmatism.

2. Geological setting

The main Karoo basin is a retro-arc foreland basin that developed north of the Cape fold belt in response to the subduction of the paleao-Pacific plate beneath the Gondwana plate in the late Paleozoic and early Mesozoic (Catuneanu, 2004a). Early compression and tectonic loading during the Cape orogeny at 290-215 Ma (Hälbich et al., 1983; Hälbich and Cornell, 1983; Gresse et al., 1992; Hansma et al., 2015) developed a foredeep marking the onset of sedimentation within the Karoo basin. Later, orogenic progradation initiated a back-bulge and the formation of several northern subordinate basins, such as the Springbok Flats, Kalahari and Ellisras basins (Catuneanu, 2004a, 2004b). The main Karoo basin represents an asymmetric depository which preserves a maximum of 6 km of Late-Carboniferous to Middle-Jurassic sedimentary units in the south that progressively taper out to the north. The lithostratigraphic units reflect a changing depositional environment from glacial to deep marine (Dwyka), shallow marine to deltaic (Ecca), fluvial (Beaufort) and eolian (Stormberg) (Smith et al., 1993; Catuneanu et al., 1998, 2005). Similar sedimentary sequences in,

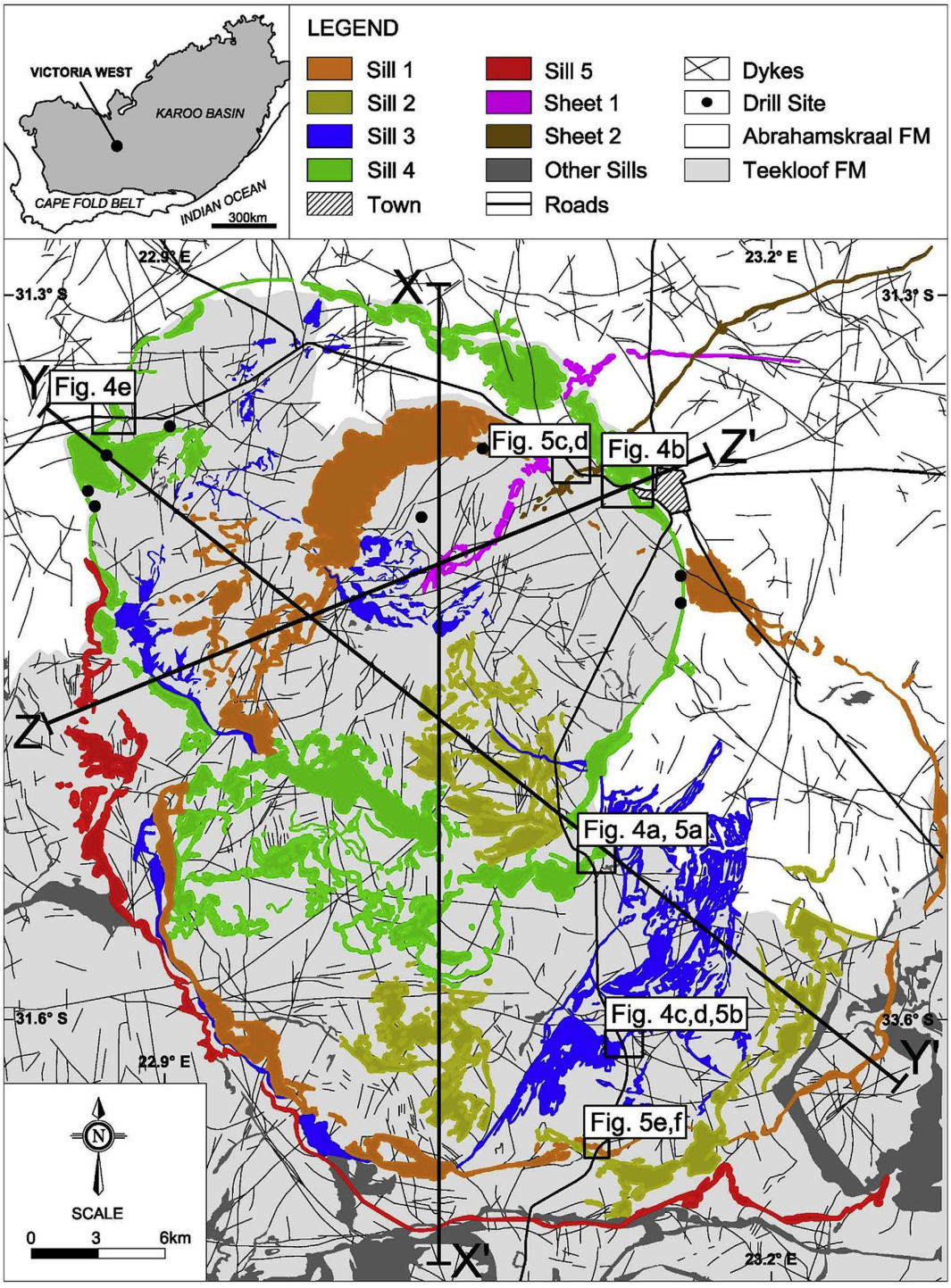

(caption on next page)

Fig. 2. Geological map of the Victoria West area of the Karoo basin showing saucer-shaped sills (coloured sills 1 to 5), curved sheets (coloured sheets 1 and 2), dykes (thin black lines) as well as sills that does not form part of this study (grey). Black circles indicate drill sites while the thick black lines define the cross-sections X-X′, Y–Y′″ and Z-Z′ in Fig. 3. Black boxes indicate outcrops shown in Figs. 4 and 5.

e.g., Antarctica indicate the extent of the original basin. Here, it is the Devonian – Triassic, siliciclastic Beacon Supergroup that originally covered most of the continent. Triassic to Middle Jurassic erosion have largely reduced outcrops of the Beacon Supergroup to the Transantarctic Mountains in Victoria Land and several nunataks in Drönning Maud Land (Elliot and Fleming, 2000; Bernet and Gaupp, 2005; Elliot and Grimes, 2011).

In southern Africa, Karoo magmatism successively introduced a subvolcanic plumbing system of mafic sills and dykes which facilitated the outpouring of lava sequences in excess of 1.4 km thick above the largely flat sediments of the Karoo Supergroup (Marsh, 1987; Cox, 1992; Encarnacion et al., 1996; Duncan et al., 1997; Svensen et al., 2012). Recent high-precision dating of Karoo dolerites has identified several successive phases of mafic magmatism. The rapid emplacement of dolerite sills in the Karoo basin at 183.7 ± 0.6 to 182.3 ± 0.6 Ma (Duncan et al., 1997; Encarnacion et al., 1996; Jourdan et al., 2008; Svensen et al., 2007, 2012) and the Kalahari basin at 181.8 ± 1.6 to 180.0 ± 0.7 Ma (Jourdan et al., 2005) overlaps with the extrusion of the Drakensberg (182.3 ± 1.6 to 181.0 ± 2.0 Ma; Jourdan et al., 2007b) and Lebombo Groups (182.3 ± 1.6 to 181.0 ± 2.0 Ma; Jourdan et al., 2007b) along with the basaltic units of Botswana (180.7 ± 1.9 to 178.0 ± 1.6 Ma; Jourdan et al., 2005). The first appearance of regional dykes is marked by the Lebombo dyke swarm at 182.3 ± 1.7 to 181.4 ± 0.7 Ma (Jourdan et al., 2005). This was followed by the synchronous emplacement of the major Okavango (180.9 ± 1.3 to 178.4 ± 1.1 Ma; Le Gall et al., 2002; Jourdan et al., 2004), Save-Limpopo (180.4 ± 0.7 to 177.7 ± 0.8 Ma; Jourdan et al., 2007b) and the Underberg (181.7 ± 0.7 to 176.4 ± 1.2 Ma; Riley et al., 2006) dyke swarms. The emplacement of the Rooi Rand dyke swarm at 173.9 ± 3.8 to 172.1 ± 2.3 Ma represents the final dyking event and heralds the initiation of the break-up between Africa and Antarctica (Jourdan et al., 2007b).

Deep weathering of the African land surface has revealed the full extent of these overlapping and cross-cutting sills, sheet and dyke geometries. Recent borehole and geophysical data from the northern parts of the Karoo basin highlight the control of feeders to saucer-shaped sills by older, pre-existing basement structures and, as a result, the rather scattered distribution of Karoo magma feeders (Coetzee and Kisters, 2018). Moreover, the thinned Karoo stratigraphy in these northern parts of the main Karoo basin preserves significantly fewer sill complexes (Coetzee and Kisters, 2016, 2018). In contrast, the thicker strata of the central Karoo basin contains laterally extensive as well as compositionally and texturally composite sill complexes (Chevallier and Woodford, 1999; Galerne et al., 2011). Saucer-shaped sills in the central Karoo are most prominently evident as distinct ring-like structures defined by remnants of typically more than one semi-circular, inward-dipping inclined sheets surrounding inner sills seated at shallow depths within the gently-dipping sedimentary Karoo Supergroup (Chevallier and Woodford, 1999; Chevallier et al., 2001; Galerne et al., 2011). Sills commonly form isolated clusters of stacked sills and cross-cutting relationships between inclined sheets, but also textural and compositional variations indicate the multiple emplacement of sills through a number of distinct magma batches, each forming a unique set of overprinting sill geometries (Galerne et al., 2008).

Compared to sills, dykes in the central Karoo basin are volumetrically minor. Dykes typically occur either as thin (< 5 m), localised features closely associated with individual sill structures (Chevallier and Woodford, 1999) or as thicker (~30 m) dykes tens of kilometres long with east-west and north-westerly strikes (Chevallier and Woodford, 1999; Galerne et al., 2011; Neumann et al., 2011). Although dykes are commonly invoked as feeders to sills in the Karoo basin (e.g. Chevallier and Woodford, 1999; Galerne et al., 2011) due to their interconnectivity and similar ages (Svensen et al., 2012), a clear feeding relationships have yet to be established. Instead, these dyke patterns most likely represent secondary structures, arising from the shallow-level magma flow dynamics and emplacement processes of sills (Coetzee and Kisters, 2017).

3. Field data

The town of Victoria West is located in the central Karoo basin, South Africa, along the northern extremity of a regional-scale sill complex that covers an area of some 2000 km^2 (Fig. 2). The area is underlain by Permian sandstones and purple-red shales of the Abrahamskraal and Teekloof Formations of the Beaufort Group (Smith et al., 1993; Veevers et al., 1994c). The majority of dolerite intrusions is represented by saucer-shaped sills emplaced into the gently (< 5–10°) south-east dipping sedimentary country rocks. In the field, saucers are easily recognized by their inclined sheets that form circular ridges, whereas the remnants of outer sills cap distinct flat-topped mountains in the Karoo landscape. Contact and intrusive relationships between dolerites and wall rocks are only rarely exposed and extensive scree slopes largely restrict structural observations to road cuts and deeply incised river valleys. These sites are central to the ground truthing of existing geological maps and satellite imagery and were used for the validation of the orientation of contacts and the internal structures of the dolerite sheets.

In addition, aeromagnetic and drill hole data were used to reconstruct overlapping sill geometries. Both high and low resolution magnetic data proved crucial in visualizing inclined sheets eroded away or obscured on surface. In these images the thick and steeply dipping inclined sheets are easily distinguished from the non-magnetic country rocks and thin dykes. Topographic ridges underlain by inclined sheets with similar dip directions were traced along strike for lateral continuity to establish their overall outline and shape. Individual saucers were identified where inclined sheets define inward dipping ring-shaped structures. Percussion boreholes drilled to depths of some 250 m for groundwater studies in the late 1990's by the Council for Geoscience (Chevallier et al., 2001) provided subsurface data on sill depths and thicknesses (Fig. 2).

4. Results

4.1. Dolerite intrusions

4.1.1. Saucer-shaped sills

The Victoria West sill complex consists of no fewer than five individual saucer-shaped sills that form a cluster of nested, overlapping and cross-cutting geometries arranged along a north-westerly trending axis (Fig. 2). Saucer-shaped sills in the area are composed of bedding-parallel inner and outer sills connected by transgressive inclined sheets. Saucers are exposed at different stratigraphic levels within the south-east dipping Beaufort Group sediments. We refer to the stratigraphically higher level structures as sills 1 and 4, while lower level structures are termed sills 2, 3 and 5 (Fig. 3). Lower level saucers, with the exception of the smaller sill 2, generally represent elongated shapes with larger diameters (37.0–46.5 km) to that of the overlying, more circular saucers (20.3 × 33.5 km) (see Table 1 for structural data). However, the increased thickness (60–100 m) of sills 1 and 4 accentuates their regional dominance and exposure in the field compared to the much thinner (5–15 m) sills 2, 3 and 5 (Figs. 2 and 3).

Drill holes indicate the sub-surface occurrence of inner sills at

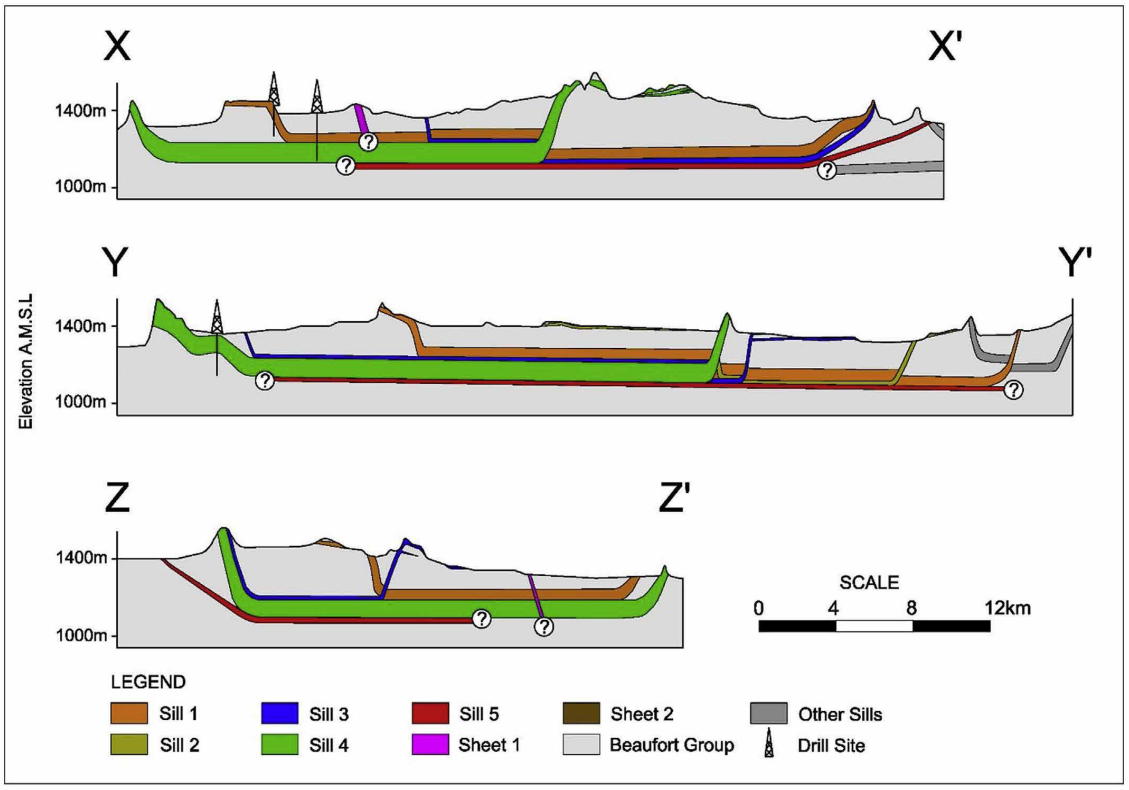

Fig. 3. Cross-sections along lines X-X′, Y–Y′ and Z-Z′ as shown in Fig. 2.

depths between 30 m and 200 m, with the exception of the outcropping dome-like structure along the north-western rim of sill 4 (Figs. 2 and 3). The areal extent of each inner sill is defined by the commonly well-preserved bounding inclined sheets that extend upwards at angles up to 35° (Fig. 4a). Drill-hole intersections show the transition from inner sill to inclined sheet coincides with a significant drop in thickness, particularly along sills 1 and 4, by as much as 30 m.

Outer sills typically occur as single, gently dipping (< 5°) sheets, but often show a series of flat, concordant segments linked by gently dipping steps cutting through the wall rocks (Fig. 4b). Locally along the intrusion plane, outer sills are developed as thin (< 1 m) concordant sheets that exhibit distinct stepping patterns and blunt terminations (Fig. 4c and d). In places, steps coincide with a marked narrowing in sill width that resembles sill bridges between off-set magma fingers (e.g. Pollard et al., 1975; Nicholson and Pollard, 1985).

4.1.2. Apophyses

Sections across inclined sheets along road cuts typically show the presence of several apophyses parallel or sub-parallel to the main inclined sheets (Fig. 4a, e, 5a). These features are well preserved in outcrop, but are below the resolution of geophysical imagery when they may provide important information about the propagation and growth of inclined sheets in sill complexes. The thin (0.05–1 m) apophyses commonly occur within the footwall rocks adjacent to inclined sheets of saucer-shaped sills (Fig. 4a). Two types of apophyses can be distinguished, including (1) steep dipping (45–55°), single or en-echelon sheet geometries several meters in cross-sectional length and not rooted or connected to adjacent inclined sheets, and (2) shallow dipping (< 45°) short, curved or bulbous structures rooted in inclined sheets (Fig. 4a, e, f). Furthermore, protruding sheets form, in many places, low-angle, cross-cutting steps at bedding planes and taper out, commonly controlled by a single joint plane (Fig. 4a, e, f).

Table 1
Structural data of saucer-shaped sills and curved sheets of the Victoria West sill complex.

Name	Saucer-shaped Sills					Curved Sheets	
	Sill 1	*Sill 2*	*Sill 3*	*Sill 4*	*Sill 5*	*Sheet 1*	*Sheet 2*
Geometry	Circular, rounded	Circular, rounded	Elongated, irregular	Oval, rounded	Elongated, irregular	Curved	Curved
Length (km)	33.5	13.0	32.0	27.0	± 46.5	21.0	22.8
Width (km)	32.5	13.0	20.5	20.3	± 24.3		
Inner sill area (km^2)	765	144	± 395	450	± 890		
Orientation			NW-SE	NW-SE	NW-SE	NE-SW	NE-SW
Thickness (m) [inner sill - inclined sheet]	80–60	< 15	~15	100–70	~8	< 20	< 20

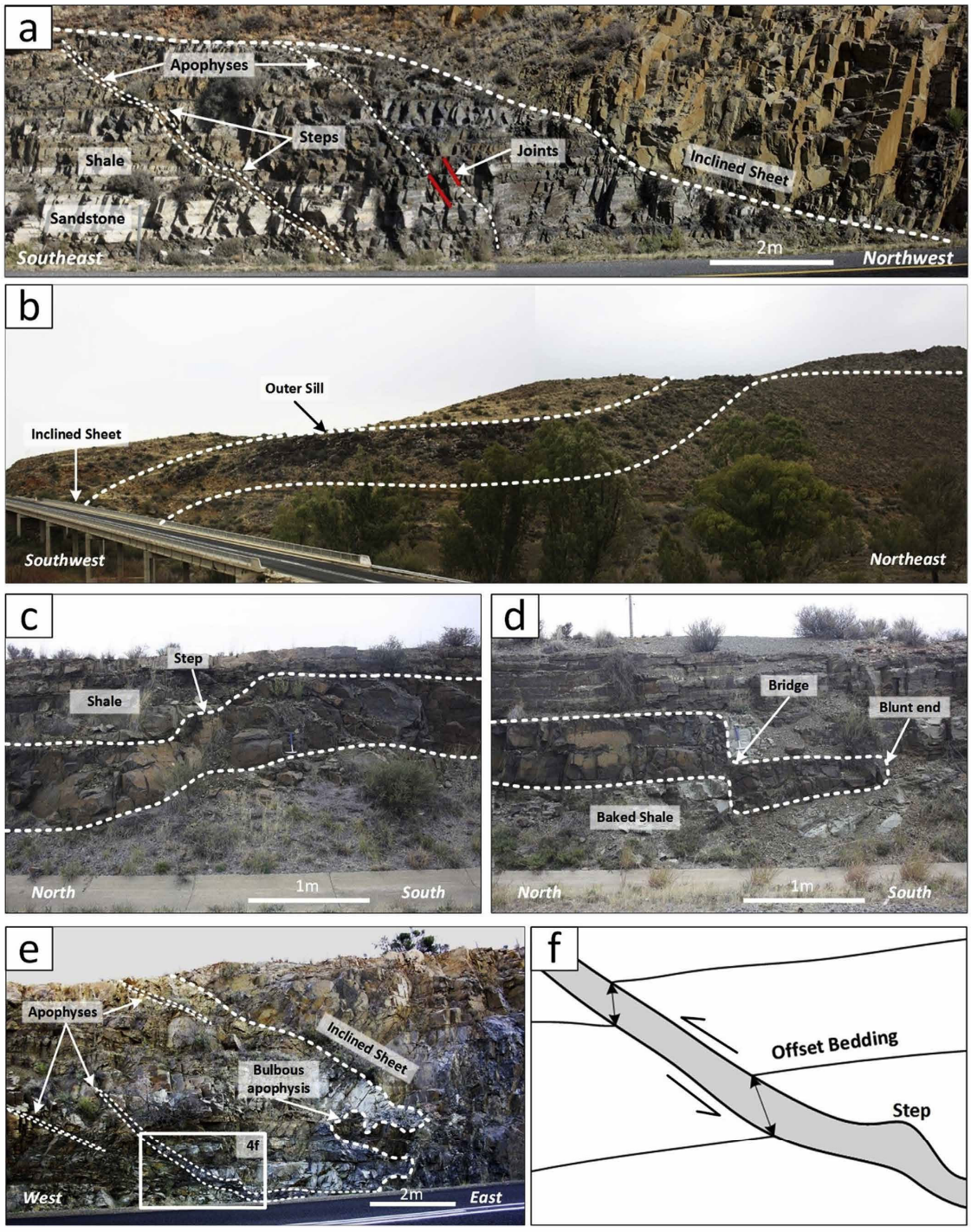

Fig. 4. (a) Footwall contact of sill 4 with planar and en-echelon arrays of apophyses not rooted to the adjacent inclined sheet. (b) Outer sill exposure of sill 4 with concordant segments interchanging with steeper ramps. (c) and (d) Local outer sill geometries of sill 3 showing transgressive steps, bridges and blunt terminations. (e) Footwall contact of sill 4 with several apophyses rooted in the adjacent inclined sheet. (f) An inset of the apophysis in (e) showing the sense of shear (half-arrows) and dilation (double-sided arrows) inferred by the wall rock offset.

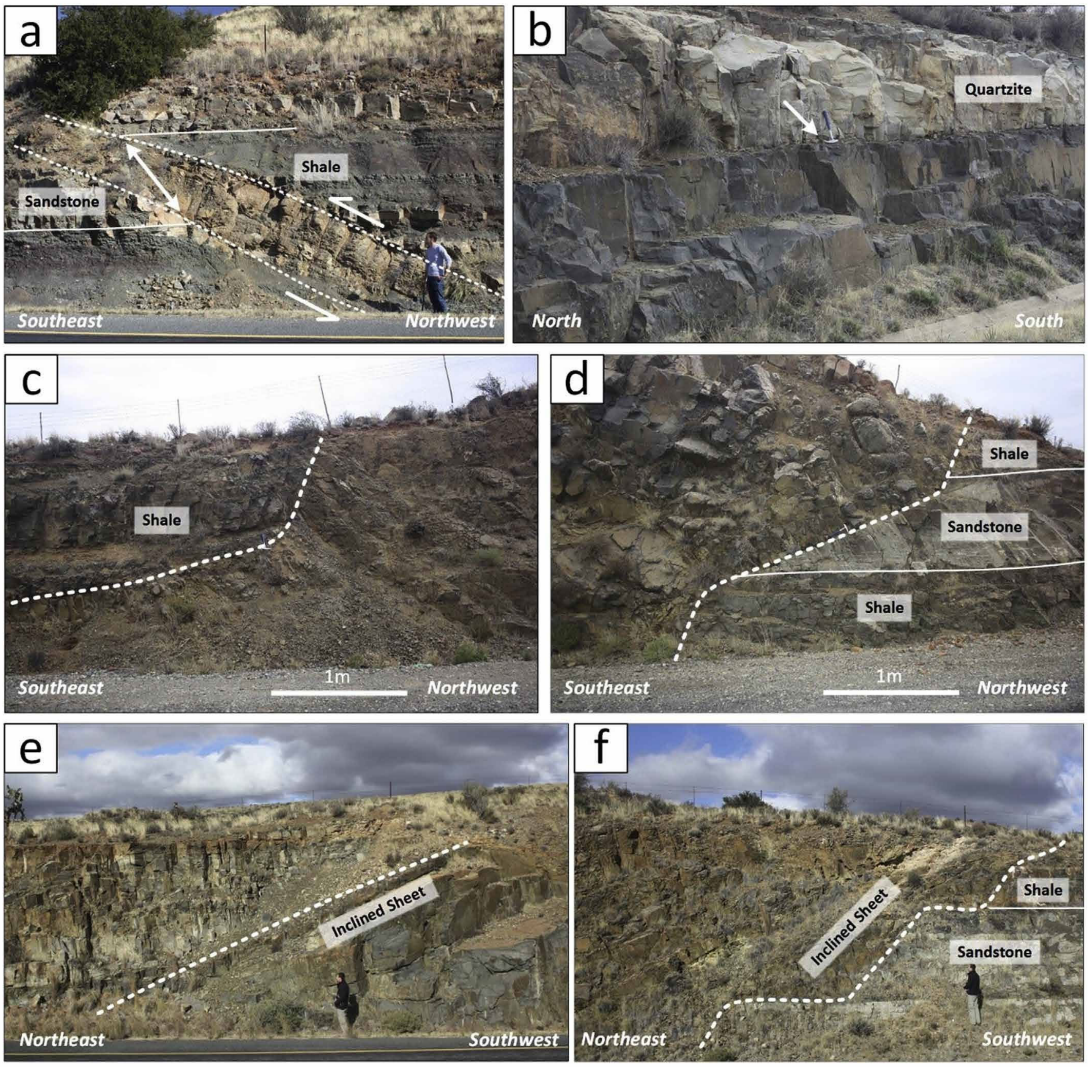

Fig. 5. (a) A single thick (1–2 m) apophysis located tens of meters from the footwall contact of the inclined sheet of sill 4. The sense of shear and dilation is indicated by half- and double-sided arrows respectively based on wall rock offset. (b) Flat outer sill of sill 3 seated along the basal contact of a quartzite unit. (c) Hanging-wall and (d) footwall contact of sheet 2. The dip angle of the footwall contact decreases in sandstone and steepens in shale. (e) Smooth hanging-wall and (f) step-like footwall contact of the inclined sheet of sill 1.

4.1.3. Curved sheets

Two regional, cross-cutting sheets, i.e. sheets 1 and 2 (Fig. 2), do not describe the characteristic ring-like geometry observed for inclined sheets. These sheets are confined to the north-eastern parts of the Victoria West sill complex (Figs. 2 and 3). The sheets form < 20 m thick, south-east dipping (~20° dips) transgressive dolerite sheets (Fig. 5c and d), but without any connection to flat inner or outer sills. Outcrops delineate an overall curved strike extent, some 22.0–23.8 km in length, tapering out laterally to the northeast and southwest (Fig. 2).

4.2. Wall-rock relationships

Cross-sections of sills and sheets along road cuts generally reveal sharp contacts and narrow (< 0.5 m) chilled zones devoid of host rock inclusions, dolerite fragments and calcite veins (Figs. 4 and 5). Wall rocks adjacent to dolerite intrusions lack damage zones and signs of deformation, but display discolouration and recrystallized textures associated with thermal baking along dolerite contacts (Figs. 4d and 5b).

Dolerite sheets commonly exploit specific lithologies or lithological contacts within the host-rock sequence. Flat inner and outer sills are usually confined to shale layers (Fig. 4c and d) and, where exposed, typically beneath prominent quartzite units (Fig. 5b). Transgressive inclined and curved sheets are characterised by distinct hanging-wall and footwall contacts. Hanging- and footwall contacts are typically smooth and cross-cut the country rocks at shallow angles between 24° and 35° (Fig. 5c, e). However, footwall contacts, particularly of sill 1,

occasionally display step-like geometries consisting of bedding-concordant segments along sandstone and shale boundaries alternating with steeper (40–70°) transgressive segments confined to a single lithological unit (Fig. 5d, f). Furthermore, the diverse lithological units exposed along the respective hanging- and footwall contacts (Fig. 5c–f) indicate that inclined sheets formed through the uplift and shear displacement of overlying strata, a fundamental factor in the development of saucer-shaped sills (e.g. Polteau et al., 2008; Galland et al., 2009; Galerne et al., 2011). Shear fractures induced along the peripheries of inner sills and exploited by inclined sheets accommodate uplift equal to the thickness of the inner sill (e.g. Thomson, 2007; Coetzee and Kisters, 2016). Therefore, wall rocks exposed in the hanging-wall next to inclined sheets represents strata at lower stratigraphic levels compared to the adjacent footwall rocks. This shear movement is also evident on a small scale along the intrusion plane of apophyses where host-rocks are typically displaced over distances greater than or equal to their thickness (Figs. 4f and 5a).

4.3. Spatial and temporal relationships

Cross-cutting and overlapping intrusive relationships provide insights into the successive emplacement of sills (Figs. 2 and 3). Sill 1 is, with the exception of sill 5, cross-cut by all other sill structures suggesting an early timing for this saucer. Sill 2 intersects sill 1 to the south while the inclined sheet of sill 3 also transgresses both sill 1 and 2. Likewise, the abrupt change in outcropping rocks found along the eastern and southern reaches of the inclined sheet of sill 4 implies sills 1, 2 and 3 were subsequently truncated and uplifted by sill 4. Sill 5 represents the lower-most saucer that seemingly envelopes the base of sills 1 to 4. The lack of cross-cutting relationship with any other saucer suggests sill 5 represents the youngest sill of the Victoria West complex. While the intersection of sheets 1 and 2 with sill 1 reveal a later timing for these intrusions (Fig. 2), their emplacement age relative to the other sills is not clear due to their restricted occurrence within the sill complex.

To summarize, sill 1 represents the first dolerite intrusion followed consecutively by sill 2, sill 3, sill 4 and sill 5 as the youngest intrusive while the exact emplacement age of the two curved sheets remain uncertain.

4.4. Sill nesting

Field relationships and drill hole data allow for the reconstruction of the likely three-dimensional structure of the stacked sills and curved sheets (Fig. 6) and, based on their saucer-shaped geometry, the likely, although inferred, position of feeders to the sills. The midpoints of the sills are clustered along a north-western axis over a distance of some 20 km (Fig. 6). Sills 1 and 5 coincide near the centre of the study area while the midpoints of sills 2 and 3 are located 5–7 km to the southeast and southwest, respectively. Sill 4 is more isolated and occurs some 10 km towards the northwest. Conversely, the isolated occurrence of the curved sheets (sheets 1 and 2), seemingly without connections to inner or outer sills, suggest a different emplacement style to the sills of the main Victoria West sill complex.

5. Discussion

5.1. Emplacement controls – rigidity contrasts and stress barriers

The Victoria West sill complex shares many similarities with sill complexes described from elsewhere in the Karoo (Chevallier and Woodford, 1999; Galerne et al., 2011). The sills highlight the role of the subhorizontal, well-stratified Karoo wall-rock sequence for dolerite emplacement, both on a regional (Figs. 2 and 3) and local scale (Figs. 4 and 5). Numerical, experimental and field studies have demonstrated the significance of compositional heterogeneities of layered host rocks for the changeover from steep feeder structures to subhorizontal, bedding-parallel sills, the so-called dyke-sill transition (e.g., Gudmundsson, 1995, 2011; Gudmundsson and Brenner, 2001; Kavanagh et al., 2006; Menand et al., 2010; Rivalta et al., 2015). Magma ascent though the crust is fracture controlled (Clemens and Mawer, 1992; Gudmundsson, 1995). In homogeneous rocks, the propagation of magmatic feeder dykes or sheets depends primarily on the regional stress field, the driving magma pressure and the magnitude and orientation of tensile stresses at the fracture tip of the magma-filled fracture (hydrofracture) (Pollard and Holzhausen, 1979; Gudmundsson, 2006). In a horizontal sedimentary sequence, layers with different mechanical properties exert a significant control on the propagation path of feeder dykes or inclined sheets. These mechanical variations may promote or arrest and/or deflect the propagation of magma feeders. There are three main factors that are considered to promote the deflection of steep magma feeders into sills; namely (1) discontinuities, such as bedding planes, (2) abrupt changes in rigidity (or stiffness, or Young's Modulus, E) between adjacent layers, and (3) stress barriers, where elevated compressive stresses in rigid layers compared to softer layers inhibit further vertical propagation of the magma-filled fracture (Kavanagh et al., 2006; Menand, 2008; Gudmundsson, 2011). Hooke's law formulates a linear relationship between strain and stress that depends on the respective rigidity (E) of rocks. Layers with a higher rigidity in a horizontally layered sequence undergoing layer-parallel shortening, experience larger stresses than less rigid or softer layers (Kavanagh et al., 2006; Gudmundsson and Philipp, 2006; Gudmundsson, 2011). Under such conditions, the vertical propagation of a feeder is inhibited if compressive stresses in the relatively stiff layers exceed the tensile stresses at the tip of the advancing hydrofracture (stress barrier). As a result, the vertical magma feeder may be arrested and/or deflected along the interface between layers with pronounced differences in rigidity. The formation of sills is facilitated by the presence of well-developed bedding anisotropies (discontinuities) and extensional fracturing parallel to regional subhorizontal shortening. Hence, it is commonly the combination of these three processes - the presence of discontinuities, rigidity contrasts between layers and stress barriers – that contribute to the dyke-sill transition (Kavanagh et al., 2006; Menand, 2008; Menand et al., 2010; Gudmundsson, 2011; Rivalta et al., 2015).

Cross-cutting relationships demonstrate the progressive growth of the Victoria sill complex through the underaccretion of successively emplaced magma batches tightly below earlier emplaced sills (Fig. 3). The controls of the earliest emplaced sill 1 on the emplacement of subsequent sills is particularly prominent in the two north and northwest trending sections (Fig. 3, X-X′ and Y–Y′), more or less parallel to the long axis of the complex. While Young's moduli of rocks show a large range between < 1 to ca. 100 GPa (Palmström and Singh, 2001), the rigidity of dolerite (30–100 GPa) is considerably higher compared to that of sandstone (15–50 GPa) and shale (5–30 GPa), with shale being the softest of the three main units in the Victoria West area. This may explain the consistent underaccretion of magma batches and underlines the role of pronounced differences in rigidity and/or stress barriers as the main factors for the dyke-sill transition. The magmatic underaccretion also accounts for the characteristic nested structure of the saucer-shaped sills and the displacement and uplift of sedimentary strata above the composite sill complex (Fig. 2). The significance of stress barriers for sill emplacement also agrees with the observation that localised sill outcrops are typically capped by sandstones along the sandstone-shale interface (Fig. 5b).

Importantly, rigid layers in a horizontal sequence only act as stress barriers under horizontal compression. When a layered sequence experiences horizontal extension, the decrease in compressive stress in the rigid layers is greater than that in softer layers so that rigid layers facilitate the propagation of vertical hydrofractures and the dyke-sill transition is promoted in softer layers (e.g. Gudmundsson, 1995; 2011; Gudmundsson and Brenner, 2001). This implies an emplacement of the Victoria West complex under very low deviatoric stresses or in a mildly

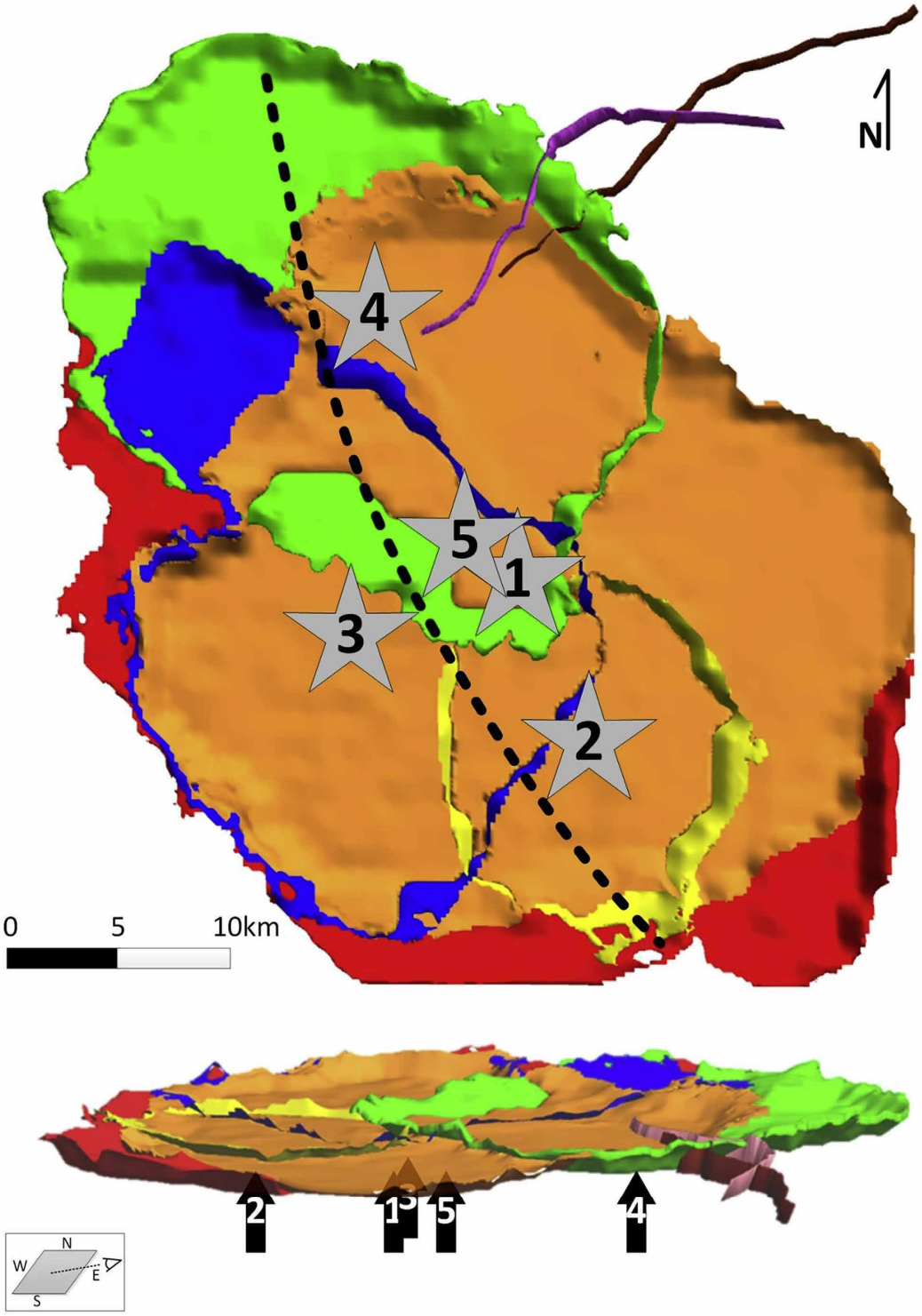

Fig. 6. A three-dimensional illustration of the Victoria West sills and curved sheets with stars/arrows showing the underlying feeder connections and their emplacement sequence. The broken line delineates the curvature of a possible underlying feeder sheet.

compressional stress regime. The implications of this are discussed further below.

5.2. Inclined sheets and apophyses

The growth of saucer-shaped sills is well demonstrated and interpreted to occur through a number of distinct stages, starting with the emplacement of the basal inner sill, followed by the formation of the transgressive inclined sheet and later flat outer sill (Malthe-Sørenssen et al., 2004; Kavanagh et al., 2006; Mathieu et al., 2008; Polteau et al., 2008; Galland et al., 2009; Galerne et al., 2011; Magee et al., 2016). Concordant inner and outer sills are largely controlled by host rock anisotropies (Kavanagh et al., 2006; Menand, 2008; Gudmundsson, 2011) and, in the case of the Victoria West complex, by earlier emplaced sills. Inclined sheets represent the infill of shear fractures formed along the periphery of the inner sill due to doming and shear failure of the overburden rocks during sill inflation and propagation (Pollard, 1973; Pollard and Johnson, 1973; Thomson and Hutton, 2004; Goulty and Schofield, 2008; Galland et al., 2009; Galerne et al., 2011; Montanari et al., 2017).

The apparent mismatch between stepped footwall and smooth hangingwall contacts along some inclined sheets, particularly that of sill 1 (Fig. 5f), is at variance with the typically planar inclined sheet surfaces observed elsewhere in the Victoria West area and the wider Karoo basin (e.g. Galerne et al., 2011; Schofield et al., 2010). Furthermore, the general lack of xenoliths or wall rock fragments within inclined sheets suggests magma stoping has very little effect on the geometry of wall rock contacts. While, the emplacement mechanism whereby shear fractures are formed and subsequently infilled by magma are not usually associated with step-like contacts, the presence of rigidity contrasts in the stratigraphic sequence during regional shortening may lead to a strain refraction that causes propagating shear fractures to deviate from their usual linear paths. The deflection of subvertical shear fractures in weaker shale units into parallelism with rigid sandstone layers may create step-like magma propagation paths (Fig. 8a). Once reverse displacement and dilation takes place along the fracture surfaces, the hanging-wall separates and moves upward relative to the footwall (Fig. 8b) creating a disconnect between the in-situ step-like footwall contact and the now corresponding smooth hangingwall contact. Conversely, upwards displacement of the hanging wall creates an inverse contact relationship at higher stratigraphic levels with a step-like hanging-wall contact next to a smooth footwall contact (Fig. 8b).

The general predominance of thick concordant sills in the Victoria West sill complex compared to thinner, low angle transgressive inclined sheets (Table 1) and apophyses (Fig. 4a, e) highlights a preference for horizontal fracture propagation and provides additional evidence for tectonic shortening during the emplacement of sills in the Karoo basin.

Meter-scale apophyses are common in the footwall of inclined sheets and the associated shear displacement (Fig. 4f) suggests that they are related to the formation processes of inclined sheets. Lack of exposure may account for the presence of isolated sheets not connected to the larger inclined sheets (Figs. 4a and 5a), but their steeper dip, longer cross-sectional length and occasional increased thickness indicates the isolated sheets to be related to a more distinct emplacement mechanism compared to their stubby and curved equivalents (Fig. 4e).

Experimental models by Montanari et al. (2017) show that shear failure along the margins of inner sills is rarely restricted to a single fracture or fault. Instead, the stress distribution at the magma front of the inner sill introduces an array of sub-parallel reverse faults that are subsequently exploited by magma (Fig. 7a). A drop in magma pressure and resulting deflation of the inner sill may limit magma breakout to a finite length (Fig. 7b) depending on magma viscosity and the properties of the immediate wall rocks. Once magma pressures have been restored and the inner sill has sufficiently inflated, renewed uplift and arching of overburden rocks may reactivate overlying reverse faults or form new

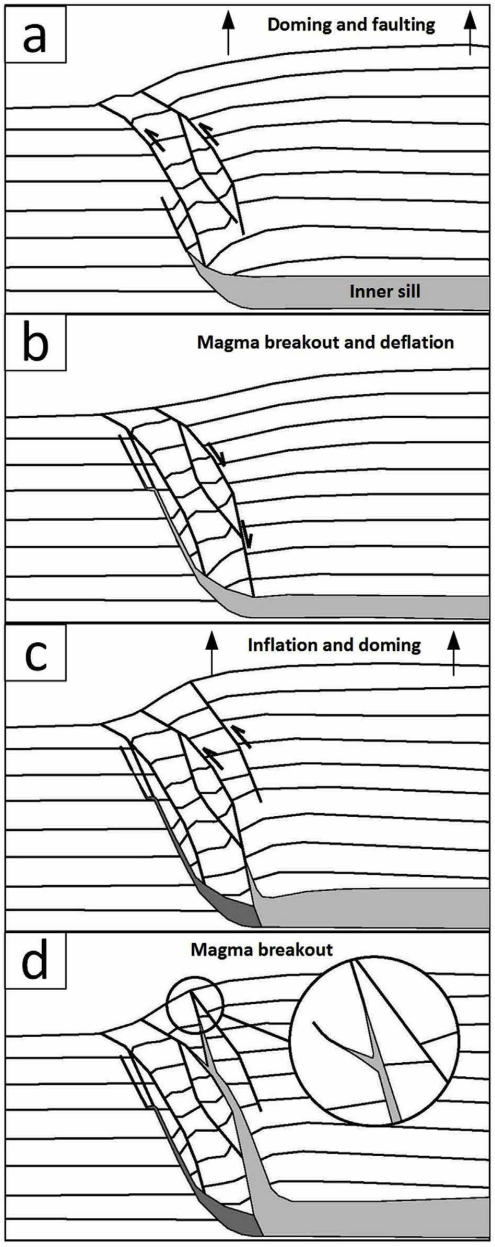

Fig. 7. Diagrammatic sketches illustrating the proposed stages in the development of apophyses in the footwall rocks of inclined sheets. Refer to the text for more information.

fractures that accommodate additional magma breakouts (Fig. 7c) (Pollard, 1973; Pollard and Johnson, 1973; Galland et al., 2009). The periodic inflation and deflation of the inner sill will initiate several magma breakouts that overlie and cut off preceding breakouts (Fig. 7d) until a preferred flow path is established and the main inclined sheet is formed. Unsuccessful or failed flow paths at the inner sill-inclined sheet

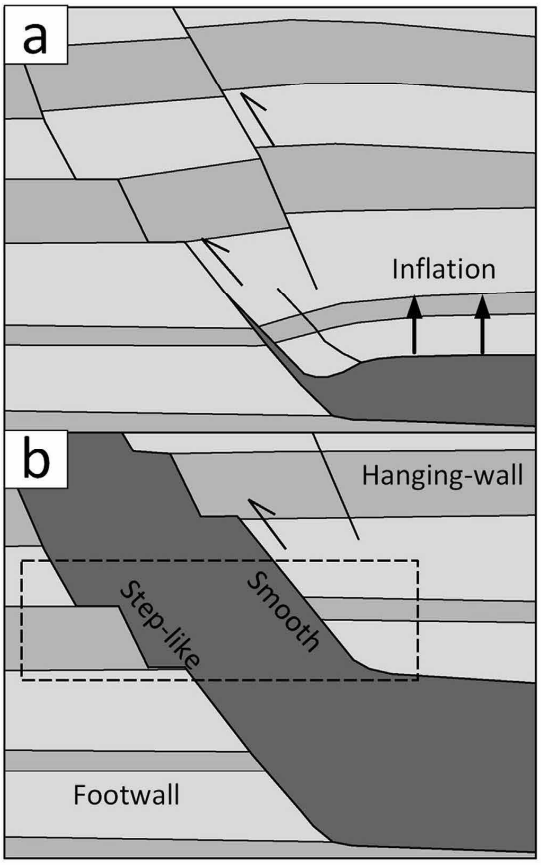

Fig. 8. A diagrammatic sketch illustrating how the infill of shear fractures influenced by layer anisotropies can form inclined sheets seemingly with both smooth and step-like contacts in outcrop exposures.

transition likely represent the longer, steep dipping apophyses (Fig. 7d).

Conversely, the short, curved apophyses protruding directly from inclined sheets (Fig. 4e) are likely related to a more localised emplacement mechanism that arise during the upwards propagation of inclined sheets. The typical divergent extension fractures induced at the tip of an advancing magma front and the preference for one path over the other may produce localised flow paths that are subsequently abandoned (Fig. 7d) (Pollard, 1973; Mathieu et al., 2008). The inflation and growth of the steeper branch at the expense of the shallow dipping branch will consistently produce short apophyses in the footwall rocks (Fig. 7d). Therefore, shear failure at the inner sill boundary likely produce thicker apophyses that extend upwards into the overlying strata whereas splitting of the wall rocks by the advancing inclined sheet generate short, curved apophyses at higher stratigraphic positions.

5.3. Potential sill feeders

The Karoo LIP was constructed through several, spatially distinct and successively emplaced magma pulses (Marsh, 1987; Duncan et al., 1997; Jourdan et al., 2007b; Neumann et al., 2011). Even in individual sill complexes, such as the Golden Valley sill complex, geochemical data allows for the distinction of up to six discrete magma batches of which three are preserved in sills and the other three in localised dykes (Galerne et al., 2008). In the Victoria West area, cross-cutting and stacked sill geometries (Figs. 2 and 3) illustrate that each saucer represents a separate intrusive event and the sills document at least five separate magma pulses in the area. The localization of multiple magma batches within an area less than 2000 km^2 also requires a feeder structure that repeatedly accommodated magma ascent. In the thinner stratigraphy of the northern Karoo basin, the base of many saucer-shaped sills is made up of funnel-shaped feeders seated within the Proterozoic basement rocks. In many places, these funnels seem to be controlled by older basement faults and pre-Karoo dykes or dyke swarms. This has been interpreted to indicate the influence and re-utilization of pre-existing structures on magma dispersal controlling the location of magma feeders in the Karoo LIP (Coetzee and Kisters, 2018). However, in the southern parts of the up to 6 km thick Karoo Supergroup, the well-layered, thick sedimentary sequence rather promotes sill-to-sill feeding relationships (e.g. Cartwright and Hansen, 2006; Magee et al., 2014, 2016; Schofield et al., 2017).

Sills 3, 4 and 5 show significant overshoots compared to the topmost sill 1 in the north-westerly direction of the sill complex (Fig. 3, Y–Y'). The distinct north-westerly trend defined by the midpoints of the five saucer-shaped sills likely define the outline of a feeder, such as an inclined sheet of a larger underlying saucer as commonly envisaged for sill-feeding-sill networks (e.g. Magee et al., 2016; Cartwright and Hansen, 2006; Thomson and Schofield, 2008). Notably, the strike of the feeder corresponds to the typical north-northwest trend of other major structures in the central Karoo, such as the Cradock and Golden Valley dykes (Chevallier and Woodford, 1999; Galerne et al., 2008; Neumann et al., 2011). Although these dykes have been shown to be chemically unrelated to the emplacement of surrounding sill complexes, their similar orientation highlight a preferred regional emplacement path that may be linked to the prevailing stress field across the Karoo basin. While the evidence for the location of the feeder is tentative, the successive emplacement and underaccretion of magma batches implies the reutilization of one or very similar feeder pathways over time and even after cooling and solidification of the previous magma batch. This underlines the significance of pre-existing structures such as faults or earlier sheets, dykes and dyke swarms, not only in the basement, but also higher in the stratigraphy, for the emplacement and distribution of Karoo magmatism (Elburg and Goldberg, 2000; Jourdan et al., 2004, 2006; Hastie et al., 2014; Coetzee and Kisters, 2018).

5.4. Regional implications

The actual causes and processes of the break-up of Gondwana and the associated magmatism, whether plume-related (Cox, 1989; White and McKenzie, 1989; Storey et al., 1992; Storey, 1995; Storey and Kyle, 1997; White, 1997; Elliot and Fleming, 2000; Curtis et al., 2008) or associated with regional plate-tectonic processes (Encarnacion et al., 1996; Hawkesworth et al., 1999; Coetzee and Kisters, 2018), are controversially discussed. A number of studies postulate that the actual fragmentation of Gondwana was preceded by regional shortening related to subduction processes along the margins of Gondwana (e.g. Cox, 1992; Grantham, 1996; Grantham et al., 2018).

The growth of the Victoria West sill complex through magmatic underaccretion and the lateral propagation of dolerite sills over tens of kilometres are consistent with an emplacement of the sills during regional subhorizontal, albeit mild, shortening. Dolerite dykes are of mainly localised extent (Fig. 2) and either related to the emplacement of sills (Coetzee and Kisters, 2017) or volumetrically minor compared to the regional sill complexes in the main Karoo basin. The major Okavango, Lebombo and Save dyke swarms occur to the north and east of the main Karoo basin and define a well-developed triple junction centered around Mwanezi in southern Zimbabwe (Fig. 1). While this has commonly been related to their emplacement around a plume head (Cox, 1989; White and McKenzie, 1989; Storey et al., 1992; Storey,

1995; Storey and Kyle, 1997; White, 1997; Curtis et al., 2008), numerous works have also emphasized the controls of pre-existing lithospheric structures, but also fault zones or older dyke swarms on the emplacement of the Karoo dykes (Elburg and Goldberg, 2000; Jourdan et al., 2004, 2006; Hastie et al., 2014).

While speculative, there are two observations that may help explain the different styles of sills versus regional dyke emplacement in different parts of the Karoo LIP. Firstly, the total amount of sills probably accounts for as much as 30% of the Karoo basin's thickness with an estimated volume of ca. 350 000 km^3 (Chevallier and Woodford, 1999; Svensen et al., 2012). Given the sheer volume of Karoo sills and Drakensberg flood basalts, it is conceivable that loading through the mafic magmas and ensuing thermal subsidence led to the flexuring of the lithosphere in the region of the Karoo basin. This effect may have been exacerbated by the extraction and transfer of the mafic magmas from the underlying mantle and into the crust. Secondly, recent high-precision age data (Svensen et al., 2012) also indicate sill emplacement over a very brief period of time (ca. 500 ka) and, by and large, prior to the emplacement of dyke swarms along the margins of the main Karoo basin (Fig. 1). Similarly, the emplacement of some 0.5×10^6 km^3 of Ferrar Group sills and lavas at 183.6 ± 1 Ma across Antarctica would have initiated subsidence, particularly along Dronning Maud Land (Fig. 9) (Encarnacion et al., 1996; Elliot and Fleming, 2000). Thermal subsidence and lithospheric flexure in regions underlain by the Karoo and Beacon Supergroups, respectively, and intruded by sill complexes will induce uplift and extension in the surrounding regions that have not been intruded by large sill complexes. Extensional stresses concentrating along crustal weaknesses such as the cratonic boundaries between south-eastern Africa and Antarctica are likely to have intensified this effect. This may have led to the formation of the northern Lebombo dyke swarms. Similar loading and subsidence in the northern, elongated Kalahari basin created an additional area that further amplified the rift along southeast Africa (Fig. 9). The progressive uplift of the Lebombo region relative to the subsiding sedimentary basins, became the focal point for extensional tectonics and associated magmatism through the emplacement of the Okavango, Save-Limpopo, Underberg and Rooi Rand dyke swarms. Thus, we speculate that in addition to mantle processes, the original basin architecture and later thermal subsidence associated with the emplacement of vast sub-volcanic systems in the upper crust has contributed to the plumbing architecture of the Karoo LIP.

6. Conclusions

The following conclusions can be drawn from this study:

1. The nested structure of the Victoria West sill complex is made up of five distinct, successively emplaced, saucer-shaped sills. Growth of the complex occurred by magmatic underaccretion of later magma batches below earlier emplaced sills.
2. The magmatic underaccretion suggests that earlier sills acted as stress barriers for later sills. This also implies an emplacement of the sill complex under low deviatoric stresses or during mild shortening, prior to Gondwana break-up.

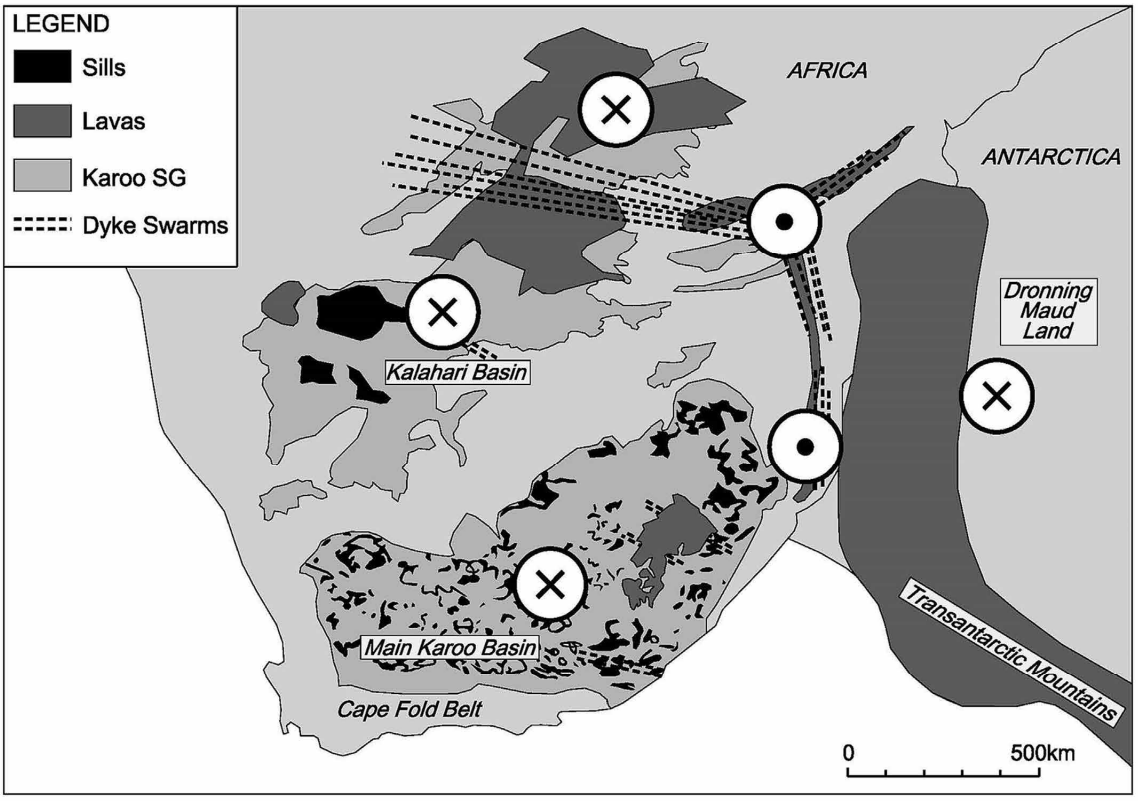

Fig. 9. Gondwana reconstruction showing the likely subsidence associated with mafic intrusive and extrusive rocks in the Karoo and Kalahari basins as well as Donning Maud Land, Antarctica in relation to uplift along the south-eastern margin of Africa.

3. The occurrence of five nested saucer-shaped sills over an area of 2000 km^2 indicates the repeated reactivation of feeder structures, probably through sill-feeding-sill networks, even after full crystallization of earlier magma batches. This agrees with findings from studies elsewhere in the Karoo LIP that emphasize the significance of pre-existing structures for the dispersal of the Karoo magmatism (e.g., Elburg and Goldberg, 2000; Jourdan et al., 2006; Coetzee and Kisters, 2018).
4. Dolerite apophyses are common in the footwall of inclined sheets around inner sills. The apophyses are interpreted to represent earlier used, but failed arms intruded into shear fractures along the fronts of the propagating inner sills that did not grow into fully developed inclined sheets. The abandonment of the apophyses points to a trial-and-error mechanism of sheet propagation.
5. The spatial disconnect between sills and dyke swarms in the Karoo LIP may be the result of the lithospheric loading and flexuring caused by the sheer volume and thermal subsidence of earlier emplaced sills in the main Karoo basin. Thermal subsidence in the central parts of the basins and associated lithospheric flexure and extension along the margins of the basins has led to a swap of the regional stress field and the emplacement of dyke swarms surrounding the main Karoo basin. This would imply that the mode of occurrence of the mafic Karoo magmatism – sills versus dyke swarms – is also determined by the inherited basin and lithospheric architecture.

Acknowledgements

We would like to express our gratitude to the Council for Geoscience for the sharing of historical data without which this study would not have been possible. We particularly want to thank the farm owners of Ganskraal and Jasfontein for their assistance in accessing study sites. We acknowledge the contribution of the anonymous reviewers in improving the content of the paper.

Appendix A. Supplementary data

Supplementary data to this article can be found online at https://doi.org/10.1016/j.jafrearsci.2019.103517.

References

Bernet, M., Gaupp, R., 2005. Diagenetic history of triassic sandstone from the Beacon Supergroup in central Victoria land, Antarctica. N. Z. J. Geol. Geophys. 48, 447–458.
Cartwright, J., Hansen, D.M., 2006. Magma transport through the crust via interconnected sill complexes. Geology 34, 929–932. Basin Res. 10, 417–439.
Catuneanu, O., 2004a. Retroarc foreland systems—evolution through time. J. Afr. Earth Sci. 38, 225–242.
Catuneanu, O., 2004b. Basement control on flexural profiles and the distribution of foreland facies: the Dwyka Group of the Karoo Basin, South Africa. Geology 32, 517–520.
Catuneanu, O., Hancox, P.J., Rubidge, B.S., 1998. Reciprocal Flexural Behaviour and Contrasting Stratigraphies: a New Basin Development Model for the Karoo Retroarc Foreland System, South Africa.
Catuneanu, O., Wopfner, H., Eriksson, P.G., Cairncross, B., Rubidge, B.S., Smith, R.M.H., Hancox, P.J., 2005. The Karoo basins of south-central Africa. J. Afr. Earth Sci. 43, 211–253.
Chevallier, L., Woodford, A., 1999. Morpho-tectonics and mechanism of emplacement of the dolerite rings and sills of the western Karoo, South Africa. S. Afr. J. Geol. 102, 43–54.
Chevallier, L., Goedhart, M., Woodford, A.C., 2001. The Influences of Dolerite Sill and Ring Complexes on the Occurrence of Groundwater in Karoo Fractured Aquifers: A Morpho-Tectonic Approach. Water Resource Commission Reports. WRC Report No. 937/1/01: 165.
Clemens, J.C., Mawer, C.K., 1992. Granitic magma transport by fracture propagation. Tectonophysics 204, 339–360.
Coetzee, A., Kisters, A.F.M., 2016. The 3D geometry of regional-scale dolerite saucer complexes and their feeders in the Secunda Complex, Karoo basin. J. Volcanol. Geotherm. Res. 317, 66–79.
Coetzee, A., Kisters, A.F.M., 2017. Dyke-sill relationships in Karoo dolerites as indicators of propagation and emplacement processes of mafic magmas in the shallow crust. J. Struct. Geol. 97, 172–188.
Coetzee, A., Kisters, A.F.M., 2018. The elusive feeders of the Karoo Large Igneous Province and their structural controls. Tectonophysics 747, 146–162.
Cox, K.G., 1989. The role of mantle plumes in the development of continental drainage patterns. Nature 342, 873–877.
Cox, K.G., 1992. Karoo igneous activity, and the early stages of the break-up of Gondwanaland. In: In: Storey, B.C., Alabaster, T., Pankhurst, R.J. (Eds.), Magmatism and the Causes of Continental Break-Up, vol. 68. Geological Society of London Special Publication, pp. 37–148.
Curtis, M.L., Riley, T.R., Owens, W.H., Leat, P.T., Duncan, R.A., 2008. The form, distribution and anisotropy of magnetic susceptibility of Jurassic dykes in H.U. Sverdrupfjella, Dronning Maud Land, Antarctica. Implications for dyke swarm emplacement. J. Struct. Geol. 30, 1429–1447.
Duncan, R.A., Hooper, P.R., Rehacek, J., Marsh, J.S., Duncan, A.R., 1997. The timing and duration of the Karoo igneous event, southern Gondwanaland. J. Geophys. Res. 102, 18127–18138.
Elburg, M., Goldberg, A., 2000. Age and geochemistry of Karoo dolerite dykes from northeast Botswana. J. Afr. Earth Sci. 31, 539–554.
Elliot, D.H., Fleming, T.H., 2000. Weddell triple junction: the principal focus of Ferrar and Karoo magmatism during initial breakup of Gondwana. Geology 28, 539–542.
Elliot, D.H., Grimes, C.G., 2011. Triassic and Jurassic strata at Coombs Hills, south Victoria Land: stratigraphy, petrology and cross-cutting breccia pipes. Antarct. Sci. 23 (3), 268–280.
Encarnacion, J., Fleming, T.H., Elliot, D.H., Eales, H.V., 1996. Synchronous emplacement of Ferrar and Karoo dolerites and the early break-up of Gondwana. Geology 24, 535–538.
Galerne, C.Y., Neumann, E., Planke, S., 2008. Emplacement mechanisms of sill complexes: information from the geochemical architecture of the golden valley sill complex, South Africa. J. Volcanol. Geotherm. Res. 177, 425–440.
Galerne, C.Y., Galland, O., Neumann, E., Planke, S., 2011. 3D relationships between sills and their feeders: evidence from the Golden Valley Sill Complex (Karoo basin) and experimental modelling. J. Volcanol. Geotherm. Res. 202, 189–199.
Galland, O., Planke, S., Neumann, E.R., Malthe-Sørenssen, A., 2009. Experimental modelling of shallow magma emplacement: application to saucer-shaped intrusions. Earth Planet. Sci. Lett. 277, 373–383.
Goulty, N.R., Schofield, N., 2008. Implications of simple flexure theory for the formation of saucer-shaped sills. J. Struct. Geol. 30, 812–817.
Grantham, G.H., 1996. Aspects of jurassic magmatism and faulting in western dronning Maud land, Antarctica: implications for Gondwana breakup. In: In: Storey, B.C., King, E.C., Livermore, R.A. (Eds.), Weddell Sea Tectonics and Gondwana Break-Up, vol. 108. Geological Society Special Publication, pp. 63–71.
Grantham, G.H., Eglington, B.M., Macey, P.H., Ingram, B.A., Rademeyer, M., Kaiden, H., Manhica, V., 2018. The chemistry of Karoo-age andesitic lavas along the northern Mozambique coast, southern Africa and possible implications for Gondwana breakup. S. Afr. J. Geol. 121, 3.
Gresse, P.G., Theron, J.N., Fitch, F.J., Miller, J.A., 1992. Tectonic inversion and radiometric resetting of the basement in the Cape Fold Belt. In: de Wit, M.J., Ransome, I.G.D. (Eds.), Inversion Tectonics of the Cape Fold Belt, Karoo and Cretaceous Basins of Southern Africa. Balkema, Rotterdam, Netherlands, pp. 217–228.
Gudmundsson, A., 1995. Infrastructure and mechanics of volcanic systems in Iceland. J. Volcanol. Geotherm. Res. 64, 1–22.
Gudmundsson, A., 2006. How local stresses control magma-chamber ruptures, dyke injections, and eruptions in composite volcanoes. Earth Sci. Rev. 79, 1–31.
Gudmundsson, A., 2011. Deflection of dykes into sills at discontinuities and magma-chamber formation. Tectonophysics 500, 50–64.
Gudmundsson, A., Brenner, S.L., 2001. How hydrofractures become arrested. Terra. Nova 13, 456–462.
Gudmundsson, A., Philipp, S.L., 2006. How local stress fields prevent volcanic eruptions. J. Volcanol. Geotherm. Res. 158, 257–268.
Hälbich, I.W., Cornell, D.H., 1983. Metamorphic history of the Cape fold belt. In: In: Söhnge, A.P.G., Hälbich, I.W. (Eds.), Geodynamics of the Cape Fold Belt, vol. 12. Special Publications of the Geological Society of South Africa, Johannesburg, pp. 131–148.
Hälbich, I.W., Fitch, F.J., Miller, J.A., 1983. Dating the Cape orogeny. In: In: Söhnge, A.P.G., Hälbich, I.W. (Eds.), Geodynamics of the Cape Fold Belt, vol. 12. Special Publications of the Geological Society of South Africa, Johannesburg, pp. 75–100.
Hansma, J., Tohver, E., Schrank, C., Jourdan, F., Adams, D., 2015. The timing of the Cape orogeny: new 40Ar/39Ar age constraints on deformation and cooling of the Cape fold belt, South Africa. Gondwana Res. 32, 122–137.
Hastie, W.W., Watkeys, M.K., Aubourg, C., 2011. Significance of magnetic and petrofabric in Karoo-feeder dykes, northern Lebombo. Tectonophysics 513, 96–111.
Hastie, W.W., Watkeys, M.K., Aubourg, C., 2014. Magma flow in dyke swarms of the Karoo LIP: implications for the mantle plume hypothesis. Gondwana Res. 25, 736–755.
Hawkesworth, C., Kelley, S., Turner, S., Le Roex, A., Storey, B., 1999. Mantle processes during Gondwana break-up and dispersal. J. Afr. Earth Sci. 28, 239–261.
Jourdan, F., Féraud, G., Bertrand, H., Kampunzu, A.B., Tshoso, G., Le Gall, B., Tiercelin, J.J., Capiez, P., 2004. The Karoo triple junction questioned: evidence from 40Ar/39Ar Jurassic and Proterozoic ages and geochemistry of the Okavango dike swarm (Botswana). Earth Planet. Sci. Lett. 222, 989–1006.
Jourdan, F., Féraud, G., Bertrand, H., Kampunzu, A.B., Tshoso, G., Watkeys, M.K., Le Gall, B., 2005. The Karoo large igneous province: brevity, origin, and relation with mass extinction questioned by new 40Ar/39Ar age data. Geology 33, 745–748.
Jourdan, F., Féraud, G., Bertrand, H., Watkeys, M.K., Kampunzu, A.B., Le Gall, B., 2006. Basement control on dyke distribution in Large Igneous Provinces: case study of the Karoo triple junction. Earth Planet. Sci. Lett. 241, 307–322.
Jourdan, F., Fe´raud, G., Bertrand, H., Watkeys, M.K., Renne, P.R., 2007a. Distinct brief major events in the Karoo large igneous province clarified by new 40Ar/39Ar ages on

the Lesotho basalts. Lithos 98, 195–209.
Jourdan, F., Féraud, G., Bertrand, H., Watkeys, M.K., 2007b. From flood basalts to the inception of oceanization: example from the 40Ar/39Ar high-resolution picture of the Karoo large igneous province. Geochem. Geophys. Geosyst. 8, 989–1006.
Jourdan, F., Feraud, G., Bertrand, H., Watkeys, M.K., Renne, P.R., 2008. The 40Ar/39Ar ages of the sill complex of the Karoo large igneous province: Implications for the Pliensbachian-Toarcian climate change. Geochem. Geophys. Geosyst. 9.
Kavanagh, J.L., Menand, T., Sparks, R.S.J., 2006. An experimental investigation of sill formation and ropagation in layered elastic media. Earth Planet. Sci. Lett. 245, 799–813.
Klausen, M.B., 2009. The Lebombo monocline and associated feeder dyke swarm: diagnostic of a successful and highly volcanic rifted margin? Tectonophysics 468, 42–62.
Le Gall, B., Tshoso, G., Jourdan, F., Fe´raud, G., Bertrand, H., Tiercelin, J.J., Kampunzu, A.B., Modisi, M.P., Dyment, M., Maia, J., 2002. 40Ar/39Ar geochronology and structural data from the giant Okavango and related mafic dike swarms, Karoo igneous province, Botswana. Earth Planet. Sci. Lett. 202, 595–606.
Le Gall, B., Tshoso, G., Dyment, J., Kampunzu, A.B., Jourdan, F., Feraud, G., Bertrand, H., Aubourg, C., Vetel, W., 2005. The Okavango giant mafic dyke swarm (NE Botswana): its structural significance within the Karoo Large Igneous Province. J. Struct. Geol. 27, 2234–2255.
Magee, C., Jackson, C.A.L., Schofield, N., 2014. Diachronous sub-volcanic intrusion along deep-water margins: insights fromthe Irish Rockall basin. Basin Res. 26, 85–105.
Magee, C.J., Muirhead, J.D., Karvelas, A., Holford, S.P., Jackson, C.A.L., Bastow, I.D., Schofield, N., Stevenson, C.S.T., McLean, C., McCarthy, W., Shtukert, O., 2016. Lateral magma flow in mafic sill complexes. Geosphere 12 (3), 809–841.
Malthe-Sørenssen, A., Planke, S., Svensen, H., Jamtveit, B., 2004. Formation of saucer-shaped sills. In: In: Breitkreuz, C., Petford, N. (Eds.), Physical Geology of High-Level Magmatic Systems, vol. 234. Geological Society, London, Special Publications, pp. 215–227.
Marsh, J.S., 1987. Basalt geochemistry and tectonic discrimination within continental flood basalt provinces. J. Volcanol. Geotherm. 32, 35–49.
Mathieu, L., Van Wyk de Vries, B., Holohan, E.P., Troll, V.R., 2008. Dykes, cups, saucers and sills: analogue experiments on magma intrusion into brittle rocks. Earth Planet. Sci. Lett. 271, 1–13.
Menand, T., 2008. The mechanics and dynamics of sills in layered elastic rocks and their implications for the growth of laccoliths and other igneous complexes. Earth and Planetary Letters 267, 93–99.
Menand, T., Daniels, K.A., Benghiat, P., 2010. Dyke propagation and sill formation in a compressive tectonic environment. J. Geophys. Res. 115, b08201.
Montanari, D., Bonini, M., Corti, G., Agostini, A., Del Ventisette, C., 2017. Forced folding above shallowmagma intrusions: insights on supercritical fluid flow from analogue modelling. J. Volcanol. Geotherm. Res. 345, 67–80.
Neumann, E., Svensen, H., Galerne, C.Y., Planke, S., 2011. Multistage evolution of dolerites in the Karoo large igneous province, Central South Africa. J. Petrol. 52, 959–984.
Nicholson, R., Pollard, D.D., 1985. Dilation and linkage of en echelon cracks. J. Struct. Geol. 5, 583–590.
Palmström, A., Singh, R., 2001. The deformation modulus of rock masses. Tunn. Undergr. Space Technol. 16, 3.
Pollard, D.D., 1973. Derivation and evaluation of a mechanical model for sheet intrusions. Tectonophysics 19, 233–269.
Pollard, D.D., Holzhausen, G., 1979. On the mechanical interaction between a fluid-filled fracture and the earth's surface. Tectonophysics 53, 27–57.
Pollard, D.D., Johnson, A.M., 1973. Mechanics of growth of some laccolithic intrusions in the Henry Mountains, Utah, II. Bending and failure of overburden layers and sill formation. Tectonophysics 18, 311–354.
Pollard, D.D., Muller, O.H., Dockstader, D.R., 1975. The form and growth of fingered sheet intrusions. Geol. Soc. Am. Bull. 86, 351–363.
Polteau, S., Mazzini, A., Galland, O., Planke, S., Malthe-Sorenssen, A., 2008. Saucer-shaped intrusions: occurrences, emplacement and implications. Earth Planet. Sci. Lett. 266, 195–204.
Riley, T.R., Curtis, M.L., Leat, P.T., Watkeys, M.K., Duncan, R.A., Millar, I.L., Owens, W.H., 2006. Overlap of Karoo and ferrar magma types in KwaZulu-natal, South Africa. J. of Petrography 47 (3), 541–566.
Riley, T.R., Millar, I.L., Watkeys, M.K., Curtis, M.L., Leat, P.T., Klausen, M.B., Fanning, C.M., 2004. U–Pb zircon (SHRIMP)ages for the Lebombo rhyolites, South Africa:refining the duration of Karoo volcanism. J. Geol. Soc. (Lond.) 161, 547–550.
Rivalta, E., Taisne, B., Bunger, A.P., Katz, R.F., 2015. A review of mechanical models of dike propagation: schools of thought, results and future directions. Tectonophysics 638, 1–42.
Schofield, N., Holford, S., Millett, J., Brown, D., Jolley, D., Passey, S.R., Muirhead, D., Grove, C., Magee, C., Murray, J., Hole, M., Jackson, C.A.L., Stevenson, C., 2017. Regional magma plumbing and emplacement mechanisms of the Faroe-Shetland Sill Complex: implications formagma transport and petroleum systems within sedimentary basins. Basin Res. 29, 41–63.
Schofield, N., Stevenson, C., Reston, T., 2010. Magma fingers and host rock fluidization in the emplacement of sills. Geology 38, 63–66.
Smith, R.M.H., Eriksson, P.G., Botha, W.J., 1993. A review of the stratigraphy and sedimentary environments of the Karoo-aged basins of Southern Africa. J. Afr. Earth Sci. 16, 143–169.
Storey, B.C., 1995. The role of mantle plumes in continental breakup: case histories from Gondwanaland. Nature 377, 301–308.
Storey, B.C., Kyle, P.R., 1997. An active mantle mechanism for Gondwana breakup. S. Afr. J. Geol. 100, 283–290.
Storey, B.C., Alabaster, T., Hole, M.J., Pankhurst, R.J., Wever, H.E., 1992. Role of subduction plate boundary forces during the initial stages of Gondwana break-up: evidence from the proto-Pacific margin of Antarctica. In: In: Storey, B.C., Alabaster, T., Pankhurst, R.J. (Eds.), Magmatism and the Causes of Continental Break-Up, vol. 68. Geological Society of London Special Publication, pp. 149–163.
Svensen, H., Sverre, P., Chevallier, L., Malthe-Sørenssen, A., Corfu, F., Jamtveit, B., 2007. Hydrothermal venting of greenhouse gases triggering Early Jurassic global warming. Earth Planet. Sci. Lett. 256, 554–566.
Svensen, H., Corfu, F., Polteau, S., Hammer, O., Planke, S., 2012. Rapid magma emplacement in the Karoo large igneous province. Earth Planet. Sci. Lett. 325–326, 1–9.
Thomson, K., 2007. Determining magma flow in sills, dykes and laccoliths and their implications for sill emplacement mechanisms. Bull. Volcanol. 70, 183–201.
Thomson, K., Hutton, D., 2004. Geometry and growth of sill complexes: insights using 3D seismic from the North Rockall Trough. Bull. Volcanol. 66, 364–375.
Thomson, K., Schofield, N., 2008. Lithological and Structural Controls on the Emplacement and Morphology of Sills in Sedimentary Basins, vol. 302. Geological Society, London, Special Publications, pp. 31–44.
Uken, R., Watkeys, M.K., 1997. An interpretation of mafic dyke swarms and their relationship with major mafic magmatic events on the Kaapvaal Craton and Limpopo Belt. S. Afr. J. Geol. I. 100 (4), 341–348.
Veevers, J.J., Cole, D.I., Cowan, E.J., 1994. Southern Africa: Karoo basin and Cape fold belt. In: Veevers, J.J., Powell, C.McA. (Eds.), Permian-Triassic Pangean Basins and Foldbelts along the Panthalassan Margin of Gondwanaland. Geol. Soc. America, Boulder, Colorado, Memoir 184, pp. 223–279.
White, R.S., 1997. Mantle plume origin for the Karoo and Ventersdorp flood basalts, South Africa. S. Afr. J. Geol. 100, 271–282.
White, R.S., McKenzie, D., 1989. Magmatism at rift zones: the generation of volcanic continental margins and flood basalts. J. Geophys. Res. 94, 7685–7729.

Chapter 6: Spatial variations of sills

This chapter constitutes a presentation of the submitted research paper: ***Spatial variations of sills and implications for magma dispersal across the Karoo basin***[1] by Coetzee and Kisters. The formatting was merely adopted to reflect the journal style and has not been accepted as yet

This paper was first authored by André Coetzee with standard supervision entailing academic guidance and editorial support from Alex Kisters. The following aspects were carried out independently by André Coetzee: (1) field work and data collection, (2) data consolidation, processing and interpretation, (3) preparation and submission of the manuscript.

[1]Coetzee, A., Kisters, A.F.M., in submission to Gondwana Research (assigned manuscript no: GR-S-19-00657). *Spatial variations of sills and implications for magma dispersal across the Karoo basin.*

Gondwana Research: Submitted for review 19 Nov 2019

Gondwana Research

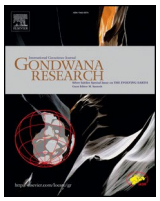

Spatial variations of sills and implications for magma dispersal across the Karoo basin

A. Coetzee[a], A.F.M. Kisters[a]

[a] *Department of Earth Sciences, University of Stellenbosch, Private Bag X1, Stellenbosch 7602, South Africa*

ARTICLE INFO

Article history:
Received 19
November 2019

Keywords:
Saucer-shaped sills
Dolerite intrusions
Sill-fed dykes
Karoo Basin
Dyke patterns

ABSTRACT

The Karoo Large Igneous Province (c. 183 Ma) is dominated by an extensive network of sill complexes, dyke networks, curved sheets and hydrothermal vent structures that show spatially distinct variations throughout the Karoo basin. These variations in emplacement style and size of sills are explained in terms of three main, interrelated factors, namely overburden thickness or emplacement depth, changes in sedimentary facies of the host Karoo Supergroup and feeder proximity. Sills emplaced at shallow depths (<500 m) are confined to the northern extremities of the Karoo basin and typically show small (< 10 km) diameters with thicknesses rarely exceeding 40 m. The shallowly emplaced sills are closely associated with dense, systematic dyke networks developed above the sills. Sills emplaced at intermediate emplacement depths (c. 700 m) in the central Karoo basin are marked by larger diameters (> 30 km) and thicknesses up to 100 m, with more irregular, non-systematic dyke patterns. At greater depths (<2 km) and in the southern parts of the Karoo basin, mega-sills reach diameters of 50 – 80 km and thicknesses of up to 35 m. These deeper seated sills are typically not associated with local dyke networks. The asymmetric distribution of sedimentary facies and southward thickening of formations further influenced sill emplacement processes. Thick shale-rich sequences in the southern Karoo basin facilitate sill emplacement through internal deformation and ductile flow while their thinner more sandstone-rich equivalents in the north involve a component of brittle roof uplift, resulting in thinner sills. Additionally, differential magma pressures and proximity to basement feeders also play a leading role in the emplacement of magma by modifying the spreading rate and inflation of sills. Overall, the rapid emplacement of sills and their dispersed stratigraphic occurrence from the basal Dwyka to the Stormberg Group is more consistent with numerous distributed feeders seated in rocks of the Kalahari craton and Namaqua-Natal metamorphic belt rather than the unidirectional influx of magma related to a mantle plume situated along the east coast of southern Africa.

Introduction

Interconnected sills and sill-saucer structures form the principal dolerite geometries in the main Karoo basin of South Africa intruding the subhorizontal sediments of the Karoo Supergroup over an area in excess of 1000 000 km2 (Chevallier and Woodford, 1999; Galerne et al., 2011; Svensen et al., 2012; Coetzee and Kisters, 2016, 2018; Coetzee et al., 2019). Field and geochronological studies suggest that regional dyke swarms, largely confined to the north-east of the Karoo LIP, are most likely not the feeders to these sill complexes (Encarnacion et al., 1996; Duncan et al., 1997; Jourdan et al., 2004, 2005, 2007a, 2007b, 2008; Riley et al., 2004, 2006; Le Gall et al., 2002; Svensen et al., 2007, 2012; Hastie et al., 2014; Coetzee and Kisters, 2018). Instead, field relationships and flow fabrics in intrusives indicate the presence of several isolated igneous centres emplaced along cratonic boundaries and crustal weaknesses, such as basement faults or older dyke swarms (Hastie et al., 2014; Coetzee and Kisters, 2018). Magma dispersal through numerous, distributed sites across the craton also represents a more efficient feeder system that can account for the rapid emplacement (<500 ka) of the voluminous (>350 000 km3) sills across the main Karoo basin (Duncan et al., 1997; Encarnacion et al., 1996; Jourdan et al., 2008; Svensen et al., 2007, 2012). All this implies that the regional-scale sill complexes were able to accommodate the lateral, long-range transfer and emplacement of the mafic magmas. The sill complexes, thus, represent the backbone of an extensive shallow-crustal magma plumbing system (Duncan et al., 1997; Chevallier and Woodford, 1999; Schofield et al., 2010; Galerne et al., 2011; Svensen et al., 2012; Coetzee and Kisters, 2016, 2018; Coetzee et al., 2019).

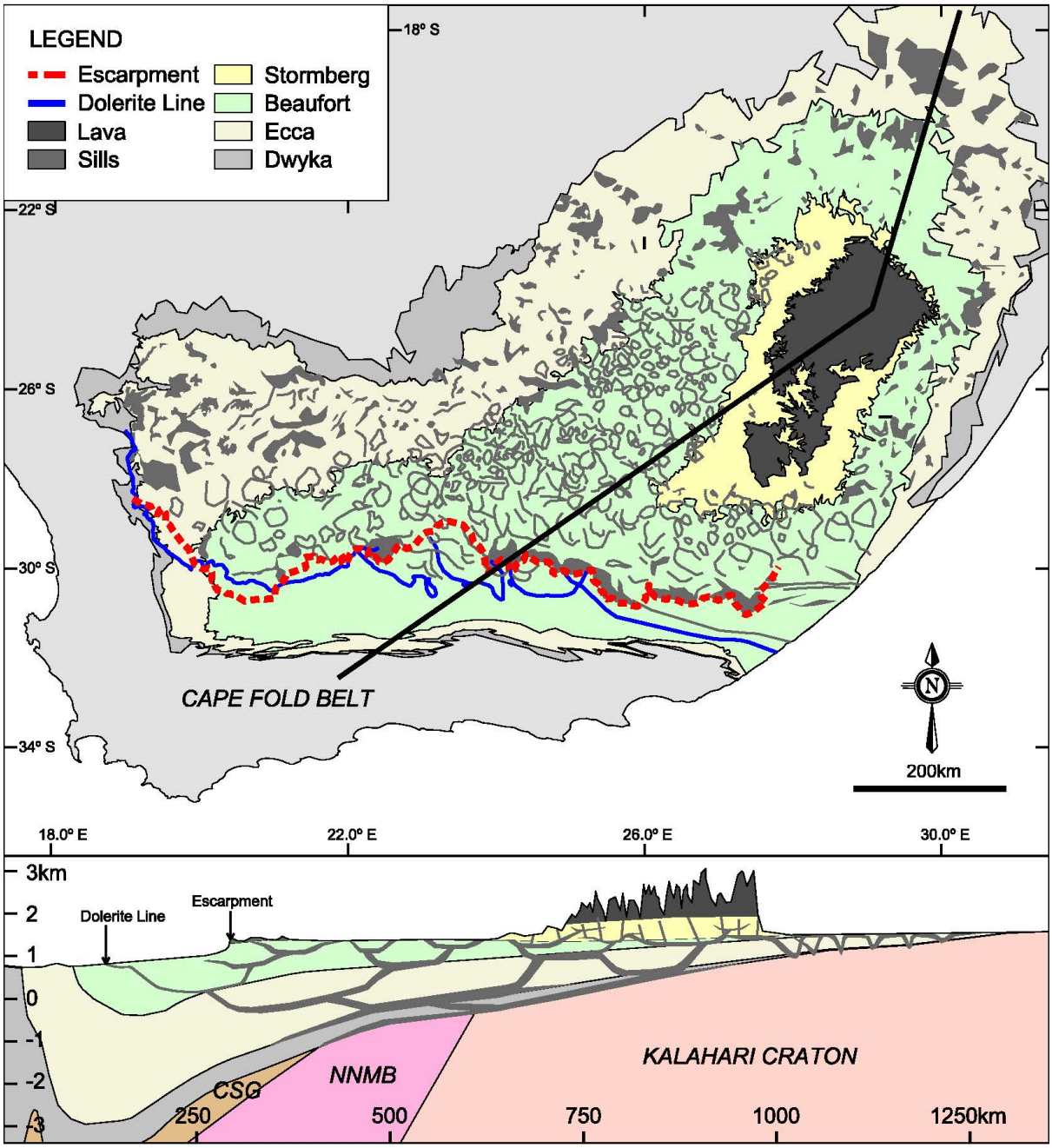

Fig. 1. A geological map of the Karoo basin with a regional cross-section showing the different sill structures from the thin northern extremities to the Cape Fold Belt in the south. CSG – Cape Supergroup, NNMB – Namaqua-Natal Metamorphic Belt.

Studies on the geometry and emplacement of Karoo dolerite sills have traditionally relied on the, in large parts, excellent outcrop conditions in the semi-arid Karoo region. More recently, extensive sub-surface geophysical and drill hole data sets established through mining and exploration provide additional information about the deeper-level geometry and connectivity of this magma plumbing system in the Karoo Supergroup (Encarnacion et al., 1996; Duncan et al., 1997; Uken and Watkeys, 1997; Chevallier and Woodford, 1999; Elburg and Goldberg, 2000; Chevallier et al., 2001; Le Gall et al., 2002, 2005; Jourdan et al., 2004, 2005, 2007a, 2007b, 2008; Riley et al., 2004, 2006; Svensen et al., 2006, 2007, 2012; Klausen, 2009; Hastie et al., 2011, 2014; Scheiber-Enslin et al., 2014; Coetzee and Kisters, 2016, 2017, 2018; Coetzee et al., 2019). The predominance of sills is commonly understood to highlight the role of rigidity contrasts and stress barriers exerted by the Karoo Supergroup as steep basement feeders are interpreted to deflect into subhorizontal sills initiated by the mechanical stratification of the sedimentary succession. Given the pronounced asymmetry of the Karoo basin, thickness and facies variations across the basin, but also the diversity of basement rocks and structures should exert significant controls on sill emplacement. Variations of sill geometries and sizes, feeders and emplacement controls have, to date, not been described when this has clear implications for our understanding of the dispersal of Karoo magmatism on a continental scale. Hence, the main aim of this paper is to describe the geometry of sills and associated structures along a north-south transect across

the Karoo basin. We will also discuss the likely factors that have controlled these variations. We integrate field, geophysical and drill hole data from the northern and central Karoo basin with data from better exposed dolerite structures in the southern Karoo in order to develop a north-south distribution model for the Karoo magmatism.

1. The Karoo basin and Karoo Large Igneous Province

Karoo sills and dykes are intrusive into largely subhorizontal, late Carboniferous to early Jurassic and mainly clastic sedimentary rocks of the Karoo Supergroup. Dramatic thickness and facies variations of the sedimentary succession testify to the pronounced asymmetry of the original Karoo basin (e.g., Johnson, 1991, Catuneanu et al., 1998) with the Karoo Supergroup reaching maximum cumulative thicknesses of > 6 km in the south to pinching out against basement rocks of the Kalahari Craton in the north (Fig. 1). Basement rocks to the Karoo Supergroup are heterogeneous with large variations in age, internal structure and composition across the basin. In the north, the basin is underlain by Archaean TTG-greenstone rocks and Archaean to Proterozoic cover sequences of the Kalahari Craton. In the south, the deeper parts of the basin are made up of Mesoproterozoic gneisses and metasediments of the Namaqua-Natal

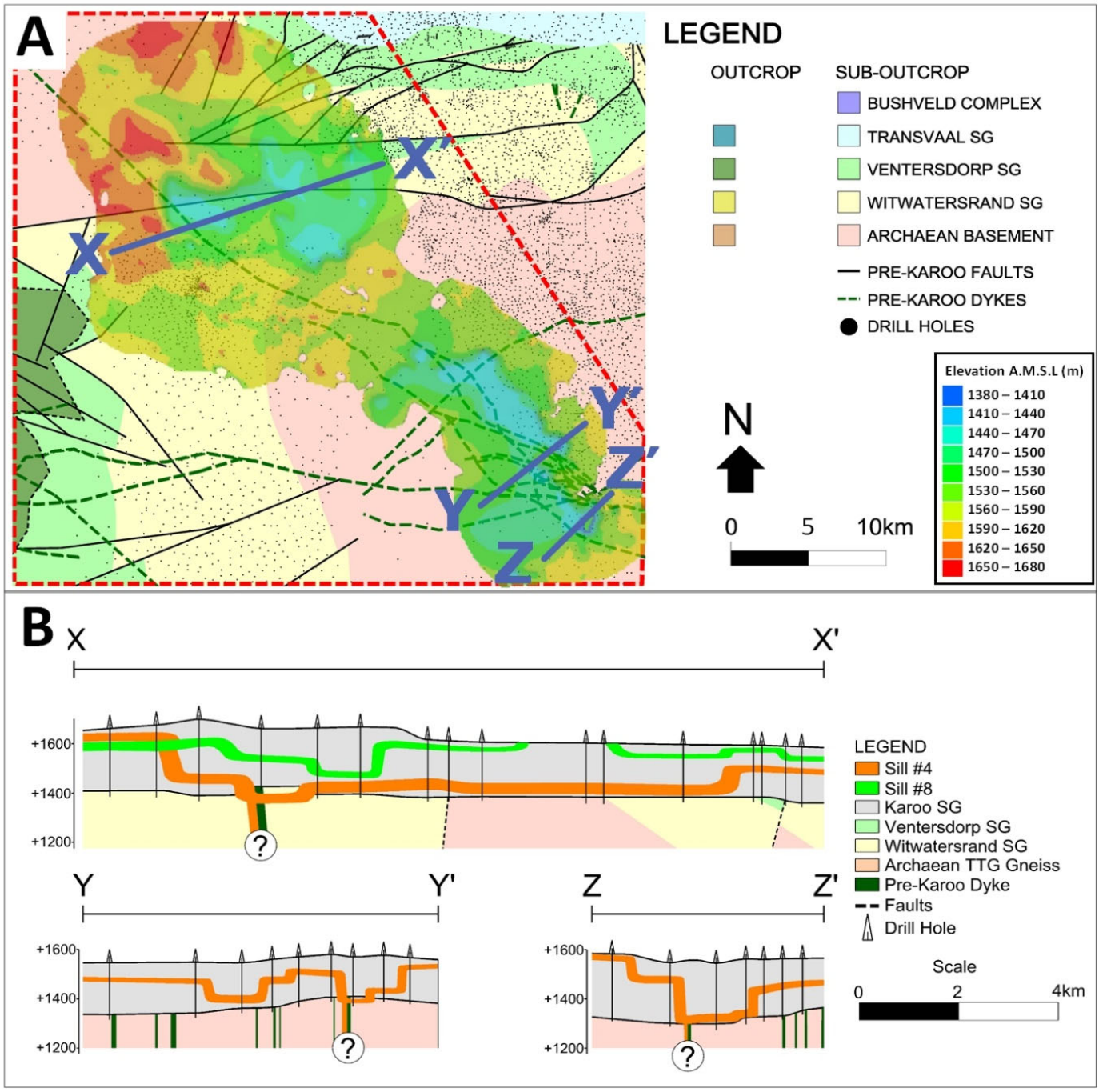

Fig. 2. (a) Geological map and (b) cross-sections of circular and elongate saucer-shaped sills in the northern Karoo basin that dip towards feeders seated along older basement dykes (modified after Coetzee and Kisters, 2018).

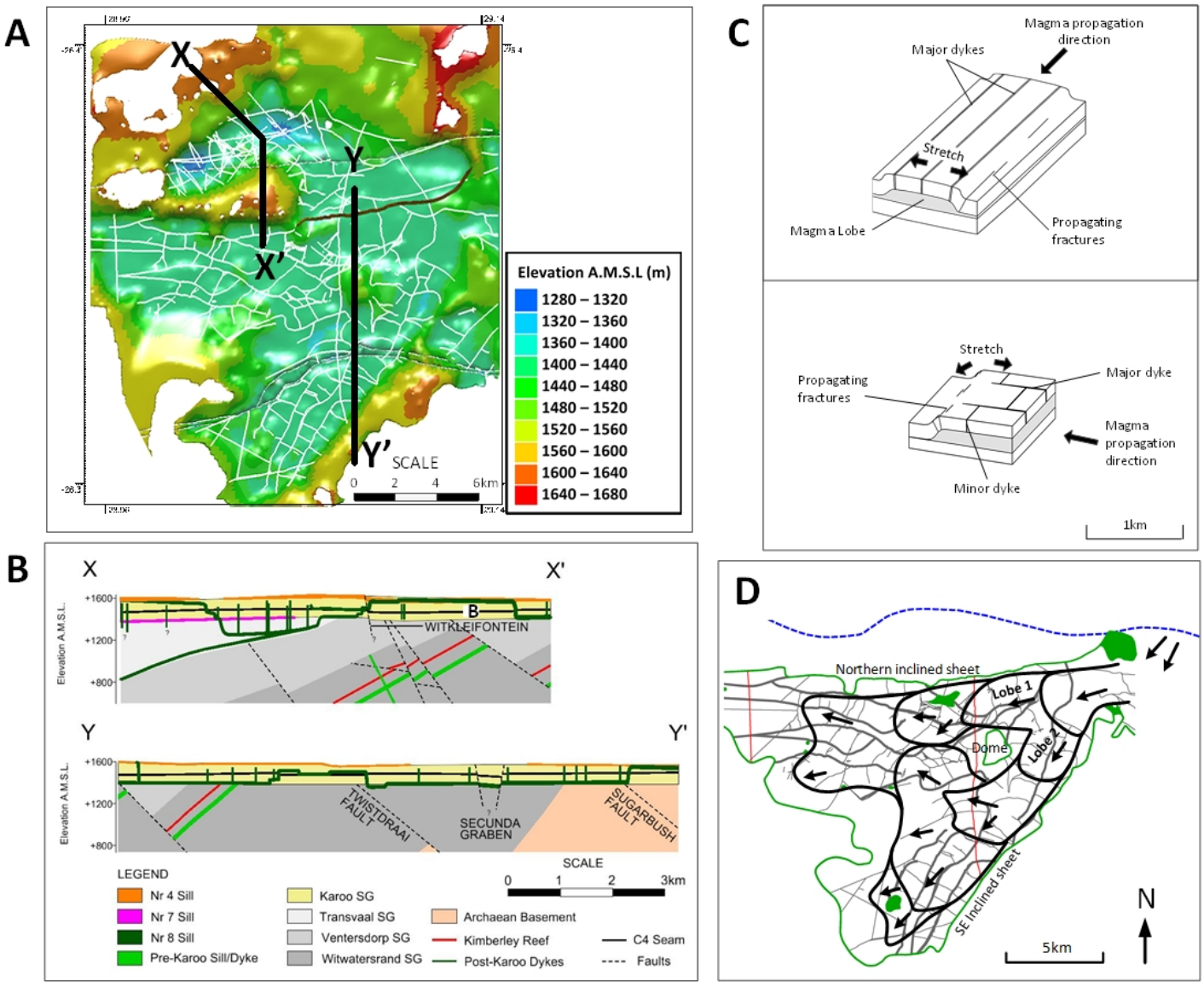

Fig. 3. (a) Geological map and (b) cross-section showing dyke networks rooted in underlying saucer-shaped sills in the northern Karoo basin. (c) Schematic and (d) plan view illustrations of dyke formation during lobate magma emplacement processes (modified after Coetzee and Kisters, 2017).

metamorphic belt. The high-grade rocks are, in turn, overlain by the Ordovician to Carboniferous (500-330 Ma) Cape Supergroup forming a gently south-dipping wedge beneath the Karoo Supergroup that gradually tapers northwards from a maximum thickness of 8-10 km in the south to the north, where it is not developed. In the far west of the basin, the Karoo Supergoup unconformably overlies Neoproterozoic to early Phanerozoic metasedimentary sequences of the Nama and Vanrhynsdorp Groups. In the south, the basin is bounded by the Cape Fold Belt (CFB) whose formation is closely linked to Karoo sedimentation and the overall asymmetric architecture of the basin. The north verging retro-arc fold-and-thrust belt developed between the mid-Permian and late-Triassic (ca. 270-210 Ma) and is thought to have formed during northward-directed subduction and convergence and associated accretion of terranes along the southern, leading edge of Gondwana (Catuneanu, 2004). Orogenic loading and unloading cover rocks existed above the current topographic level at ca. 1200 m a.s.l. (Hanson et al., 2009). This highlights the lateral continuity of the basal contact of the Drakensberg lavas at some 2000 m a.s.l. along the CFB not only influenced the migration of the stratigraphic hinge line separating proximal and distal sectors within the Karoo basin, but also created the characteristic high-rise topography that served as a source of sedimentary material (Catuneanu et al., 1998). The presence of recycled sediments in the upper Beaufort Group (Johnson, 1991) and Witteberg quartzite pebbles within the Stormberg Group units reflects the emergence of an uplifted and steep sloping proximal sector from the early Triassic (Catuneanu et al., 1998). Further inland, however, the basal contact of the Drakensberg Group lavas indicates the upper limit of the Karoo Supergroup (Stormberg Group) at ca. 1850 – 2000 m a.s.l., considerably higher than the current topography of the surrounding Karoo basin at 1300 – 1600 m a.s.l. Likewise, Stormberg Group xenoliths within Cretaceous kimberlite diatremes along the north-western margin of the basin indicate an additional 850 m of sedimentary

Therefore, it is evident that in addition to the high-level topography in southern Karoo basin, the overall sedimentary pile across the entire basin was also significantly thicker during the onset of Karoo

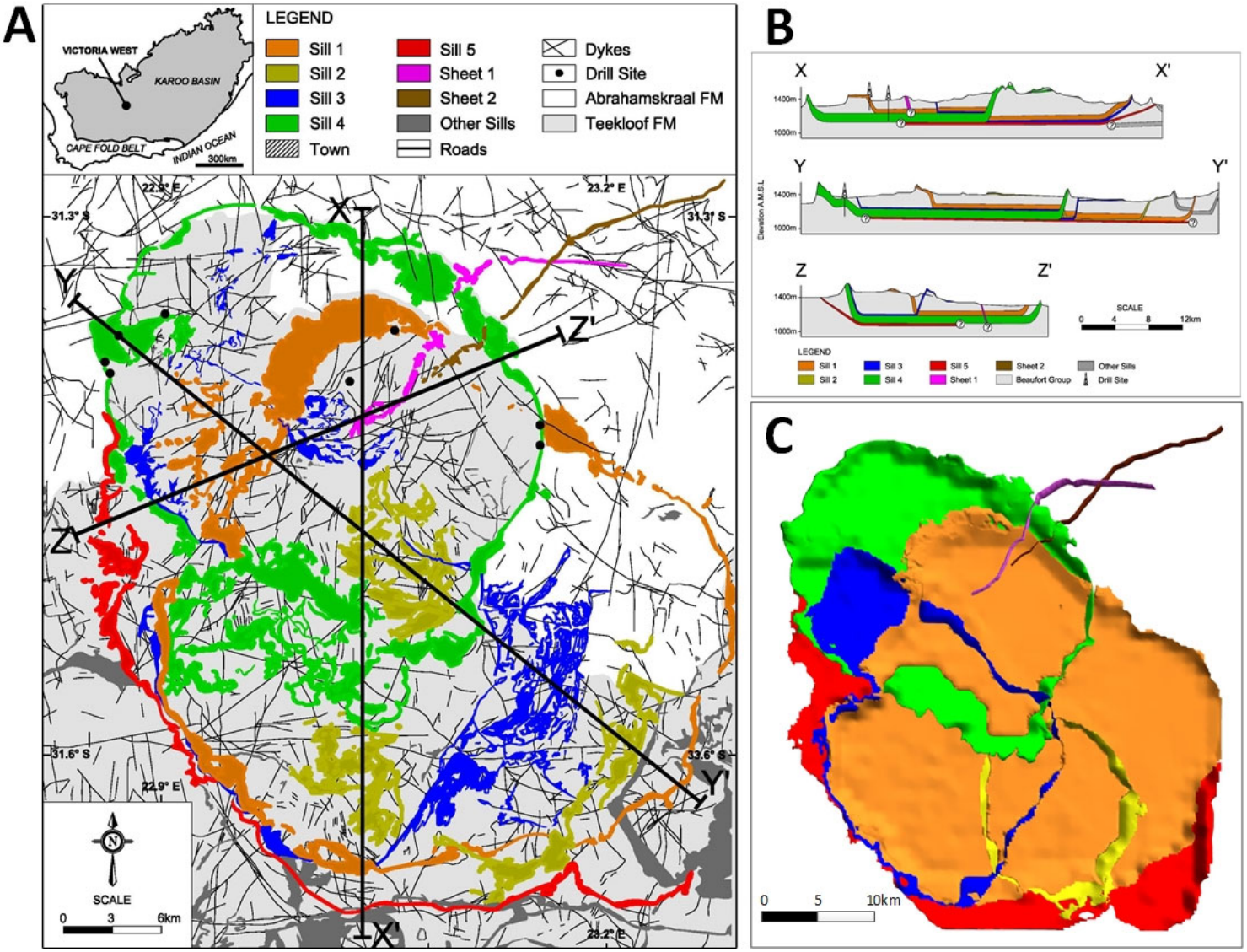

Fig. 4. (a) Geological map, (b) cross-sections and (c) three-dimensional model of a nested sill complex in the central Karoo basin with associated dyke networks and curved sheets (modified after Coetzee et al., 2019).

magmatism at 183 Ma compared to the current preserved stratigraphy. We now compare the distinct differences in sedimentary facies and structural features of sills from north to south across the Karoo basin (Fig. 1).

1.1. Northern Karoo basin

In the northern parts of the Karoo basin, the Karoo Supergroup reaches a maximum thickness of 200 - 350 m (Fig. 1). The basal Dwyka Group is a thin unit (<10 m) of tillite interbedded with varve shales (Johnson et al., 2006). The distribution of the Dwyka Group is influenced by an irregular palaeo-topography of the Archaean and Paleoproterozoic basement and commonly pinch out against basement highs. The overlying Ecca Group comprises the Vryheid Formation, a deltaic and near-shore sequence marked by up to five coal seams separated by about 20 m of sand- and siltstone layers. The Vryheid Formation is under- and overlain by the respective shale-rich Pietermaritzburg and Volksrust Formations. The topmost Beaufort Group (Adelaide Subgroup) is, where developed, made up of shales of the Normandien Formation (Johnson et al., 2006).

Karoo-age intrusives in the northern Karoo basin mainly occur as single-level sill complexes (Fig. 1, 2) and closely-spaced, but localised and short, interconnected dyke networks (Fig. 3) (Coetzee and Kisters, 2016, 2017, 2018). Most saucer-shaped sills represent relatively small, circular or oval, elongate structures with diameters below 10 km and thicknesses of less than 40 m (Fig. 2a). However, sills with larger diameters up to 25 km and thicknesses below 15 m are also occur (Coetzee and Kisters, 2016, 2018). Their inner sills are typically emplaced along the basement and Dwyka-Ecca Group contacts at 1320 - 1450 m a.s.l. (Fig. 2b, 3b). This suggests a paleo-depth of emplacement of ca. 500 m. Single or multiple funnel-shaped zones extend from the base of the inner sills into underlying basement rocks and likely represent the feeders to the shallow-crustal sills in the Karoo Supergroup (Fig. 2b). These funnels are commonly located around older faults and dykes (Fig. 2b) in the basement, pointing to the reutilization of pre-existing structural features by Karoo magmatism and the likely occurrence of narrow finger- or pipe-like feeder geometries (Coetzee and Kisters, 2018). However, while sill-to-sill feeding relationships are largely absent

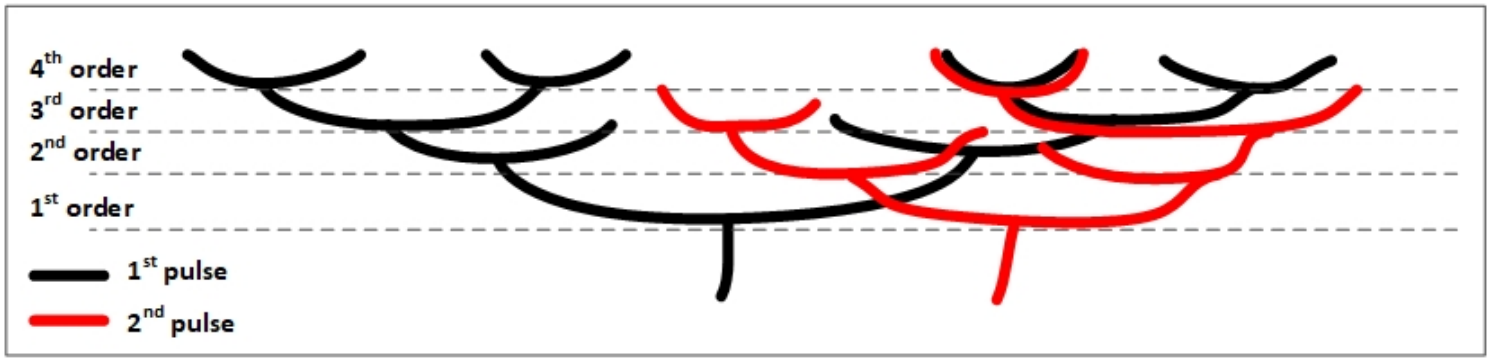

Fig. 5. Simplified diagram of the envisaged sill-to-sill feeder systems in the central Karoo basin consisting of multi-level sills emplaced through several distinct magma pulses.

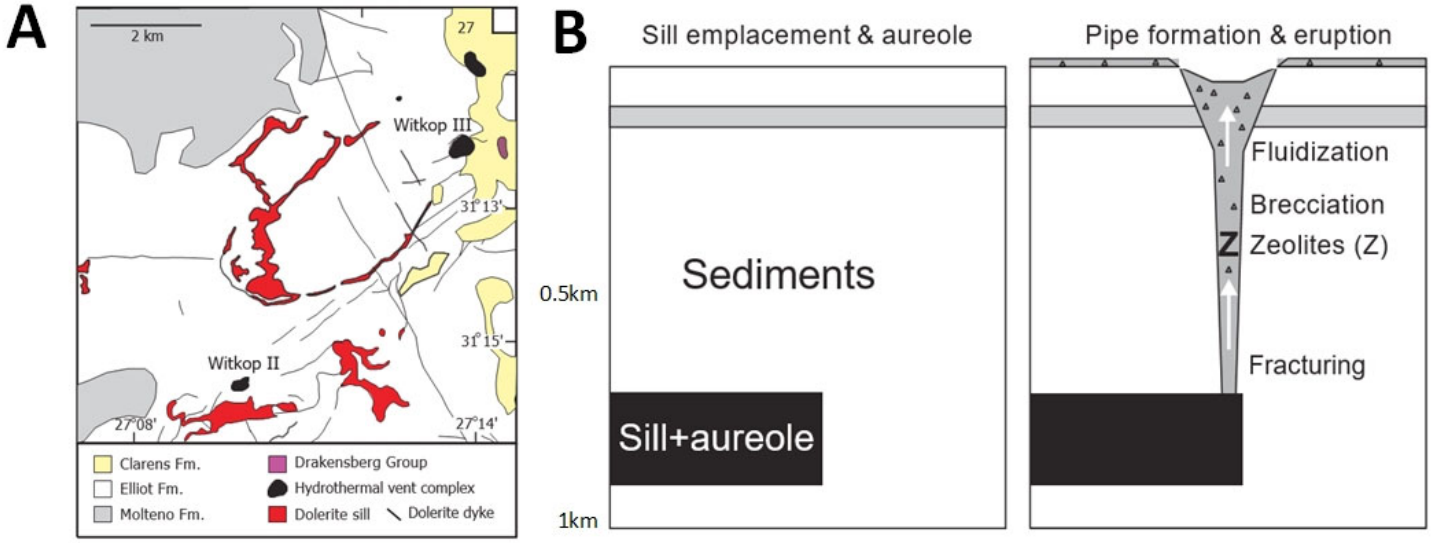

Fig. 6. (a) Geological map showing sills, dykes and hydrothermal vents in the Stormberg Group at the base of the Drakensberg lavas. (b) Proposed model for the formation of hydrothermal vent structures rooted in underlying sills.

within the sedimentary rocks of the northern Karoo basin, tilted basement strata such as the Transvaal Supergroup occasionally host extensive and gently dipping sheets that feed sills seated in the overlying Karoo Supergroup (Coetzee and Kisters, 2016).

Localised dykes are closely associated with saucer-shaped sills in the northern Karoo basin and mostly occur as thin (<5 m) structures with short strike lengths (<7 km) and curving geometries spaced at regular intervals in systematic, near-orthogonal patterns (Fig. 3a). Mining and exploration show the dykes to be rooted in underlying sills (Fig. 3b), rather than representing feeder dykes to sills. The systematic pattern of dykes and terminations of dykes against each other suggest that the dyke networks formed through the stretching and fracturing of overburden strata (Fig. 3c) during the emplacement stages of saucer-shaped sills (Fig. 3d) (e.g., Muirhead et al., 2014; Coetzee and Kisters, 2017).

1.2. Central Karoo basin

1.2.1. Beaufort Group

The Karoo Supergroup attains an overall thickness of up to 2.6 km in the central Karoo basin. The basal glaciomarine Dwyka Group consist of up to 300 m thick clast-rich, compacted diamictite, mudstone and conglomerate beds and onlaps onto bedrock of the Kalahari Craton and Namaqua-Natal Metamorphic Belt (e.g., Johnson, 2006). Dwyka Group rocks are overlain by the shallow marine to deltaic Ecca and fluvial Beaufort Groups (Fig. 1). The 0.5 - 1.3 km thick Ecca Group, consists of basal shale and mudstone units of the Prince Albert and Whitehill Formations, overlain by progressively more sandstone-bearing units of the Collingham, Vischkuil, Laingsburg, Ripon, Fort Brown, Tierberg and Skoorsteenberg, Kookfontein and Waterford Formations (Veevers et al., 1994). The up to 1.5 km thick Beaufort Group is divided into the mudstone-rich Adelaide Subgroup (Koonap, Middleton, Balfour, Abrahamskraal and Teekloof Formations) followed by the Tarkastad Subgroup (Katberg and Burgersdorp formations), the latter marked by a greater abundance of sandstone units (Veevers et al., 1994; Johnson et al., 2006).

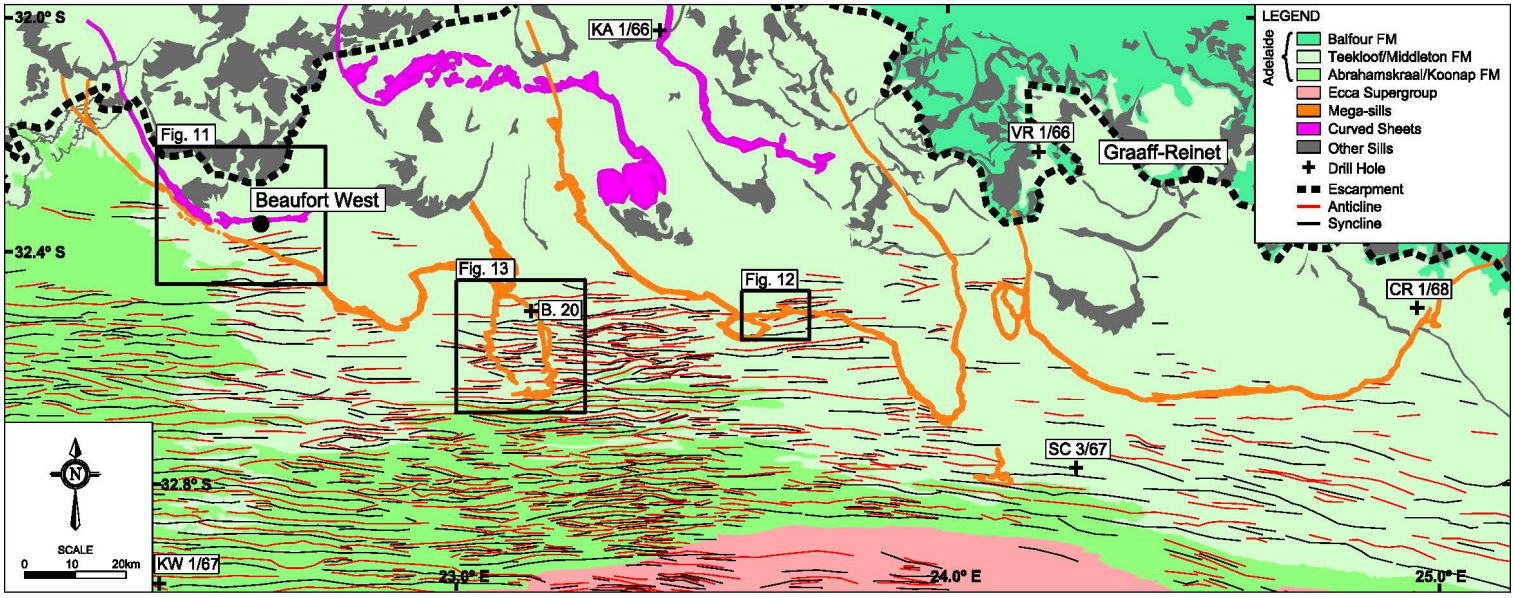

Fig. 7. Geological map of the southern Karoo illustrating the mega-sill geometries in relation to local formations of the Beaufort Group. Black outlines indicate enlarged areas shown in figures 11, 12 and 13.

Dolerite intrusions exposed in the Beaufort Group sediments of the central Karoo basin describe multi-level sill complexes, curved sheets and localised dykes (Fig. 1) (Chevallier and Woodford, 1999; Galerne et al., 2011; Svensen et al., 2012; Coetzee et al., 2019). Individual saucer-shaped sills mainly describe oval or circular outlines with considerably larger diameters in excess of 30 km (Fig. 4a) compared to sills in the north and thicknesses ranging from 50 – 100 m. Smaller sills with diameters of 4 - 13 km and thicknesses less than 15 m also occur, but are rare (Galerne et al., 2008; Coetzee et al., 2019). Inner sills are usually seated at 1150 – 1350 m a.s.l. (Fig. 4b) corresponding to a paleao-depth of 500 – 700 m (Coetzee et al., 2019). Field relationships and geochemical results show sills forming nested complexes that record the emplacement of multiple, successive magma pulses (Fig. 4c) (Schofield et al., 2010; Galerne et al., 2008, 2011; Neumann et al., 2011; Coetzee et al., 2019). The successive underaccretion of later emplaced sills below earlier emplaced sills or the location of sills below mainly sandstone units within the Beaufort Group suggests magma emplacement is largely determined by rigidity contrasts and stress barriers in the layered Karoo Supergroup (Coetzee et al., 2019). The thicker sedimentary sequence in this part of the Karoo basin promotes sill-to-sill feeding relationships between multi-level sills (Fig. 5) (e.g. Cartwright and Hansen, 2006). This is reflected by the multitude of sills found in drill holes and seismic images that apparently demonstrates interconnected networks extending from the basal Dwyka to the upper Beaufort Group (e.g. Scheiber-Enslin et al., 2014). The presence of NE trending curved sheets, some 20 km in length, that locally cross-cut and displace strata may be related to these sill-to-sill feeder networks (Fig. 4a, c) (Coetzee et al., 2019).

Dyke networks associated with sills are present, similar to those developed above sills in the northern Karoo basin. However, dyke patterns are far less systematic and commonly reveal cross-cutting and overprinting relationships that relate to multiple intrusive episodes and successively emplaced magma batches in the stacked sill complexes (Fig. 4a).

1.2.2. Stormberg Group

The mainly eolian sandstone units of the Molteno, Elliot and Clarens Formations of the Stormberg Group represent some 1.1 km of the total thickness of some 3.7 km of the Karoo Supergroup in the Lesotho region (Fig. 1) (Johnson, 1991).

Although the Stormberg Group is largely dolerite-poor compared to the rest of the Karoo basin, isolated sills, dykes and closely-spaced arrays of hydrothermal vent structures still occur (Jamtveit et al., 2004; Svensen et al., 2006; Van Zijl, 2006a; Grab and Svensen, 2011). Sills are significantly smaller (< 5 km) (Fig. 6a) and thinner (ca. 6 m) compared to those in the central Karoo and typically occur from 1600 m a.s.l up to the base of the Drakensberg Group., an approximate paleo-depth of 250 - 400 m (Jamtveit et al., 2004; Svensen et al., 2006; Van Zijl, 2006a; Grab and Svensen, 2011).

Associated dykes are less prevalent and occur as isolated segments several kilometres in length (Fig. 6a). Compared to sills and dykes, hydrothermal vent complexes are more widespread in the Stormberg Group, often comprising of sandstone pipes and brecciated sediment cones up to 700 m wide that extend upwards over several hundred meters from the larger and thicker sills confined to the underlying Beaufort Group rocks (Fig. 6b) (Chevallier and Woodford, 2002; Jamtveit et al., 2004; Svensen et al., 2006; Grab and Svensen, 2011; Chere et al., 2017).

1.3. Southern Karoo basin – the deeper basin and the dolerite line

Drill holes show the thickening of the Dwyka, Ecca and Beaufort Groups to over 5.5 km in the southern trough of the Karoo basin (Fig. 1). The sedimentary sequence is dominated by deep marine shales in the Ecca Group and braided river mudstones with minor sandstone horizons in the Beaufort Group. The southern boundary of the Karoo magmatism is known as the dolerite line. This E-W trending boundary, parallel to the CFB, is remarkably sharp and regional-scale sills are not developed further to the south and beyond this line (Fig. 1, 7). The region affected by deformation related to the CFB shows gentle, E-W trending folds and, to a lesser extent, strike-parallel thrust faults that occur from the CFB in the south up to 32.4°S in the north (Fig. 7). Folding is largely concentrated to the south-west of the study area where individual folds can be traced along strike for up to 65 km compared to the

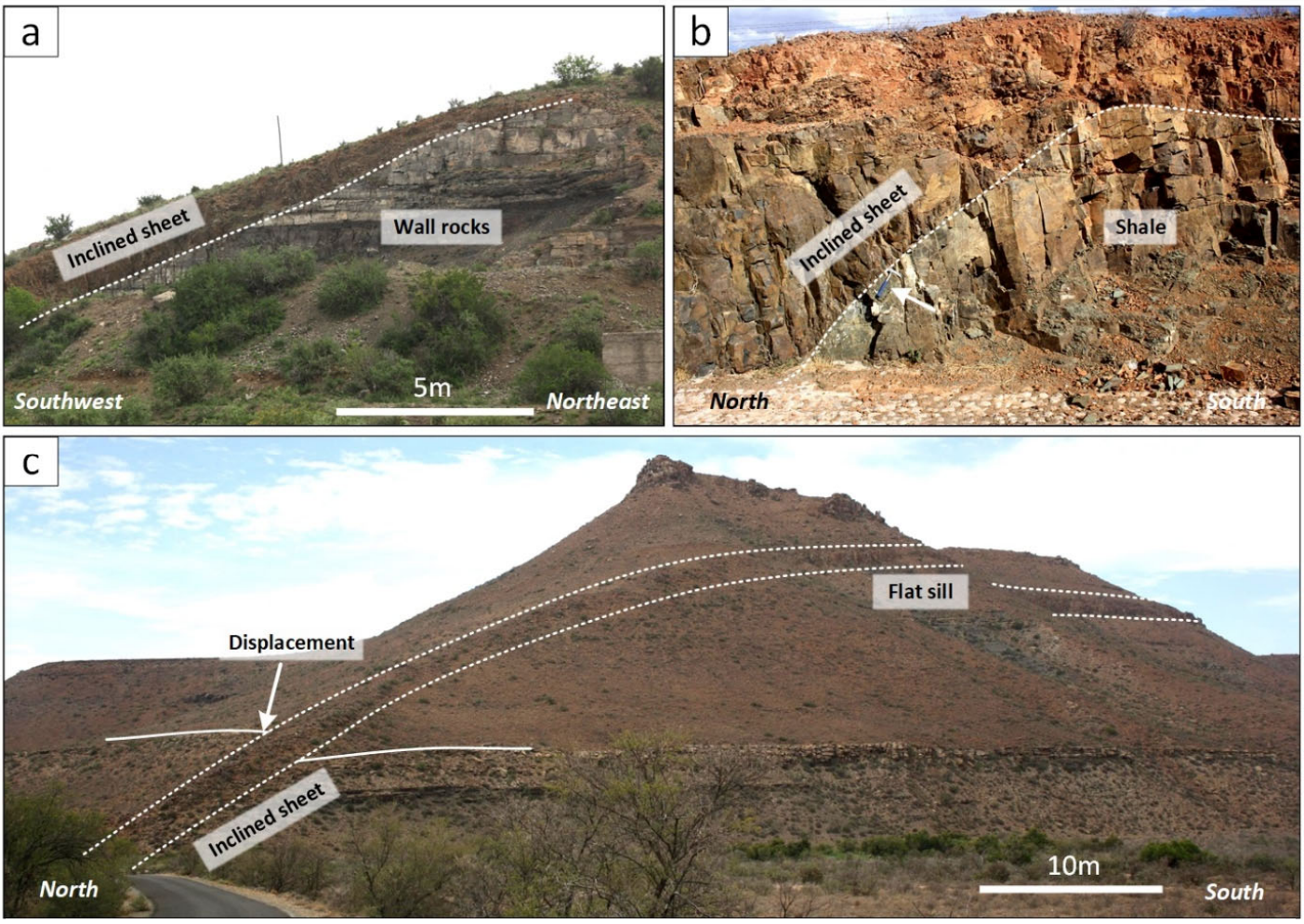

Fig. 8. Inclined sheet outcrops showing (a) steep transgression of mega-sill B; (b) step-wise transgression of mega-sill A and (c) transgression and displacement along a curved sheet flattening into a sill at a higher stratigraphic level.

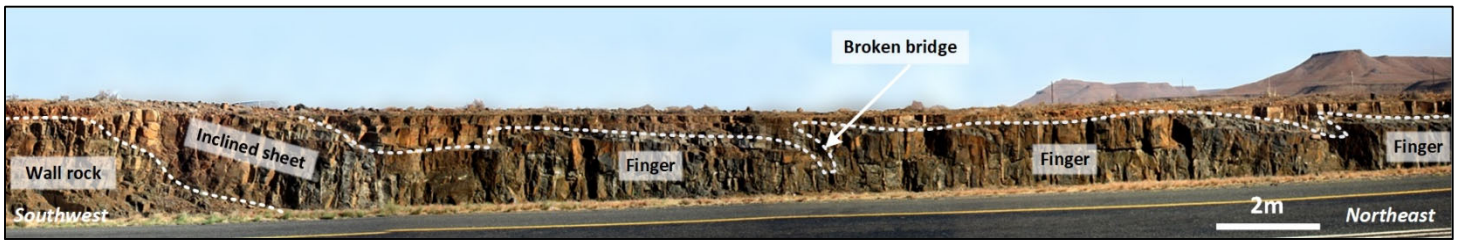

Fig. 9. Road cutting along a flat segment of the western mega-sill (see Fig. 7) exhibiting several meter-scale broken bridges.

north and east where shorter (5-10 km), discontinuous, en-echelon folds prevail. Folds are mainly upright and symmetrical with horizontal hinges and interlimb angles that tighten from ca. 160 ° in the north to ca. 120 ° in the south over an across-strike distance of some 50 km (Fig. 7). Likewise the associated bedding dips steepen from 10° in the north to over 30° to the south (Fig. 7). Overturned folds are found exclusively within the Ecca Group in front of the CFB to the far south (Fig. 7) while faulting is locally developed along steeper folds and characterised by normal displacement.

The inland extension of the Great escarpment up to a latitude of 31.9°S together with deep drill holes reveal a series of deeper-seated mega-sills, saucer-shaped sills and curved sheets confined to the upper 600 m of stratigraphy (Fig. 1, 7). Notably, localised, interconnected dyke networks commonly associated with sills seem completely absent from this region. The mega-sills represent the southernmost expression of Karoo sills and, thereby define the dolerite line and southern boundary of Karoo magmatism. Mega-sills are elongated and semi-circular structures with diameters of 50 - 100 km (Fig. 7) consisting of gently north-east dipping centres (inner sills) surrounded by steeper inclined sheets (Fig. 8a). Inner sills occur at 200 – 300 m a.s.l. (Fig. 1), corresponding to a paleo-depth in excess of 1.5 km. However, considering the differential uplift experienced in the southern Karoo compared to the rest of the basin, the emplacement depth of mega-sills was likely much deeper, up to 2 km. Inclined sheets often show step-like geometries with shallow dipping (<20°) concordant segments alternating with steeper (<50°) transgressive segments (Fig. 8b). Displacement is

evident from the abrupt change in stratigraphy along the hanging- and footwall rocks of the inclined sheets. Mega-sills reach thicknesses of 30 - 35 m, as recorded along outcrops of inclined sheets in the south. However, thicknesses gradually decrease to less than 2 - 3 m (Fig. 9) and, eventually, terminate to the north beyond the escarpment. Furthermore, the southern margin of the mega-sills is often marked by remnants of laterally connected subsidiary sills with dimensions of 4 – 9 km × 11 - 21 km (Fig. 7).

Curved sheets show E-W and NW-SE trends with some 60 – 80 km strike lengths and thicknesses of 20 – 30 m, but abrupt along strike terminations. Curved sheets are sharply transgressive and step through the Karoo Supergroup at angles up to 45° with a displacement of host rocks equal to the thickness of the dolerite sheets (Fig. 8c). In most cases, the transgressive curved sheets flatten upward into concordant sheets seated at higher stratigraphic levels (Fig. 8c). The occurrence of curved sheets here and in the central Karoo basin suggest they form an integral part of the intrusive network. Their comparable wall rock displacement, thickness and spatial association indicates similar emplacement styles to mega-sills and they likely form part of the larger sill-to-sill feeder system (Fig. 5).

Drill holes and geophysical data show no evidence of deeper-seated sills or dykes extending upwards from the basement that could have served as feeders to the sills in the southern Karoo. Here, magma feeders to the mega-sills, in particular, likely originated further north and inland, beyond the escarpment where the first sills appear at depths > 1.5 km and near basement rocks (Fig. 1). Their stratigraphic position in the lower Ecca and Dwyka groups renders these sills favourable candidates for tapping into potential basement feeders (Fig. 7). The northerly dip direction of the mega-sills and spatial occurrence of these abyssal sills suggest magma transfer and propagation occurred from north to south within this localised part of the southern Karoo basin, normal to the E-W trending CFB.

Variations in magma flow directions

Closer to the dolerite line, magma flow directions measured in the field divert from the regional N-S flow directions to SE and SW and even E-W magma flow directions. Flow directions can be established in exposures of mega-sills and curved sheets that display step-like geometries coinciding with en-echelon or broken bridge structures. These structures are commonly associated with lobate magma flow processes and the formation of magma fingers where the long axis of magma fingers is parallel to the magma flow direction (e.g. Schofield et al., 2010; Magee et al., 2019). In exposed sill sections, the margins of magma fingers are defined by elongated or rectangular slabs of wall rock extending into the sill (Fig. 9, 10a). In the measured examples, the size of magma fingers correlates with the thickness of the sill body. Meter- (Fig. 10a) and centimetre-scale fingers (Fig. 10b) occur along thinner (~3 m) sill segments (Fig. 9) whereas larger tens-of-meter-scale fingers (Fig. 10c) are associated with thicker (20 - 35 m) sills. The strike of magma fingers along the western mega-sills (Fig. 7, 11) indicates a NW-SE directed magma flow, while the curved sheet directly north thereof (Fig. 7, 11) still record N-S flow directions.

Sill geometries provide additional insight into local magma flow

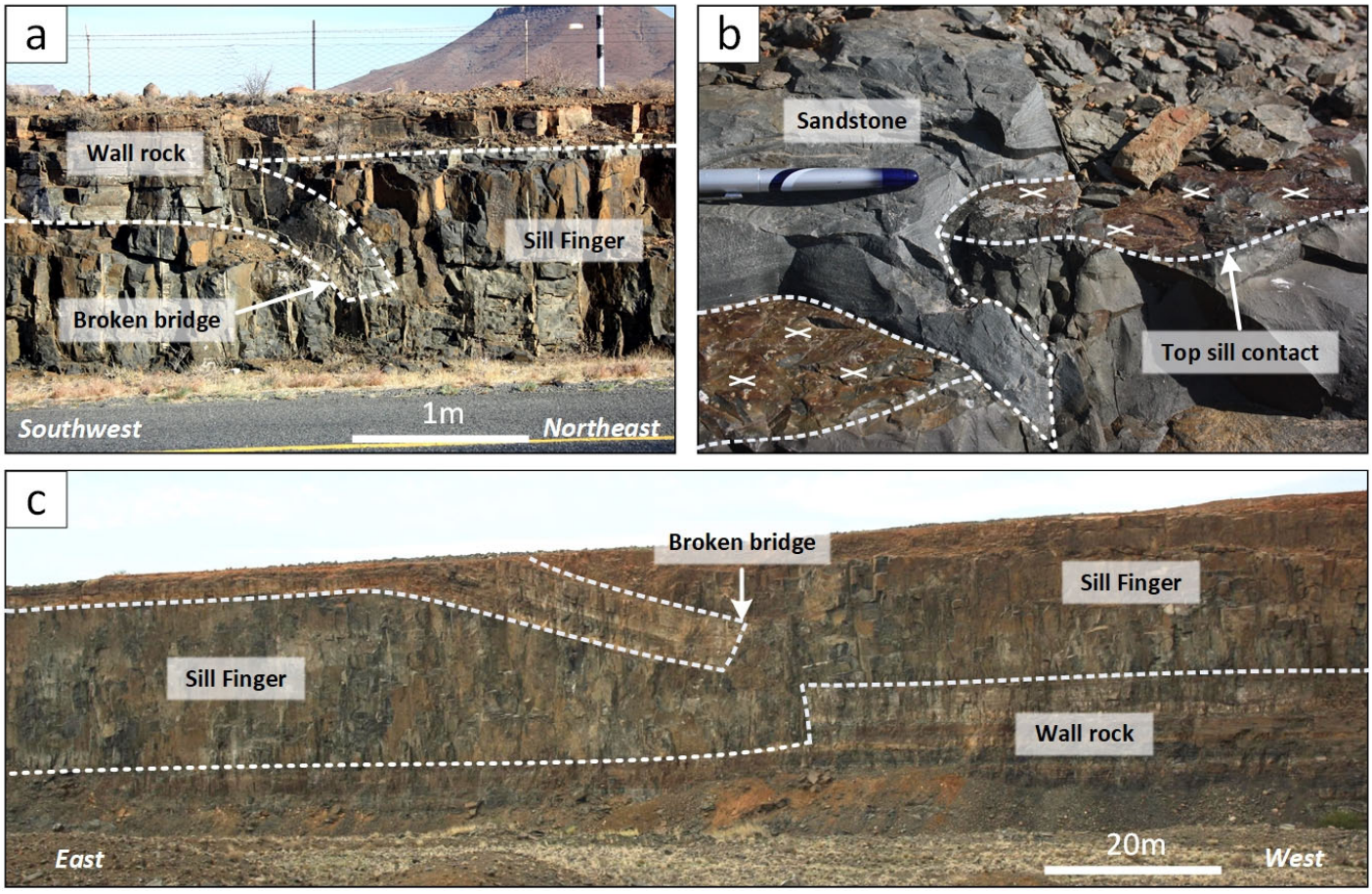

Fig. 10. Local examples of (a) meter-scale, (b) centimetre-scale and (c) tens-of-meter-scale broken bridges along mega-sills and curved sheets.

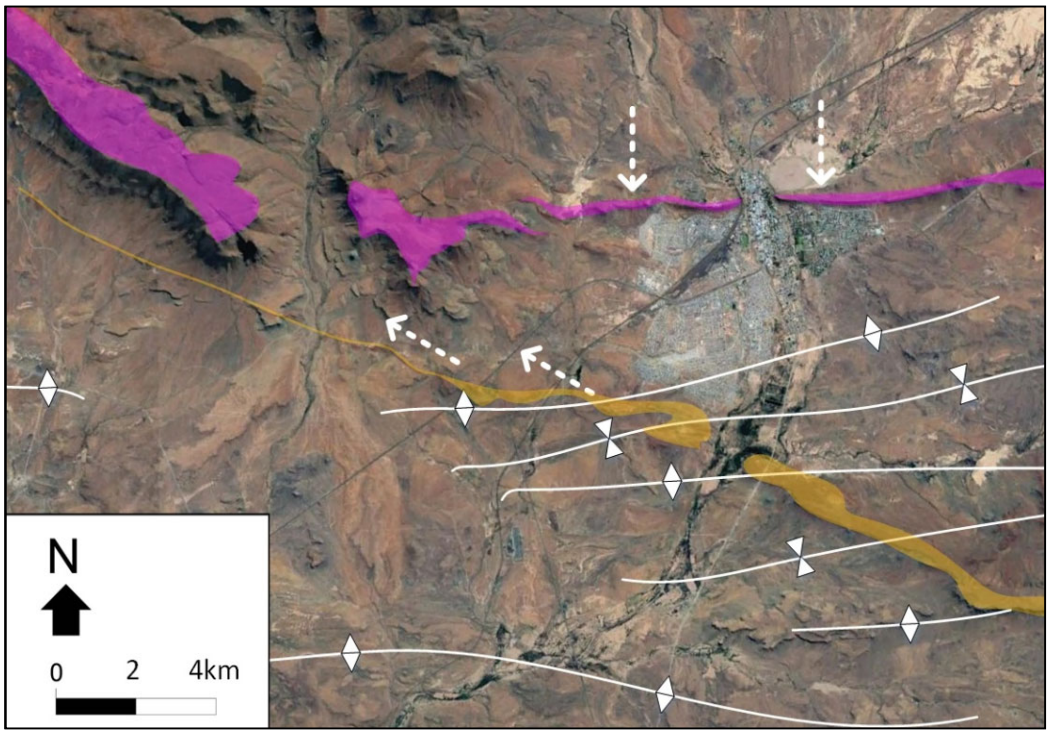

Fig. 11. Google Earth image showing local magma flow paths observed along sill bridges of the western mega-sill and adjacent curved sheet (see Fig. 7).and curved sheets.

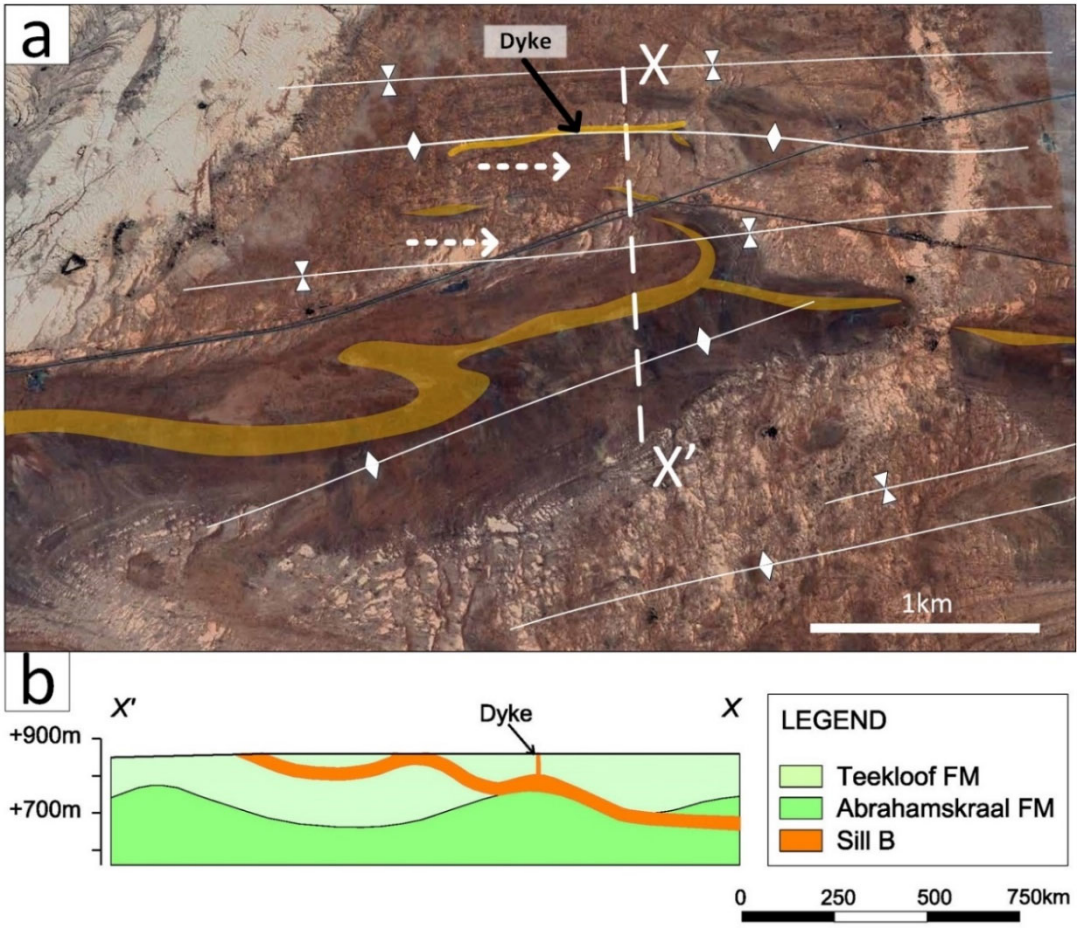

Fig. 12. (a) Google Earth image and (b) cross-section of the magma flow directions along the southern rim of the central

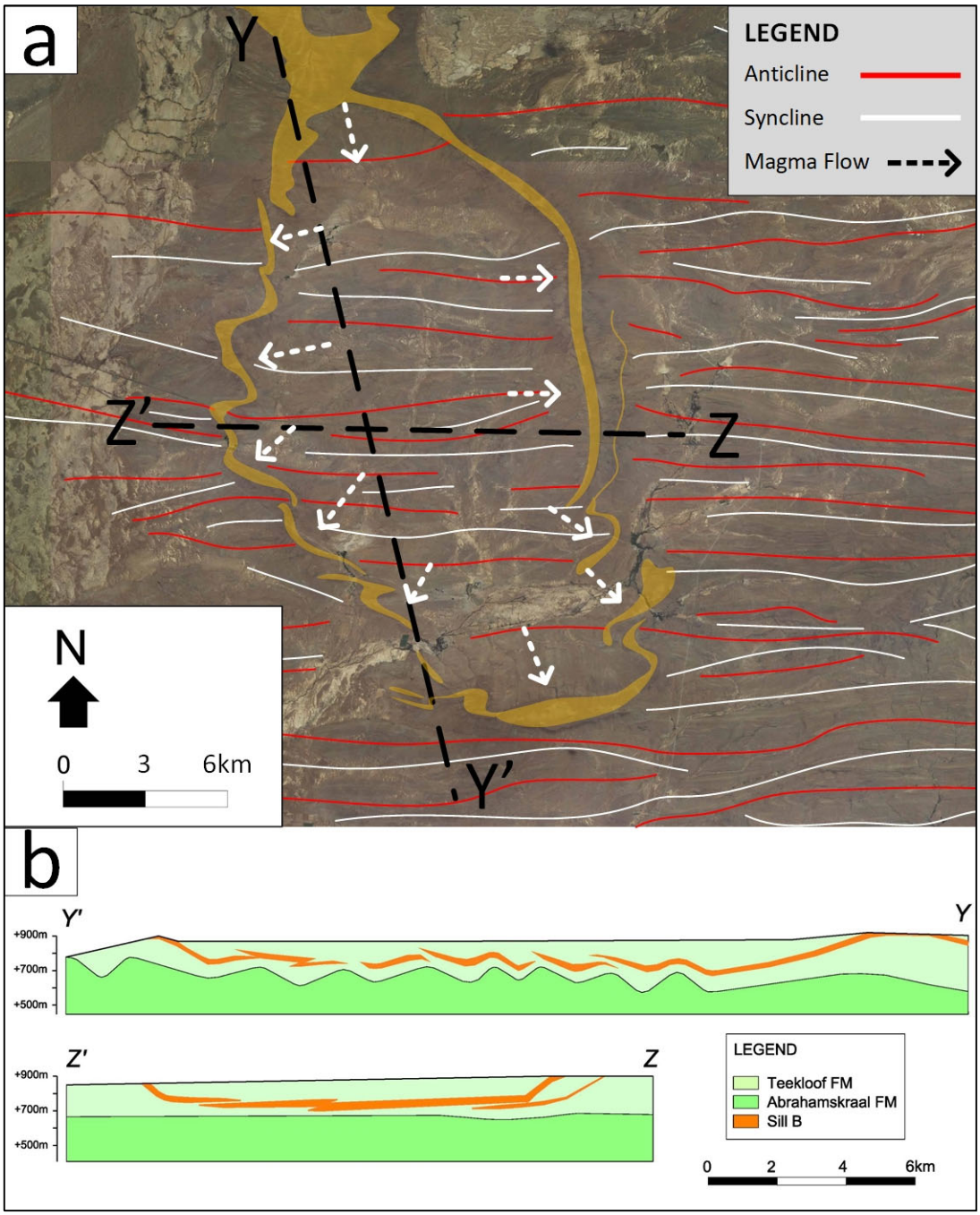

Fig. 13. (a) Google Earth image and superimposed geology indicating magma flow directions along the subsidiary sill of the western mega-sill (see Fig. 7). The undulating sill outline and en echelon geometries is controlled by the folded lower Beaufort Group sediments. (b) Cross-sections of the sill with a vertical exaggeration factor of 5. Section Y-Y' shows the sill segmentation (magma fingers) and flow (E-W) normal to the section; Z-Z' illustrates flow and sill connectivity parallel to the section line. (see Fig. 7).

directions where mega-sills and their associated subsidiary sills exploit folded strata of the Beaufort Group. The central mega-sill (Fig. 7), in particular, reveals a prominent northwards branching protrusion from its inclined sheet that cross-cuts a synform before curving into parallelism with and tapering off along the northern limb of the fold (Fig. 12a). This is likely related to an E-W magma flow channel that initially exploited the synclinal fold hinge before cross-cutting the strata and forming the inclined sheet. Likewise, the single E-W orientated dyke, some 1.5 km in length, directly north of the protruding inclined sheet indicates E-W magma injection. Given the gentle folding, dyke formation is unlikely have formed due to outer arc extension of the fold (Fig. 12b). Instead, the orientation of the dyke reflects the stretching of roof rocks associated with the E-W emplacement and inflation of elongated magma fingers (Fig. 3c) during the formation of the underlying mega-sill.

A prominent subsidiary sill found south of the westernmost mega-sill is characterised by a breakdown of the sill outline, from N to S, into several shorter, gently undulating segments as the sill cross-cuts

the gently folded Karoo strata. Individual segments show an en echelon geometry, with the separation commonly occurring on fold limbs and up to 400 m wide segments of wall rock separating individual sill segments (Fig. 13a,b). These sill segments resemble magma channels or finger-like magma flow geometries observed along sill cross-sections elsewhere (Fig. 9), albeit on a much larger scale. The orientation of individual segments and the, in all likelihood, subsurface connectivity of the segments (Fig. 13b) also points to the change in the magma flow direction to more easterly directions (Fig. 13a). This suggests folds may have delayed or prevented the southward propagation of magma, deflecting it laterally towards the east and west, and, in turn, modifying the larger sill geometry.

2. Discussion

2.1. Sill emplacement controls across the Karoo basin

Field, drill hole and geophysical data presented here indicate systematic variations of sill geometries and sizes across the Karoo basin. The main factors that probably determine these variations relate to (1) the depth of emplacement, i.e. the thickness of the overburden and the regional stress field; (2) the presence of lithologies that can initiate the deflection of steep feeders to subhorizontal sills. This aspect directly relates to facies variations in the larger Karoo basin; and (3) variations in magma pressure and distance to magma feeder zones. The following discussion evaluates the role of each of these factors and the effects they have on the geometry, size and connectivity of Karoo sills.

2.1.1. Depth of emplacement and size of sills

An estimate of the absolute depth of sill emplacement in the Karoo Supergroup is not without problems. The two main uncertainties in thickness estimates revolve around (1) the differential uplift and erosion of different parts of the basin. Higher uplifts are recorded in the south, closer to the CFB, but the absolute uplift and amounts of erosion are not well constrained; and (2) the extrusion of the Drakensberg flood basalts during sill emplacement. The outpouring and extremely rapid built up of at least 1.4 km thick Drakensberg flood basalts at the top of the Karoo Supergroup will have added a further 30-40 MPa of overburden pressure to the Karoo Supergroup over a geologically very short period (e.g., Svenson et al., 2012). Thus, pre- compared to syn- and post- Drakensberg sills will have experienced significantly different overburden pressures during their emplacement, an aspect that will be discussed below.

Analogue models highlight the close interdependence between the lateral growth of a sill and the thickness of the immediate overlying strata. The models suggest the size of saucer-shaped sills to be primarily controlled by interactions between the developing inner sill and the overburden (Pollard and Johnson, 1973; Malthe-Sørensson et al., 2004; Kavanagh et al., 2006; Galland et al., 2009; Galerne et al., 2011). At greater depths and higher overburden pressures, inner sills may grow to larger diameters before initiating roof failure and the subsequent formation of inclined sheets compared to sills emplaced at shallower depths. Along the N-S traverse across the Karoo basin, there is an overall trend for sills to be smaller in the north compared to the southern parts of the Karoo basin. These variations follow the asymmetry and southward deepening of the basin and the emplacement of sills at progressively larger depths in the south (Fig. 14). The smaller (<5 – 13 km) sill diameters in the Stormberg Group and the thin northern extremities of the Karoo basin correspond to an overall shallow emplacement depth of 250 m and 500 m, respectively (Fig. 14). In contrast, larger (>30 km) diameter sills in the central Karoo basin intruded at intermediate palaeo-depths up to 700 m (Fig. 14). Mega-sills with diameters >50 km characterise sills at deeper levels emplaced at palaeo-depths of up to 2 km (Fig. 14). Notably, both small (5 - 10 km) and large-diameter sills (15 – 35 km) occur at comparable stratigraphic levels in the north-eastern (Coetzee and Kisters, 2016, 2018) and central Karoo basin (Galerne et al., 2008; Coetzee et al., 2019). This may reflect sill emplacement at depth before and during the extrusion of the overlying Drakensberg flood basalts and, hence, varying overburden pressures at a given location in response to the rapid loading of the crust.

The thickness of the overburden and emplacement level also controls the occurrence of associated interconnected dyke networks. Based on the emplacement depths of sills in the northern and central Karoo basin, the formation of dyke networks above sills seems restricted to depths less than 700 m, corresponding to overburden pressures of < 18-20 Mpa (Fig. 14). This relation probably reflects a combination of (1) lower confining pressures that promote extensional fracturing and dyking (e.g., Muirhead et al., 2014; Coetzee and Kisters, 2017), and (2) the presence of anisotropies, particularly joints systems, that can be exploited by the interconnected and typically high-angle dyke networks. However, hydrothermal vent complexes are not as well constrained by overburden thickness.

2.1.2. Sedimentary facies and sill emplacement

North-south facies variations are the result of the asymmetry and progressive contraction of the Karoo basin with time and the uplift and unroofing of the CFB in the south. Thick, marine shales dominate the deeper southern parts of the basin, succeeded by coarser sedimentary rocks and increasing sandstone-shale ratios in the central-northern parts as the basin contracts with time (Johnson, 1997). In the layered Karoo Supergroup, the formation of bedding-parallel sills can be seen to be promoted by the presence of mechanical anisotropies, mainly in the form of stress barriers (e.g., Gudmundsson, 1995, 2011; Gudmundsson and Brenner, 2001; Kavanagh et al., 2006; Menand et al., 2010; Coetzee et al., 2019). The commonly higher rigidity (Young's modulus, E) of sandstone units compared to shale renders sandstone units as stress barriers, particularly in the mildly compressive regional stress field during sill emplacement and prior to Gondwana break up (e.g., Grantham et al., 2019; Coetzee et al., 2019). As a result, many dolerites have intruded below massive sandstone units and within shale, recording the deflection of steep magma feeders and promoting the lateral propagation of the mafic magmas as sills preferentially in shale units. Sill emplacement in shales is facilitated by the rather viscoelastic deformation and ductile flow of shale compared to the elastic, brittle behaviour of sandstone units. The thick deep-marine shales of the Ecca and fluvial mudstones of the Beaufort Groups in the south, thus, provide favourable horizons for sill emplacement compared to the thinner sandstone units in the north of the basin. This may also explain the near-absence of sills within the thick eolian sandstone units of the Stormberg Group. Not only did the sandstone units represent stress barriers that halted the propagation of feeders, the emplacement of sills was further impeded by the brittle behaviour of the rigid package compared to the underlying shale-rich Beaufort and Ecca Groups.

A contributing factor to the deeper emplacement of sills in the southern parts of the basin are increased fluid pressures in deeper seated shale units. Experimental studies by Gressier et al., (2010) conclude that high fluid pressures confined to deeply buried, impermeable, suprahydrostatically pressured and low rigidity shales promote the emplacement of deep-seated sills in sedimentary basins. This is likely an additional factor that controls the emplacement of

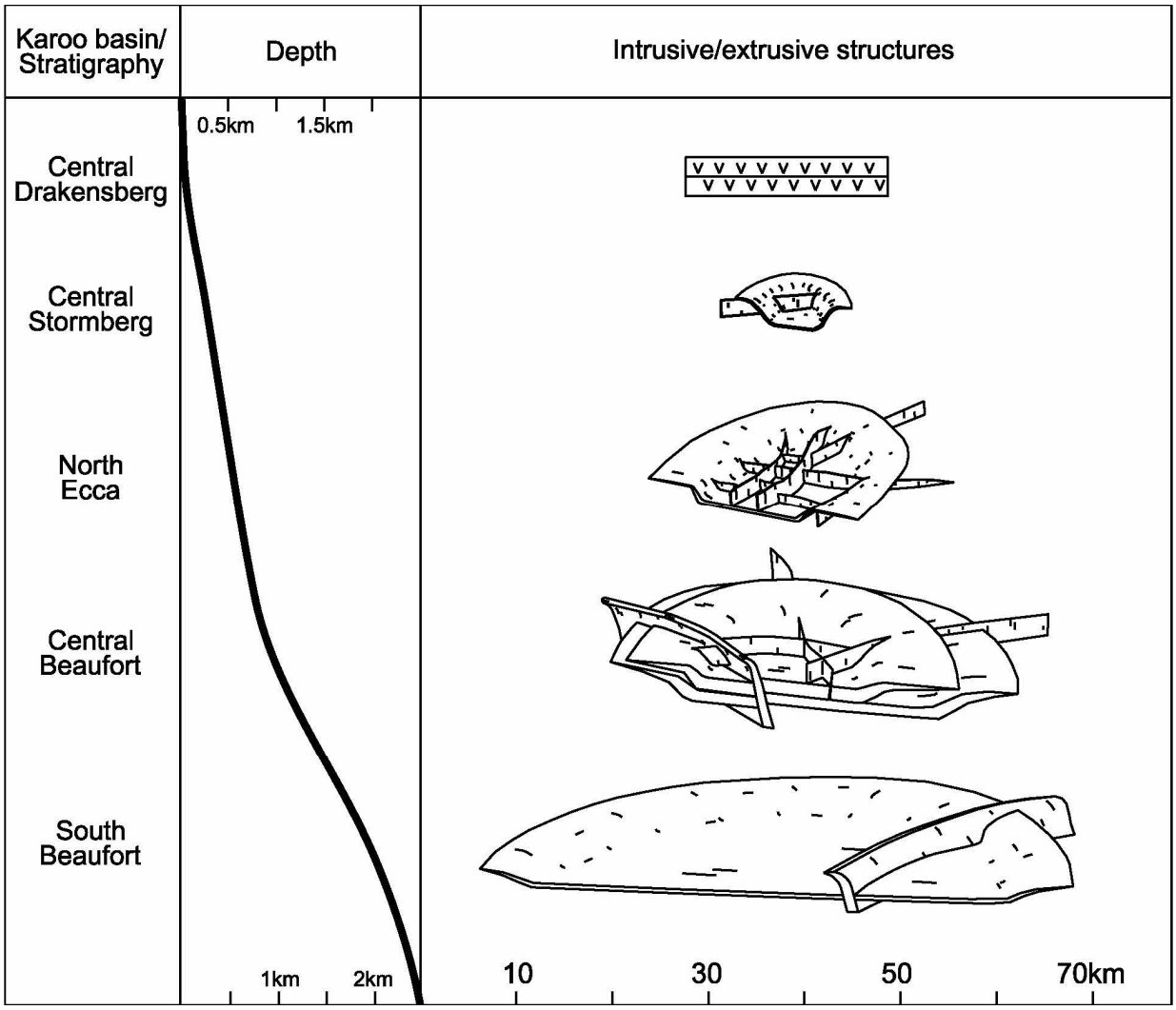

Fig. 14. Schematic illustration of dolerite intrusions found in certain parts of the Karoo basin along a depth profile in relation to the capping Drakensberg Group lavas. From Chevallier and Woodford (1999), Jamtveit et al. (2004), Svensen et al. (2006), Van Zijl (2006a), Grab and Svensen (2011), Galerne et al. (2011), Svensen et al. (2012), Coetzee and Kisters (2016, 2017, 2018), Coetzee et al. (2019).

the southern mega-sills at depth. Injection of sills into thick shale units may also account for the near absence of dyke networks in the deeper southern Karoo basin, since the low-rigidity shales accommodate sill emplacement by internal deformation and ductile flow rather than brittle fracturing.

In contrast, the emplacement of thick regional-scale sills in water-saturated layers at shallower depths, notably the upper Beaufort Group, is likely to be responsible for the formation of hydrothermal vent structures. Rapid vaporisation of pore-fluids at pressures exceeding the confining pressure of the overlying and poorly lithified Stormsberg Group enable phreatic explosions to reach the palaeo-surface prior to the extrusion of flood basalts. The overall low concentration of dolerite intrusions in the Stormberg Group may also be related to water-saturated layers inhibiting the effective upwards migration of magma from the underlying Beaufort Group sediments.

2.1.3. Magma pressures, proximity to feeders and sill emplacement

The emplacement of sills and associated structures is also influenced by the driving magma pressures, and variations thereof, and proximity to basement feeders. Away from basement feeders, magma pressures will decrease as a result of the cooling of the magmas and associated increase in viscosity and the shear resistance against wall rocks and wall-rock deformation during sill propagation (e.g., Magee et al., 2016). Magma injected at higher driving pressures is likely to accelerate the lateral spreading rate of sills. This will induce overburden failure and formation of inclined sheets at an earlier stage during sill inflation and thereby limit the lateral extent of the sill. This is evident from the small, single-level saucer-shaped sills in the northern Karoo basin that connect directly to feeders reutilizing older basement faults and dyke swarms. In contrast, decreasing magma pressures away from feeders and within sill-to-sill networks would promote slower spreading and propagation rates and, as a result, favour larger sills. It is already evident from this, that several independent factors influence the propagation and size of sills.

2.2. Implications for regional magma transport

The large volumes of mafic magma emplaced and erupted over a narrow time interval across southern Africa and Antarctica have traditionally been explained by a mantle-plume model (e.g. Cox,

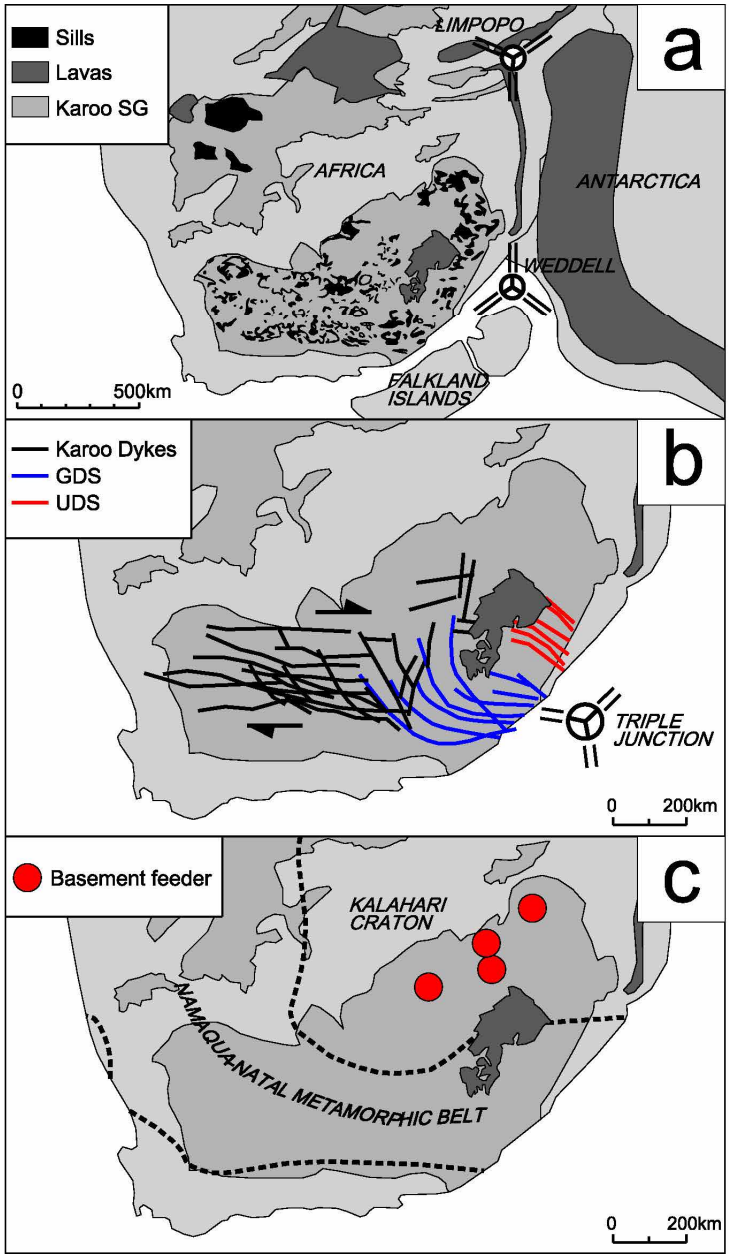

Fig. 15. Proposed regional magma feeder models to the Karoo sills based on (a) mantle plumes situated along rift margins of southern Africa (after Elliot and Fleming, 2000), (b) the formation of a failed rift system or E-W dextral shear zone (after Chevallier and Woodford, 1999) and (c) basement feeders exploiting pre-existing faults and dykes (after Coetzee and Kisters, 2018)

1992; White, 1997; Elliot and Fleming, 2000). The contemporaneous emplacement of the Karoo and Ferrar LIP's at some 183 Ma (Encarnacion et al., 1996; Elliot and Fleming, 2000) is evidence of a common magma source with plume heads suggested to be located at the Limpopo and Weddell triple junctions (Fig. 15a). Notably, the Weddell triple junction, typically regarded as the primary source of mantle derived magmas to the Ferrar LIP (e.g. Elliot and Fleming, 2000, 2004), is also located along the eastern margin of the Karoo basin (Fig. 15a). However, while low-Ti lavas from the Karoo and Ferrar LIP's show geochemical similarities (Elliot and Fleming, 2000), sill feeders injecting magma westwards into the Karoo basin from magma sources near the Weddell triple junction have yet to be identified. An alternative model proposes the formation of an east-west dextral shear zone or failed rift system defined by the prevailing EW and NE strike direction of dykes across the central Karoo basin as evidence for east-west magma injection (Fig. 15b) (Chevallier and Woodford, 1999, 2002). However, these dykes, with the exception of the Gap and Underberg dyke swarms in the east, are largely secondary and accommodation structures related to the emplacement of multi-level sill complexes (Coetzee and Kisters, 2018). Moreover, geochronology data and xenoliths of older sills in the dykes indicate the intrusion of the dyke swarm after sill emplacement (Fig. 15b) (Riley et al., 2006; Svensen et al., 2012).

There are a number of reasons that seem to argue against the injection of the magma from an eastern point source. Due to the nature of sill-to-sill networks, transport of magma over hundreds of kilometres would generate an upwards cascading structure (Fig. 5). In this scenario, sills should be observed to cut up stratigraphy from east to west, but sills actually occur throughout the Karoo stratigraphy. Furthermore, if magma transport was from a point source to the east, a higher density of sills would be expected close to the magma source compared to the west, which is not realized either in the Karoo basin.

The occurrence of sills throughout the stratigraphy of the Karoo Supergroup, from the basal Dwyka to the upper Beaufort Group in the central Karoo basin, is more consistent with thermal incubation beneath southern Africa and the presence of numerous, rather distributed magma feeders, each feeding separate sill complexes from different locations (Fig. 15c). Subsurface borehole and geophysical data also suggest the control of feeders around pre-existing basement anisotropies such as older faults or dyke swarms (Coetzee and Kisters, 2018). The location of such magma feeders in highly deformed basement rocks of the thinner lithospheric structure of the Namaqua-Natal metamorphic belt seems plausible considering the successful injection of magma through the pronounced lithospheric thickness of the Kalahari craton (Fig. 15c) (Coetzee and Kisters, 2018). In contrast, deformation and associated lithospheric thickening in the CFB to the south of the Karoo basin may have prevented injection of mantle derived magmas (Fig. 1), resulting in the absence of basement feeders and deep-level sills in the southernmost parts of the basin. This area likely represents the confluence of north to south magma flow from distributed feeders emplaced in rocks of the Namaqua-Natal metamorphic belt and the Kalahari craton with the dolerite line defining the lateral limit of sills to transport magma. This is accentuated by folding and thrusting in the frontal parts of the CFB that impedes and deflects sill propagation away from the regional flow direction into smaller localised channels (Fig. 11, 12, 13).

3. Conclusion

The emplacement style of dolerite sills is evaluated in relation to the basal level of the Drakensberg Group lavas at different sites across the Karoo basin to develop a regional magma emplacement and distribution model. The following conclusions can be made:

1. The size and geometry of dolerite sills is partly a function of emplacement depth. At shallow depths (< 500 m) sills are small (< 10 km), less than 40 m thick and interconnected with dense 'cracked-lid' dyke networks developed above sills. Magma emplacement at intermediate depths (500 – 700 m) is characterised by larger (> 30 km) and thicker (50 - 100 m) sills forming nested sill-in-sill geometries fed through intricate sill-to-sill networks. Dyke networks here typically form non-systematic patterns above the sills. Mega-sills, some 50 km wide and 35 m thick, are more prevalent at advanced depths

(< 2 km) while local dykes are largely absent. The occasional occurrence of both large and small diameter sills at comparable stratigraphic levels across the Karoo basin may be related to emplacement at depths prior to and during the outpouring of the Drakensberg Group lavas.

2. Regional facies variations of the Karoo Supergroup exert additional controls on sill emplacement. Thick (>100 m), low-rigidity, shale-rich sequences of the Ecca and Beaufort Group in the southern Karoo basin largely facilitate sill emplacement and inflation through internal deformation and ductile flow. In contrast, sill emplacement in thinner, equivalent shale units in the north has to involve a component of roof uplift, resulting in commonly thinner sills. Conversely, the thick, rigid and brittle sandstone sequences of, e.g., the Stormberg Group in the central-northern Karoo basin likely served as stress barriers to advancing magma feeders, also impeding sill inflation. This may explain dolerite-poor nature of the uppermost Karoo Supergroup. The exclusive occurrence of hydrothermal vent structures in the Stormberg Group is likely related to sill emplacement in water-saturated layers of the upper Beaufort Group sediments.
3. Differential magma pressures and proximity to basement feeders further influence the emplacement of sills. Higher driving magma pressures close to basement feeders promote rapid strata uplift and overburden failure which results in smaller sill diameters. In contrast, lower magma pressures within sill-to-sill networks leads to slower spreading rates producing larger and thicker sills.
4. Borehole and geophysical data indicate the presence of numerous basement feeders to overlying sills in the northern parts of the Karoo basin. The feeders mainly re-utilized older basement faults or pre-existing dykes and dyke swarms. The presence of basement feeders in the northern parts of the basin and predominance of sill-to-sill feeding contacts further south suggest a north to south magma transport across the basin. This magma propagation direction is corroborated by a lack of deep-level feeders and local magma flow directions along the dolerite line in the south of the basin.
5. The emplacement style and stratigraphic occurrence of sills across the Karoo basin is more consistent with many distributed feeders emplaced within the underlying basement rocks than a single plume-related source along the east coast of southern Africa.

Although this study shows that the size and geometry of sills is determined by a number of interrelated factors – magma pressure, depth, lithology and wall-rock deformation, mechanical layering, and fluid pressure - a clear distinction of the contribution of each is currently not possible. Furthermore, the limited information on magma sources to the Karoo LIP highlights the need for further investigation to better constrain their origin. Basin-wide geochemical analyses of sill complexes should provide crucial insights into the spatial distribution of different magma batches and, in turn, possibly highlight the locations of feeders beneath the Karoo basin.

4. References

Catuneanu, O. (2004). Basement control on flexural profiles and the distribution of foreland facies: The Dwyka Group of the Karoo Basin, South Africa. Geology 32, 517–520.

Catuneanu, O., Wopfner, H., Eriksson, P.G., Cairncross, B., Rubidge, B.S., Smith, R.M.H., Hancox, P.J. (2005). The Karoo basins of south-central Africa. Journal of African Earth Sciences 43, 211–253.

Chevallier, L., Woodford, A. (1999). Morpho-tectonics and mechanism of emplacement of the dolerite rings and sills of the western Karoo, South Africa. South African Journal of Geology 102, 43–54.

Chevallier, L., Woodford, A. (2002). Hydrogeology of the Main Karoo Basin: Current Knowledge and Future Research Needs. WRC Report No TT 179/02.

Chere, N., Linol, B., De Wit, M. (2017). Lateral and temporal variations of black shales across the southern Karoo Basin - Implications for shale gas exploration. South African Journal of Geology 120, 541-564.

Coetzee, A., Kisters, A.F.M. (2016). The 3D geometry of regional-scale dolerite saucer complexes and their feeders in the Secunda Complex, Karoo Basin. J. Volcanol. Geotherm. Res. 317, 66-79.

Coetzee, A., Kisters, A.F.M. (2017). Dyke-sill relationships in Karoo dolerites as indicators of propagation and emplacement processes of mafic magmas in the shallow crust. J. Structural Geology 97, 172-188.

Coetzee, A., Kisters, A.F.M. (2018). The elusive feeders of the Karoo Large Igneous Province and their structural controls. Tectonophysics 747, 146–162.

Coetzee, A., Kisters, A.F.M., Chevallier, L. (2019). Sill complexes in the Karoo LIP: Emplacement controls and regional implications. Journal of African Earth Sciences 158, 103517.

De Beer, C.H., 1995. Fold interference from simultaneous shortening in different directions: the Cape fold belt syntaxis. Journal of African Earth Sciences 21, 157–169.

Duncan, R.A., Hooper, P.R., Rehacek, J., Marsh, J.S., Duncan, A.R. (1997). The timing and duration of the Karoo igneous event, southern Gondwanaland. J. Geophys. Res. 102, 18127-18138.

Elliot, D., Fleming, T.H. (2000). Weddell triple junction: The principal focus of Ferrar and Karoo magmatism during initial breakup of Gondwana. Gondwana Research 7, 223-237.

Elliot, D., Fleming, T.H. (2004). Occurrence and Dispersal of Magmas in the Jurassic Ferrar Large Igneous Province, Antarctica. Geology 28, 539-542.

Encarnacion, J., Fleming, T.H., Elliot, D.H., Eales, H.V., 1996. Synchronous emplacement of Ferrar and Karoo dolerites and the early break-up of Gondwana. Geology 24, 535-538.

Galerne, C.Y., Neumann, E., Planke, S., 2008. Emplacement mechanisms of sill complexes: information from the geochemical architecture of the golden valley sill complex, South Africa. J. Volcanol. Geotherm. Res. 177, 425-440.

Galerne, C.Y., Galland, O., Neumann, E., Planke, S. (2011). 3D relationships between sills and their feeders: evidence from the Golden Valley Sill Complex (Karoo Basin) and experimental modelling. Journal of Volcanology and Geothermal Research 202, 189–199.

Galland, O., Planke, S., Neumann, E.R., Malthe-Sørenssen, A. (2009). Experimental modelling of shallow magma emplacement: application to saucer-shaped intrusions. Earth and Planetary Science Letters 277, 373–383.

Grab, S., Svensen, H. (2011). Rock doughnut and pothole structures of the Clarens Fm. Sandstone in the Karoo Basin, South Africa: Possible links to Lower Jurassic fluid seepage. Geomorphology 131, 14–27.

Gresse, P.G., Theron, J.N., Fitch, F.J. and Miller, J.A., 1992. Tectonic inversion and radiometric resetting of the basement in the Cape Fold Belt. In: M.J. de Wit and I.G.D. Ransome (Editors). Inversion tectonics of the Cape Fold Belt, Karoo and Cretaceous Basins of Southern Africa. Balkema, Rotterdam, Netherlands, 217–228.

Gresse, P.G., Germs, G.J.B. (1993). The Nama foreland basin: sedimentation, major unconformity bounded sequences and multisided active margin advance. Precambrian Research, 63, 247-272.

Gressier, J., Mourgues, R., Bodet, L., Matthieu, J., Galland, G., Cobbold, P. (2010). Control of pore fluid pressure on depth of emplacement of magmatic sills: An experimental approach. Tectonophysics 489, 1–13.

Gudmundsson, A., 1995. Infrastructure and mechanics of volcanic systems in Iceland. Journal of Volcanology Geothermal Research 64, 1–22.

Gudmundsson, A., 2011. Deflection of dykes into sills at discontinuities and magma chamber formation. Tectonophysics 500, 50–64.

Gudmundsson, A., Brenner, S.L., 2001. How hydrofractures become arrested. Terra. Nova 13, 456–462.

Hälbich, I.W., Fitch, F.J. and Miller, J.A., 1983. Dating the Cape Orogeny. In: A.P.G. Söhnge and I.W. Hälbich (Editors), Geodynamics of the Cape Fold Belt. Special Publications of the Geological Society of South Africa, Johannesburg, 12, 75–100.

Hansma, J., Tohver, E., Schrank, C., Jourdaan, F. and Adams, D., 2015. The

timing of the Cape Orogeny: New 40Ar/39Ar age constraints on deformation and cooling of the Cape Fold Belt, South Africa. Gondwana Research 32, 122-137.

Hanson, E.K., Moore, J.M., Bordy, E.M., Marsh, J.S., Howarth, G., Robey, J.V.A. (2009). Cretaceous erosion in central South Africa: evidence from upper-crustal xenoliths in kimberlite diatremes. South African Journal of Geology 112, 125-140.

Hastie, W.W., Watkeys, M.K., Aubourg, C., 2014. Magma flow in dyke swarms of the Karoo LIP: implications for the mantle plume hypothesis. Gondwana Research. 25, 736-755.

Jamtveit, B., Svensen, H., Podladchikov, Y., Plank, S. (2004). Hydrothermal vent complexes associated with sill intrusions in sedimentary basins. Physical Geology of High-Level Magmatic Systems. Geological Society, London, Special Publications, 234, 233-241.

Johnson, M.R., van Vuuren, C.J., Visser, J.N.J., Cole, D.I., Wickens, H.de V., Christie, A.D.M., Roberts, D.L., Brandl, G., 2006. Sedimentary rocks of the Karoo Supergroup. In: Johnson, M.R., Anhaeusser, C.R., Thomas, R.J. (Eds.), The Geology of South Africa, Geological Society of South Africa and Council for Geoscience, pp. 461–499.

Johnson, M.R. (1991). Sandstone petrography, provenance and plate tectonic setting in Gondwana context of the southeastern Cape-Karoo Basin. South African Journal of Geology 94, 137-154.

Jourdan, F., G. Féraud, H. Bertrand, A. B. Kampunzu, G. Tshoso, B. Le Gall, J. J. Tiercelin, and P. Capiez (2004), The Karoo triple junction questioned: Evidence from 40Ar/39Ar Jurassic and Proterozoic ages and geochemistry of the Okavango dike swarm (Botswana), Earth Planet. Sci. Lett., 222, 989–1006.

Jourdan, F., G. Féraud, H. Bertrand, A. B. Kampunzu, G. Tshoso, M. K. Watkeys, and B. Le Gall (2005), The Karoo large igneous province: Brevity, origin, and relation with mass extinction questioned by new 40Ar/39Ar age data, Geology, 33, 745–748.

Jourdan, F., Féraud, G., Bertrand, H., Watkeys, M.K., Kampunzu, A.B., Le Gall, B. (2006). Basement control on dyke distribution in Large Igneous Provinces: Case study of the Karoo triple junction. Earth and Planetary Science Letters 241, 307– 322.

Jourdan, F., G. Fe´raud, H. Bertrand, M. K. Watkeys, and P. R. Renne (2007a), Distinct brief major events in the Karoo large igneous province clarified by new 40Ar/39Ar ages on the Lesotho basalts, Lithos, 98, 195–209.

Jourdan, F., Féraud, G., Bertrand, H.,Watkeys, M.K. (2007b). From flood basalts to the inception of oceanization: example from the 40Ar/39Ar high-resolution picture of the Karoo large igneous province. Geochemistry, Geophysics, Geosystems 8, 989–1006.

Kavanagh, J.L., Menand, T., Sparks, R.S.J., 2006. An experimental investigation of sill formation and propagation in layered elastic media. Earth Planetary Science Letters. 245, 799–813.

Lanci, L., Tohver, E., Wilson, A., Flint, S. (2013). Upper Permian magnetic stratigraphy of the lower Beaufort Group, Karoo Basin. Earth and Planetary Science Letters 375, 123–134.

Le Gall, B., G. Tshoso, F. Jourdan, G. Fe´raud, H. Bertrand, J. J. Tiercelin, A. B. Kampunzu, M. P. Modisi, M. Dyment, and J. Maia (2002), 40Ar/39Ar geochronology and structural data from the giant Okavango and related mafic dike swarms, Karoo igneous province, Botswana, Earth Planet. Sci. Lett., 202, 595–606.

Lindique, A., De Wit, M.J., Ryberg, T., Weber, M., Chevallier, L. (2011). Deep crustal profile across the southern Karoo basin and beattie magnetic anomaly, south africa: an Integrated interpretation with tectonic implications. South African Journal of Geology 114, 265-292.

Magee, C., Jackson, C.A.L., Schofield, N. (2013). The influence of normal fault geometry on igneous sill emplacement and morphology. Geology 41(4), 407–410.

Magee, C., Jackson, C.A.L., Schofield, N. (2014). Diachronous sub-volcanic intrusion along deep-water margins: insights fromthe Irish Rockall Basin. Basin Research 26, 85–105.

Magee, C.J., Muirhead, J.D., Karvelas, A., Holford, S.P., Jackson, C.A.L., Bastow, I.D., Schofield, N., Stevenson, C.S.T., McLean, C., McCarthy, W., Shtukert, O. (2016). Lateral magma flow in mafic sill complexes. Geosphere 12 (3), 809-841.

Menand, T., Daniels, K.A., Benghiat, P., 2010. Dyke propagation and sill formation in a compressive tectonic environment. Journal of Geophysical Research 115, b08201.

Paton, D.A., Macdonald, D.I.M., Underhill, J.R. (2006). Applicability of thin or thick skinned structural models in a region of multiple inversion episodes; southern Africa. Journal of Structural Geology 28, 1933–1947.

Riley, T. R. Curtis, M.L., Leat, P.T. Watkeys, M.K., Duncan, R.A., Millar, I.L., Owens, W.H. (2006). Overlap of Karoo and Ferrar Magma Types in KwaZulu-Natal, South Africa. J. of Petrography 47(3), 541–566.

Scheiber-Enslin, S.E., Webb, S.J., Ebbing, J. (2014). Geophysically plumbing the main Karoo basin, South Africa. South African Journal of Geology 117, 2.

Schofield, N., Stevenson, C., Reston, T., 2010. Magma fingers and host rock fluidization in the emplacement of sills. Geology 38, 63-66.

Svensen, H., Corfu, F., Polteau, S., Hammer, O., Planke, S., 2012. Rapid magma emplacement in the Karoo large igneous province. Earth Planet. Sci. Lett. 325-326, 1-9.

Svensen, H., Jamtveit, B., Plank, S., Chevallier, L. (2006). Structure and evolution of hydrothermal vent complexes in the Karoo Basin, South Africa. Journal of the Geological Society 163, 671–682.

Tankard, A., Welsink, H., Aukes, P., Newton, R., Stettler, E. (2009). Tectonic evolution of the Cape and Karoo basins of South Africa. Marine and Petroleum Geology 26, 1379-1412.

Thomson, K., Hutton, D. (2004). Geometry and growth of sill complexes: insights using 3D seismic from the North Rockall Trough. Bull Volcanol 66,364–375.

Van Zijl, J.S.V. (2006a). Physical characteristics of the Karoo sediments and mode of emplacement of the dolerites. South African Journal of Geology 9, 329-334.

Van Zijl, J.S.V. (2006b). A review of the resistivity structure of the Karoo Supergroup South Africa, with emphasis on the dolerites: A study in anisotropy. South African Journal of Geology 109, 315-328.

Veevers, J.J., Cole, D.I., Cowan, E.J., 1994c. Southern Africa: Karoo basin and Cape Fold Belt. In: Veevers, J.J., Powell, C.McA. (Eds.), Permian-Triassic Pangean Basins and Foldbelts along the Panthalassan Margin of Gondwanaland. Geol. Soc. America, Boulder, Colorado, Memoir 184, 223–279.

Chapter 7: Conclusion and future outlook

7.1 Conclusion

This thesis set out to understand the controls that govern the emplacement of sills and their underlying feeder systems and how this relates to the overall geodynamic environment during Karoo magmatism. It is clear from field relationships in addition to the drill hole and geophysical data presented herein that sill complexes and their feeders play a dominant role in facilitating the rapid emplacement of huge volumes of magma through the crust. Despite remaining uncertainties, there is sufficient evidence to conclude that sills are fed from feeders exploiting pre-existing weaknesses within the competent basement rocks of the Kalahari craton. Furthermore, the multitude of feeders and their distributed occurrence suggests the emplacement of magmas across much of the Kalahari craton rather than originating from a few isolated feeders or plume heads located along the rift between southern Africa and Antarctica (Fig. 7.1a). Instead, the emplacement of Karoo sill feeders through the Kalahari craton is more consistent with thermal incubation of the sub-continental mantle beneath Gondwana.

Conversely, the central Karoo basin is marked by nested sill complexes formed through multiple distinct, successively emplaced, saucer-shaped sills. Sill complexes expand and grow by magmatic underaccretion of later magma batches below earlier emplaced sills. The spatial overlap of several unique saucer-shaped sills within a localised area suggests the reutilization of feeder structures and emphasizes the importance of pre-existing structures for Karoo magma dispersal. Moreover, magmatic underaccretion indicates earlier emplaced sills act as stress barriers to later sill intrusion which is characteristic of a compressive stress field.

This indicates an abrupt changeover in the regional stress field during Karoo magmatism from compressive during sill emplacement at 184-182 Ma to extensional during the intrusion of dyke swarms from 182 Ma onwards. Considering the rapid emplacement of sills in the Karoo (<500 ka) (Svensen et al., 2012) and other basins it is conceivable that their sheer volume would result in lithospheric loading and subsidence (Fig. 7.1b). Lithospheric flexure within the basins and subsequent extension along their margins may have initiated a swap in the regional stress field and induced the emplacement of dyke swarms along cratonic boundaries (Fig. 7.1b).

Sills described throughout the Karoo basin highlighted a distinct north-south progression in sill diameter and emplacement style that is likely controlled not only by depth but also facies changes and proximity to feeders. Shallow emplacement depths (<500 m) are confined to the northern parts of the Karoo basin and associated with small (<25 km), single-level sill complexes and numerous systematic dykes. Intermediate emplacement depths (500-700 m) prevailed in the central Karoo basin and is characterised by larger (<50 km) nested sill complexes with more disordered dyke patterns. Advanced emplacement depths (<1.5 km) are characteristic of the southern Karoo basin and marked by mega-sills up to 100 km wide and the complete absence of dykes.

The presence of basement feeders in the northern Karoo and predominance of sill-to-sill feeding networks in the central and southern Karoo suggest a north to south magma transport across the basin which opposes current beliefs (e.g. Chevallier and Woodford, 1999, 2002; Elliot and Fleming, 2000) of magma injection from the Weddell triple junction along the eastern margin of the basin (Fig. 7.1.a). Overall, it is evident from the close spatial relationship of saucer-shaped sills and pre-existing basement structures, sill-to-sill feeder

networks elsewhere in the Karoo basin in addition to dyke swarms largely confined to pre-existing crustal weaknesses that the mode of emplacement of Karoo magmatism was determined by inherited basin and lithospheric architecture.

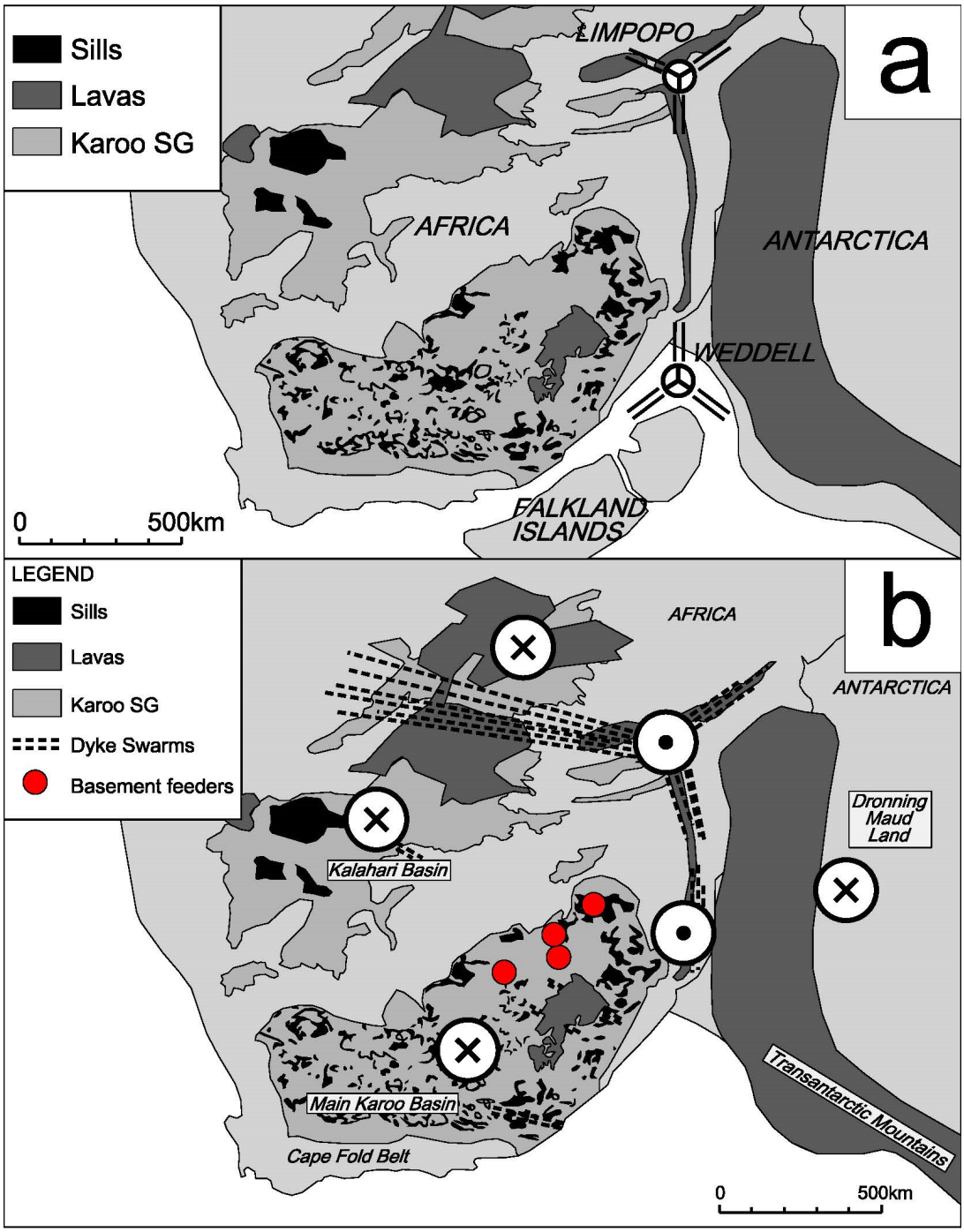

Figure 7.1: *Gondwana reconstructions showing the (a) current mantle plume model for Karoo magmatism and (b) the proposed feeder model based on basement feeders in the northern Karoo basin.*

7.2 Future outlook

The spatial distribution of sill feeders and the thermal incubation model proposed herein challenges the commonly held view of how sill complexes are fed across the Karoo basin. However, locating actual feeders within the basement rocks remain problematic and highlights the need for further investigation. Additional drilling work and seismic imaging are perhaps not the best methods to effectively locate such feeders especially considering their likely narrow extent. Instead, large-scale geochemical analyses of nested sill complexes across the Karoo basin and, to a lesser extent, dating of dolerite intrusions found in deep mining operations may be able to provide further insight into the spatial distribution of magma sources to the Karoo LIP. Importantly, the results will also have implications for other LIP's, notably the Ferrar LIP, which to date relies on models that support magma injection over thousands of kilometres from mantle plumes located near the Weddell triple junction (Fig. 7.1a) (e.g. Elliot and Fleming, 2000). Such investigations will require large-scale data collection and multi-disciplinary collaboration. Therefore, until such time, we will have to continue to rely on well-preserved field exposures and subsurface data to shape our understanding.

REFERENCES

Chevallier, L., Woodford, A. (1999). Morpho-tectonics and mechanism of emplacement of the dolerite rings and sills of the western Karoo, South Africa. South African Journal of Geology 102, 43–54.

Chevallier, L., Woodford, A. (2002). Hydrogeology of the Main Karoo Basin: Current Knowledge and Future Research Needs. WRC Report No TT 179/02.

Elliot, D., Fleming, T.H. (2000). Weddell triple junction: The principal focus of Ferrar and Karoo magmatism during initial breakup of Gondwana. Gondwana Research 7, 223-237.

Svensen, H., Corfu, F., Polteau, S., Hammer, O., Planke, S. (2012). Rapid magma emplacement in the Karoo large igneous province. Earth Planet. Sci. Lett. 325–326, 1–9.

Appendix A: Research outputs

Peer-reviewed articles:

Coetzee, A. & Kisters, A.F.M. (2018). ***The elusive feeders of the Karoo Large Igneous Province and their structural controls***. *Tectonophysics, 747-748, 146-162.*

[1]Coetzee, A. & Kisters, A.F.M., Chevallier, L. (2019). ***Sill complexes in the Karoo LIP: emplacement controls and regional implications***. Journal of African Earth Sciences 158, 103517.

Article under review:

Coetzee, A. & Kisters, A.F.M., in submission to Gondwana Research (assigned manuscript no: GR-S-19-00657). ***Spatial variations of sills and implications for magma dispersal across the Karoo basin***.

Conference abstracts:

Coetzee, A. & Kisters, A.F.M., July 2018. Oral presentation: ***The elusive feeders of the Karoo LIP and their structural controls***. 2018 Geocongress, Johannesburg.

Appendix B: Data

Chapter 4 - Craton-hosted sill feeders

Due to confidentiality the drilling data used in this chapter cannot be made public but can be requested from the university for research purposes.

Chapter 5 - Sill emplacement controls

The below represents the drill collars and digitized logs from the Victoria West area.

BOREID	LAT	LONG	ELEV
G40014	-31.43076	22.71315	1320.000
G40015	-31.42956	22.71260	1316.000
G40016	-31.42960	22.71255	1316.000
G40016A	-31.42966	22.71251	1316.000
G40017	-31.42974	22.71245	1316.000
G40018	-31.43081	22.71319	1320.000
G40019	-31.43066	22.71347	1320.000
G40020	-31.43064	22.71347	1320.000
G40021	-31.38928	22.85531	1400.000
G40022	-31.38929	22.85521	1401.381
G40064	-31.38930	22.85495	1403.762
G40065	-31.38931	22.85469	1405.587
G40066	-31.38918	22.85789	1393.427
G40067	-31.40287	22.84600	1333.410
G40068	-31.40285	22.84590	1334.000
G40069	-31.40293	22.84621	1333.666
G40070	-31.40300	22.84646	1333.685
G40071	-31.40310	22.84685	1334.216
G40072	-31.40276	22.84555	1333.106
G40073	-31.40969	22.85027	1357.733
G40074	-31.40970	22.85024	1358.465
G40075	-31.40973	22.85015	1359.424
G40076	-31.40975	22.85007	1360.000
G40077	-31.40959	22.85053	1351.000
G40077A	-31.40956	22.85053	1351.115
G40078	-31.40950	22.85072	1347.590
G40079	-31.40328	22.84753	1334.677
G40080	-31.37752	22.88543	1340.000
G40081	-31.37734	22.88536	1340.682
G40082	-31.37771	22.88532	1340.094
G40083	-31.37760	22.88493	1341.918
G40186	-31.38324	23.03531	1356.952
G40187	-31.38341	23.03537	1355.829
G40188	-31.38432	23.03570	1351.222
G40189	-31.38442	23.03570	1350.989
G40190	-31.37659	22.88567	1339.064
G40191	-31.40241	22.84864	1335.927
G40192	-31.43784	23.12592	1342.000

G40193	-31.43784	23.12576	1341.769
G40194	-31.43784	23.12566	1341.143
G40195	-31.43786	23.12602	1340.981
G40196	-31.43788	23.12612	1339.400
G40197	-31.43790	23.12632	1337.400
G40198	-31.43784	23.12536	1339.615
G40199	-31.44827	23.12605	1315.000
G40200	-31.44825	23.12587	1315.000
G40201	-31.44825	23.12560	1315.000
G40203	-31.44825	23.12465	1315.000
G40204	-31.44826	23.12595	1315.000
G40205	-31.44827	23.12615	1315.000
G40205A	-31.44825	23.12615	1315.000
G40206	-31.44827	23.12635	1315.000
G46001	-31.38464	23.03570	1350.100
G46002	-31.38534	23.03570	1347.422
G46003	-31.38848	23.03658	1340.000
G46004	-31.38748	23.03658	1341.780
G46005	-31.38923	23.03629	1338.400
G46005A	-31.38923	23.03627	1338.400

BOREID	FROM	TOLITHO	THICK	STRAT	MAIN
G40014	0	4	4	OVB	SST
G40014	4	22	18		SST
G40014	22	26	4		SLT
G40014	26	28	2		SST
G40014	28	29	1	SILL	DO
G40014	29	48	19		SLT
G40014	48	56.5	8.5		SST
G40014	56.5	82	25.5		SLT
G40014	82	88	6		SST
G40014	88	91	3		SLT
G40014	91	95.5	4.5		SST
G40014	95.5	103	7.5		SLT
G40014	103	204	101	SILL	DO
G40014	204	204	0	EOH	EOH
G40015	0	4.5	4.5	OVB	SST
G40015	4.5	7	2.5	SILL	DO
G40015	7	14	7		SLT
G40015	14	23	9		SST
G40015	23	37	14		SLT
G40015	37	38	1		SST
G40015	38	41	3		SLT
G40015	41	42	1		SST
G40015	42	48	6		SLT
G40015	48	49	1		SST
G40015	49	58	9		SLT
G40015	58	60	2		SST
G40015	60	66	6		SLT
G40015	66	76	10		SST
G40015	76	88	12		SLT
G40015	88	90	2		SST
G40015	90	100	10		SLT
G40015	100	100	0	EOH	EOH
G40016	0	4	4	OVB	DO
G40016	4	27	23	SILL	DO
G40016	27	27	0	EOH	EOH
G40016A	0	4	4	OVB	DO
G40016A	4	45.5	41.5		DO
G40016A	45.5	49	3.5		SLT
G40016A	49	50.5	1.5		SST

G40016A	50.5	60.5	10		SLT
G40016A	60.5	61	0.5		SST
G40016A	61	62	1		SLT
G40016A	62	66.5	4.5		SLT
G40016A	66.5	76	9.5		SST
G40016A	76	78	2		SLT
G40016A	78	79.5	1.5		SST
G40016A	79.5	87	7.5		SLT
G40016A	87	90.5	3.5		SST
G40016A	90.5	91	0.5		SLT
G40016A	91	92	1		SST
G40016A	92	102.5	10.5		SLT
G40016A	102.5	107.5	5		SST
G40016A	107.5	112.5	5		SLT
G40016A	112.5	114.5	2		SST
G40016A	114.5	122.5	8		SLT
G40016A	122.5	130	7.5		SST
G40016A	130	147	17		SST
G40016A	147	148.5	1.5		SLT
G40016A	148.5	151.5	3		SST
G40016A	151.5	163	11.5		SLT
G40016A	163	165.6	2.6		SST
G40016A	165.6	168.5	2.9	SILL	DO
G40016A	168.5	169.5	1		SST
G40016A	169.5	252	82.5	SILL	DO
G40016A	252	252	0	EOH	EOH
G40017	0	5	5	OVB	DO
G40017	5	32.5	27.5		SLT
G40017	32.5	69.5	37	SILL	DO
G40017	69.5	75.5	6		SST
G40017	75.5	77.5	2		SLT
G40017	77.5	78	0.5		SST
G40017	78	86.5	8.5		SLT
G40017	86.5	89.5	3		SST
G40017	89.5	101.5	12		SLT
G40017	101.5	106.5	5		SST
G40017	106.5	114	7.5		SLT
G40017	114	125	11		SST
G40017	125	152	27		SLT
G40017	152	164.5	12.5		SST
G40017	164.5	252	87.5	SILL	DO
G40017	252	252	0	EOH	EOH
G40018	0	4	4	OVB	DO
G40018	4	20.5	16.5		SLT
G40018	20.5	21.5	1		SST
G40018	21.5	27	5.5		SLT
G40018	27	30	3		SST
G40018	30	44	14		SLT
G40018	44	45	1		SST
G40018	45	50	5		SLT
G40018	50	57.5	7.5		SST
G40018	57.5	73	15.5		SLT
G40018	73	75	2		SST
G40018	75	86	11		SLT
G40018	86	99.5	13.5		SST
G40018	99.5	118	18.5		SLT
G40018	118	126.5	8.5		SST
G40018	126.5	134	7.5		SLT
G40018	134	252	118	SILL	DO
G40018	252	252	0	EOH	EOH
G40019	0	3	3	OVB	DO
G40019	3	51.5	48.5	SILL	DO
G40019	51.5	65.5	14		SLT

G40019	65.5	114.5	49	SILL	DO
G40019	114.5	116.5	2		SLT
G40019	116.5	127	10.5	SILL	DO
G40019	127	132	5		SLT
G40019	132	132	0	EOH	EOH
G40020	0	3	3	OVB	SST
G40020	3	8	5		SST
G40020	8	20	12		SLT
G40020	20	22	2		SST
G40020	22	27.5	5.5		SLT
G40020	27.5	32.5	5		SST
G40020	32.5	40	7.5		SLT
G40020	40	42	2		SST
G40020	42	45	3		SLT
G40020	45	61.5	16.5		SST
G40020	61.5	109.5	48	SILL	DO
G40020	109.5	151	41.5		SST
G40020	151	153	2		DO
G40020	153	155.5	2.5		SST
G40020	155.5	252	96.5	SILL	DO
G40020	252	252	0	EOH	EOH
G40021	0	6	6		SST
G40021	6	7.5	1.5		SLT
G40021	7.5	14	6.5		SST
G40021	14	15	1		SLT
G40021	15	98.5	83.5	SILL	DO
G40021	98.5	102	3.5		SST
G40021	102	118.5	16.5	SILL	DO
G40021	118.5	130	11.5		SST
G40021	130	167	37		SLT
G40021	167	168	1		SST
G40021	168	171.5	3.5		SLT
G40021	171.5	173	1.5		SST
G40021	173	182.5	9.5		SLT
G40021	182.5	183	0.5		SST
G40021	183	252	69		SLT
G40021	252	252	0	EOH	EOH
G40022	0	1	1	OVB	SST
G40022	1	8	7		SLT
G40022	8	18	10		SST
G40022	18	100.5	82.5	SILL	DO
G40022	100.5	101	0.5		SST
G40022	101	121	20	SILL	DO
G40022	121	132.5	11.5		SST
G40022	132.5	163.5	31		SLT
G40022	163.5	175	11.5		SST
G40022	175	189	14		SLT
G40022	189	210	21		SST
G40022	210	217	7		SLT
G40022	217	221	4		SST
G40022	221	227	6		SLT
G40022	227	243	16		SST
G40022	243	252	9		SLT
G40022	252	252	0	EOH	EOH
G40064	0	2.5	2.5		SST
G40064	2.5	66.5	64	SILL	DO
G40064	66.5	91	24.5		SST
G40064	91	100	9		SLT
G40064	100	104	4		SST
G40064	104	117	13	SILL	DO
G40064	117	128	11		SST
G40064	128	130	2		DO
G40064	130	133	3		SST

G40064	133	135	2		SLT
G40064	135	140	5		SST
G40064	140	252	112		SLT
G40064	252	252	0	EOH	EOH
G40065	0	5	5	OVB	DO
G40065	5	48	43	SILL	DO
G40065	48	72	24		SST
G40065	72	73	1		SLT
G40065	73	108	35		SST
G40065	108	121	13	SILL	DO
G40065	121	135	14		SLT
G40065	135	144.5	9.5		SST
G40065	144.5	150	5.5		SLT
G40065	150	150	0	EOH	EOH
G40066	0	0.5	0.5	OVB	SST
G40066	0.5	5.5	5		SST
G40066	5.5	8.5	3		SLT
G40066	8.5	10.5	2		SST
G40066	10.5	111.5	101	SILL	DO
G40066	111.5	112	0.5		SST
G40066	112	113	1	SILL	DO
G40066	113	114.5	1.5		SST
G40066	114.5	115.5	1	SILL	DO
G40066	115.5	128	12.5		SST
G40066	128	128	0	EOH	EOH
G40067	0	0.5	0.5	OVB	SST
G40067	0.5	55.5	55	SILL	DO
G40067	55.5	97.5	42		SST
G40067	97.5	98.5	1	SILL	DO
G40067	98.5	100.5	2		SST
G40067	100.5	101.5	1	SILL	DO
G40067	101.5	103	1.5		SST
G40067	103	105.5	2.5	SILL	DO
G40067	105.5	115	9.5		SST
G40067	115	116	1		SLT
G40067	116	134	18		SST
G40067	134	135	1		SLT
G40067	135	136	1		SST
G40067	136	143	7		SLT
G40067	143	150	7		SST
G40067	150	150	0	EOH	EOH
G40068	0	3.5	3.5	OVB	DO
G40068	3.5	19.5	16	SILL	DO
G40068	19.5	23.5	4		SST
G40068	23.5	43.5	20		DO
G40068	43.5	97	53.5		SST
G40068	97	97.5	0.5		DO
G40068	97.5	102	4.5		SST
G40068	102	105.5	3.5		DO
G40068	105.5	120	14.5		SST
G40068	120	120	0	EOH	EOH
G40069	0	2	2	OVB	GRD
G40069	2	19.5	17.5		SST
G40069	19.5	105.5	86	SILL	DO
G40069	105.5	108	2.5		SST
G40069	108	108	0	EOH	EOH
G40070	0	2.5	2.5	OVB	GRD
G40070	2.5	70	67.5		SST
G40070	70	146	76	SILL	DO
G40070	146	151	5		SST
G40070	151	156	5		DO
G40070	156	156	0	EOH	EOH
G40071	0	5	5	OVB	GRD

G40071	5	14	9		SST
G40071	14	39	25		SLT
G40071	39	41.5	2.5		SST
G40071	41.5	77.5	36		SLT
G40071	77.5	80	2.5		SST
G40071	80	84.5	4.5		SLT
G40071	84.5	92	7.5		SST
G40071	92	120.5	28.5		SLT
G40071	120.5	138	17.5		SST
G40071	138	139	1		SLT
G40071	139	146.5	7.5		SST
G40071	146.5	234	87.5		DO
G40071	234	238	4		SST
G40071	238	242	4		SLT
G40071	242	252	10		SST
G40071	252	252	0	EOH	EOH
G40072	0	1	1	OVB	GRD
G40072	1	6	5		SLT
G40072	6	8	2		SST
G40072	8	22.5	14.5		SLT
G40072	22.5	27	4.5		SST
G40072	27	178	151		SLT
G40072	178	180	2		SST
G40072	180	184	4		SLT
G40072	184	194	10		SST
G40072	194	248	54		SLT
G40072	248	256.5	8.5	SILL	DO
G40072	256.5	298	41.5		SLT
G40072	298	298	0	EOH	EOH
G40073	0	0.5	0.5	OVB	DO
G40073	0.5	74	73.5	SILL	DO
G40073	74	90.5	16.5		SST
G40073	90.5	101	10.5	SILL	DO
G40073	101	109	8		SST
G40073	109	110	1	SILL	DO
G40073	110	138.5	28.5		SST
G40073	138.5	140	1.5	SILL	DO
G40073	140	153	13		SST
G40073	153	180	27		SLT
G40073	180	181.5	1.5		SST
G40073	181.5	192	10.5		SLT
G40073	192	198.5	6.5	SILL	DO
G40073	198.5	199.5	1		SST
G40073	199.5	246.5	47		SLT
G40073	246.5	248.5	2		SST
G40073	248.5	295	46.5		SLT
G40073	295	298	3		SST
G40073	298	298	0	EOH	EOH
G40074	0	4	4	OVB	DO
G40074	4	86	82	SILL	DO
G40074	86	87.5	1.5		SST
G40074	87.5	93	5.5		SLT
G40074	93	97.5	4.5	SILL	DO
G40074	97.5	152.5	55		SST
G40074	152.5	252	99.5		SLT
G40074	252	252	0	EOH	EOH
G40075	0	16.5	16.5	OVB	DO
G40075	16.5	31	14.5		SST
G40075	31	43.5	12.5		SLT
G40075	43.5	91	47.5	SILL	DO
G40075	91	96.5	5.5		SST
G40075	96.5	97.5	1	SILL	DO
G40075	97.5	122	24.5		SST

G40075	122	123	1		SLT
G40075	123	124	1		SST
G40075	124	131	7		SLT
G40075	131	134	3		SST
G40075	134	145	11		SLT
G40075	145	152	7		SST
G40075	152	152.5	0.5		DO
G40075	152.5	204	51.5		SLT
G40075	204	204	0	EOH	EOH
G40076	0	11.5	11.5	OVB	DO
G40076	11.5	39.5	28	SILL	DO
G40076	39.5	40	0.5		SST
G40076	40	42.5	2.5		SLT
G40076	42.5	44.5	2		DO
G40076	44.5	45	0.5		SLT
G40076	45	84	39	SILL	DO
G40076	84	87	3		SLT
G40076	87	108.5	21.5		SST
G40076	108.5	111.5	3		SLT
G40076	111.5	114	2.5		SST
G40076	114	121	7		SLT
G40076	121	122	1		SST
G40076	122	130	8		SLT
G40076	130	138	8		SST
G40076	138	146	8		SLT
G40076	146	152.5	6.5		SST
G40076	152.5	153.5	1	SILL	DO
G40076	153.5	154	0.5		SST
G40076	154	174.5	20.5		SLT
G40076	174.5	176	1.5		SST
G40076	176	183	7		SLT
G40076	183	184	1		SST
G40076	184	186	2		SLT
G40076	186	190	4		SST
G40076	190	240	50		SLT
G40076	240	240	0	EOH	EOH
G40077	0	4.5	4.5	OVB	DO
G40077	4.5	18	13.5		SLT
G40077	18	26	8		SST
G40077	26	27.5	1.5	SILL	DO
G40077	27.5	28	0.5		SLT
G40077	28	91	63	SILL	DO
G40077	91	91	0	EOH	EOH
G40077A	0	4.5	4.5	OVB	SLT
G40077A	4.5	18	13.5		SLT
G40077A	18	26	8		SST
G40077A	26	27.5	1.5	SILL	DO
G40077A	27.5	28	0.5		SLT
G40077A	28	117	89	SILL	DO
G40077A	117	120	3		SST
G40077A	120	138	18	SILL	DO
G40077A	138	160	22		SST
G40077A	160	162	2		SLT
G40077A	162	163.5	1.5	SILL	DO
G40077A	163.5	252	88.5		SLT
G40077A	252	252	0	EOH	EOH
G40078	0	4	4	OVB	SLT
G40078	4	18	14		SLT
G40078	18	23	5		SST
G40078	23	30	7		SLT
G40078	30	39	9		SST
G40078	39	43.5	4.5		SLT
G40078	43.5	44	0.5		SST

G40078	44	45.5	1.5		SLT
G40078	45.5	49.5	4		SST
G40078	49.5	58	8.5		SLT
G40078	58	61.5	3.5		SST
G40078	61.5	150	88.5	SILL	DO
G40078	150	202.5	52.5		SLT
G40078	202.5	203	0.5		SST
G40078	203	252	49		SLT
G40078	252	252	0	EOH	EOH
G40079	0	5	5	OVB	GRD
G40079	5	18	13		SLT
G40079	18	20.5	2.5		SST
G40079	20.5	41.5	21		SLT
G40079	41.5	44.5	3		SST
G40079	44.5	80.5	36		SLT
G40079	80.5	83	2.5		SST
G40079	83	86.5	3.5		SLT
G40079	86.5	95.5	9		SST
G40079	95.5	101.5	6		SLT
G40079	101.5	102	0.5		SST
G40079	102	106.5	4.5		SLT
G40079	106.5	108.5	2		SST
G40079	108.5	113.5	5		SLT
G40079	113.5	114	0.5		SST
G40079	114	134	20		SLT
G40079	134	142	8		SST
G40079	142	145.5	3.5		SLT
G40079	145.5	156.5	11	SILL	DO
G40079	156.5	253	96.5		SST
G40079	253	255	2		SLT
G40079	255	260	5		SST
G40079	260	260	0	EOH	EOH
G40080	0	3	3	OVB	DO
G40080	3	66.5	63.5	SILL	DO
G40080	66.5	72.6	6.1		SST
G40080	72.6	73.4	0.8		SLT
G40080	73.4	109.5	36.1		SST
G40080	109.5	110.5	1		SLT
G40080	110.5	111	0.5		SST
G40080	111	114	3		SLT
G40080	114	114	0	EOH	EOH
G40081	0	2.5	2.5	OVB	DO
G40081	2.5	70.5	68	SILL	DO
G40081	70.5	72	1.5		SST
G40081	72	75.5	3.5	SILL	DO
G40081	75.5	113.5	38		SST
G40081	113.5	114.5	1		SLT
G40081	114.5	115	0.5		SST
G40081	115	126.5	11.5		SLT
G40081	126.5	130	3.5		SST
G40081	130	139	9		SLT
G40081	139	140.5	1.5		SST
G40081	140.5	144	3.5		SLT
G40081	144	147.5	3.5		SST
G40081	147.5	149	1.5		SLT
G40081	149	176.5	27.5		SST
G40081	176.5	177.5	1	SILL	DO
G40081	177.5	194.5	17		SLT
G40081	194.5	200	5.5		SST
G40081	200	201	1		SLT
G40081	201	206	5	SILL	DO
G40081	206	218	12		SLT
G40081	218	218	0	EOH	EOH

G40082	0	0.5	0.5	OVB	DO
G40082	0.5	65	64.5	SILL	DO
G40082	65	65	0	EOH	EOH
G40083	0	3	3	OVB	DO
G40083	3	73	70	SILL	DO
G40083	73	73.5	0.5		SST
G40083	73.5	75	1.5		DO
G40083	75	76	1		SST
G40083	76	76	0	EOH	EOH
G40186	0	5	5	OVB	DO
G40186	5	12	7		SST
G40186	12	13	1		SLT
G40186	13	19	6		SST
G40186	19	20.5	1.5		SLT
G40186	20.5	25	4.5		SST
G40186	25	38.5	13.5		SLT
G40186	38.5	40.5	2		SST
G40186	40.5	47.5	7		SLT
G40186	47.5	53.5	6		SST
G40186	53.5	67	13.5		SLT
G40186	67	70.5	3.5		SST
G40186	70.5	89	18.5		SLT
G40186	89	96	7		SST
G40186	96	103	7		SLT
G40186	103	106	3		SST
G40186	106	145	39		SLT
G40186	145	147	2		SST
G40186	147	149.5	2.5		SLT
G40186	149.5	151	1.5		SST
G40186	151	160.5	9.5		SLT
G40186	160.5	161.5	1		SST
G40186	161.5	199	37.5		SLT
G40186	199	199	0	EOH	EOH
G40187	0	4	4	OVB	DO
G40187	4	23	19		SST
G40187	23	25	2		SLT
G40187	25	27	2		SST
G40187	27	28	1		SLT
G40187	28	30.5	2.5		SST
G40187	30.5	36.5	6		SLT
G40187	36.5	43	6.5		SST
G40187	43	45	2		SLT
G40187	45	55	10		SST
G40187	55	64	9		SLT
G40187	64	71	7		SST
G40187	71	77	6		SLT
G40187	77	79	2		SST
G40187	79	82	3		SLT
G40187	82	96.5	14.5		SST
G40187	96.5	103	6.5		SLT
G40187	103	106	3		SST
G40187	106	149.5	43.5		SLT
G40187	149.5	151	1.5		SST
G40187	151	151	0	EOH	EOH
G40188	0	0.5	0.5	OVB	GRD
G40188	0.5	2.5	2	OVB	SLT
G40188	2.5	30	27.5	SILL	DO
G40188	30	34	4		SST
G40188	34	35	1		SLT
G40188	35	46.5	11.5		SST
G40188	46.5	47	0.5		SLT
G40188	47	48.5	1.5		SST
G40188	48.5	49	0.5		SLT

G40188	49	52.5	3.5		SST
G40188	52.5	53	0.5		SLT
G40188	53	55	2		SST
G40188	55	56.5	1.5		SLT
G40188	56.5	64.5	8		SST
G40188	64.5	68	3.5		SLT
G40188	68	70.5	2.5		SST
G40188	70.5	84	13.5		SLT
G40188	84	95.5	11.5		SST
G40188	95.5	101	5.5		SLT
G40188	101	102.5	1.5		SST
G40188	102.5	103	0.5		SLT
G40188	103	103	0	EOH	EOH
G40189	0	3	3	OVB	GRD
G40189	3	34	31	SILL	DO
G40189	34	37	3		SST
G40189	37	39	2		SLT
G40189	39	55	16		SST
G40189	55	56	1		SLT
G40189	56	64	8		SST
G40189	64	82	18		SLT
G40189	82	96	14		SST
G40189	96	100	4		SLT
G40189	100	100	0	EOH	EOH
G40190	0	0.5	0.5	OVB	GRD
G40190	0.5	99	98.5	SILL	DO
G40190	99	100	1		SST
G40190	100	100	0	EOH	EOH
G40191	0	4	4	OVB	GRD
G40191	4	12	8		SLT
G40191	12	14	2		SST
G40191	14	17	3		SLT
G40191	17	19	2		SST
G40191	19	20	1		SLT
G40191	20	30	10		SST
G40191	30	39	9		SLT
G40191	39	40	1		SST
G40191	40	43	3		SLT
G40191	43	44	1		SST
G40191	44	47.5	3.5		SLT
G40191	47.5	48	0.5		SST
G40191	48	60.5	12.5		SLT
G40191	60.5	63	2.5		SST
G40191	63	67.5	4.5		SLT
G40191	67.5	68	0.5		SST
G40191	68	71	3		SLT
G40191	71	72	1		SST
G40191	72	80	8		SLT
G40191	80	84	4		SST
G40191	84	88	4		SLT
G40191	88	90.5	2.5		SST
G40191	90.5	91	0.5		SLT
G40191	91	95.5	4.5		SST
G40191	95.5	100.5	5		SLT
G40191	100.5	101	0.5		SST
G40191	101	109	8		SLT
G40191	109	110.5	1.5		SST
G40191	110.5	111.5	1		DO
G40191	111.5	112	0.5		SST
G40191	112	117	5		DO
G40191	117	137	20		SST
G40191	137	138	1		SLT
G40191	138	140.5	2.5		SST

G40191	140.5	141.5	1		SLT
G40191	141.5	144.5	3		SST
G40191	144.5	252.5	108	SILL	DO
G40191	252.5	253.5	1		SST
G40191	253.5	254	0.5		DO
G40191	254	260	6		SST
G40191	260	260	0	EOH	EOH
G40192	0	5	5	OVB	DO
G40192	5	60	55	SILL	DO
G40192	60	60.5	0.5		SST
G40192	60.5	73.5	13	SILL	DO
G40192	73.5	80.5	7		SLT
G40192	80.5	96.5	16		SST
G40192	96.5	100.5	4		SLT
G40192	100.5	103	2.5		SST
G40192	103	104.5	1.5		SLT
G40192	104.5	111.5	7		SST
G40192	111.5	125	13.5		SLT
G40192	125	132	7		SST
G40192	132	135	3		SLT
G40192	135	136.5	1.5		SST
G40192	136.5	141.5	5		SLT
G40192	141.5	142	0.5		SST
G40192	142	195.5	53.5		SLT
G40192	195.5	201	5.5		SST
G40192	201	204	3		SLT
G40192	204	205	1		SST
G40192	205	208	3		SLT
G40192	208	212	4		SST
G40192	212	224.5	12.5		SLT
G40192	224.5	225.5	1		SST
G40192	225.5	232.5	7		SLT
G40192	232.5	233	0.5		SST
G40192	233	242	9		SLT
G40192	242	243.5	1.5		SST
G40192	243.5	245.5	2		SLT
G40192	245.5	246	0.5		SST
G40192	246	247	1		SLT
G40192	247	250	3		SST
G40192	250	250	0	EOH	EOH
G40193	0	3	3	OVB	DO
G40193	3	15.5	12.5		SLT
G40193	15.5	18	2.5		SST
G40193	18	115	97	SILL	DO
G40193	115	115.2	0.2		SST
G40193	115.2	117	1.8	SILL	DO
G40193	117	118	1		SST
G40193	118	119	1		SLT
G40193	119	121.5	2.5		SST
G40193	121.5	150	28.5	SILL	DO
G40193	150	163	13		SST
G40193	163	169	6		SLT
G40193	169	170	1		SST
G40193	170	179	9		SLT
G40193	179	180	1		SST
G40193	180	185.5	5.5		SLT
G40193	185.5	186.5	1		SST
G40193	186.5	195.5	9		SLT
G40193	195.5	197.5	2		SST
G40193	197.5	199.5	2		SLT
G40193	199.5	201	1.5		SST
G40193	201	204	3		SLT
G40193	204	206.5	2.5		SST

G40193	206.5	229	22.5		SLT
G40193	229	230	1		SST
G40193	230	236	6		SLT
G40193	236	238	2		SST
G40193	238	241	3		SLT
G40193	241	243	2		SST
G40193	243	249	6		SLT
G40193	249	250	1		SST
G40193	250	250	0	EOH	EOH
G40194	0	17.5	17.5		SLT
G40194	17.5	18	0.5		SST
G40194	18	117	99	SILL	DO
G40194	117	122.5	5.5		SST
G40194	122.5	150.5	28	SILL	DO
G40194	150.5	160.5	10		SST
G40194	160.5	161.5	1		SLT
G40194	161.5	163.5	2		SST
G40194	163.5	165.5	2	SILL	DO
G40194	165.5	169	3.5		SLT
G40194	169	170.5	1.5		SST
G40194	170.5	178.5	8		SLT
G40194	178.5	179.5	1		SST
G40194	179.5	194.5	15		SLT
G40194	194.5	198	3.5		SST
G40194	198	215	17		SLT
G40194	215	216	1		SST
G40194	216	222	6		SLT
G40194	222	230	8		SST
G40194	230	237	7		SLT
G40194	237	243	6		SST
G40194	243	245.5	2.5		SLT
G40194	245.5	249	3.5		SST
G40194	249	250	1		SLT
G40194	250	250	0	EOH	EOH
G40195	0	0.5	0.5	OVB	DO
G40195	0.5	60	59.5	SILL	DO
G40195	60	63.5	3.5		SST
G40195	63.5	65.5	2		SLT
G40195	65.5	71.5	6		SST
G40195	71.5	73.5	2		SLT
G40195	73.5	90.5	17		SST
G40195	90.5	91	0.5	SILL	DO
G40195	91	96.5	5.5		SST
G40195	96.5	97.5	1	SILL	DO
G40195	97.5	100.5	3		SLT
G40195	100.5	102	1.5		SST
G40195	102	104	2		SLT
G40195	104	106	2		SST
G40195	106	108	2		SLT
G40195	108	113.5	5.5		SST
G40195	113.5	131.5	18		SLT
G40195	131.5	132	0.5		SST
G40195	132	136.5	4.5		SLT
G40195	136.5	140.5	4		SST
G40195	140.5	142	1.5		SLT
G40195	142	146.5	4.5		SST
G40195	146.5	192.5	46		SLT
G40195	192.5	202	9.5		SST
G40195	202	203	1		SLT
G40195	203	212.5	9.5		SST
G40195	212.5	240	27.5		SLT
G40195	240	247.5	7.5		SST
G40195	247.5	252	4.5		SLT

G40195	252	252	0	EOH	EOH
G40196	0	5.5	5.5	OVB	DO
G40196	5.5	58	52.5	SILL	DO
G40196	58	75	17		SST
G40196	75	76.5	1.5		SLT
G40196	76.5	77.5	1		SST
G40196	77.5	78	0.5		SLT
G40196	78	80.5	2.5		SST
G40196	80.5	83	2.5		SLT
G40196	83	84.5	1.5		SST
G40196	84.5	85	0.5	SILL	DO
G40196	85	86.5	1.5		SST
G40196	86.5	94.5	8		SLT
G40196	94.5	95	0.5	SILL	DO
G40196	95	101	6		SLT
G40196	101	112	11		SST
G40196	112	118.5	6.5		SLT
G40196	118.5	119.5	1		SST
G40196	119.5	135.5	16		SLT
G40196	135.5	150	14.5		SST
G40196	150	150	0	EOH	EOH
G40197	0	5	5	OVB	DO
G40197	5	55.5	50.5	SILL	DO
G40197	55.5	59.5	4		SST
G40197	59.5	60.5	1	SILL	DO
G40197	60.5	64.5	4		SST
G40197	64.5	65.5	1	SILL	DO
G40197	65.5	66.5	1		SST
G40197	66.5	67.5	1	SILL	DO
G40197	67.5	69.5	2		SST
G40197	69.5	71	1.5		SLT
G40197	71	72.5	1.5		SST
G40197	72.5	74	1.5		SLT
G40197	74	75	1		SST
G40197	75	76.5	1.5		SLT
G40197	76.5	80	3.5		SST
G40197	80	84	4		SLT
G40197	84	84.5	0.5		SST
G40197	84.5	85.5	1	SILL	DO
G40197	85.5	86.5	1		SST
G40197	86.5	87.5	1	SILL	DO
G40197	87.5	95	7.5		SST
G40197	95	104.5	9.5		SLT
G40197	104.5	108.5	4		SST
G40197	108.5	109.5	1	SILL	DO
G40197	109.5	110.5	1		SST
G40197	110.5	116.5	6		SLT
G40197	116.5	118	1.5		SST
G40197	118	132.5	14.5		SLT
G40197	132.5	134.5	2		SST
G40197	134.5	135.5	1		SLT
G40197	135.5	141.5	6		SST
G40197	141.5	162.5	21		SLT
G40197	162.5	163.5	1		SST
G40197	163.5	167.5	4		SLT
G40197	167.5	168	0.5		SST
G40197	168	174	6		SLT
G40197	174	174	0	EOH	EOH
G40198	0	0.5	0.5	OVB	SST
G40198	0.5	11	10.5		SST
G40198	11	13	2		SLT
G40198	13	18	5		SST
G40198	18	28	10		SLT

G40198	28	30	2		SST
G40198	30	31.5	1.5		SLT
G40198	31.5	36.5	5		SST
G40198	36.5	37.5	1		SLT
G40198	37.5	47.5	10		SST
G40198	47.5	49	1.5		SLT
G40198	49	61	12		SST
G40198	61	65.5	4.5	SILL	DO
G40198	65.5	66.5	1		SST
G40198	66.5	67.5	1	SILL	DO
G40198	67.5	84.5	17		SST
G40198	84.5	90.5	6		SLT
G40198	90.5	93	2.5		SST
G40198	93	100	7		SLT
G40198	100	101.5	1.5		SST
G40198	101.5	107	5.5		SLT
G40198	107	111.5	4.5		SST
G40198	111.5	115	3.5		SLT
G40198	115	126	11		SST
G40198	126	138	12		SLT
G40198	138	141	3		SST
G40198	141	144	3		SLT
G40198	144	146	2		SST
G40198	146	150	4		SLT
G40198	150	154.5	4.5	SILL	DO
G40198	154.5	160	5.5		SLT
G40198	160	162	2		SST
G40198	162	164	2		SLT
G40198	164	166.5	2.5		SST
G40198	166.5	168.5	2		SLT
G40198	168.5	169	0.5	SILL	DO
G40198	169	169.5	0.5		SST
G40198	169.5	204.5	35	SILL	DO
G40198	204.5	205.5	1		SST
G40198	205.5	260	54.5	SILL	DO
G40198	260	260	0	EOH	EOH
G40199	0	5.5	5.5	OVB	DO
G40199	5.5	67.5	62	SILL	DO
G40199	67.5	72	4.5		SST
G40199	72	73	1		SLT
G40199	73	76	3		SST
G40199	76	79.5	3.5		SLT
G40199	79.5	80.5	1		SST
G40199	80.5	81	0.5		SLT
G40199	81	82.5	1.5		SST
G40199	82.5	83	0.5		SLT
G40199	83	92.5	9.5		SST
G40199	92.5	93	0.5		SLT
G40199	93	107.5	14.5		SST
G40199	107.5	116.5	9		SLT
G40199	116.5	117.5	1		SST
G40199	117.5	119.5	2		SLT
G40199	119.5	120.5	1		SST
G40199	120.5	142.5	22		SLT
G40199	142.5	143.5	1		SST
G40199	143.5	156	12.5		SLT
G40199	156	160	4		SST
G40199	160	174	14		SLT
G40199	174	175.5	1.5	SILL	DO
G40199	175.5	178.5	3		SST
G40199	178.5	186.5	8		SLT
G40199	186.5	187	0.5		SST
G40199	187	192	5		SLT

G40199	192	194.5	2.5		SST
G40199	194.5	196	1.5		SLT
G40199	196	197.5	1.5		SST
G40199	197.5	225.5	28		SLT
G40199	225.5	227.5	2		SST
G40199	227.5	229.5	2		SLT
G40199	229.5	230	0.5		SST
G40199	230	233.5	3.5		SLT
G40199	233.5	234	0.5		SST
G40199	234	235.5	1.5		SLT
G40199	235.5	236	0.5		SST
G40199	236	238	2		SLT
G40199	238	240	2		SST
G40199	240	246	6		SLT
G40199	246	249.5	3.5		SST
G40199	249.5	252	2.5		SLT
G40199	252	252	0	EOH	EOH
G40200	0	5.5	5.5	OVB	DO
G40200	5.5	20	14.5	SILL	DO
G40200	20	30.5	10.5		SLT
G40200	30.5	33	2.5		SST
G40200	33	36	3		SLT
G40200	36	40.5	4.5		SST
G40200	40.5	125	84.5	SILL	DO
G40200	125	152	27		SST
G40200	152	156	4		SLT
G40200	156	163	7		SST
G40200	163	173.5	10.5		SLT
G40200	173.5	182.5	9		SST
G40200	182.5	192.5	10		SLT
G40200	192.5	195	2.5		SST
G40200	195	221.5	26.5		SLT
G40200	221.5	222	0.5		SST
G40200	222	222.5	0.5		SLT
G40200	222.5	227.5	5		SST
G40200	227.5	229.5	2		SLT
G40200	229.5	231.5	2		SST
G40200	231.5	241	9.5		SLT
G40200	241	242.5	1.5		SST
G40200	242.5	245.5	3		SLT
G40200	245.5	252	6.5		SST
G40200	252	252	0	EOH	EOH
G40201	0	0.5	0.5	OVB	GRD
G40201	0.5	7	6.5		SLT
G40201	7	11	4		SST
G40201	11	16	5		SLT
G40201	16	17	1		SST
G40201	17	18	1		SLT
G40201	18	23	5		SST
G40201	23	25	2		SLT
G40201	25	33	8		SST
G40201	33	34.5	1.5		SLT
G40201	34.5	35	0.5		SST
G40201	35	40.5	5.5		SLT
G40201	40.5	41.5	1		SST
G40201	41.5	45.5	4		SLT
G40201	45.5	49.5	4		SST
G40201	49.5	50.5	1		SLT
G40201	50.5	60.5	10		SST
G40201	60.5	61.5	1	SILL	DO
G40201	61.5	62.5	1		SST
G40201	62.5	94	31.5	SILL	DO
G40201	94	101.5	7.5		SLT

G40201	101.5	113.5	12	SILL	DO
G40201	113.5	116.5	3		SST
G40201	116.5	195	78.5	SILL	DO
G40201	195	223.5	28.5		SST
G40201	223.5	224.5	1	SILL	DO
G40201	224.5	235.5	11		SST
G40201	235.5	236.5	1		SLT
G40201	236.5	242	5.5		SST
G40201	242	245.5	3.5		SLT
G40201	245.5	250	4.5		SST
G40201	250	251	1		SLT
G40201	251	252	1		SST
G40201	252	252	0	EOH	EOH
G40203	0	3	3	OVB	SLT
G40203	3	7	4		SLT
G40203	7	15.5	8.5		SST
G40203	15.5	16	0.5		SLT
G40203	16	18.5	2.5		SST
G40203	18.5	19.5	1		SLT
G40203	19.5	21	1.5		SST
G40203	21	81	60		SLT
G40203	81	85.5	4.5		SST
G40203	85.5	99	13.5		SLT
G40203	99	102	3		SST
G40203	102	119	17		SLT
G40203	119	121	2		SST
G40203	121	132.5	11.5		SLT
G40203	132.5	133	0.5		SST
G40203	133	136.5	3.5		SLT
G40203	136.5	137	0.5		SST
G40203	137	144.5	7.5		SLT
G40203	144.5	146	1.5		SST
G40203	146	151	5		SLT
G40203	151	153.5	2.5		SST
G40203	153.5	155.5	2		SLT
G40203	155.5	156.5	1		SST
G40203	156.5	186	29.5		SLT
G40203	186	265.5	79.5	SILL	DO
G40203	265.5	267.5	2		SLT
G40203	267.5	269.5	2		SST
G40203	269.5	270	0.5		SLT
G40203	270	280	10		SST
G40203	280	280	0	EOH	EOH
G40204	0	2	2	OVB	DO
G40204	2	8.5	6.5		SLT
G40204	8.5	9	0.5		SST
G40204	9	13	4		SLT
G40204	13	14	1		SST
G40204	14	15	1		SLT
G40204	15	17	2	SILL	DO
G40204	17	17.5	0.5		SST
G40204	17.5	103.5	86	SILL	DO
G40204	103.5	108.5	5		SST
G40204	108.5	110.5	2		SLT
G40204	110.5	147	36.5		SST
G40204	147	155	8		SLT
G40204	155	159	4		SST
G40204	159	160.5	1.5		SLT
G40204	160.5	161	0.5		SST
G40204	161	174.5	13.5		SLT
G40204	174.5	179.5	5		SST
G40204	179.5	185.5	6		SLT
G40204	185.5	186	0.5		SST

G40204	186	193	7		SLT
G40204	193	195.5	2.5		SST
G40204	195.5	205.5	10		SLT
G40204	205.5	207.5	2		SST
G40204	207.5	225.5	18		SLT
G40204	225.5	227.5	2		SST
G40204	227.5	229	1.5		SLT
G40204	229	230	1		SST
G40204	230	238.5	8.5		SLT
G40204	238.5	240.5	2		SST
G40204	240.5	246	5.5		SLT
G40204	246	252	6		SST
G40204	252	252	0	EOH	EOH
G40205	0	4	4	OVB	DO
G40205	4	41.5	37.5	SILL	DO
G40205	41.5	56.5	15		SST
G40205	56.5	58.5	2		SLT
G40205	58.5	108	49.5		SST
G40205	108	109.5	1.5		SLT
G40205	109.5	110	0.5		SST
G40205	110	111	1		SLT
G40205	111	112	1		SST
G40205	112	114	2		SLT
G40205	114	115	1		SST
G40205	115	142	27		SLT
G40205	142	142.5	0.5		SST
G40205	142.5	155.5	13		SLT
G40205	155.5	159.5	4		SST
G40205	159.5	161	1.5		SLT
G40205	161	162	1		SST
G40205	162	189	27		SLT
G40205	189	190	1		SST
G40205	190	190	0	EOH	EOH
G40205A	0	8	8	OVB	DO
G40205A	8	42	34	SILL	DO
G40205A	42	45.5	3.5		SST
G40205A	45.5	52	6.5		SLT
G40205A	52	53.5	1.5		SST
G40205A	53.5	55	1.5		SLT
G40205A	55	58	3		SST
G40205A	58	60.5	2.5		SLT
G40205A	60.5	61.5	1		SST
G40205A	61.5	64	2.5		SLT
G40205A	64	79	15		SST
G40205A	79	80	1		SLT
G40205A	80	85	5		SST
G40205A	85	90	5		SLT
G40205A	90	95.5	5.5		SST
G40205A	95.5	99	3.5		SLT
G40205A	99	102.5	3.5		SST
G40205A	102.5	103.5	1		SLT
G40205A	103.5	105	1.5		SST
G40205A	105	158	53		SLT
G40205A	158	161	3		SST
G40205A	161	260	99		SLT
G40205A	260	260	0	EOH	EOH
G40206	0	0.5	0.5	OVB	GRD
G40206	0.5	2.5	2		SLT
G40206	2.5	30	27.5		SST
G40206	30	34.5	4.5		SLT
G40206	34.5	35	0.5		SST
G40206	35	37	2		SLT
G40206	37	40	3		SST

G40206	40	44	4		SLT
G40206	44	48.5	4.5		SST
G40206	48.5	50.5	2		SLT
G40206	50.5	56.5	6		SST
G40206	56.5	74	17.5		SLT
G40206	74	76	2		SST
G40206	76	82	6		SLT
G40206	82	83	1		SST
G40206	83	90	7		SLT
G40206	90	94	4		SST
G40206	94	96	2		SLT
G40206	96	100	4		SST
G40206	100	101.5	1.5		SLT
G40206	101.5	102	0.5		SST
G40206	102	155	53		SLT
G40206	155	160	5		SST
G40206	160	174.5	14.5		SLT
G40206	174.5	179.5	5		SST
G40206	179.5	225	45.5		SLT
G40206	225	225	0	EOH	EOH
G46001	0	3	3	OVB	GRD
G46001	3	34	31	SILL	DO
G46001	34	37	3		SST
G46001	37	39	2		SLT
G46001	39	55	16		SST
G46001	55	56	1		SLT
G46001	56	64	8		SST
G46001	64	82	18		SLT
G46001	82	96	14		SST
G46001	96	100	4		SLT
G46001	100	119	19		SST
G46001	119	120	1		SLT
G46001	120	129	9		SST
G46001	129	139	10		SLT
G46001	139	148	9		SST
G46001	148	150	2		SLT
G46001	150	150	0	EOH	EOH
G46002	0	4	4	OVB	GRD
G46002	4	55.5	51.5	SILL	DO
G46002	55.5	78.5	23		SST
G46002	78.5	81.5	3		SLT
G46002	81.5	82	0.5		SST
G46002	82	83.5	1.5		SLT
G46002	83.5	87.5	4		SST
G46002	87.5	91	3.5		SLT
G46002	91	92.5	1.5		SST
G46002	92.5	100	7.5		SLT
G46002	100	103	3		SST
G46002	103	108	5		SLT
G46002	108	114.5	6.5		SST
G46002	114.5	116	1.5		SLT
G46002	116	118	2		SST
G46002	118	120	2		SLT
G46002	120	120	0	EOH	EOH
G46003	0	2	2	OVB	GRD
G46003	2	14	12		SLT
G46003	14	15.5	1.5		SST
G46003	15.5	16.5	1		SLT
G46003	16.5	36	19.5		SST
G46003	36	42	6		SLT
G46003	42	105.5	63.5	SILL	DO
G46003	105.5	111	5.5		SST
G46003	111	112	1		SLT

G46003	112	129	17		SST
G46003	129	130	1		SLT
G46003	130	132	2		SST
G46003	132	140	8		SLT
G46003	140	143.5	3.5		SST
G46003	143.5	151	7.5		SLT
G46003	151	151	0	EOH	EOH
G46004	0	3.5	3.5	OVB	SLT
G46004	3.5	10.5	7		SLT
G46004	10.5	14.5	4		SST
G46004	14.5	15	0.5		SLT
G46004	15	24.5	9.5		SST
G46004	24.5	26.5	2		SLT
G46004	26.5	27.5	1		SST
G46004	27.5	91	63.5	SILL	DO
G46004	91	106	15		SST
G46004	106	107	1		SLT
G46004	107	113	6		SST
G46004	113	114	1		SLT
G46004	114	121	7		SST
G46004	121	122	1		SLT
G46004	122	123	1		SST
G46004	123	124.5	1.5		SLT
G46004	124.5	127	2.5		SST
G46004	127	139	12		SLT
G46004	139	140.5	1.5		SST
G46004	140.5	142	1.5		SLT
G46004	142	150	8		SST
G46004	150	150	0	EOH	EOH
G46005	0	2	2	OVB	SLT
G46005	2	8	6		SLT
G46005	8	9	1		SST
G46005	9	27	18		SLT
G46005	27	29	2		SST
G46005	29	31	2		SLT
G46005	31	33	2		SST
G46005	33	36	3		SLT
G46005	36	45	9		SST
G46005	45	51	6		SLT
G46005	51	98	47	SILL	DO
G46005	98	98	0	EOH	EOH
G46005A	0	2	2	OVB	SLT
G46005A	2	8	6		SLT
G46005A	8	9	1		SST
G46005A	9	27	18		SLT
G46005A	27	28.5	1.5		SST
G46005A	28.5	31	2.5		SLT
G46005A	31	33	2		SST
G46005A	33	36	3		SLT
G46005A	36	45	9		SST
G46005A	45	51	6		SLT
G46005A	51	116	65	SILL	DO
G46005A	116	118	2		SST
G46005A	118	119	1		SLT
G46005A	119	124	5		SST
G46005A	124	131	7		SLT
G46005A	131	132	1		SST
G46005A	132	133.5	1.5		SLT
G46005A	133.5	135.5	2		SST
G46005A	135.5	138	2.5		SLT
G46005A	138	144	6		SST
G46005A	144	146.5	2.5		SLT
G46005A	146.5	150	3.5		SST

G46005A	150	151	1		SLT
G46005A	151	157	6		SST
G46005A	157	161	4		SLT
G46005A	161	161	0	EOH	EOH

Chapter 6 - Spatial variations of sills

All drilling and geophysical data is available from the Council for Geoscience or from the below literature:

Cole, D.I., Robey, K., Chevallier, L. and Viljoen, J., 2011. The geology of shales with a gas potential in the Main Karoo Basin of South Africa and impact of hydraulic fracturing on groundwater. Council for Geoscience Report 2011-0142. Council for Geoscience Western Cape Regional Office (Bellville), 43p.

Cawthorn, R.G., 2012. Distribution of Dolerite Sills in the Karoo Supergroup. LASI 5 Conference, Port Elizabeth, South Africa, 28-29.

Lindique, A., De Wit, M.J., Ryberg, T., Weber, M., Chevallier, L. (2011). Deep crustal profile across the southern Karoo basin and beattie magnetic anomaly, south africa: an Integrated interpretation with tectonic implications. South African Journal of Geology 114, 265-292.

Rowsell, D.M. and De Swardt, A.M.J. (1976). Diagenesis in Cape and Karroo sediments, South Africa, and its bearing on their hydrocarbon potential. Transactions, Geological Society of South Africa, 79, 81-145.

Scheiber-Enslin, S.E. (2015). Integrated Geophysical Investigation of the Karoo Basin, South Africa. PhD Thesis University of the Witwatersrand, 292pp.

Scheiber-Enslin, S.E., Webb, S.J., Ebbing, J. (2014). Geophysically plumbing the main Karoo basin, South Africa. South African Journal of Geology 117, 2.